Strength, Durability, Ductility and Fire Performance of Concrete Containing Waste Rubber Tyre Ash and Rubber Fiber as Partial Replacement of Fine Aggregate

by

TRILOK GUPTA

Department of Civil Engineering

A Thesis

Submitted

in partial fulfillment of the requirements of the degree of

Doctor of Philosophy

to

MALAVIYA NATIONAL INSTITUTE OF TECHNOLOGY JAIPUR

JAIPUR

February, 2016

MALAVIYA NATIONAL INSTITUTE OF TECHNOLOGY JAIPUR,
JAIPUR

CANDIDATE'S DECLARATION

I hereby certify that the work which is being presented in the thesis entitled "**Strength, Durability, Ductility and Fire Performance of Concrete Containing Waste Rubber Tyre Ash and Rubber Fiber as Partial Replacement of Fine Aggregate**" in partial fulfillment of the requirements for the award of the degree of Doctor of Philosophy and submitted in the Department of Civil Engineering, Malaviya National Institute of Technology Jaipur, is an authentic record of my own work carried out at Department of Civil Engineering, MNIT Jaipur and CTAE, Udaipur during a period from July 20, 2012 to July 29, 2015 under the supervision of Dr. Sandeep Chaudhary, Associate Professor, Civil Engineering, MNIT Jaipur and Dr. Ravi K. Sharma, Professor, Civil Engineering, CTAE, MPUAT, Udaipur.

The matter presented in this thesis has not been submitted by for the award of any other degree of this or any other Institute.

Date: 29-02-2016

Trilok Gupta
ID No. 2012RCE9005

This is to certify that the above statement made by the candidate is true to the best of our knowledge.

(Dr. Ravi Kr. Sharma)
External Supervisor
Professor
Department of Civil Engineering
CTAE Udaipur-313001 (India)

(Dr. Sandeep Chaudhary)
Supervisor
Associate Professor
Department of Civil Engineering
MNIT Jaipur-302017 (India)

MALAVIYA NATIONAL INSTITUTE OF TECHNOLOGY JAIPUR,
JAIPUR

CERTIFICATE

This is to certify that the thesis report entitled, "**Strength, Durability, Ductility and Fire Performance of Concrete Containing Waste Rubber Tyre Ash and Rubber Fiber as Partial Replacement of Fine Aggregate"** which is being submitted by **Trilok Gupta, ID: 2012RCE9005,** for the partial fulfillment of the degree of **Doctor of Philosophy** in **Civil Engineering** in the Malaviya National Institute of Technology Jaipur, has been carried out by him under our supervision and guidance.

Date: 29-02-2016

(Dr. Ravi Kr. Sharma)
External Supervisor
Professor
Department of Civil Engineering
CTAE Udaipur-313001 (India)

(Dr. Sandeep Chaudhary)
Supervisor
Associate Professor
Department of Civil Engineering
MNIT Jaipur-302017 (India)

ACKNOWLEDGEMENT

Behind every achievement lies an unfathomable sea of gratitude to those who nurtured it, without whom it would have never seen the light of the day. I am fully indebted to the strength and countless blessings received from almighty, the good wishes and never-ending support from each of my teachers, friends, colleagues and members of the family. The favors received from each of them in completing this work are immense and immeasurable.

I take this opportunity to extend my most sincere gratitude and thanks to my supervisors, Dr. Sandeep Chaudhary, MNIT Jaipur and Prof. Ravi Kr. Sharma, CTAE, Udaipur. I fall short of words to thank them for their constant endeavor and enthusiasm throughout my research work. The technical and moral support provided by them draws no parallels. This work would have been impossible without their guidance and would have never been completed without their perception to put things in to right perspective.

I also wish to thank Prof. Ravindra Nagar, Prof. A.K. Vyas, Prof. R.C. Gupta, Prof. A.B. Gupta, Dr. Rajesh Gupta, Dr. S.K. Tiwari, Dr. Vinay Agrawal, Dr. Sandeep Shrivastava, Dr. Sanjay Mathur, Dr. Urmila Brighu, Dr. Sumit Khandelwal, Dr. Mahendra Choudhary, Dr. Putul Haldar and other eminent faculty members of MNIT Jaipur for their valuable support and comments which helped in refining the work at different stages. I am grateful for the unceasing help provided by Dr. B.S. Singvi, Head, Department of Civil Engineering, CTAE, Udaipur and Prof. Gunwant Sharma, Head, Department of Civil Engineering, MNIT Jaipur during the study.

Earnest gratitude are also extended to the Prof. I.K. Bhat, Director, MNIT Jaipur and Dr. B.P. Nandwana, Dean, CTAE Udaipur for allowing me to utilize the research facilities in the Institute and also providing support from the Institute whenever it was required for the progress of this study.

I would like to thank Dr. Bhavna Tripathi, Salman Siddique, Pankaj Chaudhary, Priyansha Mehra, Rupesh Gawas, and all other colleagues and friends for their constant support. A special thanks also to the technical and support staff (Sh. M.L. Gupta and Sh. Mohan Lal Borana) of Department of Civil Engineering at CTAE, Udaipur and at MNIT Jaipur for their support throughout this study.

I owe a special thanks to Sh. Lalit Kumar Guglani, Chief Manager (Project), Central Institute of Plastic Engineering and Technology, Jaipur, Govt. of India, for allowing performing the tests for elastic modulus of waste rubber fibers.

I would like to thank my family members for being and bearing with me ever always. The incessant support of my wife, Mrs. Shalini Gupta, the blessings of my mother & father and most of all my sons Neel and Naman who have showered their affection with patience and wash away the daylong fatigue with their sweet smiles greeting me at the door step every time. I also wish to thank with all sincerity, Mrs. Sandeep Chaudhary and other family members of Dr. Sandeep Chaudhary for their cooperative behavior.

Date: February 29, 2016 (Trilok Gupta)
Jaipur

ABSTRACT

River sand is generally used as filler for gaps of coarse aggregates in concrete. At present, river sand is becoming expensive due to higher cost of transportation from river beds. Judiciary and Governments have therefore imposed ban on extraction of river sand from the river bed beyond a certain depth causing a shortage of fine aggregates. Consequently, concrete industry has been forced to look for alternative materials of river sand as fine aggregate. It is therefore desirable to investigate the use of cheaper, easily available and sustainable alternative materials to natural sand. Large quantities of waste rubber tyres are produced every year and accumulation of these tyres is a major problem. Waste rubber tyres can be used as in the concrete as replacement of fine aggregate (FA). This would not only solve the problem of accumulation of tyres but will also save natural resources.

Though, a number of studies have been undertaken on the properties of rubberised concrete; most of the studies are limited to a single w/c ratio and very few studies are available on use of rubber ash and rubber fibers in concrete, combined use of rubber ash and rubber fibers, waste rubber aggregate with silica fume, ductility properties of waste rubber concrete, and various properties of waste rubber concrete at elevated temperature (different exposure duration).

Therefore, the present study has been carried out for three different w/c ratios for strength, durability and ductility studies of concrete containing rubber fiber and rubber ash as partial replacement of fine aggregate and silica fume as partial replacement of cement. Study has also been carried out for strength, durability and ductility of rubber fiber concrete subjected to elevated temperatures.

It is concluded from the studies carried out that rubber ash and rubber fiber enhance the ductility properties of concrete. The compressive strength is adversely affected and the other strength and durability properties are marginally affected. The partial replacement of cement by silica fume is found to enhance the strength, durability and ductility properties of rubberized concrete.

To sum up, the rubberized concrete can be utilized where ductility is a major concern rather than strength and the rubberized concrete with silica fume can be used where strength is a concern along with ductility.

LIST OF CONTENTS

LIST OF FIGURES

LIST OF TABLES

CHAPTER 1

INTRODUCTION AND LITERATURE REVIEW

1.1 INTRODUCTION

River sand is generally used as filler for gaps of coarse aggregates in concrete. Now a days, river sand is becoming expensive due to the higher cost of transportation from river beds. Mining of river sand also creates serious environmental problems (Bederina *et al.*, 2013). Judiciary and Governments have therefore imposed ban on extraction of river sand from the river bed beyond a certain depth causing a shortage of fine aggregates. Consequently, concrete industry has been forced to look for alternative materials of river sand as fine aggregate (Prakash, 2007; Pofale and Quadri, 2013). Detailed study is therefore required to investigate the use of cheaper, easily available and sustainable alternative materials to natural sand.

Large quantities of waste rubber tyres are produced every year. Accumulation of discarded tyres is a major problem as degradation of these tyres is very difficult because of the highly complex configuration of the ingredient materials (Toutanji, 1996; Sunthonpagasit and Duffey, 2004).

Waste rubber tyres can be used as in the concrete as replacement of fine aggregate (FA). This would not only solve the problem of accumulation of tyres but will also save natural resources (Oikonomou and Mavridou, 2009; Ozbay *et al.* 2011; Wang *et al.* 2013).

Though a number of experimental studies are available for rubberised concrete and encouraging results have been reported, the rubberised concrete is still in early stages of practical application in field. The rubberised concrete has been used in foundation, sidewalk, parking lot and tennis court in state of Arizona, USA (Kaloush *et al.*, 2005). Further, waste rubber tyre is being used in rubberised asphalt concrete in many parts of the world.

In this chapter, a thorough review of published work on utilization of waste rubber tyre particles as partial replacement of sand (fine aggregate) in concrete is presented. In addition, various durability, ductility parameters along with effect of elevated temperature on waste rubber concrete are also discussed.

1.2 LITERATURE REVIEW

A number of studies are available for different properties of rubberized concrete

1.2.1 Workability

Properties of concrete are affected by inclusion of waste rubber tyre. There are two parallel views regarding effect of waste rubber tyre particles on workability. The decrease in workability was reported by Olivares and Barluenga (2004), Batayneh *et al.* (2008), Oikonomou and Mavridou (2009) and Ozbay *et al.* (2011) whereas an increase in workability was reported by Khaloo *et al.* (2008) and Aiello and Leuzzi (2010).

Sukontasukkul and Chaikaew (2006) observed reduction in workability of concrete with waste rubber aggregate. It was reported that the water requirement increases with the increase of waste rubber aggregate and as the average particle size of the waste rubber aggregate decrease. Reda Taha *et al.* (2008) observed reduction in slump of concrete with increasing replacement level of natural aggregate by waste rubber aggregate. Wang *et al.* (2013) observed increase in workability with rubber replacement. Nayef *et al.* (2010) reported zero slump of a concrete mix with coarse rubber content of 20% by total coarse aggregate (CA) volume and a very low slump value for a concrete mix with fine rubber aggregate. However, it was reported that the slump of waste rubber concrete mixes can be improved by adding 5% microsilica.

Li *et al.* (2004) did not observe any significant change in workability on 15% replacement of coarse aggregate (CA) by rubber tyre chips or fibre. Khaloo *et al.* (2008) observed contrasting workability behaviour of concrete with the incorporation of fine and coarse rubber tyre aggregate as partial replacement of natural aggregate. The workability was found to increase on up to 15% replacement of sand by fine rubber aggregate, beyond which workability was found to decrease, whereas, workability of concrete with coarse rubber aggregate was found to decrease to a minimum for tyre aggregate contents of 15%. Aiello and Leuzzi (2010) reported slight improvement in workability on partial substitution of coarse or fine aggregate by waste rubber shreds.

Guneyisi *et al.* (2004) reported that the workability of waste rubber aggregate concrete with and without silica fume decreased with increase in the waste rubber aggregate content. It was also reported that the slump of concrete became negligible when rubber aggregates content became more than half of the total aggregate volume. It was further reported that the decrease in the workability was more for low w/c concrete mixes.

1.2.2 Compressive strength

Compressive strength of concrete has been observed to systematically decrease with the increase in rubber content.

Khatib and Bayomy (1999) reported significant decrease in compressive strength of concrete on replacement of fine aggregate (FA) by crumb rubber and coarse aggregate (CA) by tire chips. The reduction was attributed to (i) presence of softer rubber particles than surrounding cement matrix; and (ii) insufficient bonding between rubber particles and cement paste due to which rubber particles act like voids.

Benazzouk *et al.* (2007) observed a sharp reduction of upto 77% in compressive strength of concrete on inclusion of shredded rubber particles (upto 50% by volume) in cementitious matrix. The reduction was attributed to (i) presence of lesser stiff rubber particles than the adjacent cement paste; and (ii) cracks around the rubber particles, which accelerate the breakdown in the matrix.

Li *et al.* (2004) reported decrease in the compressive strength of concrete on replacement of 15% of volume of CA by waste tire chips or fibers. The reduction was observed to be more in case of waste tire rubber chip concrete in comparison to waste tire fiber concrete. The difference in the load transfer capabilities was cited as the reason for this. It was stated by the authors that the longer length of the fiber helps in transferring the load through interfacial forces, even after debonding from the cement matrix.

Guneyisi *et al.* (2004) observed systematic decrease in the compressive strength of concrete on replacement of aggregate by rubber (crumb and chip). The reduction in strength was attributed to the reasons mentioned by Khatib and Bayomy (1999) which have been stated earlier in this section. The compressive strength was found to increase on inclusion of silica fume. The increase was attributed to filling of voids by silica fume.

Ganjian *et al.* (2009) observed 23% decrease in the compressive strength of concrete on 10% replacement of CA by rubber chips. According to Ganjian *et al.* (2009), possible reasons for this strength reduction are: (i) soft material of rubber particles; (ii) poor bonding between rubber aggregate and cement paste; and (iii) non uniform distribution of rubber particles in the concrete.

Reda Taha *et al.* (2008) reported decrease in compressive strength on replacement of CA by chipped rubber and FA by crumb rubber for single w/c ratio (0.7). They observed more than 78% reduction in compressive strength on full replacement of CA by chip rubber and

67% reduction in compressive strength on full replacement of FA by crumb rubber. The decreases was attributed to: (i) the deformability of the rubber particles compared with the surrounding cement paste; (ii) insufficient bonding between rubber aggregates and the cement paste; and (iii) reduced concrete matrix density.

Khaloo *et al.* (2008) reported decrease in compressive strength on replacement of CA by chipped rubber and FA by crumb rubber for varied w/c ratio. They observed more than 98% reduction in compressive strength on replacement of half of CA by chipped rubber. The decrease was attributed to (i) higher air content in concrete specimen; and (ii) low modulus of elasticity of rubber with respect to mineral aggregate.

Batayneh *et al.* (2008) reported decrease in compressive strength on upto 100% replacement of FA by crumb rubber for w/c ratio 0.55. They observed more than 90% reduction in compressive strength on 100% replacement. The reduction was attributed to (i) weak aggregate paste bond; and (ii) substitution of the harder dense natural aggregate with a softer, less dense crumb rubber.

Zheng *et al.* (2008) reported decrease in compressive strength up to 45% replacement of CA by ground rubber and crushed rubber for single w/c ratio (0.45). They observed more than 53% reduction in compressive strength on 45% replacement. The reduction was attributed to: (i) replacement of CA with softer rubber particles; (ii) weak bonding between rubber aggregates and cement paste; and (iii) stress concentrations at the interface of the cement paste and rubber particles.

Son *et al.* (2011) reported about 22% reduction in compressive strength on partial replacement of aggregate by crumb rubber. Sohrabi and Karbalaie (2011) reported that the silica fume increased the compressive strength of rubberized concrete. The filling of micro voids in cement paste by silica fume producing a denser structure was cited as the reason.

Ozbay *et al.* (2011) reported a decrease in compressive strength up to 25% replacement of FA by crumb rubber for w/c ratio 0.4. They observed more than 26% reduction in compressive strength on 25% replacement and discussed (i) lesser rigidity of the rubber aggregates as compared with the surrounding cement paste; (ii) poor interface bonding; and (iii) increase in matrix porosity leading to decrease in the density, as the reasons.

Grinys *et al.* (2012) reported a decrease in compressive strength up to 30% replacement of sand by crumb rubber for w/c ratio 0.35. They observed more than 85% reduction in compressive strength on 30% replacement. The reduction was attributed to (i) presence of

more elastic and weaker rubber particles as compared to surrounding cement matrix; and (ii) replacement of higher density material with low density material.

Turki *et al.* (2012) reported a decrease in compressive strength on replacement of upto 50% FA by rubber aggregate for w/c ratio 0.5 in cement mortar. More than 84% reduction in compressive strength was reported on 50% replacement. Reduction in compressive strength was attributed to low density of rubber in comparison of the FA.

Xue and Shinozuka (2013) reported a decrease in compressive strength up to 20% replacement of CA by crumb rubber. They observed more than 47% reduction in compressive strength on 20% replacement and discussed (i) replacement of CA by low load-carrying elements; and (ii) weak interface bond, as the reasons. There was less reduction (about 38%) on addition of 7% silica fume in rubber concrete. The decrease in reduction was attributed to filling voids by nano particles and better bonding between rubber aggregate and cement paste.

Su *et al.* (2015) reported a decrease in compressive strength on upto 20% replacement of FA by granulated rubber aggregate for w/c ratio 0.37. They observed more than 10% reduction in compressive strength on 20% replacement. The reduction was attributed to: (i) replacement of FA with soft rubber aggregate; and (ii) inconsistency of the concrete mix due to low stiffness and poor surface texture.

Decrease in compressive strength has also been reported by Onuaguluchi and Panesar (2014) on replacement of upto 15% FA by crumb rubber for w/c ratio 0.47. They reported more than 40% reduction in compressive strength on 15% replacement and discussed (i) increased porosity of mixture; and (ii) low adhesion of crumb rubber to cement paste, as the reasons.

1.2.3 Flexural Strength

Flexural strength of rubberized concrete is influenced by the inclusion of waste rubber tyre. Some studies have reported enhanced flexural strength with the increase in crumb rubber content (Benazzouk *et al.* 2003; Yilmaz and Degirmenci 2009; Ganesan *et al.* 2013). However, some studies have reported reduced flexural strength with increase in the rubber content (Turatsinze and Garros 2008; Ganjian *et al.* 2009; Uygunoğlu and Topcu 2010; Aiello and Leuzzi 2010; Turki *et al.* 2012; Najim *et al.* 2012; Grinys *et al.* 2012; Liu *et al.* 2013; Gesoğlu *et al.* 2014; Su *et al.* 2015). The reduction in flexural strength may be due to the poor interface bond (Siddique *et al.* 2008).

Benazzouk *et al.* (2003) reported higher flexural strength of cement matrix on inclusion of two types of waste rubber aggregate, compact rubber aggregate and expanded rubber aggregate. The strength was found to be highest for 20% each of both types of aggregate. However, the flexural strength decreased drastically, in presence of more than 35% of any type of aggregate, due to the rupture of the rubber and cement matrix connection. Cement mortar with expanded rubber aggregate showed better flexural strength than cement mortar with compacted rubber aggregate.

Yilmaz and Degirmenci (2009) reported increase in flexural strength on 20% replacement of cement by rubber waste by and reduction on 30% replacement of cement by rubber waste.

Ganesan *et al.* (2013) reported increase in flexural strength up to 0% to 20% replacement of sand by shredded rubber for w/c ratio 0.37. They observed more than 15% increase in flexural strength on 15% replacement and 9% increase on 20% replacement of FA by shredded rubber.

Turatsinze and Garros (2008) reported decrease in flexural strength up to 25% replacement of CA by rubber aggregate for w/c ratio 0.4. They observed more than 42% reduction in flexural strength on 25% replacement of CA by rubber aggregate. The reduction was attributed to poor mechanical behaviour of rubber aggregate concrete.

Ganjian *et al.* (2009) reported decrease in flexural strength on replacement of CA by chipped rubber and cement by ground rubber for w/c ratio 0.5. They observed more than 37% reduction in flexural strength on 10% replacement of CA by chipped rubber. The reduction was attributed to weak bonding between rubber aggregates and the cement paste.

Uygunog˘lu and Topcu (2010) reported decrease in flexural strength up to 50% replacement of FA by rubber particles for w/c ratios 0.40, 0.43, 0.47 and 0.51. They observed more than 55% reduction in flexural strength on 50% replacement of FA by rubber particles. No sudden collapse of rubberized specimens was observed under bending load during the flexural test.

Aiello and Leuzzi (2010) reported decrease in flexural strength on replacement of CA by rubber shreds and FA by rubber particles for w/c ratio 0.6. More than 28% reduction in flexural strength was observed on 75% replacement of CA and more than 7% reduction was observed on 75% replacement of FA. The reduction was attributed to poor mechanical behaviour of rubber aggregate concrete. The coarse rubber chips were found to avoid the sudden failure.

Turki *et al.* (2012) reported decrease in flexural strength on upto 50% replacement of FA by rubber aggregate for w/c ratio 0.5. They observed more than 72% reduction in flexural strength on 50% replacement of FA by rubber aggregate. The reduction was attributed to the low density of rubber.

Najim *et al.* (2012) reported decrease in flexural strength on replacement of CA and FA by rubber aggregate. They observed more than 39% reduction in flexural strength on 15% replacement of CA by rubber aggregate.

Grinys *et al.* (2012) reported decrease in flexural strength up to 30% replacement of sand by crumb rubber for w/c ratio 0.35.They observed more than 72% reduction in flexural strength on 30% replacement of sand by crumb rubber.

Liu *et al.* (2013) reported decrease in flexural strength up to 15% replacement of FA by rubber for w/c ratio 0.31. They observed more than 18% reduction in flexural strength on 15% replacement of FA by rubber content.

Gesog˘lu *et al.* (2014) reported decrease in flexural strength on replacement of CA by tire chips and FA by crumb and fine crumb rubber for w/c ratio 0.27. They observed more than 81% reduction in flexural strength on 10% replacement of CA by tyre chips and 10% replacement of FA by fine crumb rubber. Reduction in flexural strength was attributed to weak interface bond.

Su *et al.* (2015) reported decrease in flexural strength on upto 20% replacement of FA by granulated rubber aggregate for single w/c ratio (0.37). They observed more than 12% reduction in flexural strength on 20% replacement of FA by granulated rubber aggregate.

1.2.4 Density

Inclusion of rubber aggregate in concrete affects the density of concrete. Reda Taha *et al.* (2008) reported more than 12% reduction in unit weight on 50% replacement of FA by rubber aggregate at a single w/c ratio (0.7). The reduction in density was attributed to the ability of tyre rubber aggregates to entrap air in its micro voids ; and lower specific gravity of the tyre rubber aggregates in comparision to that of natural aggregate.

Zheng *et al.* (2008) reported decrease in density up to total 45% replacement of CA by ground rubber and crushed rubber for a single w/c ratio (0.45). They observed more than 16% reduction in density on 45% replacement of CA by rubber aggregate.

Yilmaz and Degirmenci (2009) reported decrease in density on replacement of cement by rubber waste in mortar. Reduction in density was attributed to (i) lesser specific gravity of rubber aggregates; and (ii) higher air content in rubberized concrete. Xue and Shinozuka (2013) reported decrease in density up to 20% replacement of CA by crumb rubber. They observed more than 16% reduction in density on 20% replacement of CA by crumb rubber. Reduction in density was attributed to low specific gravity of rubber aggregate. However, no change was observed on addition of silica fume in control and rubber fiber concrete.

Pelisser *et al.* (2011) observed decrease in density on replacement of aggregate by rubber waste. They observed more than 13% reduction in density on replacement of natural aggregate by rubber waste. However, only 9% reduction in density was observed on addition of 15% silica fume in rubber concrete.

Nayef *et al.* (2010) observed decrease in density on replacement of FA by fine rubber and CA by coarse rubber for a single w/c ratio (0.55). They observed more than 22% reduction in density on 20% replacement of natural aggregate by rubber aggregate. Reduction in density was resulted in lighter concrete.

1.2.5 Abrasion resistance

The abrasion due to movement of objects leads to the deterioration of concrete surface. A concrete should have high abrasion resistance from durability aspect.

Increase in depth of wear (abrasion resistance) has been reported by Ozbay *et al.* (2011) on replacement of upto 25% FA by crumb rubber for a single w/c ratio (0.4) in cement mortar. They observed more than 20% increase in depth of wear on 25% replacement of FA by crumb rubber.

Increase in weight loss due to abrasion has been reported by Sukontasukkul and Chaikaew (2006) on replacement of CA and FA by crumb rubber. They observed more than 900% increases in weight loss on 20% replacement of FA by crumb rubber.

Decrease in mass loss due to abrasion has been reported by Segre and Joekes (2000) on inclusion of powdered tyre rubber as additive (0% to 10%) for single w/c ratio (0.36). They observed more than 300% reduction in mass loss on 10% addition of powdered tyre rubber.

Gesog˘lu *et al.* (2014) reported decrease in depth of wear on replacement of CA by tire chips and FA by crumb and fine crumb rubber for w/c ratio 0.27. They observed more than

81% reduction in depth of wear on 20% replacement of aggregate by rubber particles. The reduction was attributed to the ability of the rubber particles to hold the paste together.

1.2.6 Water absorption

The water absorption of concrete gives an insight of the internal microstructure as it is related to the internal porosity of the concrete specimen.

Turatsinze and Garros (2008) observed an increase of about 30% in the porosity on 25% replacement of the CA by rubber. The increase was attributed to higher air content resulting in reduced compaction of the concrete. Oikonomou and Mavridou (2009) reported decrease in water absorption on upto 15% replacement of FA by tire rubber.

Yilmaz and Degirmenci (2009) reported decrease in water absorption on inclusion of rubber waste as cement (20% to 30%) in mortar. It was reported that the rubber aggregates do not absorb water hence the inclusion of rubber aggregates reduced the amount of water absorbed.

Ganjian *et al.* (2009) reported increase in water absorption on replacement of CA by chipped rubber and cement by ground rubber in concrete. Increase in water absorption was attributed to poor interface bond.

Uygunogˇlu and Topcu (2010) reported increase in water absorption on replacement of FA by rubber particles for w/c ratios 0.4, 0.43, 0.47 and 0.51. They observed about more than 18% increase in water absorption on 50% replacement of FA by rubber particles. Increase in water absorption was attributed to (i) the entrapment of air; and (ii) the increase in the voids in the cement paste.

Bjegović *et al.* (2011) reported decrease in water absorption on replacement up to total 15% volume of aggregate by granulated, shredded and small granulated rubber particles. They observed more than 78% decrease in water absorption on 15% replacement of natural aggregate by rubber particles.

Gesogˇlu and Guneyisi (2011) reported increase in water absorption on replacement of CA by tire chips and FA by crumb and fine crumb rubber for w/c ratio 0.27. They observed more than 4.2% increase in water absorption on 25% replacement of FA by crumb rubber.

Bravo and Brito (2012) reported increase in water absorption on replacement of natural aggregate by tyre rubber aggregate for single w/c ratio (0.35). They observed more than 2.5% increase in water absorption on 15% replacement of natural aggregate by rubber aggregate.

The poor bonding in between rubber/cement paste transition zones was held responsible for the increase.

Sukontasukkul and Chaikaew (2012) reported increase in water absorption on up to 30% replacement of FA by crumb rubber for single w/c ratio (0.47). It was reported that rubber particles have the property of water insolvablility due to which the air bubbles were trapped at the surface of rubber particles at the time of mixing. This made the interface of cement paste and rubber particles more porous.

Onuaguluchi and Panesar (2014) reported increase in water absorption on replacement of FA by crumb rubber for a single w/c ratio (0.47). They observed more than 7% increase in water absorption on 15% replacement of FA by crumb rubber. Increase in water absorption was attributed to increased void content of rubberized concrete. On the other hand, addition of silica fume was found to decrease the water absorption of concrete more than 45%. The reduction in water absorption was attributed to the hydration process of silica fume resulting in filling of the voids. It was stated that the filling of voids reduced the porosity and thereby the water absorption.

1.2.7 Water permeability

Permeability is the most important parameter in determining concrete durability. An experimental study was carried out by Ganjian *et al.* (2009) to investigate the effect of replacement of CA by chipped rubber and cement by ground rubber (obtained by grinding the crumb rubber) on the water permeability for a single w/c ratio (0.5). The authors observed more than 150% increase in water permeability depth on 10% replacement of CA and 114% increase on 10% replacement of cement. This increase in water permeability was attributed to the reduction in bonding between particles in the modified concrete.

Bjegović *et al.* (2011) reported increase in water permeability on replacement of up to total 15% volume of aggregate by granulated, shredded and small granulated rubber particles. They observed more than 100% increase in water permeability on 10% replacement of natural aggregate by rubber aggregate. Increase in water permeability was attributed to higher amount of air voids entrapped around rubber surface.

Su *et al.* (2015) observed increase in water permeability up to 20% replacement of FA by granulated rubber aggregate for w/c ratio 0.37. They observed more than 215% increase in depth of water permeability on 20% replacement of FA by granulated rubber aggregate. Increase in water permeability was attributed to increased porosity of rubber concrete.

1.2.8 Shrinkage

Drying shrinkage can be defined as the change in volume due to loss of moisture to the environment. As concrete shrink, tensile stresses are developed due to restrained of material from adjacent members and will cause the crack in the concrete. The magnitude of the drying shrinkage directly depends upon the amount of moisture lost (Zhang *et al.* 2011). Drying shrinkage in concrete is important with low w/c ratio because internal water is quickly exhausted and results in rapid shrinkage. Shrinkage is a complex phenomenon because it is depends upon several factors such as proportion of mix, size, shape, density and elasticity of aggregate; w/c ratio fineness of cement, air content in concrete and use of admixtures in concrete.

Turatsinze and Garros (2008) reported decrease in restrained shrinkage cracking of self compacting concrete on upto 25% replacement of CA by rubber aggregate for single w/c ratio (0.4). The improved resistance to cracking was attributed to the enhanced strain capacity.

Uygunoglu and Topcu (2010) carried out studies for the effect of scrap rubber particles on the drying shrinkage of self compacting concrete. Up to 50% sand aggregate were replaced by scrap rubber particles and the drying shrinkage was found to increase with an increase in rubber content. The increase was attributed to the increase in porosity of mix due to rubber particles.

Bravo and Brito (2012) reported increase in total shrinkage on replacement of natural aggregate by tyre rubber aggregate for single w/c ratio (0.35). However, the drying shrinkage was not found to be affected by use of rubber aggregate.

Sukontasukkul and Tiamlom (2012) reported increase in drying shrinkage up to 30% replacement of FA by crumb rubber for single w/c ratio (0.47). Increase in drying shrinkage was attributed to the (i) decrease in internal restraint; and (ii) increase of more flexible material.

Nguyen *et al.* (2012) reported increase in restrained shrinkage on replacement of FA (0% to 30%) by rubber aggregate for a single w/c ratio (0.47) in mortar. The replacement was found to delay the shrinkage cracking.

Yung *et al.* (2013) reported increase in drying shrinkage on replacement of FA (0% to 20%) by rubber powder for a single w/c ratio (0.35). They observed, more than 95% increase in drying shrinkage on 20% replacement of FA by rubber powder. The minor capability of deformation of rubber powder was cited as the reason for increase in drying shrinkage.

1.2.9 Carbonation

Ingress of carbon dioxide into concrete through voids and its reaction with hydrated cement paste is known as carbonation (Papadaks *et al.* 1992). The chemical reaction of carbonation is as follows (Broomfield 2007):

$$CO_2 + H_2O \rightarrow H_2CO_3 \tag{1.1}$$

$$H_2CO_3 + Ca(OH)_2 \rightarrow CaCO_3 + 2H_2O \tag{1.2}$$

The carbonation though not harmful in itself, reduces the pH of concrete which results in the increase in the chances of corrosion of steel in concrete. Carbonation depends on CO_2 concentration present in the environment, humidity of the atmosphere and w/c ratio. According to Roy *et al.* (1999), the maximum rate of carbonation is achieved in the range of 50% to 75% relative humidity.

Bravo and Brito (2012) reported increase in carbonation depth on replacement of natural aggregate (0% to 15%) by tyre rubber aggregate for single w/c ratio (0.35). More than 56% increase in carbonation depth was observed on 15% replacement of natural aggregate by rubber aggregate. The increase in carbonation depth was attributed to (i) the more water demand of rubber content, required to maintain the workability; and (ii) the more void volume between rubber aggregate and the cement paste.

1.2.10 Corrosion and chloride diffusion

The high pH value of 12-13 protects steel bars from corrosion by formation of a passive layer (Broomfield 2007).

The process of corrosion may be defined by the following equations:

$$Fe = Fe^{++} + 2e^{-} \tag{1.3}$$

$$\frac{O_2}{2} + H_2O + 2e^{-} = 2HO^{-} \tag{1.4}$$

Chloride attack is a major deterioration mechanism for corrosion of reinforcing steel bars (Ababneh 2002). Porosity in the concrete facilitates the ingress of chlorides. The alkanity of concrete gets reduced by the chloride attack. Further, in the presence of oxygen and moisture, a local cell is formed causing anodic and cathodic reactions at same time (Hausmann 1964 and 1967). This breaks the passive layer and initiates the corrosion in steel bars.

Theoretically, two type of corrosion is possible in steel bars of reinforced concrete: (i) microcell corrosion, in which anode and cathode are very near; and (ii) macrocell corrosion, in which anode and cathode are bit far (Sangoju *et al.* 2011).

Very few studies are available on chloride-ion penetration of concrete containing waste rubber aggregate.

More resistance against the diffusion of chloride ion was reported by Al-Akhras and Smadi (2004) for rubberized mortar, containing rubber particles (tyre rubber ash) as partial replacement of sand for a single w/c ratio (0.65). It was stated that that the filling of the voids by the rubber ash prevented the diffusion of chloride.

Gesoglu and Guneyisi (2007) reported decrease in the penetration of chloride ions on partial replacement of FA by crumb rubber and CA by tire chips in concrete. The chloride ion permeability was found to increase upto 59% on 25% replacement of total aggregate by rubber. The increase in permeability was however found to be controlled on addition of silica fume.

Oikonomou and Mavridou (2009) reported decrease in chloride-ion penetration of cement mortar on replacement of FA (0% to 15%) by granulated tyre rubber. More than 35% reduction in chloride-ion penetration was observed on 15% replacement of FA by rubber aggregate.

Reduction in chloride-ion penetration has been reported by Bjegović *et al.* (2011) on replacement up to total 15% of volume of aggregate by granulated, shredded and small granulated rubber particles. The reduction was attributed to better fillment of voids between rubber and natural aggregate, causing higher homogeneity and uniform distribution of ingredients.

Gesog˘lu and Guneyisi (2011) reported increase in chloride-ion penetration on partial replacement of FA (0% to 25%) by crumb rubber for a single w/c ratio (0.35). More than 45% increase in chloride-ion penetration was observed on 25% replacement of FA by crumb rubber. However, chloride-ion penetration was found to slightly improve on extending the curing period from 28 to 90 days. Further, the chloride ion permeability of rubberized concrete was found to decrease on addition of fly ash.

No trends of variation in chloride-ion penetration were observed by Bravo and Brito (2012) on replacement of natural aggregate (0% to 15%) by tyre rubber aggregate for single

w/c ratio (0.35). They observed decrease in chloride-ion penetration up to 5% replacement of natural aggregate by rubber aggregate and subsequently an increase for higher replacement ratios.

Dong *et al.* (2013) observed increase in chloride-ion penetration on replacement of FA by crumb rubber. They observed more than 40% increase in chloride-ion penetration on 1% replacement of natural aggregate by crumb rubber and more than 20% increase on 30% replacement. Increase in voids at the interface of cement paste and rubber aggregates was described as the reason for the increase in chloride-ion penetration.

Onuaguluchi and Panesar (2014) observed an uneven trend in chloride-ion penetration on replacement of FA by crumb rubber for a single w/c ratio (0.47). They observed about 18%, 25% and 12% decrease in chloride-ion penetration on 5%, 10% and 15% replacement of FA by crumb rubber. The chloride-ion penetration was found to decrease on inclusion of silica fume.

1.2.11 Acid attack

Acid attack affects the long term durability of concrete structure as it may cause expansion, cracking and deterioration (Cullu and Arslan 2014).

The deterioration process of concrete starts when sulphuric or hydrochloride acids attack surface of concrete. Sulphuric acid produces gypsum and hydrochloride acid produces calcium chloride when these react with cement. The chemical reaction is shown in following equations (Miyamoto *et al.* 2014):

$$Ca(OH)_2 + H_2SO_4 = CaSO_4.2H_2O \quad (1.5)$$

$$Ca(OH)_2 + 2HCl = CaCl_2 + 2H_2O \quad (1.6)$$

Azevedo *et al.* (2012) reported increase in mass loss, due to sulphuric acid attack, on partial replacement of sand (0% to 15%) by rubber waste for a single w/c ratio (0.35). More than 35% increase in mass loss was reported on 15% replacement of sand by rubber waste. However, the acid resistance of rubberized concrete was found to be better than control mix on addition of fly ash and metakaolin.

Raghavan *et al.* (1998) studied the effect of alkaline environment on rubber shreds and found little effect of alkaline environment on rubber shreds. It was therefore assumed that the rubber shreds would not be affected by the alkaline environment in the mortar.

1.2.12 Static modulus of elasticity

Studies have also been reported for the modulus of elasticity of rubberized concrete and mortar. Reduction in the elastic modulus of rubberized concrete/mortar has been reported in such studies and this indicates higher flexibility which may be viewed as a positive gain for concrete according to Al-Tayeb *et al.* (2013).

Schimizze *et al.* (1994) reported a reduction of 72% in the static modulus of elasticity on replacement of FA by fine rubber crumbs and coarse chipped rubber.

Zheng *et al.* (2008) reported a decrease in the static modulus of elasticity on replacement of the CA by ground and crushed rubber with an increase in the replacement level from 0% to 45%. More than 29% and 49% decrease in static modulus of elasticity was observed on replacement of 45% CA by ground rubber and crushed rubber respectively.

Mavroulidou and Figueiredo (2010) observed a greater reduction in the static modulus of elasticity on replacement of FA by rubber aggregate as in comparison to the case of replacement of CA by coarse rubber aggregate.

Guenisiyi *et al.* (2004) reported decrease in modulus of elasticity on replacement of FA by crumb rubber and CA by rubber chips for w/c ratios 0.4 and 0.6. They observed about 20% reduction in modulus of elasticity for w/c ratio 0.6 on 50% replacement of total aggregate volume by rubber content. The use of silica fume was found to slightly improve the modulus of elasticity of rubberized concrete even though the improvement was small.

Turatsinze and Garros (2008) reported decrease in static modulus on partial replacement of rounded siliceous gravel (4 mm-10 mm) by rubber aggregate (4 mm-10 mm) for w/c ratio 0.4. The decrease was attributed to the low modulus of elasticity of rubber aggregate. No specific trend was found for the variation.

Ganjian *et al.* (2009) reported decrease in static modulus of elasticity on replacement of CA by chipped rubber and cement by ground rubber for w/c ratio 0.50. The reduction was attributed to the low modulus of elasticity of rubber.

Pelisser *et al.* (2011) reported more than 49% decrease (on an average) in static modulus of elasticity on replacement of 10% sand aggregate by rubber waste (size less than 4.8 mm) for w/c ratios 0.40, 0.45 and 0.60. The lower modulus of elasticity of rubber in comparison to the elastic modulus of sand was cited as the reason for the same.

Atahan *et al.* (2012) reported decreasing trend in static modulus of elasticity up to 100% replacement of FA and CA by crumb rubber for a single w/c ratio (0.52). The decrease in elastic modulus was found to be about 96% on 100% replacement of aggregate by rubber.

Sukontasukkul and Tiamlom (2012) reported decrease in static modulus of elasticity on replacement of FA (0% to 30% by volume) by crumb rubber. The decrease was found to be more for the smaller size of crumb rubber. The flaky shape of large size particles providing a spring like effect was cited as the reason for the same.

Al-Tayeb *et al.* (2013) reported decrease in static modulus of elasticity on partial substitution of sand (up to 20% by volume) for a single w/c ratio (0.48). More than 22% reduction in static modulus of elasticity was reported on 20% replacement of FA by crumb rubber.

Xue and Shinozuka (2013) reported decrease in static modulus of elasticity on replacement of CA with scrapped tire rubber crumb. More than 40% reduction in static modulus of elasticity was reported on 20% replacement. The static modulus of rubberized concrete was found to increase on partial replacement of cement by silica fume; however, the static modulus was still lower than that of normal concrete.

Onuaguluchi and Panesar (2014) reported decrease in static modulus of elasticity on replacement of FA (0% to 15% by volume) by crumb rubber for a single w/c ratio (0.47). More than 29% reduction in static modulus of elasticity was reported on 15% replacement of FA by crumb rubber. The reduction in static modulus of elasticity was attributed to the substitution of stiff FA with very low elastic modulus crumb rubber aggregate. The reduction was found to be controlled on coating of crumb rubber by lime stone powder and addition of silica fume.

1.2.13 Dynamic modulus of elasticity

The rubber aggregate have very low stiffness as compared to natural aggregate, therefore the addition of rubber aggregate lowers the modulus of elasticity of the resulting concrete thereby reducing the dynamic modulus of elasticity.

Benazzouk *et al.* (2003) reported lower dynamic modulus of elasticity of rubberized concrete as compared to control concrete. The increase in mixing water and the low elasticity of modulus of rubber aggregate were deduced as the reasons for the reduction. The reduction was found to be greater in case of soft aggregate with alveolar surfaces than in the case of aggregate with smooth surface.

Skripkiunas *et al.* (2007) observed a reduction of about 1% -2% in the dynamic modulus of elasticity of concrete on 3% replacement of FA by crumb rubber. The lower modulus of rubber as compared to the FA (sand) was discussed as the reason.

Benazzouk *et al.* (2007) reported about 76% decrease in the dynamic modulus of elasticity of cementitious matrix on 50% replacement of FA by rubber. However, the w/c ratios for the control concrete and the corresponding rubberized concrete were not kept the same. The ability of the rubber particles to absorb ultrasonic waves was deduced as the reason for the same.

Zheng *et al.* (2008) reported decrease in dynamic modulus of elasticity on replacement of CA by ground and crushed scrap rubber tire for w/c ratio 0.45. A decrease of 29% and 25% was reported for 45% replacement by ground rubber and crushed rubber respectively. No reason was attributed for the reductions.

Oikonomou and Mavridou (2009) reported decrease in dynamic modulus of cement mortar on replacement of sand (0% to 15%) by tire rubber granules in cement mortars. More than 68% reduction was observed on 15% replacement of FA by tire rubber. Reduction in dynamic modulus of elasticity was attributed to the tendency of the rubber towards the absorption of ultrasonic waves.

Uygunog˘lu and Topcu (2010) reported decrease in dynamic modulus of elasticity of self consolidating mortar on partial replacement of FA (0% to 50%) by scrap tire rubber. More than 68% reduction in dynamic modulus of elasticity was observed on 50% replacement of FA by rubber particles. The increase in the porous structure was attributed as the reason for the same.

Rahman *et al.* (2012) reported decrease in dynamic modulus of elasticity of self compacting concrete on replacement of fines (28%) by rubber particles for a single w/c ratio (0.47). More than 18% reduction in dynamic modulus of elasticity was observed. It was stated that the flexible rubber particles improve the dampening effect.

1.2.14 Energy absorption capacity and Impact resistance

Concrete is a brittle material with high rigidity. High impact resistance and more energy absorption capacity are required in many applications such as shock absorbers, foundation pads of machinery, railway buffers etc. Additional ingredients are required to improve the properties of concrete in some situations where these requirements are not fulfilled. Few

studies have been carried out on the energy absorption capacity and impact resistance of rubber concrete.

Topcu (1995) reported a decrease in elastic energy capacity and increase in plastic energy capacity of the concrete on replacement of CA and FA by coarse rubber chips and fine rubber chips respectively. It was stated that concrete becomes ductile on addition of rubber and starts behaving like elastic material.

Khaloo *et al.* (2008) carried out a study on concrete containing high volume chip rubber as partial replacement of CA and crumb rubber as partial replacement of FA. The toughness was reported to be highest for 25% concentration of both the types of rubber particles as a part of the total aggregate volume.

Sukontasukkul and Chaikaew (2006) carried out flexural tests on concrete pedestrian blocks and reported an increase in toughness of concrete blocks on partial replacement of FA and CA by crumb rubber.

Aiello and Leuzzi (2010) also carried out flexural tests on rubberized concrete and reported a significant increase in the energy absorption for up to 75% replacements of CA/FA by rubber shreds.

Reda Taha *et al.* (2008) reported higher impact resistance on up to 100% replacement of CA by chipped rubber and FA by crumb rubber for a single w/c ratio (0.7). Significant improvement in impact strength was observed for a replacement level of up to 50% and a reduction was observed after that though the impact resistance was still higher than the control mix even at 100% replacement. Increase in impact resistance was attributed to the relatively high flexibility of low stiffness particles at low to medium replacement leading to absorption of a considerable amount of energy.

Ozbay *et al.* (2011) reported increase in impact resistance on replacement of FA (0% to 25%) by crumb rubber for a single w/c ratio (0.4). More than 24% increase in energy absorption capacity was reported on 25% replacement of FA by crumb rubber. Increase in impact resistance was attributed to the absorption capacity of rubber. It was also reported that the low stiffness of the rubber particles allowed the rubber concrete to have a relatively high flexibility.

Atahan *et al.* (2012) reported increase in impact resistance on replacement of FA (0% to 100%) by crumb rubber for a single w/c ratio (0.52). More than 160% increase in energy absorption capacity was observed on 100% replacement of FA by crumb rubber. The increase

in impact resistance was attributed to the less brittleness and much lower elastic modulus of the rubber aggregate in comparison to concrete.

Al-Tayeb *et al.* (2013) observed increase in impact resistance on replacement of FA (0% to 20%) by crumb rubber for a single w/c ratio (0.48). More than 74% increase in impact energy was reported on 20% replacement of FA by crumb rubber. The increase in impact resistance was attributed to the ability of rubber to absorb dynamic energy.

Dong *et al.* (2013) studied the effect of coating of rubber particles by chemicals on the impact resistance of the rubberized concrete. The coating was found to increase the absorbed energy.

1.2.15 Fatigue resistance

The cement-matrix contains voids and microcracks even before any load has been applied. Concrete exposed to repetitive loading leads to increase of stress concentration around these microcracks and may finally lead to failure.

Fatigue life of the concrete is generally influenced by w/c ratio, curing period, age, type of loading (constant or variable amplitude), stress level ratio, frequency and environmental effects (temperature).

Increase in fatigue resistance has been reported by Ganesan *et al.* (2013) on inclusion of shredded rubber as FA (0% to 20%) for a single w/c ratio (0.37). The maximum increase was found for 15% rubber content.

Increase in fatigue resistance has been reported by Liu *et al.* (2013) on inclusion of rubber aggregate as FA (0% to 15%) for a single w/c ratio (0.31). It was reported that fatigue life of the rubberized concrete was more than control mix. Increase in fatigue resistance was attributed to the released energy absorption capacity of rubber, filled in internal space of the concrete, which prevents the spreading of the cracks and aggregate segregation.

1.2.16 Fire behavior

Fire is one of the most potential risks to the buildings and structures (Chan *et al.* 1996; Byström *et al.* 2013). The concrete structures can be affected greatly by the exposure to elevated temperatures. Reduction in compressive strength and static modulus along with loss in mass and increase in permeability due to elevated temperature have been reported by many researchers (Hoff *et al.* 2000; Akcaozoglu 2013; Nadeem *et al.* 2014). These changes have been reported to be affected by cooling methods of concrete subjected to elevated

temperature (Peng *et al.* 2008). The fast cooling method has been found to result in more compressive strength loss as compared to normal cooling due to wider cracks in fast cooling method (Akcaozoglu 2013; Nadeem *et al.* 2014).

Limited studies have been carried out for the effect of elevated temperature on concrete containing replacement of natural aggregate by waste rubber tyre particles (Hernández-Olivares and Barluenga 2004; Nayef *et al.* 2010; Li *et al.* 2011; Marques *et al.* 2013).

Hernandez-Olivares and Barluenga (2004) carried out study, for the effect of elevated temperature (90 minute exposure duration), on concrete containing crumb rubber aggregate as partial replacement of FA (0% to 8%) for a single w/c ratio 0.25. A reduction in explosive spalling, depth of damage and curvature of long prismatic specimens was observed due to addition of rubber fibers. The reduction in explosive spalling was attributed to the escape to water vapor through the channels formed on burning of rubber particles. Small holes were observed in the surface of the rubberized concrete specimens facing elevated temperature. No such holes were observed for control concrete. However, the reduction in compressive strength and stiffness was found to be more in case of rubberized concrete. The reduction was around 10% at 3% replacement of rubber fibers by FA.

Nayef *et al.* (2010) studied the behavior of rubberized concrete, with and without microsilica, at elevated temperature for w/c ratio 0.55. The CA was replaced by fine rubber and coarse rubber. The compressive strength was found to decrease at replacement level of more than 5% for all temperatures. An increase in strength was observed near 150 °C. This was attributed to the evaporation of free water content. It was observed that there was less reduction of compressive strength with increasing temperature in case of concrete containing fine rubber. It was stated that the rubber has more stable microstructures as it is exposed to elevated temperature and this restricts the reduction in compressive strength on exposure to elevated temperature.

A study was carried out by Li *et al.* (2011) for the effect of elevated temperature on high strength concrete reinforced with rubber particles. The study was carried out for w/c ratio of 0.35. It was observed that the loss of strength due to elevated temperature increased with increase in rubber content. The loss in strength was found to be more in case of addition of rubber fibers instead of replacement of FA. It was further reported that rubber particles increased the spalling resistance of concrete. Rubber particles of 1.2 mm size had the best

resistance against spalling whereas the rubber particles of other sizes decreased the resistance against spalling.

Guo *et al.* (2014) studied the behavior of recycled aggregate concrete containing crumb rubber at elevated temperatures. The study was carried out for w/c ratio of 0.35. The CA were replaced by recycled concrete and sand was replaced by crumb rubber. Crumb rubber was found to reduce the cracks in the concrete at elevated temperatures. This was attributed to the reason that rubber melts earlier providing a space for evaporated water in concrete to escape which otherwise would cause cracking due to increase in pore pressure. The rubber content was found to have less effect on the weight loss when subjected to temperature above 200 °C. It was stated that crumb rubber melts at temperature of around 170 °C, therefore the contribution of melting of rubber to the total weight loss is significantly less than the contribution of water evaporation and decomposition of concrete materials. It was also reported that the inclusion of rubber generally reduces the rate of concrete strength loss and the trend was more obvious for the elevated temperature. Again, this was attributed to the reason that rubber melts earlier providing a space for evaporated water in concrete to escape which otherwise would cause cracking and subsequent strength loss due to increase in pore pressure.

Marques *et al.* (2013) carried out studies on the fire behaviour of concrete made with fine and coarse recycled rubber aggregate as partial replacement of FA for w/c ratio of 0.55. The recycled rubber aggregate concrete was found to behave like void on exposure to 800 ^{0}C temperature. The decomposition of the rubber at this temperature was cited as the reason for the same. The loss in residual tensile splitting strength was found to be greater in case of recycled rubber aggregate as compared to normal concrete. It was also found that the thermal response of the concrete was affected on upto 15% replacement of FA by rubber aggregate.

1.3 OBJECTIVES OF THE STUDY

It is evident from the work reported above that although a number of studies have been undertaken on the properties of rubberised concrete; most of the studies are limited to a single w/c ratio and very few studies are available on: (i) use of rubber ash in concrete; (ii) use of rubber fibers in concrete; (iii) combined used of rubber ash and rubber fibers; (iv) waste rubber aggregate with silica fume; (v) ductility properties of waste rubber concrete; and (vi) various properties of waste rubber concrete at elevated temperature (different exposure

duration). Therefore, the present work has been carried out for three w/c ratios with following objectives:

i. To carry out strength, durability and ductility studies for concrete containing rubber ash as partial replacement of fine aggregate.

ii. To carry out strength, durability and ductility studies for concrete containing rubber fiber as partial replacement of fine aggregate.

iii. To carry out strength, durability and ductility studies for hybrid concrete containing both rubber ash and rubber fiber as partial replacement of fine aggregate.

iv. To carry out strength, durability and ductility studies for concrete containing rubber fiber as partial replacement of fine aggregate and silica fume as partial replacement of cement.

v. To carry out strength, durability and ductility studies for rubber fiber concrete subjected to elevated temperatures.

1.4 ORGANIZATION OF THESIS

The thesis has been organized in seven chapters. In each chapter, the tables and figures have presented along with the text. Separate list of figures and tables have been also included after the list of contents. The notations have been defined at the place where they appear for the first time. The contents of various chapters of the thesis are summarized as follows:

In chapter 2, physical and mechanical properties of raw materials used in the preparation of concrete mixes have been presented along with the chemical composition of raw materials. The chemical compositions were evaluated using Energy dispersive X-ray analyser (EDAX). Morphology of cement, sand, rubber ash, rubber fiber and silica fume, obtained with the help of scanning electron microscope (SEM), have also been presented in this chapter. Further, the details of concrete mixes and selection of the water cement ratio along with the replacement levels of rubber ash and rubber fibers have also been presented.

In chapter 3, properties of control and waste rubber concrete in fresh state and hardened state have been presented. The properties include microstructure, workability, compressive strength, flexural strength, density and abrasion resistance.

In chapter 4, the effect of waste rubber and silica fume on the durability properties of waste concrete has been critically examined. The examined durability properties include

water absorption, water permeability, drying shrinkage, carbonation, chloride diffusion, corrosion and acid attack (sulphuric and hydrochloride acid).

In chapter 5, the ductility assessment of waste rubber concrete has been carried out. Modulus of elasticity (static and dynamic), impact resistance and fatigue strength of concrete have been evaluated in this chapter.

In chapter 6, the detailed experimental studies have been carried out for the effect of elevated temperature on the control mix and waste rubber fiber concrete. The properties investigated include microstructure, mass loss, compressive strength, density, ultrasonic pulse velocity, static modulus of elasticity, dynamic modulus of elasticity, water permeability and chloride ion permeability.

In chapter 7, important conclusions of the study have been summarized and the recommendation has been given for future work.

CHAPTER 2

CHARACTERIZATION OF WASTE RUBBER AGGREGATE AND CONCRETE MIXES

2.1 INTRODUCTION

It is important to carry out the physical and chemical characterization of a material to ascertain its use in the concrete. This chapter deals with the basic physical and chemical properties of cement, coarse aggregate (CA), fine aggregate (FA), rubber ash (RA), rubber fibers (RF) and silica fume (SF) and concrete mixes containing these waste rubber particles.

2.2 MATERIALS

2.2.1 Cement

Ordinary Portland cement of specific gravity 3.12 confirming to 43 grade of “Binani” brand was used as per Indian standards (BIS 1989) for the concrete mixes in this study. The cement from single batch was used for preparation of all concrete mixes corresponding to a series. The physical and mechanical properties of the cement are shown in Table 2.1.

2.2.2 Fine aggregate

Locally available natural river sand (Kharka river) confirming to Zone II as per Indian standards (BIS 1970) was used as fine aggregate. The grain size analysis and physical properties of fine aggregate are given in Fig. 2.1 and Table 2.1 respectively.

2.2.3 Coarse aggregate

Crushed natural aggregate with nominal size of 20 mm and 10 mm, confirming to BIS 383 (1970) was used as coarse aggregate (CA). Equal proportions of 20 mm and 10 mm were used to prepare concrete mixes.

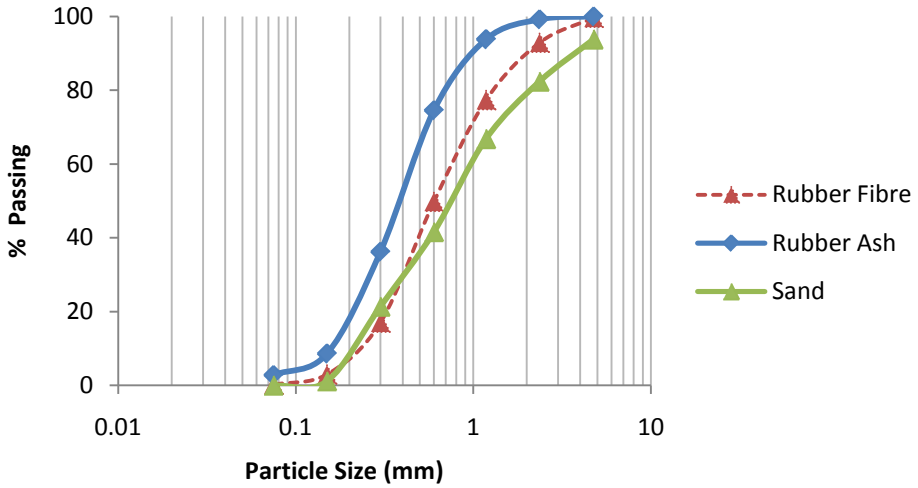

Fig. 2.1 Particle size distribution of the rubber fiber, rubber ash and fine aggregate

Table 2.1 Physical and mechanical properties of cement, aggregate, rubber ash and rubber fibers

Analysis	**Results**
Setting time of OPC cement	
Initial	115 minutes
Final	248 minutes
Compressive strength of OPC cement	
3 days	24.3 MPa
7 days	34.8 MPa
28 days	45.2 MPa
Water Absorption	
Coarse aggregate	0.5%
Fine aggregate	0.5%
Rubber fibers	0.4%
Rubber ash	0.3%
Specific gravity	
Cement	3.12
Coarse aggregate	2.59
Fine aggregate	2.56
Rubber fibers	1.07
Rubber ash	1.33
Size	
Coarse aggregate	Less than 12 mm
Fine aggregate	Less than 4.75 mm
Rubber fibers	2-5 mm & 20 mm long
Rubber ash	0.15 mm to 1.9 mm

2.2.4 Waste rubber aggregate

2.2.4.1 Rubber ash

Rubber ash particles of size ranging between 0.15 mm and 1.9 mm are obtained by pyrolysis technique (incinerating waste rubber tyres at controlled temperature of 850 ^{0}C for 72 h). The grain size analysis of rubber ash confirms to Zone II, as per BIS 383 (1970). Fig. 2.2(a) shows a photograph of rubber ash used in this study. The physical properties of the rubber ash particles are presented in Table 2.1.

2.2.4.2 Rubber fibers

These rubber fibers were 2 mm to 5 mm in width and up to 20 mm in length (aspect ratio 4 to 10) with a specific gravity of 1.07. The particle size distribution of the rubber fibers has been shown in Fig. 2.1. These rubber fibers were obtained from mechanical grinding of waste rubber tyres. The grain size analysis of rubber fibers confirms to Zone II, as per BIS 383 (1970). Fig. 2.2(b) shows a photograph of rubber fibers used in this study. The physical properties of the rubber fibers particles are presented in Table 2.1. The elastic modulus of rubber fiber was 1.72 MPa and the tensile strength was 22.8 MPa. The tests for the elastic modulus and tensile strength were conducted at the Central Institute of Plastic Engineering and Technology, Jaipur.

Fig. 2.2 (a) Rubber ash (b) Rubber fibers

2.2.5 Silica fume

Silica fume is a by-product of silicon metal production in electric furnace. It is used to improve the properties of concrete. It is usually categorized as a supplementary cementitious product. The silica fume used in the study was of “Elkem” brand.

2.2.6 Super plasticizer

Modified polycarboxylic ether based, ASTM type F super plasticizer procured from BASF was used to cast concrete specimens.

2.3 MIXTURE DETAILS

Five series of concrete with waste rubber tyre particles were cast for three water cement (w/c) ratio of 0.35, 0.45 and 0.55. In the series-I, up to 20% fine aggregate (FA) was partially replaced by rubber ash (RA) with increments of 5% (Table 2.2).

In series-II, upto 25% fine aggregate was replaced by rubber fiber with increments of 5% (Table 2.3). In series-III, 10% of fine aggregate was replaced by rubber ash and upto 25% fine aggregate was replaced by rubber fiber with increments of 5% (Table 2.4). In series IV, upto 25% fine aggregate was replaced by rubber fiber with increments of 5% and 5% of cement was replaced by silica fume and (Table 2.5). In series V, upto 25% fine aggregate was replaced by rubber fiber in increments of 5% and 10% of cement was replaced by silica fume (Table 2.6).

To maintain the workability (compaction factor of more than 0.9) and uniformity of the mixes, the amount of super-plasticizer (SP) was varied as shown in Tables 2.2-2.6.

Table 2.2 Concrete mix proportions with rubber ash (Series-I)

Mix No.	FA replacement (%)	w/c ratio	Cement (Kg)	FA (Kg)	Coarse aggregate (Kg)		RA (Kg)	SF (Kg)	SP (%)
					10mm	20mm			
T1	0	0.35	364	764	562.2	562.2	0.0	0	2.1
T2	5	0.35	364	726	562.2	562.2	19.7	0	2.2
T3	10	0.35	364	688	562.2	562.2	39.5	0	2.4
T4	15	0.35	364	650	562.2	562.2	59.2	0	2.6
T5	20	0.35	364	611	562.2	562.2	79.0	0	2.6
T6	0	0.45	364	764	562.2	562.2	0.0	0	0.5
T7	5	0.45	364	726	562.2	562.2	19.7	0	0.7
T8	10	0.45	364	688	562.2	562.2	39.5	0	1.0
T9	15	0.45	364	650	562.2	562.2	59.2	0	1.2
T10	20	0.45	364	611	562.2	562.2	79.0	0	1.6
T11	0	0.55	364	764	562.2	562.2	0.0	0	0.0
T12	5	0.55	364	726	562.2	562.2	19.7	0	0.0
T13	10	0.55	364	688	562.2	562.2	39.5	0	0.2
T14	15	0.55	364	650	562.2	562.2	59.2	0	0.5
T15	20	0.55	364	611	562.2	562.2	79.0	0	0.9

Table 2.3 Concrete mix proportions of rubber fiber concrete (Series-II)

Mix No.	FA replacement (%)	w/c ratio	Cement (Kg)	FA (Kg)	Coarse aggregate (Kg)		RF (Kg)	SF (Kg)	SP (%)
					10 mm	20 mm			
R1	0	0.35	364	764	562.2	562.2	0.0	0	2.1
R2	5	0.35	364	726	562.2	562.2	15.9	0	2.0
R3	10	0.35	364	688	562.2	562.2	31.6	0	2.0
R4	15	0.35	364	650	562.2	562.2	47.5	0	2.1
R5	20	0.35	364	611	562.2	562.2	63.5	0	2.2
R6	25	0.35	364	573	562.2	562.2	80.1	0	2.4
R7	0	0.45	364	764	562.2	562.2	0.0	0	0.5
R8	5	0.45	364	726	562.2	562.2	15.9	0	0.6
R9	10	0.45	364	688	562.2	562.2	31.6	0	0.6
R10	15	0.45	364	650	562.2	562.2	47.5	0	0.6
R11	20	0.45	364	611	562.2	562.2	63.5	0	0.6
R12	25	0.45	364	573	562.2	562.2	80.1	0	0.6
R13	0	0.55	364	764	562.2	562.2	0.0	0	0.0
R14	5	0.55	364	726	562.2	562.2	15.9	0	0.0
R15	10	0.55	364	688	562.2	562.2	31.6	0	0.0
R16	15	0.55	364	650	562.2	562.2	47.5	0	0.0
R17	20	0.55	364	611	562.2	562.2	63.5	0	0.0
R18	25	0.55	364	573	562.2	562.2	80.1	0	0.0

Table 2.4 Concrete mix proportions with combination of rubber ash and rubber fiber concrete (Series-III)

Mix No.	FA replacement (%)	w/c ratio	Cement (Kg)	FA (Kg)	Coarse aggregate (Kg)		RA (Kg)	RF (kg)	SF (Kg)	SP (%)
					10 mm	20 mm				
S1	10	0.35	364	688	562.2	562.2	39.5	0.0	0	2.0
S2	15	0.35	364	650	562.2	562.2	39.5	15.9	0	2.0
S3	20	0.35	364	611	562.2	562.2	39.5	31.6	0	2.0
S4	25	0.35	364	573	562.2	562.2	39.5	47.5	0	2.0
S5	30	0.35	364	535	562.2	562.2	39.5	63.5	0	2.0
S6	35	0.35	364	497	562.2	562.2	39.5	80.1	0	2.0
S7	10	0.45	364	688	562.2	562.2	39.5	0.0	0	0.8
S8	15	0.45	364	650	562.2	562.2	39.5	15.9	0	0.8
S9	20	0.45	364	611	562.2	562.2	39.5	31.6	0	0.8
S10	25	0.45	364	573	562.2	562.2	39.5	47.5	0	0.8
S11	30	0.45	364	535	562.2	562.2	39.5	63.5	0	0.9
S12	35	0.45	364	497	562.2	562.2	39.5	80.1	0	0.9
S13	10	0.55	364	688	562.2	562.2	39.5	0.0	0	0.0
S14	15	0.55	364	650	562.2	562.2	39.5	15.9	0	0.0
S15	20	0.55	364	611	562.2	562.2	39.5	31.6	0	0.0
S16	25	0.55	364	573	562.2	562.2	39.5	47.5	0	0.0
S17	30	0.55	364	535	562.2	562.2	39.5	63.5	0	0.0
S18	35	0.55	364	497	562.2	562.2	39.5	80.1	0	0.0

Table 2.5 Concrete mix proportions of rubber fiber concrete with 5% silica fume (Series-IV)

Mix No.	FA replacement (%)	w/c ratio	Cement (Kg)	FA (Kg)	Coarse aggregate (Kg)		RF (Kg)	SF (Kg)	SP (%)
					10 mm	20 mm			
U1	0	0.35	345.8	764	562.2	562.2	0	18.2	2.2
U2	5	0.35	345.8	726	562.2	562.2	15.9	18.2	2.2
U3	10	0.35	345.8	688	562.2	562.2	31.6	18.2	2.2
U4	15	0.35	345.8	650	562.2	562.2	47.5	18.2	2.2
U5	20	0.35	345.8	611	562.2	562.2	63.5	18.2	2.2
U6	25	0.35	345.8	573	562.2	562.2	80.1	18.2	2.4
U7	0	0.45	345.8	764	562.2	562.2	0	18.2	0.6
U8	5	0.45	345.8	726	562.2	562.2	15.9	18.2	0.6
U9	10	0.45	345.8	688	562.2	562.2	31.6	18.2	0.6
U10	15	0.45	345.8	650	562.2	562.2	47.5	18.2	0.6
U11	20	0.45	345.8	611	562.2	562.2	63.5	18.2	0.7
U12	25	0.45	345.8	573	562.2	562.2	80.1	18.2	0.7
U13	0	0.55	345.8	764	562.2	562.2	0	18.2	0.0
U14	5	0.55	345.8	726	562.2	562.2	15.9	18.2	0.0
U15	10	0.55	345.8	688	562.2	562.2	31.6	18.2	0.0
U16	15	0.55	345.8	650	562.2	562.2	47.5	18.2	0.0
U17	20	0.55	345.8	611	562.2	562.2	63.5	18.2	0.2
U18	25	0.55	345.8	573	562.2	562.2	80.1	18.2	0.2

Table 2.6 Concrete mix proportions of rubber fiber concrete with 10% silica fume (Series-V)

Mix No.	FA replacement (%)	w/c ratio	Cement (Kg)	FA (Kg)	Coarse aggregate (Kg)		RF (Kg)	SF (Kg)	SP (%)
					10 mm	20 mm			
V1	0	0.35	327.6	764	562.2	562.2	0	36.4	2.2
V2	5	0.35	327.6	726	562.2	562.2	15.9	36.4	2.2
V3	10	0.35	327.6	688	562.2	562.2	31.6	36.4	2.2
V4	15	0.35	327.6	650	562.2	562.2	47.5	36.4	2.2
V5	20	0.35	327.6	611	562.2	562.2	63.5	36.4	2.3
V6	25	0.35	327.6	573	562.2	562.2	80.1	36.4	2.4
V7	0	0.45	327.6	764	562.2	562.2	0	36.4	0.7
V8	5	0.45	327.6	726	562.2	562.2	15.9	36.4	0.7
V9	10	0.45	327.6	688	562.2	562.2	31.6	36.4	0.7
V10	15	0.45	327.6	650	562.2	562.2	47.5	36.4	0.7
V11	20	0.45	327.6	611	562.2	562.2	63.5	36.4	0.7
V12	25	0.45	327.6	573	562.2	562.2	80.1	36.4	0.8
V13	0	0.55	327.6	764	562.2	562.2	0	36.4	0.2
V14	5	0.55	327.6	726	562.2	562.2	15.9	36.4	0.2
V15	10	0.55	327.6	688	562.2	562.2	31.6	36.4	0.2
V16	15	0.55	327.6	650	562.2	562.2	47.5	36.4	0.2
V17	20	0.55	327.6	611	562.2	562.2	63.5	36.4	0.3
V18	25	0.55	327.6	573	562.2	562.2	80.1	36.4	0.3

2.4 PREPARATION OF TEST SPECIMENS

Eighty one concrete mixes were prepared using varied water cement (w/c) ratio and ratio of rubber ash/rubber fibers, with and without silica fume. The mixes were first dry-mixed for 2-3 minutes in the mixer (Fig. 2.3). When concrete mix showed desired workability for uniform rubber fiber distribution, it was placed in a mould and vibrated on table vibrator. The specimen were covered with plastic sheets and stored at room temperature for 24 hours prior to de-moulding and then concrete specimen was cured in water for 28 days, unless specified otherwise.

Fig. 2.3 Pan type mixer

2.5 EXPERIMENTAL PROCEDURE

Rubber fibers and rubber ash are a waste product of used rubber tyres, therefore detailed microstructural characteristics and chemical composition are necessary to ensure compatibility of this material with the concrete. Energy dispersive X-ray analyser (EDAX) was used, together with scanning electron microscopy (SEM) to evaluate the microstructural characteristics and chemical composition of cement, fine aggregate, rubber ash, rubber fiber and silica fume.

2.6 RESULT AND DISCUSSION

2.6.1 Cement

Fig. 2.4 and Table 2.7 show the results of EDAX analysis of cement particles. Higher peaks in Fig. 2.4 indicate a greater content of an element. A high level of calcium (Ca) is observed in Fig. 2.4 and Table 2.7 which is responsible for adhesive properties of a material.

The morphology (SEM) of cement particles at different magnifications are shown in Figs. 2.5-2.7. The SEM images show an irregular shape of the cement particles compared with silica fume particles which are regular and have smooth surfaces.

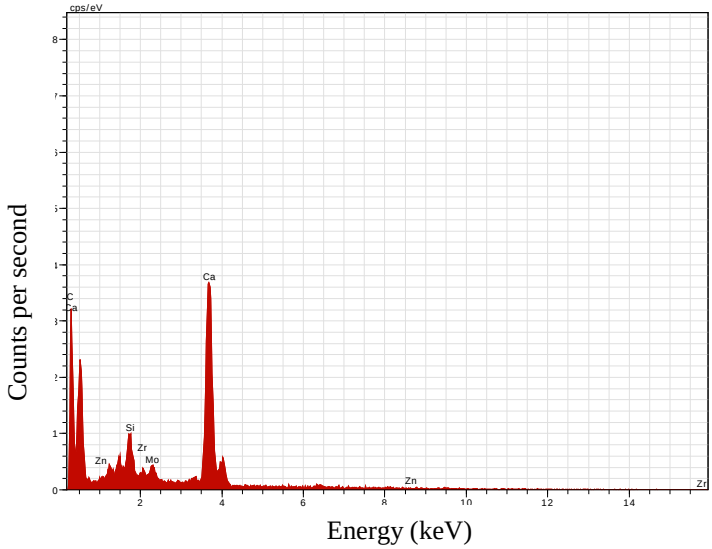

Fig. 2.4 EDAX analysis for chemical composition of cement

Table 2.7 Chemical composition of cement

Element	CaO	SiO_2	Al_2O_3	Fe_2O_3	SO_3	MgO	K_2O	LOI
Percentage (%)	62.34	20.14	4.65	3.29	2.42	2.23	0.72	1.96

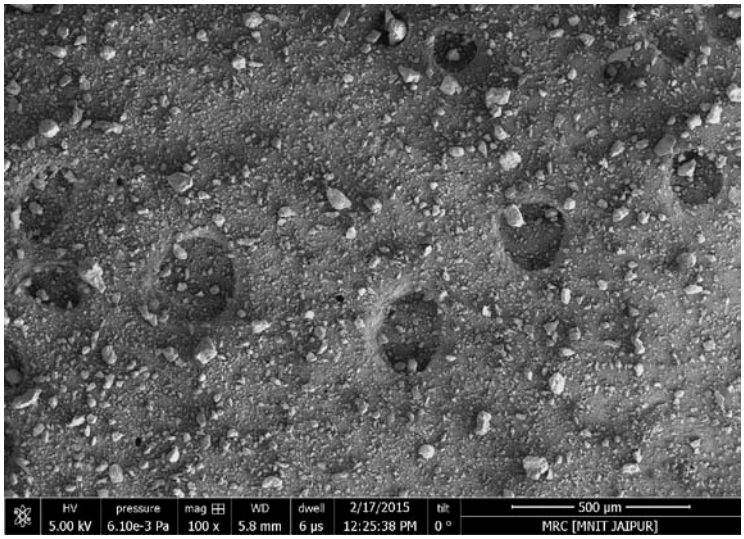

Fig. 2.5 SEM image of cement particles at 100x magnification

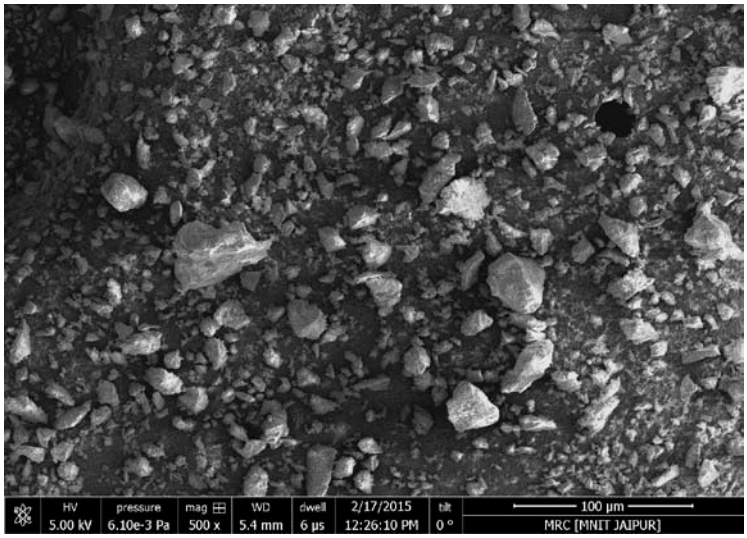

Fig. 2.6 SEM image of cement particles at 500x magnification

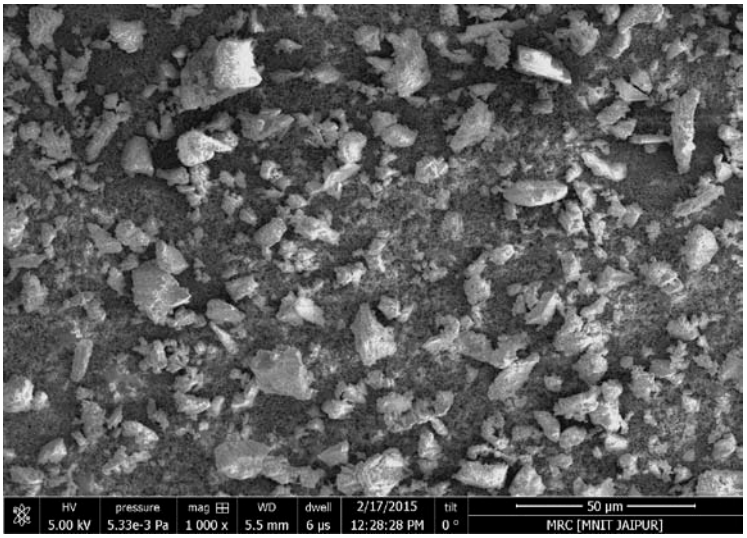

Fig. 2.7 SEM image of cement particles at 1000x magnification

2.6.2 Fine aggregate

Fig. 2.8 and Table 2.8 show the EDAX analysis of fine aggregate. A high level of oxygen (O) in the sample is observed in Fig. 2.8 and Table 2.8. The morphology (SEM) of fine aggregate particles at different magnifications is shown in Fig. 2.9-2.11. The SEM images show a smooth shape of the fine aggregate particles compared with rubber ash particles which are irregular and have rough surfaces.

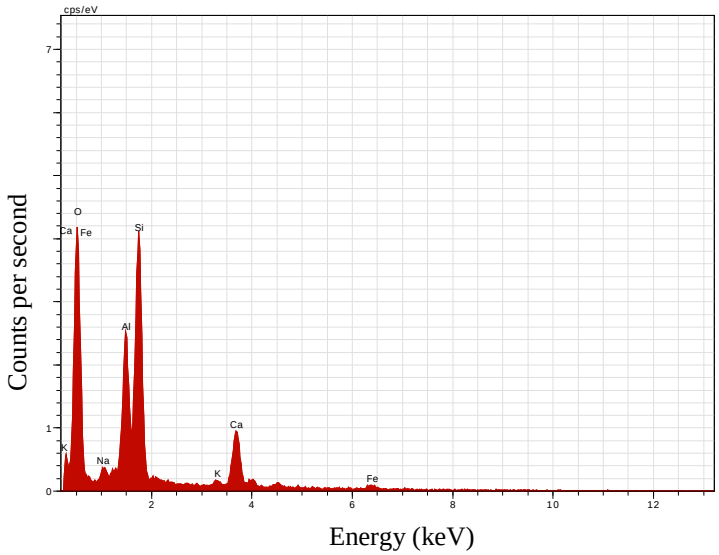

Fig. 2.8 EDAX analysis for chemical composition of fine aggregate

Table 2.8 Chemical composition of fine aggregate

Element	Oxygen (O)	Silicon (Si)	Calcium (Ca)	Aluminium (Al)	Iron (Fe)	Sodium (Na)	Potassium (K)
Percentage (%)	57.13	18.15	10.20	10.16	2.03	1.47	0.86

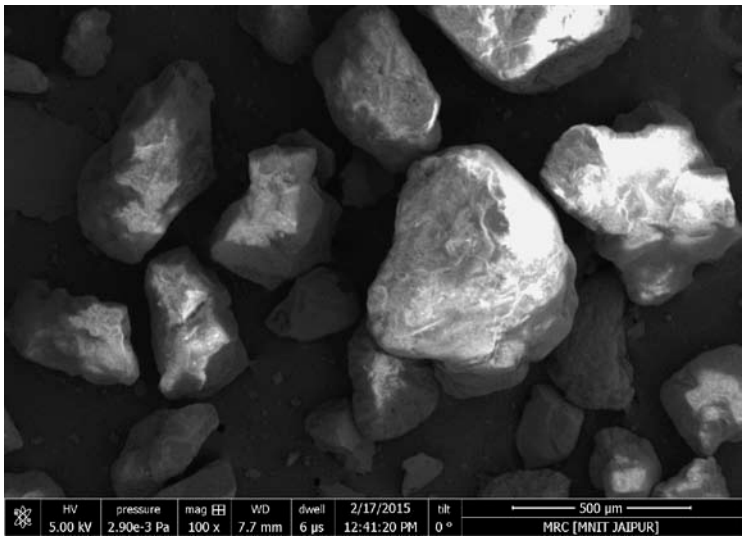

Fig. 2.9 SEM image of fine aggregate at 100x magnification

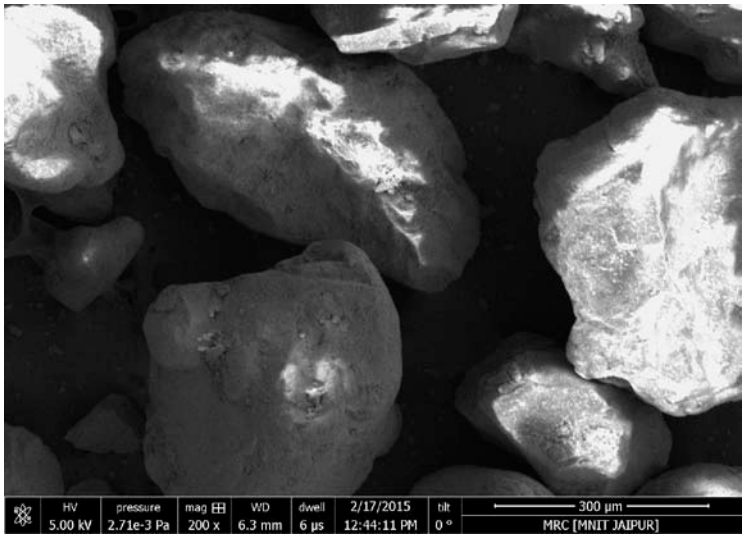

Fig. 2.10 SEM image of fine aggregate at 200x magnification

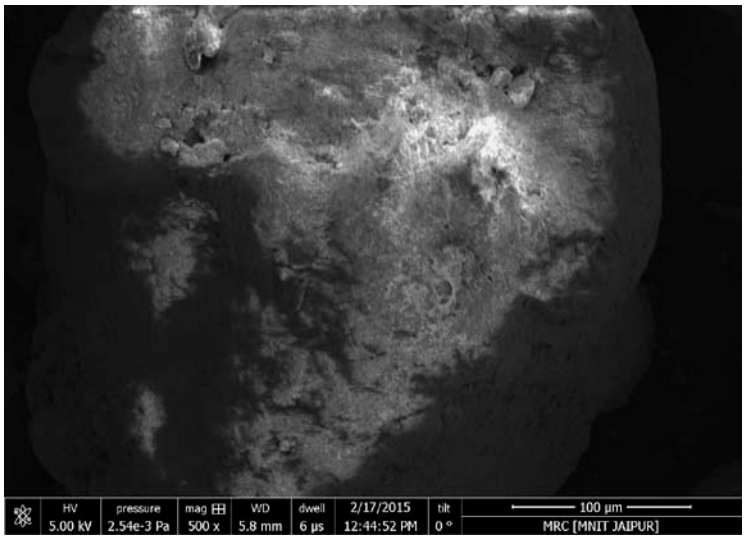

Fig. 2.11 SEM image of fine aggregate at 500x magnification

2.6.3 Rubber ash

Fig. 2.12 and Table 2.9 show the EDAX analysis for determining the chemical composition of rubber ash particles. A high level of carbon (C) is observed in Fig. 2.12 and Table 2.9. It may be noted that carbon is a soft material hence strength of waste rubber concrete is expected to be less as compared to the control mix.

The morphology (SEM) of rubber ash particles at different magnifications are shown in Figs. 2.13-2.15. The SEM images show an irregular shape of the rubber ash particles whereas fine aggregate have regular and smooth surfaces. The irregular shape may be helpful in entrapping the air during the batching process of freeze/thaw action (Richardson *et al.* 2011).

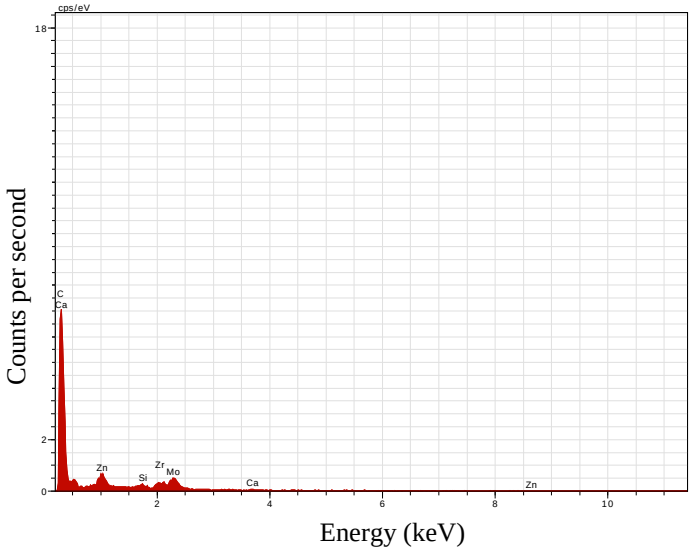

Fig. 2.12 EDAX analysis for chemical composition of rubber ash

Table 2.9 Chemical composition of rubber ash

Element	Carbon (C)	Molybdenum (Mo)	Zinc (Zn)	Zirconium (Zr)	Silicon (Si)	Calcium (Ca)
Percentage (%)	65.26	14.56	11.13	6.91	1.54	0.60

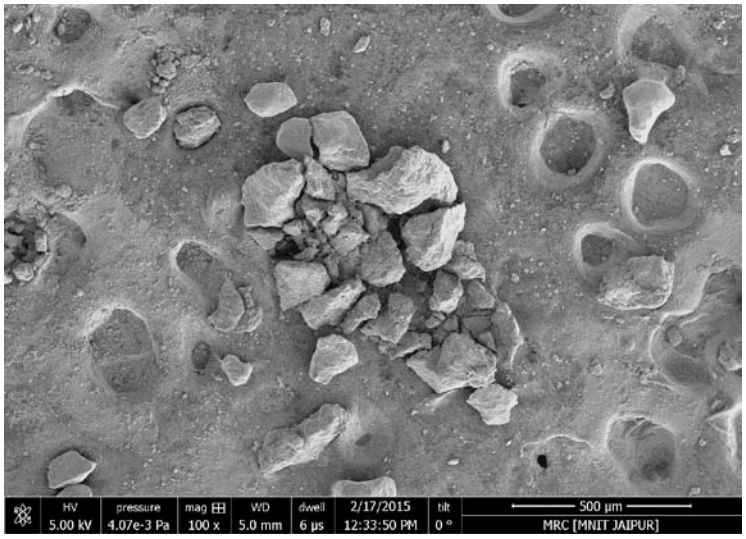

Fig. 2.13 SEM image of rubber ash at 100x magnification

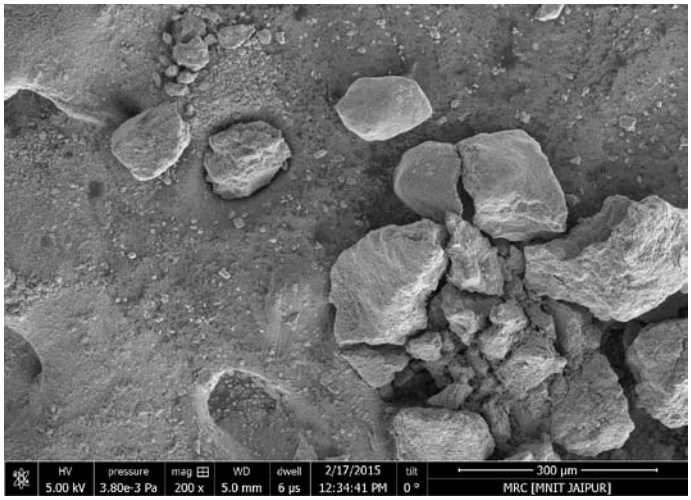

Fig. 2.14 SEM image of rubber ash at 200x magnification

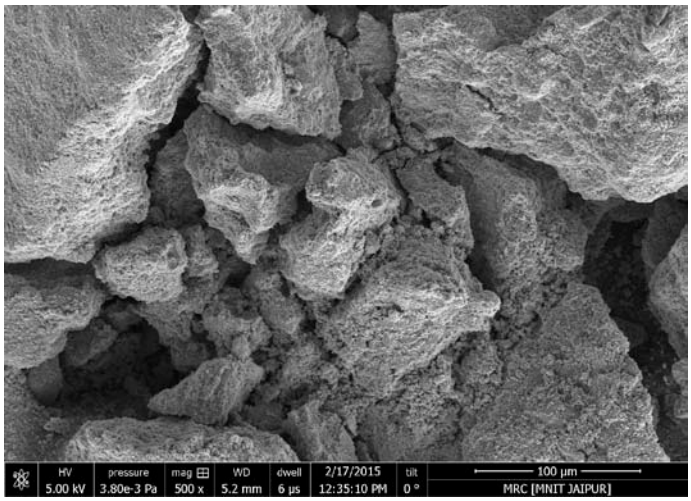

Fig. 2.15 SEM image of rubber ash at 500x magnification

2.6.4 Rubber fiber

Fig. 2.16 and Table 2.10 show the EDAX analysis of rubber fiber particles. A high level of Carbon (C) is observed in Fig. 2.16 and Table 2.10. As stated earlier, since Carbon is a soft material hence strength of waste rubber concrete is expected to be less as compared to control mix.

The shape of the rubber fiber particles can strongly influence the properties of fresh concrete and hardened concrete. The morphology (SEM) of rubber fiber particles at different magnifications are shown in Figs. 2.17-2.19. The SEM images show an irregular shape of the rubber fibers compared with fine aggregate which are regular and have smooth surfaces. The irregular shape may be helpful in entrapping the air during the batching process of freeze/thaw action (Richardson *et al.* 2011). Cavities are also observed in the Figs. which are also responsible for reduction in strength. Micro cracks within the rubber fibers were also

visible (Figs. 2.17-2.19) and these cracks indicate weak interfacial bonding between the rubber fiber and cement paste which affects the strength of rubber fiber concrete.

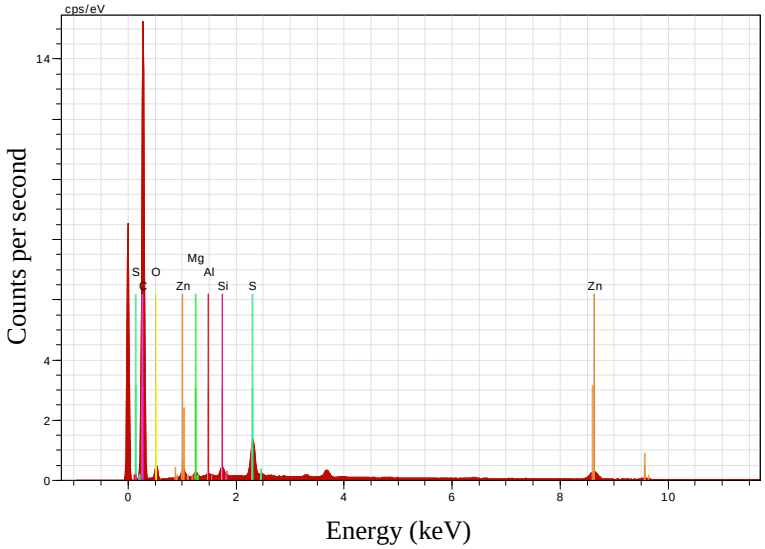

Fig. 2.16 EDAX analysis for chemical composition of rubber fiber sample

Table 2.10 Chemical composition of rubber fibers

Element	Carbon (C)	Oxygen (O)	Zinc (Zn)	Sulfur (S)	Silicon (Si)	Magnesium (Mg)	Aluminium (Al)
Percentage	87.51	9.23	1.76	1.08	0.20	0.14	0.08

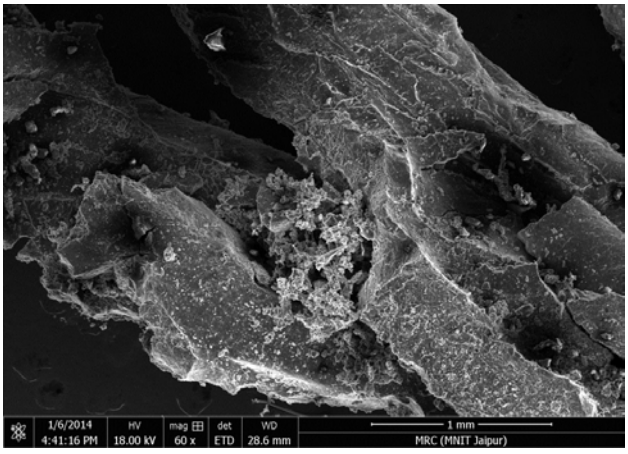

Fig. 2.17 SEM image of rubber fiber at 60x magnification

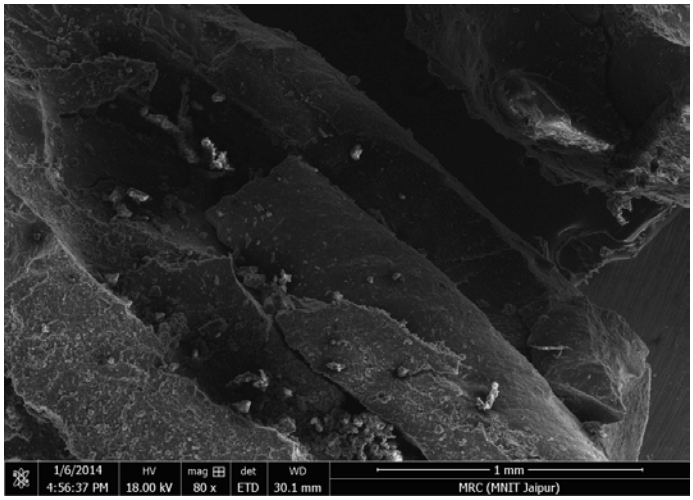

Fig. 2.18 SEM image of rubber fiber at 80x magnification

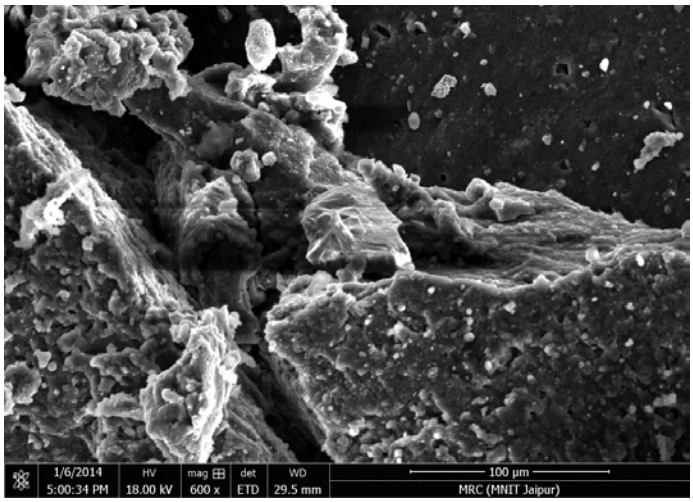

Fig. 2.19 SEM image of rubber fiber at 600x magnification

2.6.5 Silica fume

Fig. 2.20 and Table 2.11 show the EDAX analysis of silica fume particles. A high level of silica (Si), which is a very effective pozzolanic material, is observed in Fig. 2.20 and Table 2.11.

The morphology (SEM) of silica fume particles at different magnifications are shown in Figs. 2.21-2.23. The SEM images show regular shape of the silica fume particles compared with cement particles which are irregular and have rough surfaces.

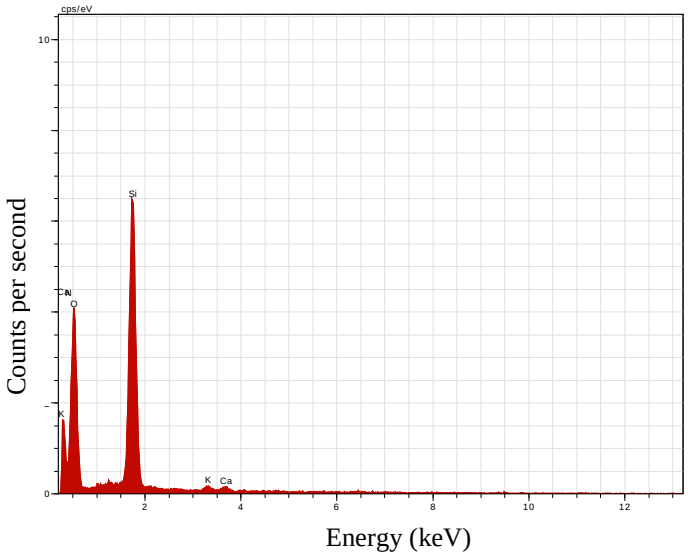

Fig. 2.20 EDAX analysis for chemical composition of silica fume

Table 2.11 Chemical composition of silica fume

Element	CaO	SiO_2	Al_2O_3	Fe_2O_3	SO_3	MgO	K_2O	LOI
Percentage	0.87	90.12	0.94	1.62	0.29	-	1.21	2.87

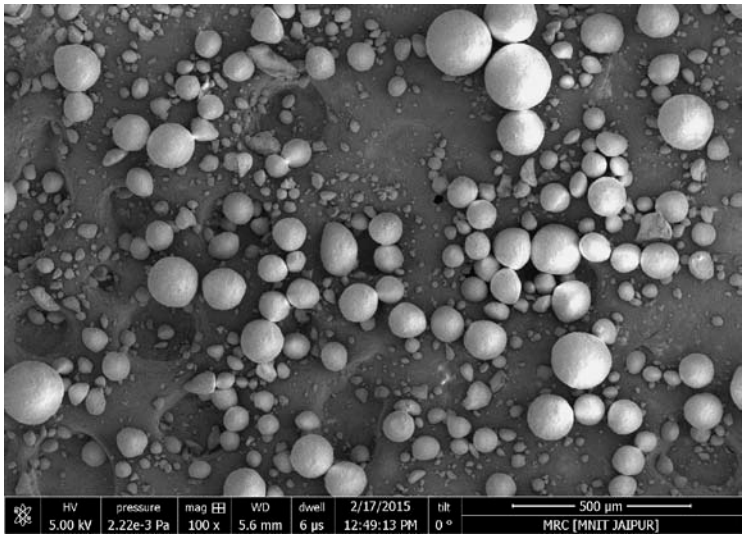

Fig. 2.21 SEM image of silica fume at 100x magnification

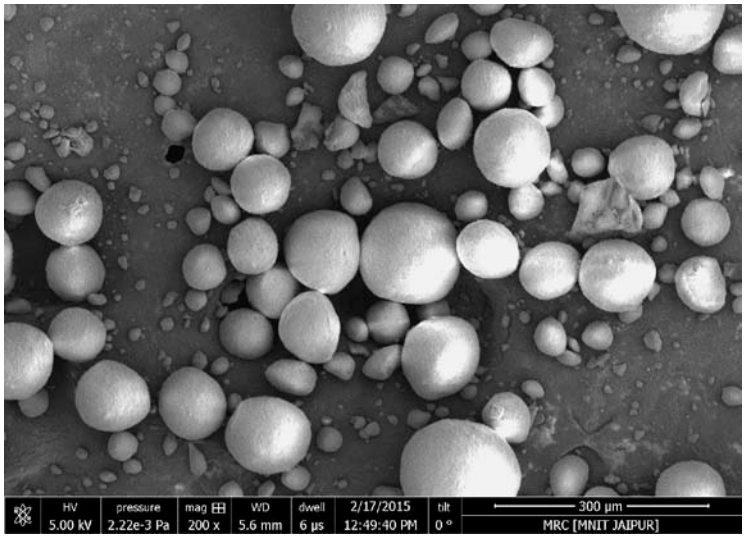

Fig. 2.22 SEM image of silica fume at 200x magnification

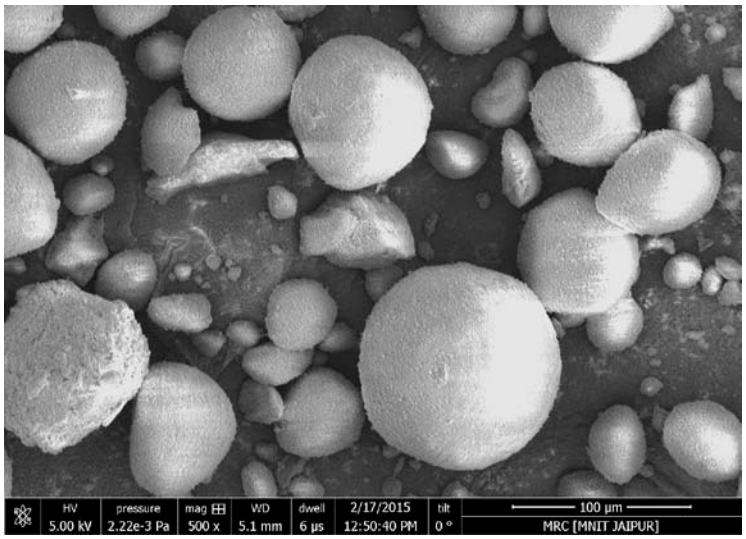

Fig. 2.23 SEM image of silica fume at 500x magnification

2.7 CONCLUSIONS

The material properties of cement, fine aggregate, rubber ash, rubber fibers and silica fume were evaluated by carrying out the experiments for specific gravity, grain size analysis, water absorption chemical composition and microstructure. Following important conclusions are drawn:

1. The specific gravity of rubber ash and rubber fiber is less than that of fine aggregate which can be helpful in production of low density concrete.
2. The rubber fiber has good tensile strength which leads to increased flexural strength of concrete.

3. Rubber ash and rubber fiber have high carbon content which leads to production of softer concrete.
4. Particle sizes of rubber ash and rubber fiber conform to the requirements of Indian Standards for fine aggregate.
5. The waste rubber ash and rubber fiber have irregular shapes as compared to fine aggregate; however rubber fibers have more irregular shape as compared to rubber ash.
6. Cavities and micro cracks are also observed in rubber ash and rubber fiber, which may reduce strength of concrete.
7. Silica fume particles have smoother surface and spherical shapes in comparison of cement particles.

CHAPTER 3

PROPERTIES OF RUBBERIZED CONCRETE IN FRESH AND HARDENED STATE

3.1 INTRODUCTION

In this chapter, the effect of partial replacement of fine aggregate (FA), by rubber ash (RA) and rubber fiber (RF), on workability of fresh concrete and mechanical properties of hardened concrete has been studied. The effect of partial replacement of cement by silica fume (SF) has also been studied for both the control concrete and rubberized concrete.

To evaluate the workability of rubberized concrete, the compaction factor and slump of fresh concrete have been examined. The mechanical properties have been evaluated in terms of compressive strength, flexural strength and abrasion resistance.

3.2 PROPERTIES IN FRESH STATE

3.2.1 Experimental procedure

In the present study, the workability of fresh concrete was examined through compaction factor test and slump cone test as per BIS 1199 (1959). A suitable percentage of admixture was used in the concrete mixes with varied w/c ratios (0.35, 0.45 and 0.55), rubber ash (0% to 20%), rubber fiber (0% to 25%) and silica fume (0% to 10%) contents to maintain same workability (compaction factor of 0.9 or more).

3.2.2 Results and discussion

The measured compaction factors and slump values together with the percentage of the admixture used for each mix are shown in Table 3.1. It can be observed from the Tables that workability is significantly affected and requirement of superplasticiser increased due to partial replacement of fine aggregate by rubber ash. It is also observed that the workability is not significantly affected and requirement of superplasticiser marginally changes on partial replacement of fine aggregate by rubber fiber.

Table-3.1 Workability of waste rubber concrete mixes

Mix No.	CF	Slump (mm)	Mix No.	CF	Slump (mm)	Mix No.	CF	Slump (mm)	Mix No.	CF	Slump (mm)	Mix No.	CF	Slump (mm)
T1	0.90	72	R1	0.90	72	S1	0.91	71	U1	0.90	71	V1	0.90	70
T2	0.90	72	R2	0.91	74	S2	0.91	71	U2	0.91	75	V2	0.91	74
T3	0.90	71	R3	0.91	74	S3	0.91	70	U3	0.91	75	V3	0.91	74
T4	0.90	70	R4	0.91	73	S4	0.91	72	U4	0.91	75	V4	0.91	74
T5	0.87	58	R5	0.91	74	S5	0.91	70	U5	0.91	74	V5	0.91	75
T6	0.92	76	R6	0.91	72	S6	0.91	69	U6	0.91	72	V6	0.91	75
T7	0.92	75	R7	0.92	76	S7	0.92	75	U7	0.92	75	V7	0.92	79
T8	0.92	75	R8	0.92	75	S8	0.92	75	U8	0.92	75	V8	0.92	78
T9	0.92	74	R9	0.92	77	S9	0.92	73	U9	0.92	78	V9	0.92	78
T10	0.91	72	R10	0.92	76	S10	0.92	73	U10	0.92	78	V10	0.92	77
T11	0.92	79	R11	0.92	75	S11	0.92	72	U11	0.92	78	V11	0.92	75
T12	0.92	80	R12	0.92	75	S12	0.92	71	U12	0.92	77	V12	0.92	75
T13	0.92	78	R13	0.92	79	S13	0.92	78	U13	0.92	80	V13	0.92	82
T14	0.92	78	R14	0.92	79	S14	0.92	77	U14	0.92	79	V14	0.92	82
T15	0.91	76	R15	0.92	78	S15	0.92	74	U15	0.92	79	V15	0.92	81
-	-	-	R16	0.92	79	S16	0.92	74	U16	0.92	78	V16	0.92	82
-	-	-	R17	0.92	77	S17	0.92	73	U17	0.92	80	V17	0.92	82
-	-	-	R18	0.92	78	S18	0.92	72	U18	0.92	80	V18	0.92	80

3.3 PROPERTIES IN HARDENED STATE

3.3.1 Experimental procedure

3.3.1.1 Density

Density of hardened concrete was measured as per BIS 516 (1959), by dividing the total weight of hardened concrete (150 mm cube) with the total volume of hardened concrete cube, expressed in kg/m^3.

3.3.1.2 Compressive and flexural strength

Compressive strength test of hardened concrete was performed on 100 mm × 100 mm × 100 mm concrete cubes at 28 days, 90 days and 365 days water cured specimen as per BIS 516 (1959). A 2000 kN capacity compression testing machine was used for this purpose (Fig. 3.1). The compressive strength test of concrete cubes exposed to natural environment (28 days water curing followed by exposure to natural environment till total age of 365 days) was also performed to simulate the actual field conditions.

Fig. 3.1 Compression testing machine

Flexural strength was determined for three specimens of each mix. The flexural strength test was performed on 100 mm × 100 mm × 500 mm concrete beams with four point loading configuration on the universal testing machine of 200 kN capacity at 7 days and 28 days as shown in Fig. 3.2.

Fig. 3.2 Flexural testing machine

3.3.1.3 Abrasion resistance

Abrasion resistance of 100 mm × 100 mm × 100 mm sized cubes was determined on 28 days cured specimens (BIS 1980). Initial weight of specimens, w_1 was measured before testing and weight, w_2 was measured after testing. Twenty gram of abrasive powder was used on abrasion testing machine for each specimen (Fig. 3.3). The speed of the disc was kept as 30 rev/min. After every twenty two revolutions, the specimen was turned about the vertical axis through an angle of 90^0 in the clockwise direction with a fresh abrasive powder of twenty

gram and it was repeated nine times thereby giving total two hundred and twenty numbers of revolutions.

The abrasion resistance was calculated in term of depth of wear using following relation:

$$t = \frac{(w_1 - w_2)V_1}{w_1 A} \tag{3.1}$$

where, t = depth of wear, V_1 = initial volume of the specimen in mm^3, and A = surface area of the specimen in mm^2.

Fig. 3.3 Abrasion testing machine

3.3.1.4 Micro-structural analysis

The microstructure of the specimen was analyzed using a scanning electron microscope (SEM) of "ZEISS" make at EHT 20 kV. Testing was performed on 10 mm × 10 mm pieces cut from concrete samples. A gold coating was applied to the surface before carrying out the analysis.

3.3.2 Result and discussion

3.3.2.1 Density

The density of the waste rubber concrete for w/c ratios 0.35, 0.45 and 0.55 at 28 days is shown in Figs. 3.4-3.6. It is seen from the Figs. that the density decreased with the increase in the replacement level of waste rubber contents for all three w/c ratios. The density of concrete without rubber fiber and silica fume decreased by 9.5%, 6.3% and 2.8% for w/c ratios 0.35, 0.45 and 0.55 respectively on 20% replacement of FA by rubber ash. Whereas, the observed decrease, on 25% replacement of FA by rubber fiber was 5.6%, 6.6%

and 4.8%, respectively. Similarly, the decrease, on replacement of FA by combine mix of 10% rubber ash and 25% rubber fiber, was 8.5%, 8.4% and 5.5% respectively. Waste rubber has a low unit weight (Yung *et al.* 2012), therefore rubberized concrete is expected to have a low density.

It may be noted that, earlier also, upto 27% reduction in density was reported by Batayneh *et al.* (2008) on replacement of 100% of the FA by crumb rubber. The low density of rubber fiber concrete may be due to low density of rubber as compared to conventional aggregate (Batayneh *et al.* 2008; Reda Taha *et al.* 2008). It may be noted that the specific gravity of rubber fibers (1.07) is much lower as compared to specific gravity of FA (2.56). Another reason for low density of rubber concrete may be the presence of entrapped air on the rough surface of fibers (Batayneh *et al.* 2008). It may be noted that SEM images reported in chapter 2 confirm the presence of large cavities on rubber fibers.

It is also observed from Figs. 3.4-3.6 that on replacement of cement by silica fume, the density increased for the control concrete as well as for the rubber fiber concrete. The density of concrete without rubber fiber increased by 1.2%, 1.4% and 1.7% for w/c ratios 0.35, 045 and 0.55 respectively, on 10% replacement of cement by SF. The density of rubber fiber concrete (25% rubber fiber) increased by 1.3%, 2.8% and 1.7% for w/c ratios 0.35, 0.45 and 0.55 respectively on 10% replacement of cement by SF.

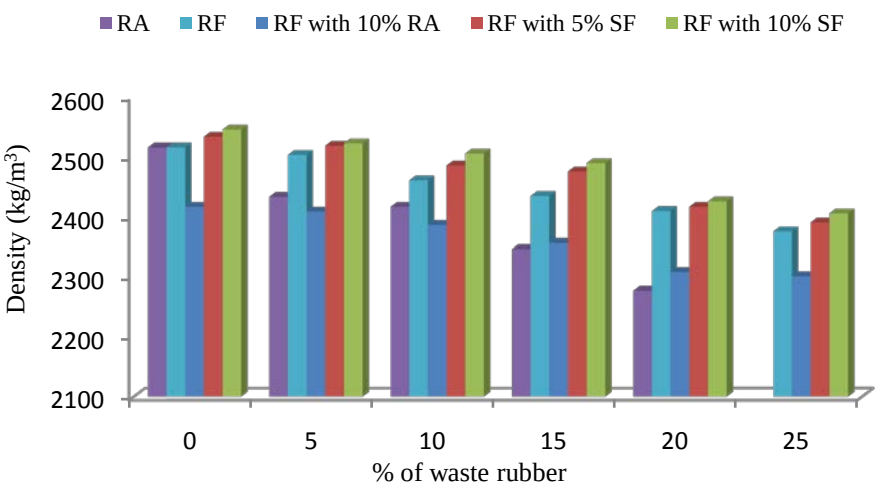

Fig. 3.4 Density of waste rubber concrete for 0.35 w/c ratio

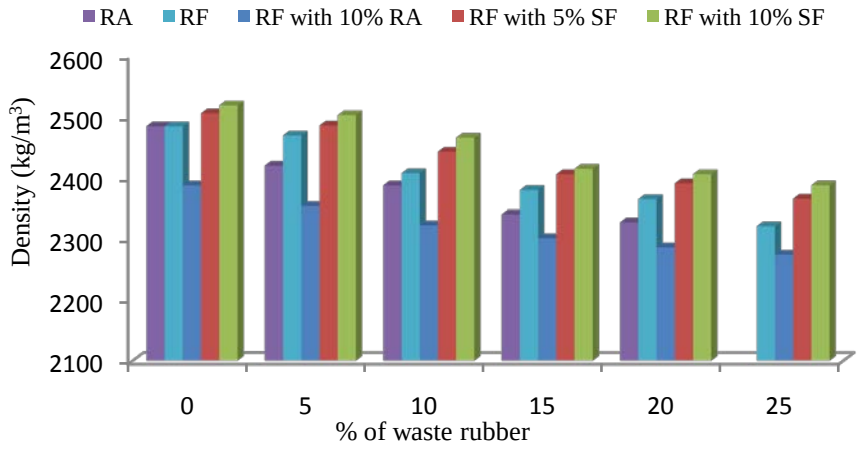

Fig. 3.5 Density of waste rubber concrete for 0.45 w/c ratio

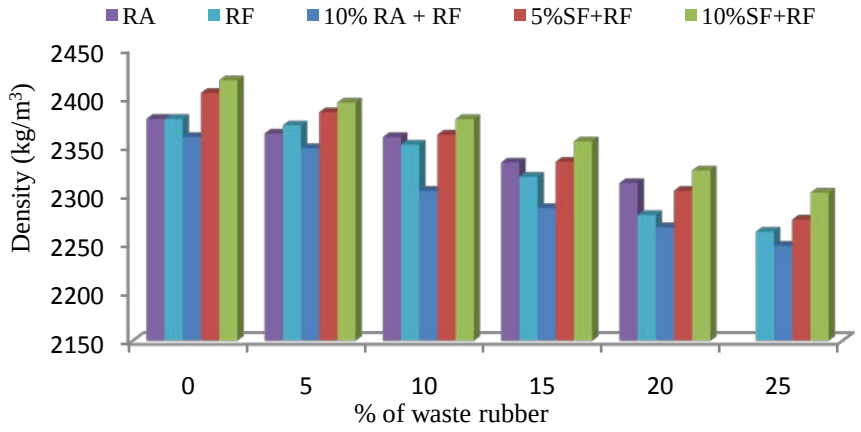

Fig. 3.6 Density of waste rubber concrete for 0.55 w/c ratio

3.3.2.2 Compressive strength

The compressive strength of the waste rubber concrete for w/c ratios 0.35, 0.45 and 0.55 at 28 days is shown in Figs. 3.7-3.9 respectively. The statistical variances of results are shown in Table 3.2.

It is observed that the compressive strength of concrete decreased with the increase in percentage of rubber ash for the w/c ratios of 0.35 and 0.45 whereas for w/c ratio 0.55, compressive strength increased marginally. Compressive strength of concrete (without rubber fiber and silica fume) decreased from 58.9 N/mm^2 and 50.4 N/mm^2 to 42.0 N/mm^2 and 45.1 N/mm^2 for w/c ratios 0.35 and 0.45 respectively and increased from 33.7 N/mm^2 to 35.6 N/mm^2 for w/c ratio 0.55 on 20% replacement of FA by rubber ash. At w/c ratio 0.55, rubber particles produce efficient packing due to higher workability of this mix which leads to higher strength. Similar behavior was also observed by Al-Akhras and Smadi (2004) in their experimental study.

It is seen from the Figs. that the compressive strength decreased with the increase in the replacement level of rubber fibers for all three w/c ratios. The strength of concrete (without rubber ash and silica fume) decreased from 58.9 N/mm^2, 50.4 N/mm^2 and 33.7 N/mm^2 to 28.4 N/mm^2, 23.6 N/mm^2 and 15.3 N/mm^2 for w/c ratios 0.35, 0.45 and 0.55 respectively on 25% replacement of FA by rubber fiber.

Similarly, it is observed from the Figs. that the compressive strength decreased with the increase in the replacement level of rubber fibers for hybrid concrete for all three w/c ratios. The strength of concrete decreased from 58.9 N/mm^2, 50.4 N/mm^2 and 33.7 N/mm^2 to 31.2 N/mm^2, 28.4 N/mm^2 and 21.2 N/mm^2 for w/c ratios 0.35, 0.45 and 0.55 respectively on replacement of FA by 10% rubber ash and 25% rubber fiber.

Reduction in compressive strength in the present study may be due to (i) replacement of hard, dense aggregate by a less dense rubber aggregate (Batayneh *et al.* 2008; Ganjian *et al.* 2009; Zheng *et al.* 2008; Grinys *et al.* 2012; Turki *et al.* 2012; Xue and Shinozuka 2013; Su *et al.* 2015); (ii) lesser stiffness of the substitute material as compared to the surrounding cement paste (Reda Taha *et al.* 2008; Khaloo *et al.* 2008; Grinys *et al.* 2012; Su *et al.* 2015); (iii) voids around the rubber particles as packing of lightweight rubber particles become difficult at high content (Ganjian *et al.* 2009; Ozbay *et al.* 2011; Onuaguluchi and Panesar 2014); (iv) higher air content in concrete specimen (Khaloo *et al.* 2008); (v) weak bond between rubber particles and the cement paste (Reda Taha *et al.* 2008; Batayneh *et al.* 2008;

Zheng *et al.* 2008; Ozbay *et al.* 2011; Xue and Shinozuka 2013; Onuaguluchi and Panesar 2014); and (vi) stress concentrations in the paste at the boundaries of the rubber aggregate (Zheng *et al.* 2008; Ozbay *et al.* 2011).

It is also observed from the Figs. that on replacement of cement by SF, the compressive strength increased for control concrete as well as rubber fiber concrete. Statistical variances of results for compressive strength are shown in Table 3.2. Compressive strength of concrete (without rubber ash and rubber fiber) increased from 58.9 N/mm^2, 50.4 N/mm^2 and 33.7 N/mm^2 to 75.2 N/mm^2, 62.7 N/mm^2 and 39.7 N/mm^2 for w/c ratios 0.35, 0.45 and 0.55 respectively on 10% replacement of cement by SF. Compressive strength of rubber fiber concrete (25% rubber fiber) increased from 28.4 N/mm^2, 23.6 N/mm^2 and 15.3 N/mm^2 to 37.9 N/mm^2, 29.9 N/mm^2 and 19.1 N/mm^2 for w/c ratios 0.35, 0.45 and 0.55 respectively on 10% replacement of cement by SF.

It may be noted that, earlier also, reduction in compressive strength on replacement of coarse aggregate by rubber crumb was found on addition of SF in rubber concrete (Xue and Shinozuka 2013). Sohrabi and Karbalaie (2011) also reported that the addition of SF was found to increase the compressive strength. Less reduction in compressive strength with SF in the present study may be due to filling of voids by nano particles and better bonding between rubber aggregate and cement paste (Xue and Shinozuka 2013; Sohrabi and Karbalaie 2011)

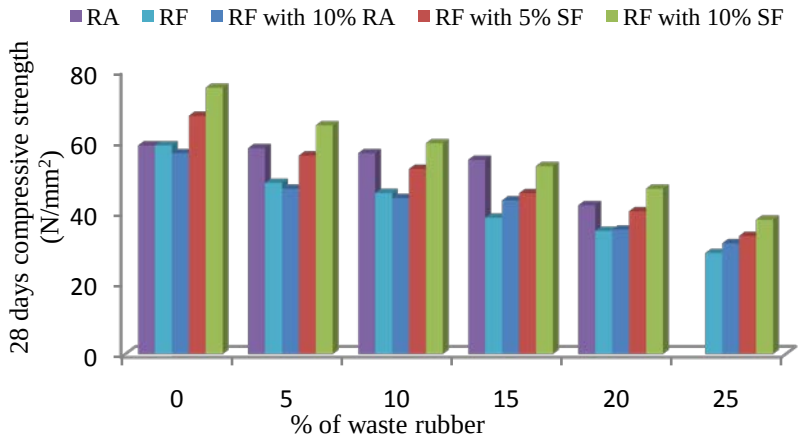

Fig. 3.7 28 days compressive strength of waste rubber concrete for 0.35 w/c ratio

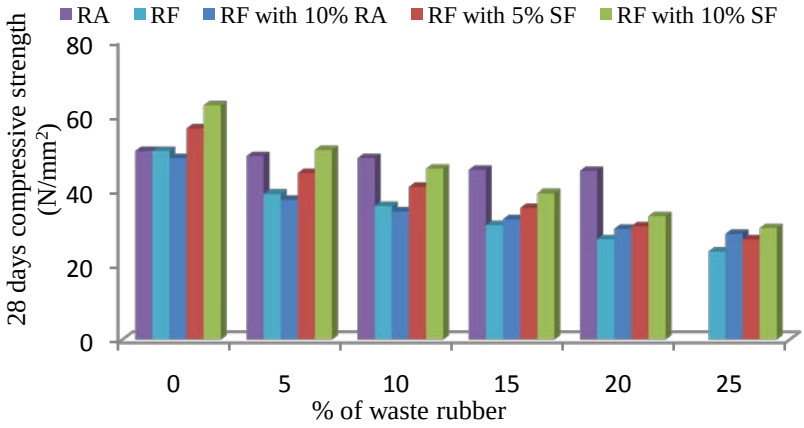

Fig. 3.8 28 days compressive strength of waste rubber concrete for 0.45 w/c ratio

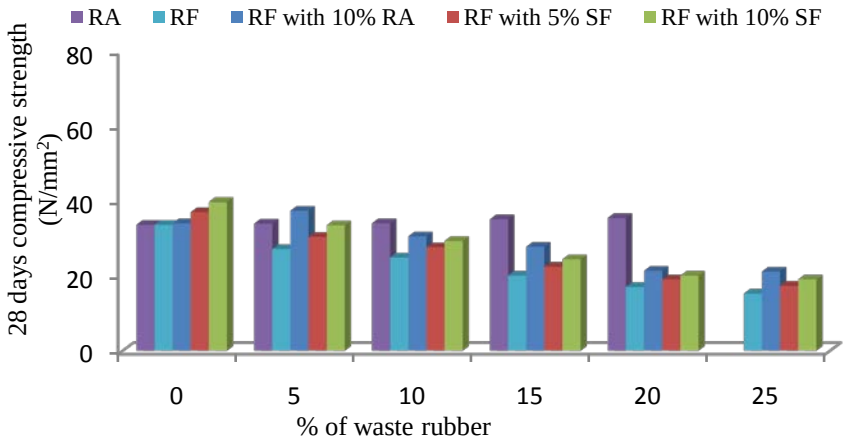

Fig. 3.9 28 days compressive strength of waste rubber concrete for 0.55 w/c ratio

Table 3.2 Statistical variances of compressive strength test results for waste rubber concrete

Mix No.	SD	COV	Mix No.	SD	COV	Mix No.	SD	COV	Mix No.	SD	COV	Mix No.	SD	COV
T1	1.13	0.02	R1	1.13	0.02	S1	4.90	0.08	U1	0.56	0.01	V1	0.67	0.01
T2	6.43	0.10	R2	1.05	0.02	S2	3.11	0.06	U2	0.21	0.01	V2	1.00	0.02
T3	1.66	0.03	R3	1.00	0.02	S3	1.01	0.02	U3	0.50	0.01	V3	1.01	0.02
T4	3.29	0.06	R4	1.05	0.02	S4	3.00	0.07	U4	1.01	0.02	V4	1.00	0.02
T5	2.65	0.06	R5	1.00	0.03	S5	1.01	0.03	U5	0.66	0.02	V5	0.52	0.01
T6	0.56	0.02	R6	0.56	0.02	S6	2.31	0.08	U6	0.55	0.02	V6	0.59	0.02
T7	3.66	0.07	R7	1.01	0.02	S7	1.36	0.03	U7	0.54	0.01	V7	1.52	0.02
T8	2.66	0.05	R8	0.50	0.01	S8	0.50	0.01	U8	1.11	0.02	V8	1.05	0.02
T9	1.58	0.03	R9	1.61	0.04	S9	1.97	0.06	U9	0.52	0.01	V9	1.54	0.03
T10	2.48	0.06	R10	0.25	0.01	S10	2.25	0.06	U10	0.79	0.02	V10	1.52	0.04
T11	1.01	0.03	R11	1.01	0.03	S11	1.57	0.05	U11	1.01	0.03	V11	0.82	0.02
T12	1.79	0.05	R12	0.53	0.02	S12	1.58	0.05	U12	0.51	0.02	V12	0.71	0.02
T13	2.87	0.08	R13	0.51	0.02	S13	1.20	0.03	U13	0.51	0.01	V13	0.61	0.01
T14	3.46	0.09	R14	0.50	0.01	S14	0.50	0.01	U14	0.50	0.02	V14	0.75	0.02
T15	2.71	0.07	R15	0.07	0.01	S15	0.64	0.02	U15	0.52	0.02	V15	1.05	0.03
-	-	-	R16	1.00	0.04	S16	1.04	0.04	U16	0.54	0.02	V16	0.63	0.02
-	-	-	R17	0.12	0.01	S17	1.04	0.05	U17	0.51	0.03	V17	0.57	0.03
-	-	-	R18	0.50	0.02	S18	0.72	0.04	U18	0.79	0.04	V18	0.57	0.03

Unit of SD (standard deviation) is N/mm^2.

The 90 days compressive strength of rubber ash concrete for various w/c ratios is shown in Figs. 3.10-3.12. The strength for w/c ratios 0.35 and 0.45 at 90 days was found to reduce as observed in the case of 28 days strength of rubber ash concrete. However, minor increase in compressive strength was observed for w/c ratio 0.55 as in the case of 28 days strength.

Compressive strength of rubber fiber concrete and hybrid concrete (10% rubber ash and varied percentage of rubber fibers) has also been shown in Figs. 3.10-3.12. Systematic reduction in compressive strength is observed with the increase of percentage of rubber fibers as was observed in the case of 28 days strength. It is also observed from the Figs. that on replacement of cement by SF, the compressive strength increased for control concrete as well as rubber fiber concrete.

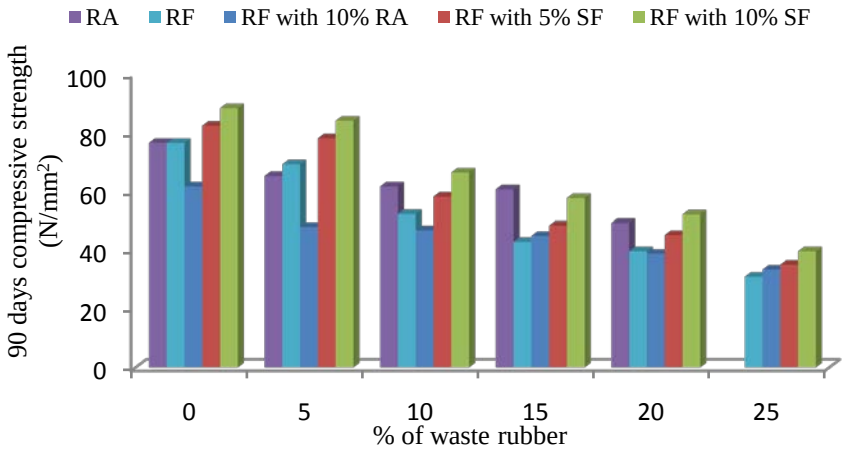

Fig. 3.10 90 days compressive strength of waste rubber concrete for 0.35 w/c ratio

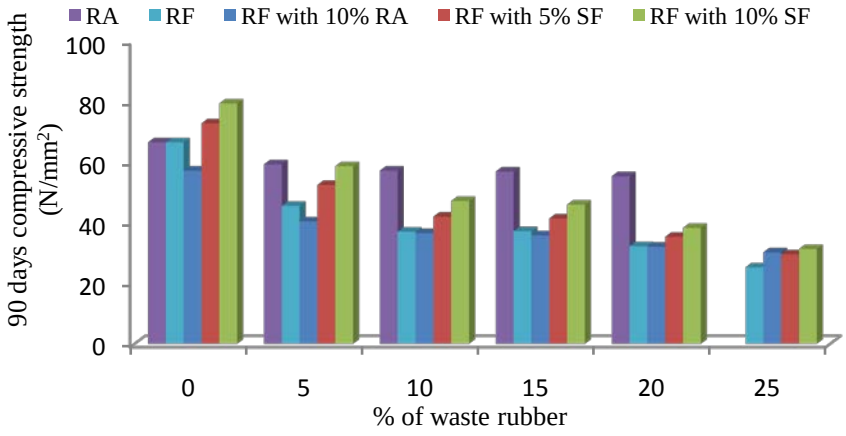

Fig. 3.11 90 days compressive strength of waste rubber concrete for 0.45 w/c ratio

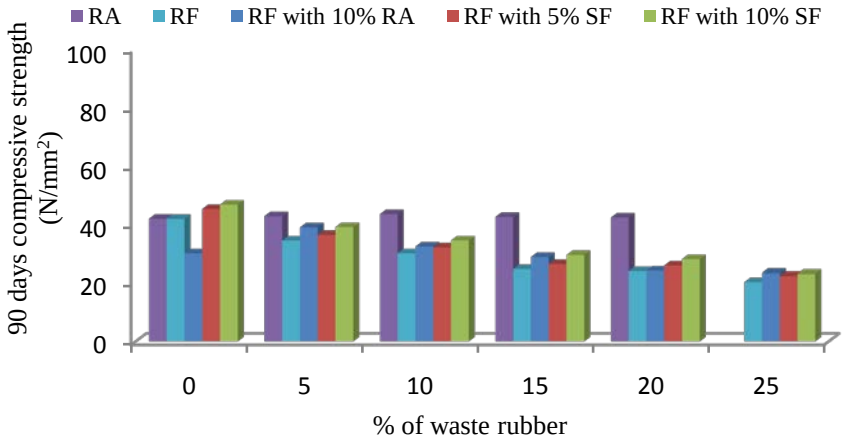

Fig. 3.12 90 days compressive strength of waste rubber concrete for 0.55 w/c ratio

The compressive strength of the waste rubber concrete for w/c ratios 0.35, 0.45 and 0.55 at 365 days is shown in Figs. 3.13-3.15. It may be noted that the specimen are water cured for 365 days in this case. It can be seen from the Figs. that the strength decreased with an increase in the rubber content as observed in the case of 28 days and 90 days strength. The strength of the concrete (without rubber ash, rubber fiber and silica fume) increased by 42.6%, 43.6% and 46.0% for w/c ratios 0.35, 0.45 and 0.55 respectively on 365 days as compared to 28 days, whereas the observed increase for rubber ash concrete (20% replacement of FA by rubber ash) was 35.0%, 26.6% and 21.5% respectively.

The compressive strength of rubber fiber concrete (25% replacement of FA by rubber fiber) increased by 35.8%, 47.0% and 74.5% for w/c ratios 0.35, 0.45 and 0.55 respectively on 365 days as compared to 28 days, whereas the observed increase for hybrid concrete (replacement of FA by mix of 10% rubber ash and 25% rubber fiber) was 15.7%, 14.6% and 17.5% respectively.

It is also observed from the Figs. that on replacement of cement by SF, the compressive strength increased for control concrete as well as for the waste rubber concrete on 365 days as compared to 28 days strength. The strength of rubber fiber concrete (25% replacement of FA by rubber fiber) with 10% SF increased by 18.2%, 45.2% and 68.1% for w/c ratios 0.35, 0.45 and 0.55 respectively on 365 days as compared to 28 days.

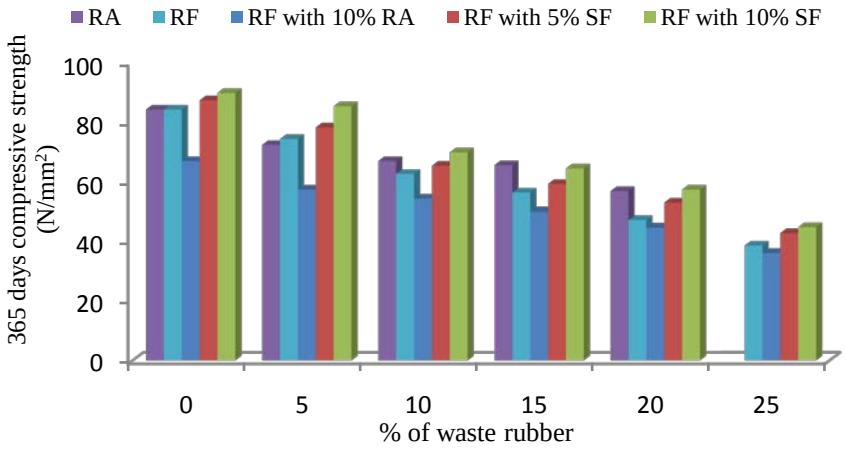

Fig. 3.13 365 days compressive strength of waste rubber concrete for 0.35 w/c ratio

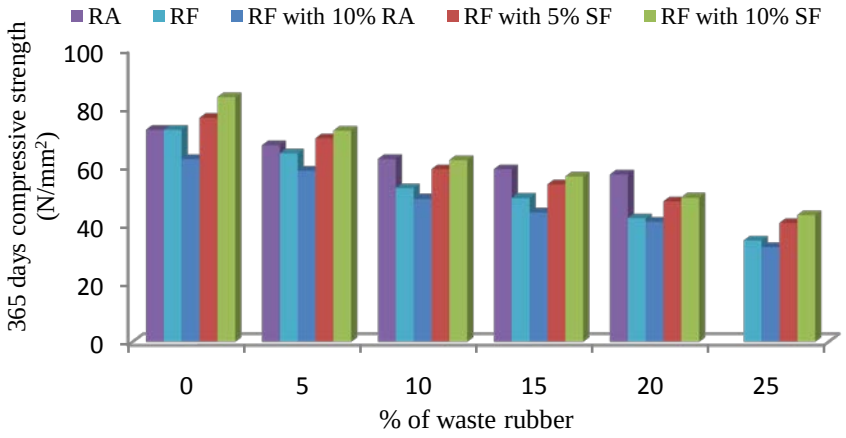

Fig. 3.14 365 days compressive strength of waste rubber concrete for 0.45 w/c ratio

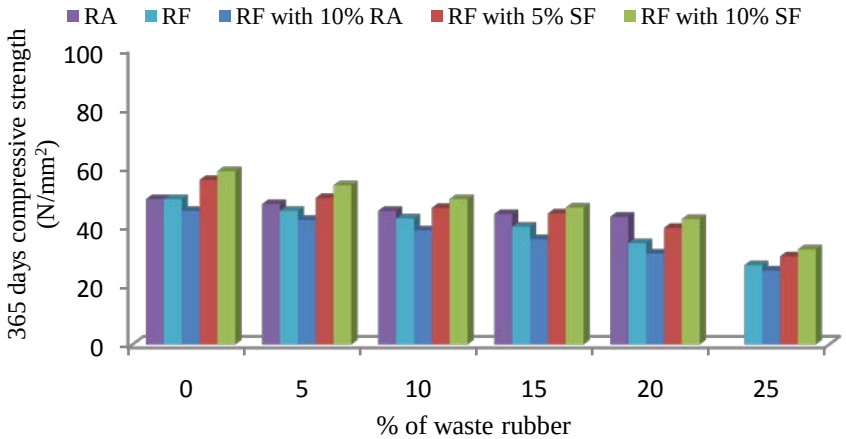

Fig. 3.15 365 days compressive strength of waste rubber concrete for 0.55 w/c ratio

The compressive strength of the waste rubber concrete, subjected to natural exposure (28 days water curing followed by exposure to natural environment till total age of 365 days), for w/c ratios 0.35, 0.45 and 0.55 is shown in Figs. 3.16-3.18. It can be seen from the Figs. that the compressive strength in case of exposure to natural environment is less than the case of water curing (Figs. 3.13-3.15) for control concrete as well as for waste rubber concrete.

The compressive strength of the control concrete (without rubber ash, rubber fiber and silica fume) decreased by 5.6%, 9.1% and 9.9% for w/c ratios 0.35, 0.45 and 0.55 respectively on adopting natural exposure as compared to water curing, whereas the decrease observed for rubber ash concrete (20% replacement of FA by rubber ash) was 11.6%, 15.6% and 16.4% respectively.

The compressive strength of rubber fiber concrete (25% replacement of FA by rubber fiber) decreased by 7.8%, 12.4% and 8.8% for w/c ratios 0.35, 0.45 and 0.55 respectively on adopting natural exposure as compared to water curing, whereas, the decrease observed for hybrid concrete (replacement of FA by 10% rubber ash and 25% rubber fiber) was 18.8%, 12.6% and 10.0% respectively.

It is also observed from the Figs. that, the compressive strength decreased for control concrete with SF as well as for the waste rubber concrete with SF on adopting natural exposure as compared to water curing. The compressive strength of rubber fiber concrete (25% replacement of FA by rubber fiber) with 10% SF decreased by 12.1%, 3.0% and 12.3% for w/c ratios 0.35, 0.45 and 0.55 respectively on adopting natural exposure as compared to water curing

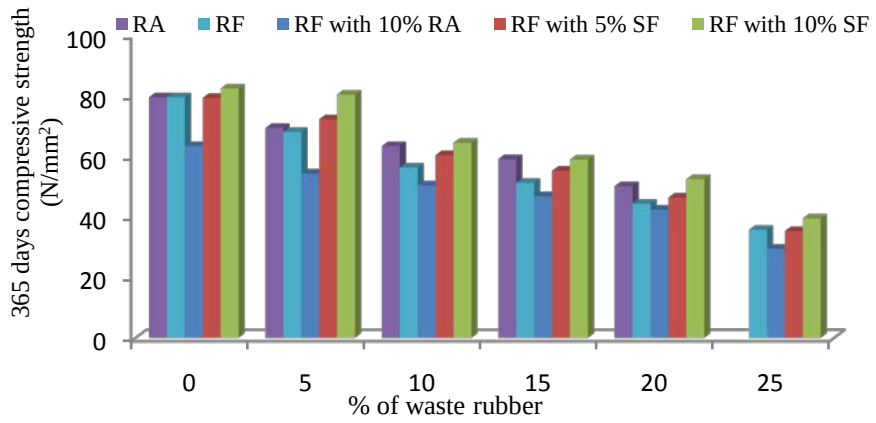

Fig. 3.16 365 days compressive strength (natural exposure) of waste rubber concrete for 0.35 w/c ratio

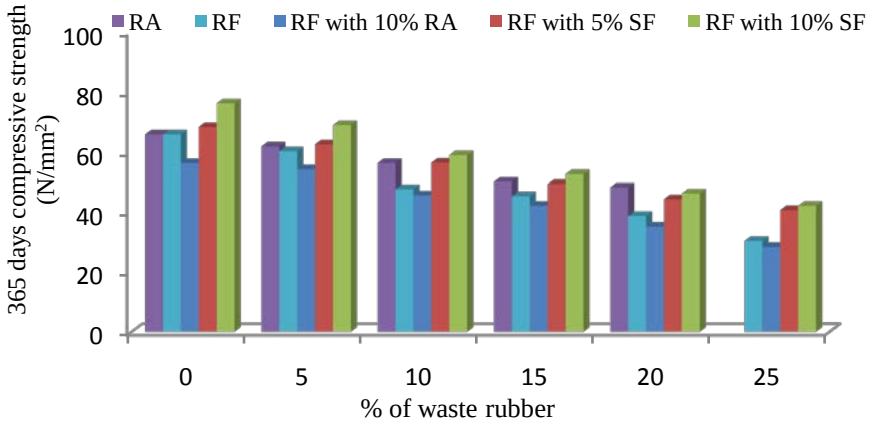

Fig. 3.17 365 days (natural exposure) compressive strength of waste rubber concrete for 0.45 w/c ratio

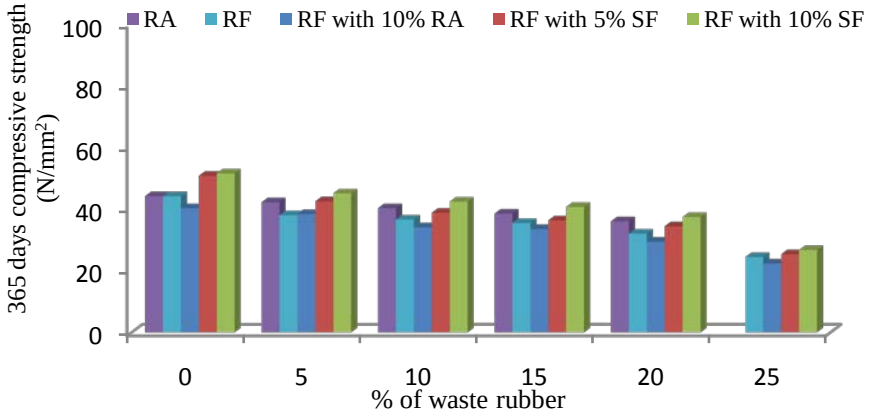

Fig. 3.18 365 days (natural exposure) compressive strength of waste rubber concrete for 0.55 w/c ratio

3.3.2.3 Flexural strength

The 7 days flexural strength for rubber ash concrete, hybrid concrete, rubber fiber concrete with and without SF is shown in Figs. 3.19-3.21. Statistical variances of results for flexural strength are shown in Table 3.3.

It is observed that the flexural strength of concrete decreased with the increase in percentage of rubber ash. The flexural strength of (without rubber fiber and silica fume) decreased by 20.5%, 29.0% and 10.5% for w/c ratios 0.35, 0.45 and 0.55 respectively on 20% replacement of FA by rubber ash.

It may be noted that, earlier also, upto 72% reduction in flexural strength was reported by Turki *et al.* (2012) on replacement of 50% of the FA by rubber aggregate. Reduction in flexural strength in the present study may be due to (i) poor mechanical behavior of rubber aggregate concrete (Turatsinze and Garros 2008; Aiello and Leuzzi 2010); (ii) lack of good bonding between rubber particles and cement paste (Ganjian *et al.* 2009; Gesog˘lu *et al.* 2014); and (iii) low density of rubber (Turki *et al.* 2012).

It is observed that the flexural strength of concrete increased with the increase in rubber content. Statistical variances of results for flexural strength are shown in Table 3.3. The flexural strength of concrete (without rubber ash and silica fume) increased by 10.2%, 16.0% and 27.3% for w/c ratios 0.35, 0.45 and 0.55 respectively on 25% replacement of FA by rubber fiber. The flexural strength of concrete (without silica fume) increased by 10.2%, 13.0% and 20.3% for w/c ratios 0.35, 0.45 and 0.55 respectively on replacement of FA by mix of 10% rubber ash and 25% rubber fiber. In this study, rubber fibers of aspect ratio 8 to 10 have been used. The increase in flexural strength is owing to fibers which provide a better bridge between propagated cracks.

It may be noted that, earlier also, upto 15% increase in flexural strength was reported by Ganesan *et al.* (2013) on replacement of 15% of the sand by shredded rubber aggregate. Benazzouk *et al.* (2003) reported that concrete with expanded/long rubber aggregate showed better flexural strength than concrete with compacted rubber aggregate. Increase in flexural strength in the present study may be due to: (i) the effect of rubber fibers (Yilmaz and

Degirmenci 2009); and (ii) gradual collapse of specimens under bending load (Uygunog˘lu and Topcu 2010).

It is also observed from Figs. 3.19-3.21 that on replacement of cement by SF, the flexural strength of concrete increased, for concrete without rubber ash and rubber fiber as well as for the rubber fiber concrete. Statistical variances of results for flexural strength are shown in Table 3.3. The flexural strength for concrete without rubber ash and rubber fiber increased by 3.9%, 9.0% and 16.8% for w/c ratios 0.35, 0.45 and 0.55 respectively on 10% replacement of cement by SF, whereas, the corresponding increase for rubber fiber concrete (25% rubber fiber) was 7.3%, 6.0% and 3.3% respectively.

The 28 days flexural strength for rubber ash concrete, hybrid concrete, rubber fiber concrete with and without SF is shown in Figs. 3.22-3.24. The flexural strength of concrete (without rubber fiber and silica fume) decreased by 32.9%, 12.5% and 27.7% for w/c ratios 0.35, 0.45 and 0.55 respectively on 20% replacement of FA by rubber ash. The flexural strength of concrete (without rubber fiber and silica fume) increased by 2.3%, 22.5% and 48.8% for w/c ratios 0.35, 0.45 and 0.55 respectively on 25% replacement of FA by rubber fiber. The flexural strength of concrete (without silica fume) increased by 1.4%, 10.9% and 9.1% for w/c ratios 0.35, 0.45 and 0.55 respectively on replacement of FA by mix of 10% rubber ash and 25% rubber fiber.

It is also observed from Figs. 3.22-3.24 that on replacement of cement by SF, the flexural strength of concrete increased, for control concrete as well as for the rubber fiber concrete. The flexural strength for control concrete increased by 1.4%, 4.4% and 2.5% for w/c ratios 0.35, 0.45 and 0.55 respectively on 10% replacement of cement by SF whereas the corresponding increase for rubber fiber concrete (25% rubber fiber) was 3.1%, 1.3% and 1.7% respectively.

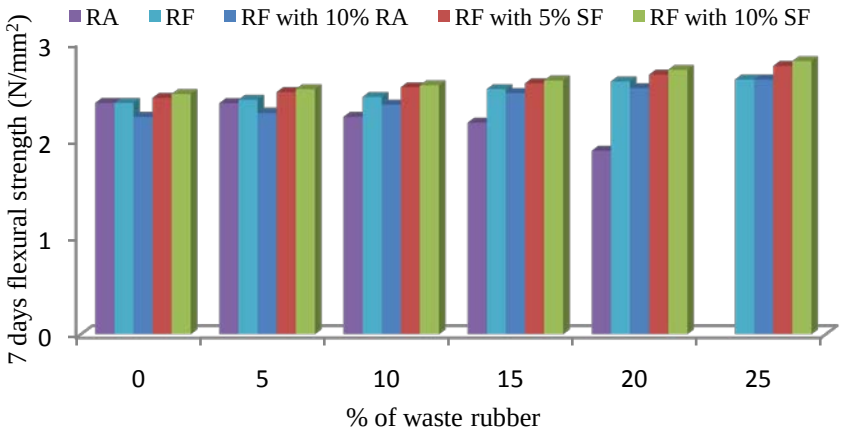

Fig. 3.19 7 days flexural strength of waste rubber concrete for 0.35 w/c ratio

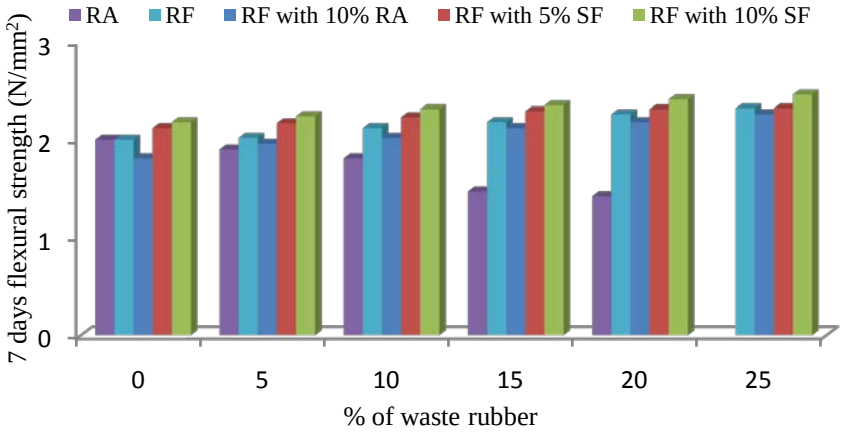

Fig. 3.20 7 days flexural strength of waste rubber concrete for 0.45 w/c ratio

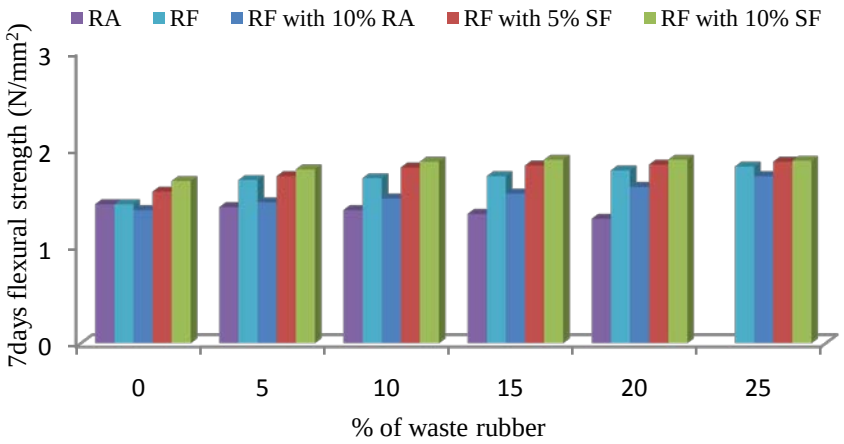

Fig. 3.21 7 days flexural strength of waste rubber concrete for 0.55 w/c ratio

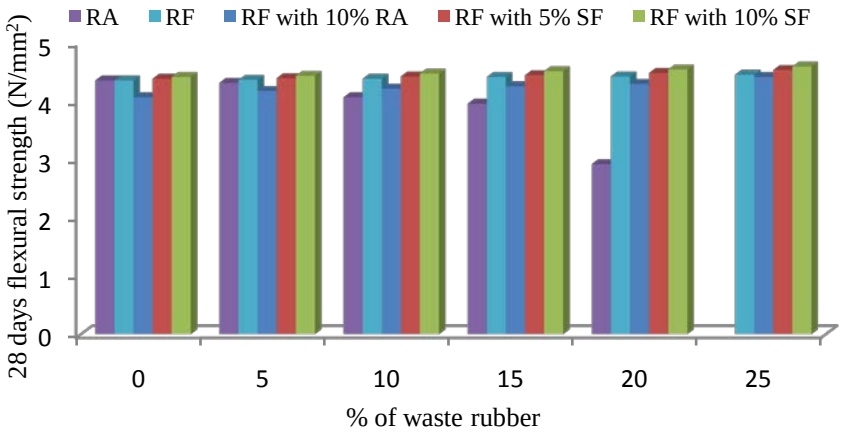

Fig. 3.22 28 days flexural strength of waste rubber concrete for 0.35 w/c ratio

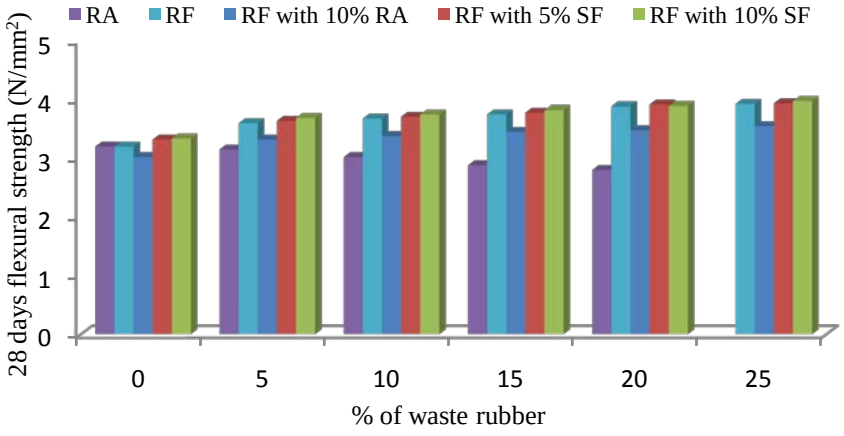

Fig. 3.23 28 days flexural strength of waste rubber concrete for 0.45 w/c ratio

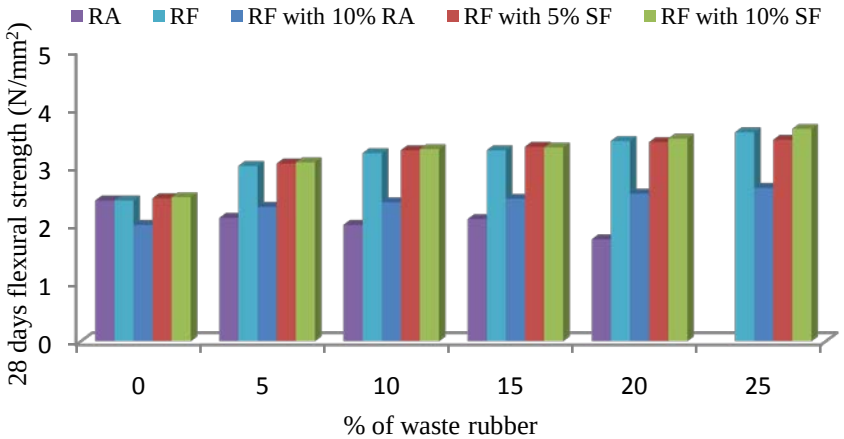

Fig. 3.24 28 days flexural strength of waste rubber concrete for 0.55 w/c ratio

Table 3.3 Statistical variances of flexural strength test results for waste rubber concrete

Mix No.	SD	COV	Mix No.	SD	COV	Mix No.	SD	COV	Mix No.	SD	COV	Mix No.	SD	COV
T1	0.43	0.09	R1	0.30	0.06	S1	0.09	0.02	U1	0.29	0.06	V1	0.15	0.03
T2	0.17	0.04	R2	0.32	0.08	S2	0.11	0.03	U2	0.24	0.05	V2	0.05	0.01
T3	0.09	0.02	R3	0.34	0.07	S3	0.22	0.06	U3	0.08	0.02	V3	0.10	0.02
T4	0.12	0.03	R4	0.27	0.06	S4	0.18	0.04	U4	0.22	0.05	V4	0.16	0.04
T5	0.28	0.09	R5	0.35	0.07	S5	0.12	0.03	U5	0.36	0.09	V5	0.03	0.01
T6	0.06	0.02	R6	0.15	0.03	S6	0.23	0.06	U6	0.22	0.05	V6	0.05	0.01
T7	0.08	0.02	R7	0.10	0.03	S7	0.20	0.07	U7	0.30	0.08	V7	0.11	0.03
T8	0.18	0.06	R8	0.20	0.05	S8	0.10	0.03	U8	0.22	0.06	V8	0.13	0.04
T9	0.12	0.04	R9	0.19	0.05	S9	0.31	0.08	U9	0.09	0.02	V9	0.12	0.03
T10	0.28	0.09	R10	0.34	0.08	S10	0.07	0.02	U10	0.06	0.02	V10	0.11	0.03
T11	0.21	0.09	R11	0.14	0.03	S11	0.06	0.02	U11	0.10	0.03	V11	0.14	0.04
T12	0.05	0.02	R12	0.07	0.02	S12	0.24	0.07	U12	0.41	0.09	V12	0.09	0.02
T13	0.05	0.02	R13	0.03	0.01	S13	0.17	0.09	U13	0.07	0.03	V13	0.12	0.05
T14	0.10	0.05	R14	0.13	0.05	S14	0.19	0.08	U14	0.10	0.03	V14	0.10	0.03
T15	0.14	0.07	R15	0.06	0.02	S15	0.19	0.09	U15	0.12	0.04	V15	0.15	0.04
-	-	-	R16	0.25	0.08	S16	0.19	0.08	U16	0.10	0.03	V16	0.15	0.05
-	-	-	R17	0.06	0.02	S17	0.12	0.05	U17	0.05	0.01	V17	0.06	0.02
-	-	-	R18	0.19	0.05	S18	0.24	0.08	U18	0.21	0.06	V18	0.13	0.04

Unit of SD (standard deviation) is N/mm^2.

3.3.2.4 Abrasion

Deterioration of concrete may take place due to abrasion caused by movement of various objects on the concrete surface. Depth of wear of concrete is measured under standard testing conditions (BIS 1980) for evaluating the abrasion. The variation in abrasion resistance of waste rubber concrete is shown in Figs. 3.25-3.27 for w/c ratio 0.35, 0.45 and 0.55. Statistical variances of results for abrasion resistance are shown in Tables 3.4.

It is observed that the depth of wear of rubber ash concrete increased with the increase of percentage of rubber ash. The depth of the wear of control concrete (without waste rubber and silica fume) increased by 26%, 21% and 22% for w/c ratios 0.35, 0.45 and 0.55 respectively on 20% replacement of FA by rubber ash. Depth of wear is 1.17 mm for control concrete with w/c ratio 0.45 whereas depth of wear marginally increased to 1.42 mm for higher replacement level of rubber ash (20%) mix at the same w/c ratio.

It is also observed from Figs. 3.25-3.27 that the depth of wear of rubber fiber concrete and hybrid concrete decreased with the increase in rubber fiber content. The depth of the wear of concrete (without rubber ash and silica fume) decreased by 33%, 39% and 15% for w/c ratios 0.35, 0.45 and 0.55 respectively on 25% replacement of FA by rubber fiber. The depth of the wear of concrete (without silica fume) decreased by 17%, 26% and 15% for w/c ratios 0.35, 0.45 and 0.55 respectively, on 10% replacement of FA by rubber ash and 25% replacement of FA by rubber fiber.

It may be noted that, earlier also, upto 81% reduction in depth of wear was reported by Gesog˘lu *et al.* (2014) on replacement of 20% of the natural aggregate by rubber particles. Decrease in depth of wear in the present study may be due to ability of the rubber fiber to hold the cement paste (Gesog˘lu *et al.* 2014).

It is also observed from Figs. 3.25-3.27 that on replacement of cement by SF, the depth of wear of concrete decreased, for control concrete as well as for the rubber fiber concrete. The depth of wear for concrete (without rubber ash and rubber fiber) decreased by 7%, 6% and 8% for w/c ratios 0.35, 0.45 and 0.55 respectively on 10% replacement of cement by SF, whereas, the observed decrease for rubber fiber concrete (25% rubber fiber) was 4%, 13% and 8% respectively.

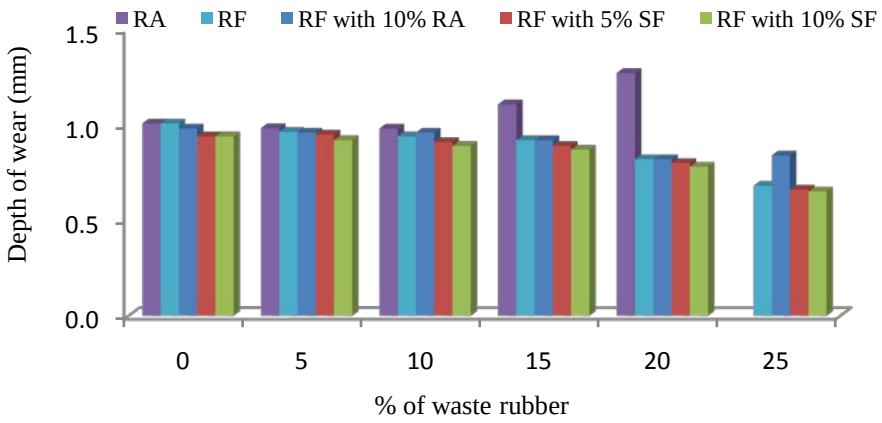

Fig. 3.25 Depth of wear of waste rubber concrete for 0.35 w/c ratio

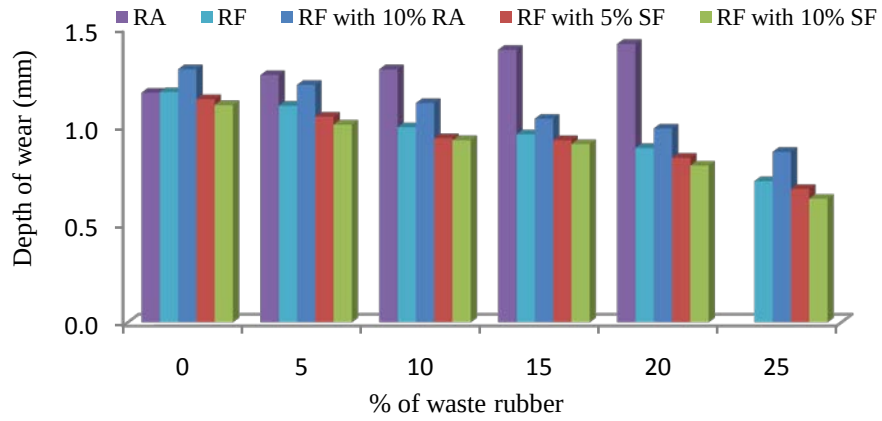

Fig. 3.26 Depth of wear of waste rubber concrete for 0.45 w/c ratio

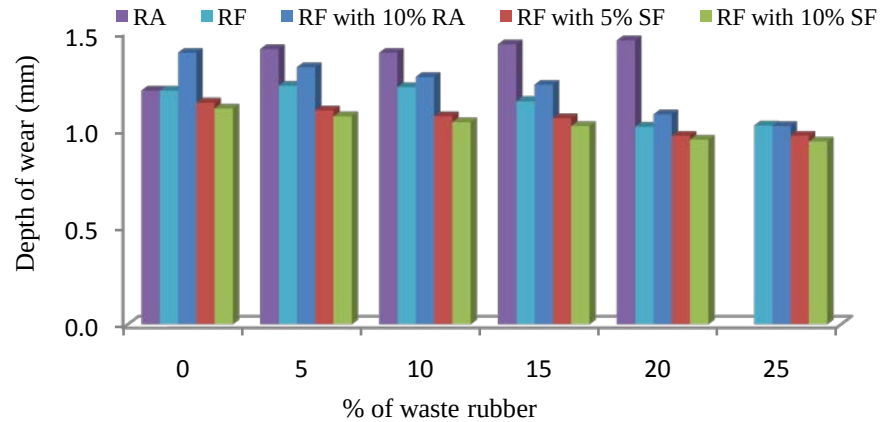

Fig. 3.27 Depth of wear of waste rubber concrete for 0.55 w/c ratio

Table 3.4 Statistical variances of abrasion resistance test results for waste rubber concrete

Mix No.	SD	COV	Mix No.	SD	COV	Mix No.	SD	COV	Mix No.	SD	COV	Mix No.	SD	COV
T1	0.07	0.06	R1	0.03	0.03	S1	0.11	0.10	U1	0.11	0.10	V1	0.02	0.02
T2	0.10	0.09	R2	0.10	0.09	S2	0.10	0.09	U2	0.10	0.09	V2	0.06	0.07
T3	0.10	0.09	R3	0.04	0.04	S3	0.10	0.09	U3	0.03	0.03	V3	0.13	0.18
T4	0.04	0.04	R4	0.04	0.04	S4	0.07	0.08	U4	0.13	0.13	V4	0.07	0.08
T5	0.13	0.09	R5	0.07	0.09	S5	0.06	0.08	U5	0.08	0.11	V5	0.08	0.12
T6	0.03	0.03	R6	0.05	0.07	S6	0.04	0.04	U6	0.03	0.05	V6	0.09	0.16
T7	0.13	0.09	R7	0.06	0.05	S7	0.06	0.04	U7	0.08	0.08	V7	0.08	0.08
T8	0.09	0.07	R8	0.07	0.07	S8	0.06	0.05	U8	0.14	0.16	V8	0.20	0.25
T9	0.06	0.05	R9	0.07	0.07	S9	0.07	0.07	U9	0.05	0.06	V9	0.12	0.11
T10	0.11	0.07	R10	0.01	0.01	S10	0.03	0.03	U10	0.06	0.07	V10	0.13	0.12
T11	0.03	0.02	R11	0.04	0.04	S11	0.08	0.07	U11	0.12	0.17	V11	0.12	0.17
T12	0.15	0.09	R12	0.04	0.05	S12	0.02	0.02	U12	0.10	0.18	V12	0.12	0.24
T13	0.04	0.03	R13	0.04	0.03	S13	0.14	0.09	U13	0.06	0.06	V13	0.08	0.08
T14	0.06	0.04	R14	0.13	0.09	S14	0.04	0.03	U14	0.09	0.09	V14	0.12	0.1
T15	0.06	0.04	R15	0.12	0.09	S15	0.01	0.01	U15	0.06	0.06	V15	0.07	0.06
-	-	-	R16	0.07	0.07	S16	0.04	0.03	U16	0.09	0.09	V16	0.11	0.1
-	-	-	R17	0.08	0.09	S17	0.05	0.05	U17	0.11	0.13	V17	0.05	0.05
-	-	-	R18	0.05	0.05	S18	0.08	0.09	U18	0.13	0.12	V18	0.09	0.09

Unit of SD (standard deviation) is mm.

It can be also seen from the results for varied w/c ratio and replacement level that the depth of wear observed in the most adverse conditions (w/c ratio 0.55) is less than permissible limits (BIS 1980). As per BIS (1980), the limit for general purpose concrete tiles is 3.5 mm and depth of wear should not exceed 2 mm for heavy duty applications. As per Bureau of Indian Standard (BIS 1980), the allowable depth of wear in concrete tiles are shown in Table 3.5.

Table 3.5 Allowable depth of wear for concrete tiles (BIS 1980)

i. For general purpose tiles
   a) Average wear 3.5 mm
   b) Wear on individual specimen 4.0 mm

ii. For heavy duty floor tiles
   a) Average wear 2.0 mm
   b) Wear on individual specimen 2.5 mm

3.3.2.5 Micro structural analysis

SEM images of the rubber ash concrete specimen are shown in Figs. 3.28-3.31. SEM images show that the rubber ash particles have an irregular shape (dark colour particles). In the Figs., cracks appear in the interface of rubber ash and cement matrix which reduce the strength of concrete. Gap in the interface of rubber ash and cement matrix can also be noticed in Figs. 3.28-3.31, and this gap reflects weak bond with cement mortar.

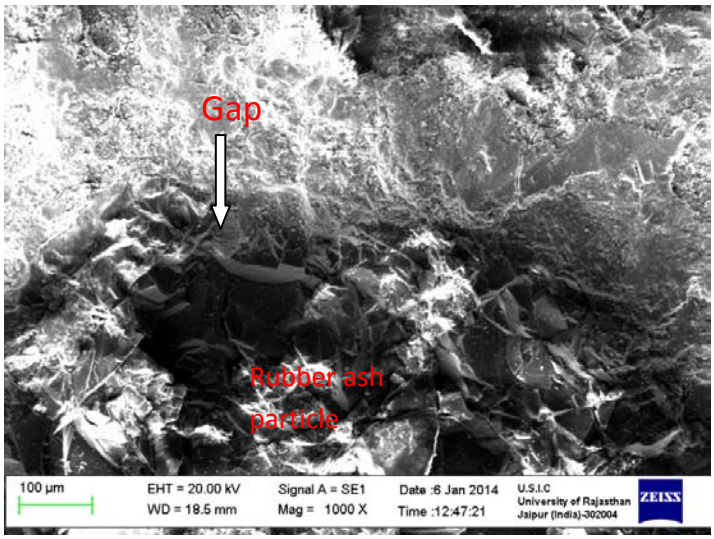

Fig. 3.28 Microstructure of waste rubber ash concrete at 1000x magnification

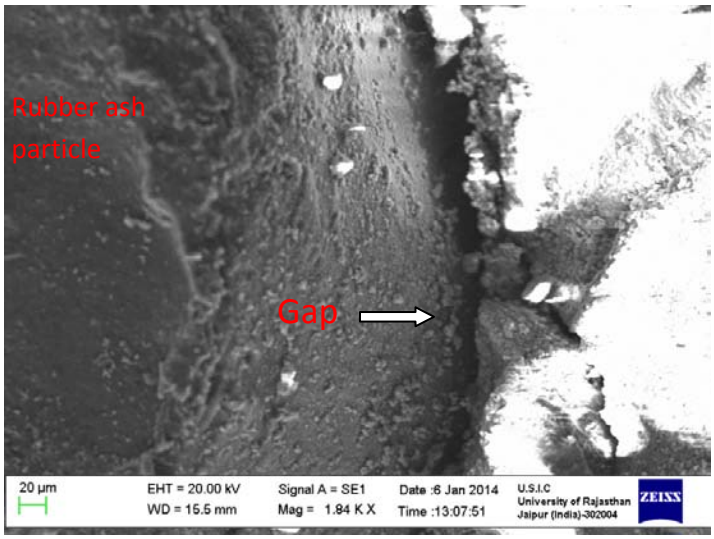

Fig. 3.29 Microstructure of waste rubber ash concrete at 1840x magnification

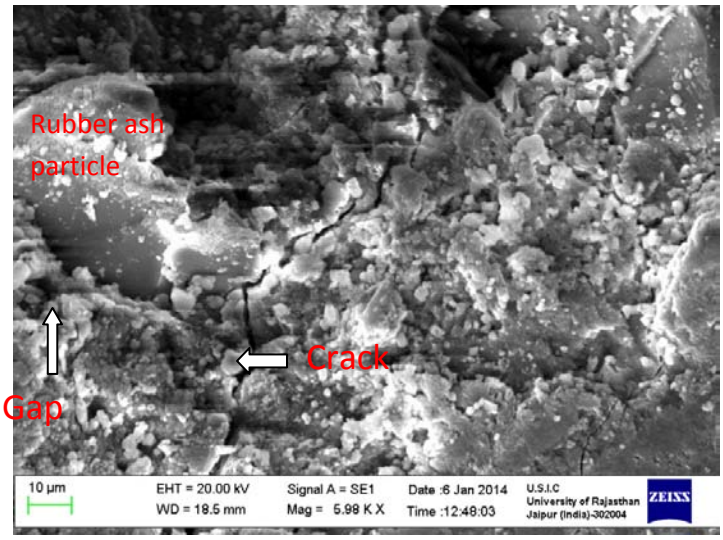

Fig. 3.30 Microstructure of waste rubber ash concrete at 5980x magnification

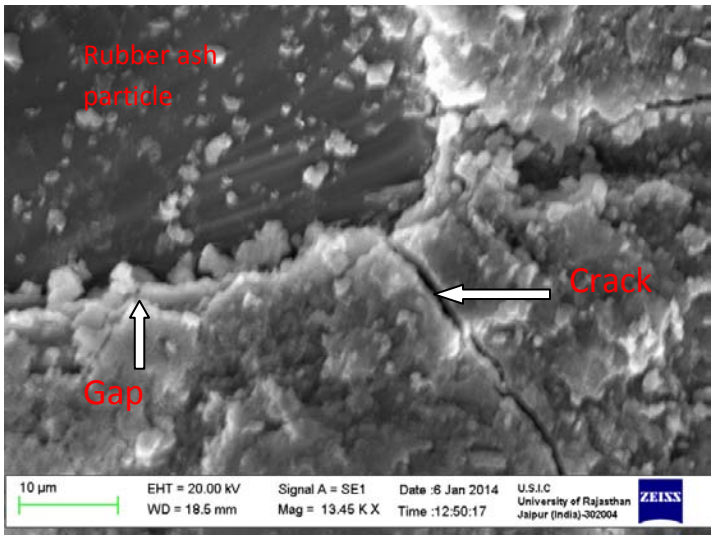

Fig. 3.31 Microstructure of waste rubber ash concrete at 13450x magnification

SEM images of the waste rubber fiber concrete are shown in Figs. 3.32-3.33. Cracks are observed in the rubber fibers in Figs. 3.32 which reduce the strength of concrete. The irregular shape of the rubber fiber particles is also observed in Fig. 3.34. Gaps in the interface of rubber aggregate and cement matrix are observed in Figs. 3.33-3.34, and this gap reflects weak bond with cement mortar and thereby cracking at the interface, which leads to the reduction in the strength of rubber fiber concrete.

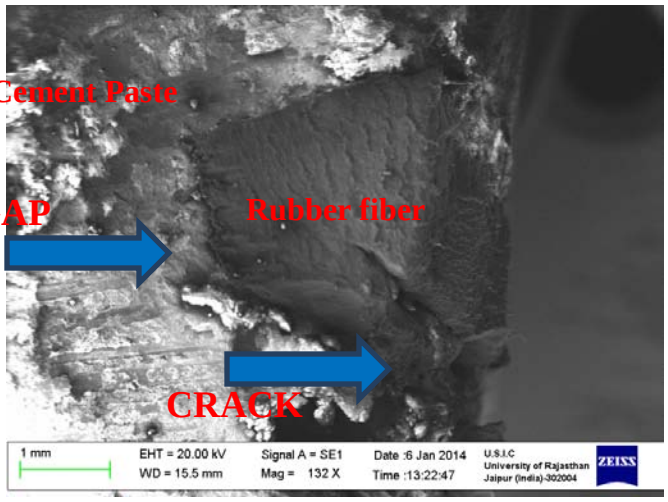

Fig. 3.32 Microstructure of waste rubber fiber concrete at 132x magnification

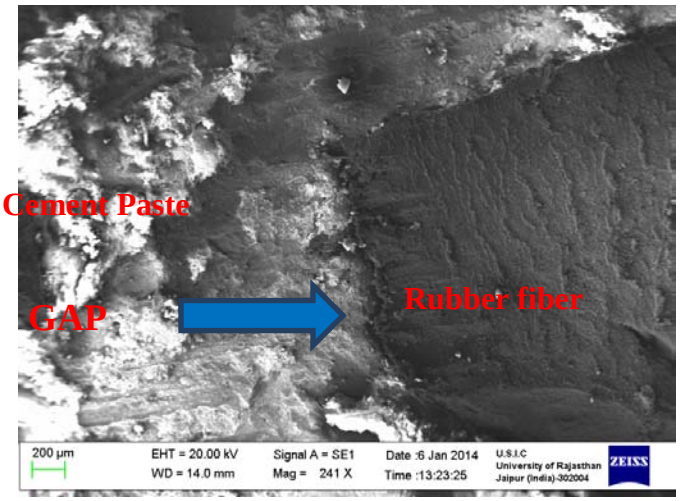

Fig. 3.33 Microstructure of waste rubber fiber concrete at 241x magnification

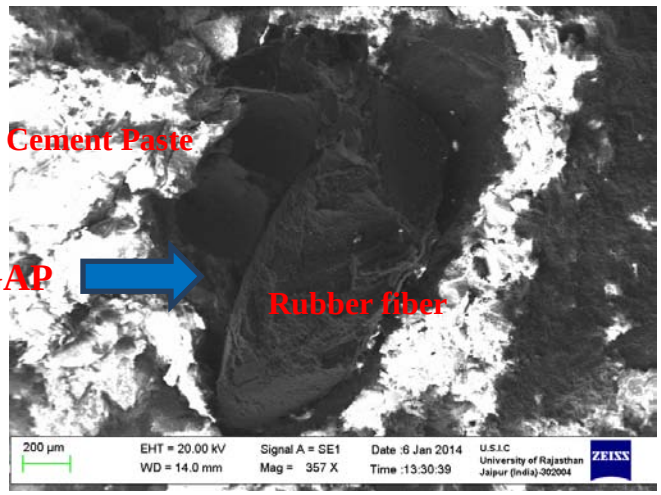

Fig. 3.34 Microstructure of waste rubber fiber concrete at 357x magnification

The SEM images of hybrid concrete are shown in Figs. 3.35 and 3.36. SEM images show that the rubber ash and rubber fiber particles have an irregular shape (dark colour particles). Large gaps in the interface of rubber particles and cement matrix are observed in the Figs. This indicates that the interfacial bonding between the rubber ash/fiber and cement paste is so weak that the cracking occurred at the interface leading to the reduction in the strength of rubber fiber concrete.

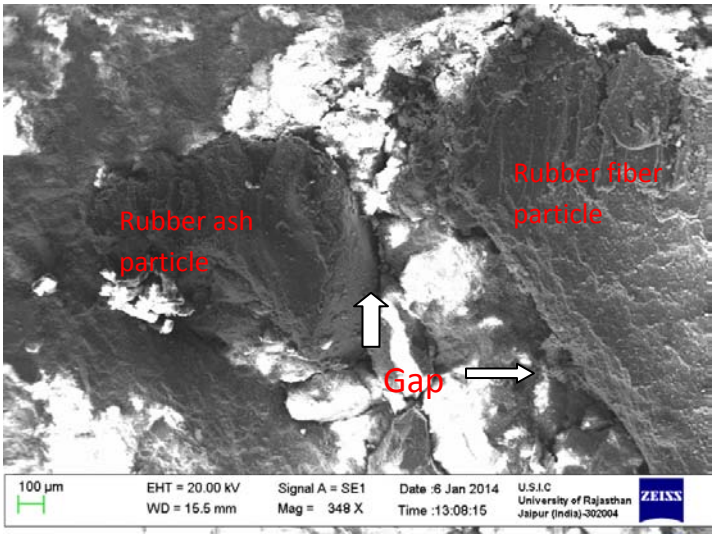

Fig. 3.35 Microstructure of hybrid concrete at 348x magnification

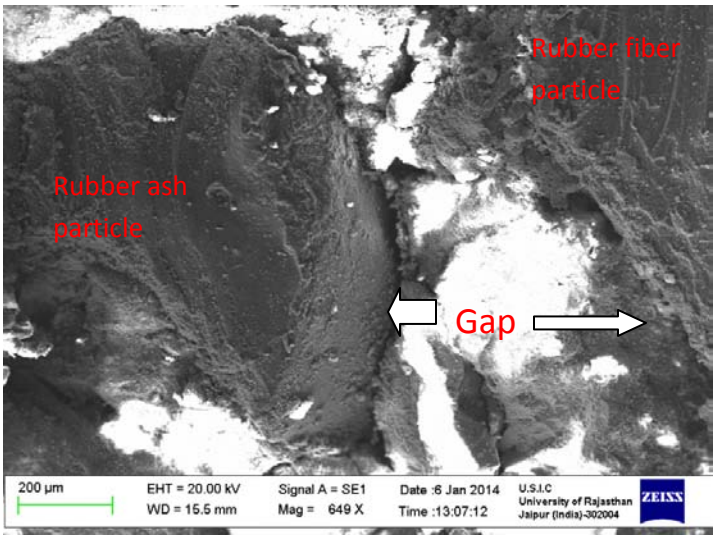

Fig. 3.36 Microstructure of hybrid concrete at 649x magnification

3.4 CONCLUSIONS

Various tests for fresh and hardened properties of waste rubber concrete were performed to assess the workability and mechanical strength of concrete along with abrasion resistance. As rubber aggregate are a product of used rubber tyres, detailed microstructural characterization of waste rubber concrete was also carried out to ensure compatibility of this material with the concrete. Following conclusions are drawn:

1. Partial replacement of fine aggregate by rubber ash decreases the workability of concrete whereas partial replacement of fine aggregate by rubber fiber does not affect the workability of concrete.
2. Partial replacement of fine aggregate by rubber ash and rubber fiber decreases the density of concrete, which is up to 9.5% in the present study.
3. Partial replacement of fine aggregate by rubber ash and rubber fiber decreases the compressive strength of concrete, which is up to 51.8% in the present study. The strength, however, increases with the inclusion of silica fume in rubberized concrete.
4. The compressive strength of waste rubber concrete at 365 days decreases on adopting natural exposure as compared to the water curing.
5. Partial replacement of fine aggregate by rubber ash decreases the flexural strength of the concrete, which is up to 32.9% in the present study whereas the partial replacement of fine aggregate by rubber fiber increases the flexural strength of the concrete, which is up to 48.8% in the present study.
6. The depth of wear of waste rubber concrete is affected by the inclusion of rubber ash, rubber fibers and silica fume. The maximum depth of wear of waste rubber concrete is less than permissible limits.
7. Micro structural analysis shows that cracking at the interface between the rubber ash/rubber fiber and cement paste which indicates weak interface.

CHAPTER 4

DURABILITY ASSESSMENT OF RUBBERIZED CONCRETE

4.1 INTRODUCTION

The durability of concrete should be ascertained along with the strength for better and longer service life. A number of parameters affect and define the durability of concrete.

(i) Water absorption gives an insight of internal microstructure whereas water permeability reflects the interconnectivity of voids.

(ii) Water permeability of concrete is the major factor, which controls several durability properties through transit of water.

(iii) Shrinkage of concrete produces the microcracks whereas carbonation is responsible for depassivation of protective layer of reinforcement bars. Shrinkage begins as soon as the hardening process of concrete starts by losing unconsumed water and can affects behaviour of concrete due to the formation of micro cracks.

(iv) Carbonation reduces the pH of concrete, which is responsible for increase in the risk of reinforcement corrosion by depassivation of the protective layer of steel reinforcement.

(v) Chloride permeability is ultimately responsible for corrosion of reinforcement bars. Chloride diffusion of chloride ions through concrete can provide insight on the permeability performance of concrete. Lower chloride permeability is desirable for durable concrete structures.

(vi) Corrosion is responsible for damages of reinforced concrete structure and pre-mature failures of the whole structures.

(vii) Acid attack may leads to the expansion, cracking and deterioration of concrete structures.

In the present study, the above durability properties of control concrete and waste rubber concrete have been evaluated by carrying out water absorption test, water permeability test, drying shrinkage test, carbonation test, chloride diffusion test, corrosion test in terms of macrocell and half cell potential and acid attack test for sulphuric acid and hydro-chloride acid. The experimental procedures and the results of above durability properties with concrete have been discussed in the subsequent sections.

4.2 EXPERIMENTAL PROCEDURE

4.2.1 Water absorption

The water absorption test was carried out as per BS 1881-122 (2011). Three oven dried specimens were placed for 24 hours in water bath. The initial weight and final weight were recorded and the percentage of water absorption was determined as per the guidelines of the codes.

4.2.2 Water permeability

The water permeability test was carried out as per German standard DIN 1048 (1991) (Fig. 4.1). Twenty eight days cured concrete cube specimens of 150 mm × 150 mm × 150 mm size were used for this study after oven drying (3 days at 55 ^{0}C). The specimen were tested for three days at a pressure of 0.5 N/mm^{2}. After three days, the specimen was split into two halves on compression testing machine as shown in Fig. 4.2 and the depth of water penetration was measured and reported as the average of 3 cubes measured to the nearest 0.1 mm.

Fig. 4.1 Water permeability apparatus

Fig. 4.2 Arrangement for splitting cubes for measurement of water permeability depth

4.2.3 Shrinkage

Drying shrinkage is particularly significant in hot-dry climatic conditions, where the concrete is dried more readily. For the drying shrinkage measurement, 75 mm × 75 mm × 300 mm concrete beams (Fig. 4.3) were cast and cured according to ASTM C157 (2008). For each mix, three specimens were cast and covered with polyethylene sheet for 24 hours. After 24 hours, the specimen were demoulded and then placed in curing tank for 28 days. Just after the curing period, stainless steel studs were glued at a distance of 212±1 mm on the top of the dry specimen and initial reading was taken out after 24 hours of mounting of studs. A mechanical strain gauge with a least count of 0.002 mm was used to observe the reading and average of two measurements (second measurement was made by reversing the specimen) was considered for each reading. Shrinkage strain was measured after seven, fifteen, thirty, forty five, sixty, ninety, one hundred eighty, two hundred seventy and three hundred sixty five days of initial reading.

Fig. 4.3 Measurement of drying shrinkage.

4.2.4 Carbonation

Accelerated carbonation test was conducted on 28 days cured concrete prisms (50 mm × 50 mm × 100 mm). The specimens were dried before the carbonation test to remove any moisture. Out of the six edges, the four longer edges were painted by resin based epoxy. This was done to ensure the penetration of the CO_2 along the length of the specimens. A carbonation chamber as shown in Fig. 4.4 was used to place the specimen with the following parameters:

a. CO_2 concentration: 5%
b. Relative humidity: 50 ± 5%
c. Temperature: 27 ± 1 °C.

After the desired CO_2 exposure (14, 21, 28, 35, 42, 56 and 90 days), three prisms from each representative concrete mix were taken out. The depth of carbonation was measured after splitting the specimens (Fig. 4.4) as per RILEM guidelines (CPC-18, 1988). The penetration depth of the CO_2 in the specimen was measured using the phenolphthalein solution. The change of the colour on application of phenolphthalein solution defined the non carbonated length.

Fig. 4.4 Carbonation chamber and Splitting of specimens after testing

4.2.5 Chloride diffusion

The steady state chloride diffusion test was carried out to obtain the chloride ion penetration resistance. The test requires a very long duration but it gives more accurate results compared to the rapid chloride permeability test. The Derian chloride permeability test apparatus (Fig. 4.5) was used for this purpose. Cylindrical samples of 50 mm thickness and 65 mm nominal diameter, cured for 28 days, were used. Upstream cell of the instrument was filled with 3%

sodium chloride (NaCl) solution (anode) while the downstream cell of the instrument was filled with distilled water (cathode). The amount of chloride which passes through specimen at a constant 30 V DC potential was measured over a period of 72 hours.

The initial chloride concentration of upstream cell (3% NaCl) was measured using a titration method. Similarly, chloride concentration of downstream cell (distilled water) was also measured by titration depending upon rate of travel of chloride ion into downstream cell. For titration purposes, a 10 mL sample was used and a few drops of potassium chromate were added as indicator. Quantity of silver nitrate ($AgNO_3$) required to change the colour of sample to reddish brick was measured.

The chloride diffusion coefficient (D_{smm}) in m^2/s was evaluated by Nernest-Planck's equation suggested by Andrade (1993):

$$Dsmm = \frac{RTL}{zF\Delta Ec_1}.J \tag{4.1}$$

where, R = gas constant (R = 8.314 J/(K mol^{-1})), T = average value of initial and final temperature (K), L = thickness of the specimen (mm), z = absolute value of ion valence (for chloride, $z=1$), F = faraday constant (F = 9.648 x 10^4 J/(V mol)), ΔE = absolute value of the potential difference between the upstream solution and the downstream solution, measured by using two reference electrodes, c_1 = activity of chloride ions, J = unidirectional flux of species j (mol/cm^2s) which depends upon monitored chloride ions.

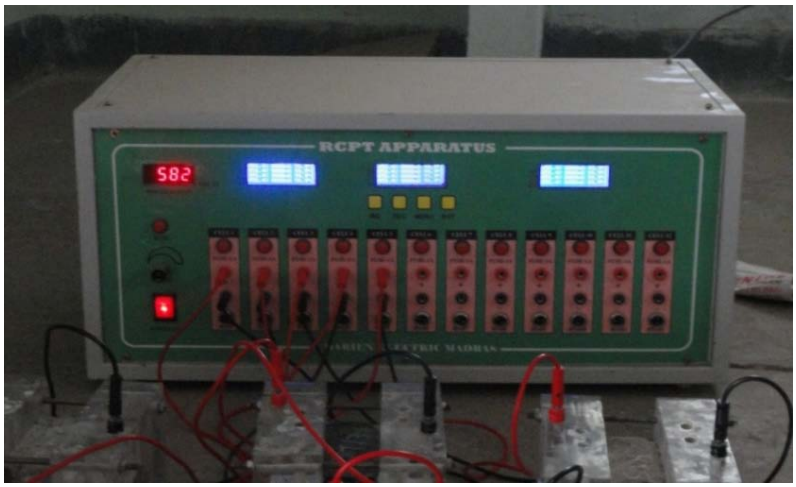

Fig. 4.5 Chloride penetration measurement apparatus

4.2.6 Corrosion

Corrosion was measured on concrete specimens of size 115 mm × 275 mm × 225 mm (150 mm + 75 mm pond) cast with three 12 mm dia TMT (Thermo Mechanically Treated) steel bars (Fig. 4.6). One steel bar was placed at a distance of 25 mm from top and another two bars were placed at a distance of 125 mm from top with equal distance from the edges. The arrangement of steel bars in this fashion was to ensure early and higher chances of corrosion. The length of the steel bar was kept as 375 mm with equal projection of bar on both side of concrete specimen. 225 mm length of bars was kept exposed in concrete and for the remaining steel bars on both sides, rubber sleeves were used to protect corrosion from outside environment. The surface of the bars was made free from any dust prior to the placement. Corrosion was measured for 18 months.

3% NaCl solution was filled up at the top of specimen in the pond (monolithic cast with specimen) for two weeks on a 28 days cured specimen dried for one month. Plastic loose fitting cover was used to minimize the evaporation of solution. The top bar was therefore subjected to chloride ion solution and moisture. An electrochemical macrocell in concrete was developed because of the availability of moisture, chloride ions and oxygen. Thus, the top bar became anodic and bottom bars became cathodic as macrocell was initiated and current flowed between them.

4.2.6.1 *Macrocell current*

The macrocell corrosion was recorded as potential difference between anode and cathode, across the 100-Ohm resister. The potential difference (V_j) was measured by the voltmeter after one week of ponding. Current (I_j) was calculated as per ASTM G109 (2005) using the following equation:

$$I_j = \frac{V_j}{100} \tag{4.2}$$

4.2.6.2 *Half-cell potential measurements*

Immediately after measuring the macrocell current, the connections between the top bars and bottom bars were removed and the half cell potential, between the reference electrode and top bar, was measured using copper-copper sulfate reference electrode.

The measured half cell potential was used to predict the probability of corrosion as per ASTM C 876 (2009) according to which:

i. There is a more than 90% probability that no corrosion will occur when potentials are more positive than -200 mV.

ii. The corrosion activities are uncertain if potentials are in the range of -200 mV to -350 mV.

iii. There is a more than 90% probability that corrosion will occur when potentials are more negative than -350 mV.

Solution was removed after two week of ponding and the specimen was allowed to dry for next two weeks.

Same cycles were repeated for next 18 months.

Fig. 4.6 Measurement of half cell potential

4.2.7 Acid attack

The control mix and waste rubber concrete were tested for resistance to acid attack over a period of 180 days. The resistance to acid attack was measured over a period of 180 days. 3% Sulphuric acid (H_2SO_4) and 3% Hydrochloric acid (HCl) was used for acid attack test. 100 mm × 100 mm × 100 mm concrete cubes were cast and cured according to ASTM C138 (2008). For each mix, thirty three specimens were cast and covered with polyethylene sheet for 24 hours. After 24 hours, the specimen were demoulded and placed in a curing tank for 28 days. Weight of all the cubes was measured and compressive strength of three cubes of each mix was measured just after the curing period. Then fifteen cubes for each mix were submerged for 7, 28, 56, 90 and 180 days duration in sulphuric acid and the remaining fifteen cubes for each mix were submerged in hydrochloric acid solution. The solution was replaced after every two weeks. The weight of the cubes and compressive strength was measured, at the end of each duration.

Fig. 4.7 Acid attack

4.2.8 Micro-structural analysis

The microstructure of the specimen was analyzed using a microscope of 90x magnification. Testing was performed on 2 cm × 2 cm pieces cut from concrete samples.

4.3 RESULTS AND DISCUSSION

4.3.1 Water absorption

The rubber content and w/c ratio influence the porosity of the concrete which affect the water absorption capacity of the concrete. The water absorption of rubber ash concrete, rubber fiber concrete, hybrid concrete and rubber fiber concrete with 5% and 10% silica fume (SF) is shown in Figs. 4.8-4.10.

The water absorption was found to change with the increase in waste rubber content. The water absorption of concrete (without rubber fiber and SF) changed by 169.1%, 16.3% and -9.1% for w/c ratios 0.35, 0.45 and 0.55 respectively on 20% replacement of FA by rubber ash. Whereas, the change observed for concrete (without rubber ash and SF) on 25% replacement of FA by rubber fiber, was 17.4%, 2.7% and -24.8% respectively. The observed change for concrete (without SF) was 28.7%, 13.9% and -29% respectively on 10% replacement of FA by rubber ash along with 25% replacement of FA by rubber fiber. .

Bjegović *et al.* (2011) reported a decrease in water absorption on replacement of up to total 15% volume of aggregate by granulated, shredded and small granulated rubber particles. They observed more than 78% decrease in water absorption on 15% replacement of natural aggregate by rubber particles. Yilmaz and Degirmenci (2009) reported decrease in water

absorption on inclusion of rubber waste as cement (20% to 30%) in mortar. The non absorption of the water by the rubber particles was described as the reason.

Uygunogˇlu and Topcu (2010) observed more than 18% increase in water absorption on 50% replacement of FA by rubber particles. Increased water absorption in the present study may be due to (i) weak bonding between rubber aggregate and cement paste (Ganjian *et al.* 2009; Sukontasukkul and Chaikaewd 2012; Onuaguluchi and Panesar 2014); (ii) the entrapment of air by the rubber aggregate (Uygunogˇlu and Topcu 2010); and (iii) greater fragility in the rubber/cement paste transition zones (Bravo and Brito 2012).

It is also observed from Figs. 4.8-4.10 that on replacement of cement by SF, the water absorption of concrete decreased, for control concrete as well as for the rubber fiber concrete. The water absorption for concrete (without rubber ash and rubber fiber) decreased by 8.9%, 9.3% and 6.4% for w/c ratios 0.35, 0.45 and 0.55 respectively on 10% replacement of cement by SF. Whereas the observed decrease for rubber fiber concrete (25% rubber fiber) was 15.7%, 13.0% and 9.5% respectively on 10% replacement of cement by SF. The reduction may be due to the hydration process of SF resulting in filling of the voids which in turn reduces the porosity and total absorbed water. It may be noted that Onuaguluchi and Panesar (2014) have also reported more than 45% reduction in water absorption on addition of silica fume.

4.3.2 Water permeability

The depth of water penetration of waste rubber concrete for w/c ratios considered in the study is shown in Figs. 4.11-4.13. Statistical variances of results for water penetration depth are shown in Table 4.1. It is seen that the depth of water penetration increased with the increase in waste rubber content for all three w/c ratio.

The depth of the water penetration of concrete (without rubber fiber and SF) increased by 113.4%, 19.7% and 20.7% for w/c ratios 0.35, 0.45 and 0.55 respectively on 20% replacement of FA by rubber ash. Whereas, the depth of the water penetration of concrete (without rubber ash and SF) increased by 43.5%, 40.5% and 23.9% respectively on 25% replacement of FA by rubber fiber. The observed increase for concrete (without SF), was 50.5%, 47.4% and 33.1% respectively on 10% replacement of FA by rubber ash along with 25% replacement of FA by rubber fiber.

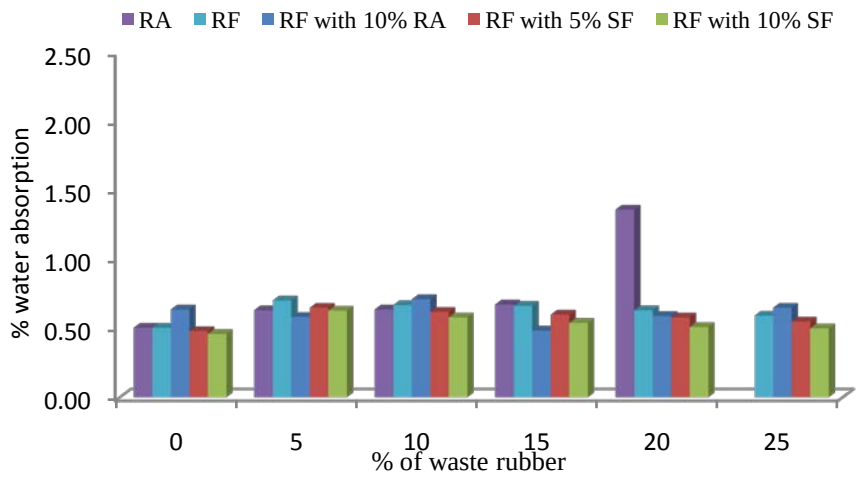

Fig. 4.8 Water absorption of waste rubber concrete for 0.35 w/c ratio

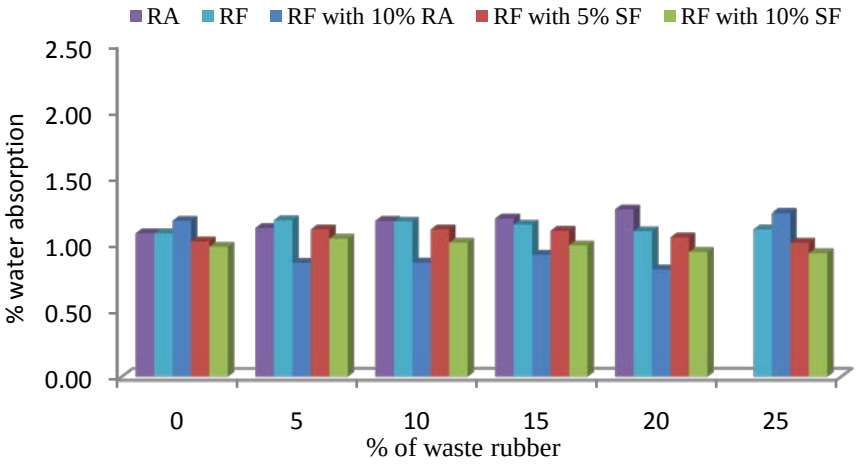

Fig. 4.9 Water absorption of waste rubber concrete for 0.45 w/c ratio

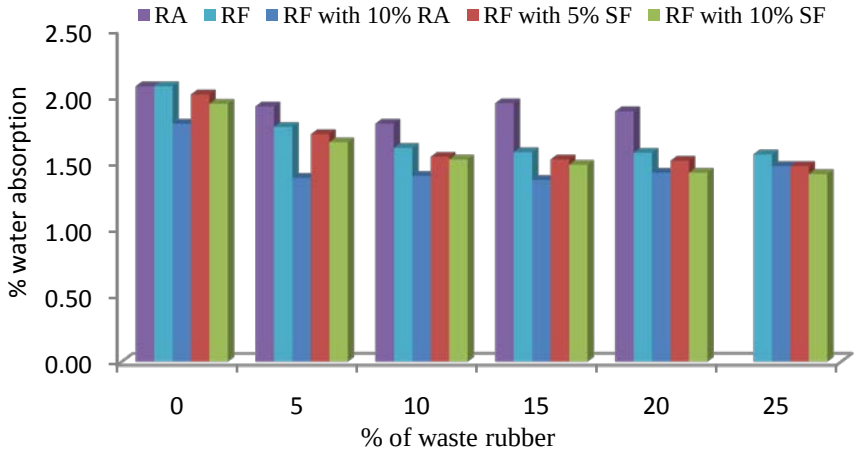

Fig. 4.10 Water absorption of waste rubber concrete for 0.55 w/c ratio

The increase in water permeability may be due to the reduction in bonding and increase in voids between rubber particles and cement paste (Ganjian *et al.* 2009; Bjegović *et al.* 2011; Su *et al.* 2014). It may be noted that, earlier also, upto 60% increase in depth of water permeability was reported by Ganjian *et al.* (2009) on 10% replacement of coarse aggregate by chipped rubber. Ganjian *et al.* (2009) classified the depth of water penetration (after 72 h) into three categories, low permeability (less than 30 mm), medium permeability (30-60 mm) and high permeability (greater than 60 mm). Rubber ash concrete shows medium permeability as the highest value of water penetration was observed as 51.4 mm (w/c ratio 0.55, 20% replacement of FA by rubber ash) except one case (w/c ratio 0.35, 20% replacement of FA by rubber ash,). The rubber fiber concrete also shows medium permeability without SF as the highest value of water penetration was observed as 52.8 mm (w/c ratio 0.55, 25% replacement of FA by rubber fiber). Similarly, the hybrid concrete also shows medium permeability as the highest value of water penetration was observed to be 56.7 mm (w/c ratio 0.55, 10% replacement of FA by rubber ash and 25% replacement of FA by rubber fiber).

It is also observed from Figs. 4.11-4.13 that on replacement of cement by SF, the depth of water penetration decreased for control concrete as well as for the rubber fiber concrete. The depth for the control concrete decreased by 20.8%, 15.5% and 11.3% for w/c ratios 0.35, 0.45 and 0.55 respectively on 10% replacement of cement by SF. The corresponding decrease for rubber fiber concrete (25% rubber fiber) was 14.0%, 11.9% and 12.1% respectively on 10% replacement of cement by SF. A medium permeability was observed for rubberized concrete on partial replacement of cement by SF.

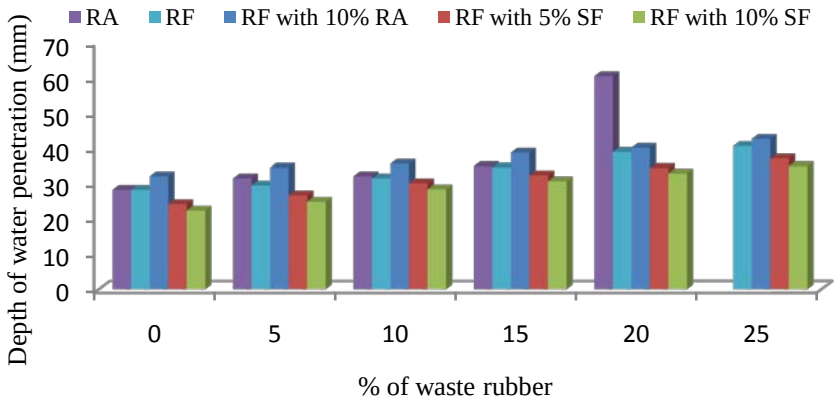

Fig. 4.11 Water penetration of waste rubber concrete for 0.35 w/c ratio

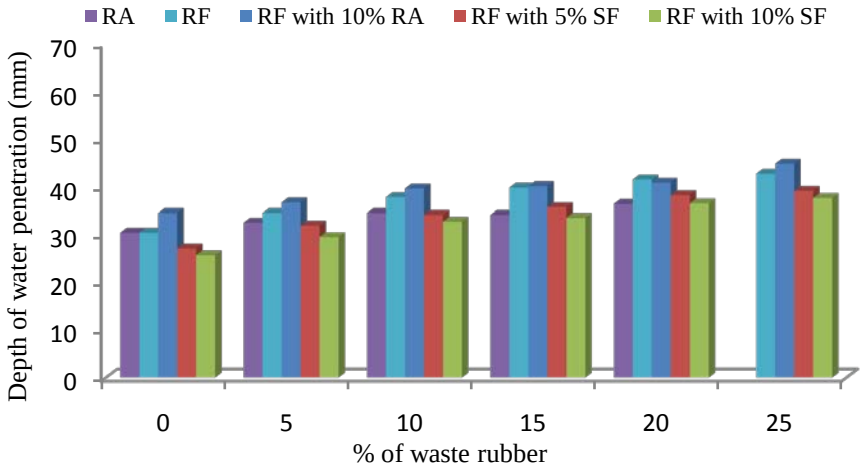

Fig. 4.12 Water penetration of waste rubber concrete for 0.45 w/c ratio

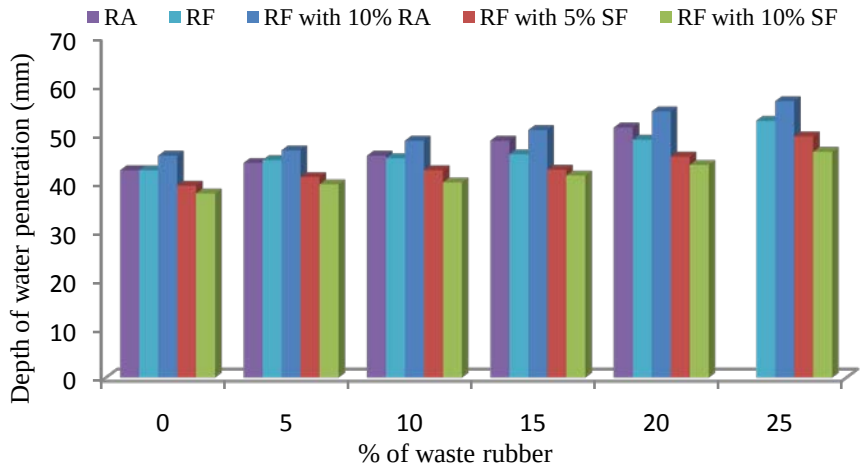

Fig. 4.13 Water penetration of waste rubber concrete for 0.55 w/c ratio

Table 4.1 Statistical variances of water permeability test results for waste rubber concrete

Mix No.	SD	COV	Mix No.	SD	COV	Mix No.	SD	COV	Mix No.	SD	COV	Mix No.	SD	COV
T1	1.30	0.04	R1	1.14	0.04	S1	1.57	0.05	U1	1.44	0.06	V1	1.11	1.01
T2	2.36	0.07	R2	0.90	0.03	S2	1.05	0.03	U2	0.90	0.03	V2	0.05	0.04
T3	2.07	0.06	R3	1.73	0.06	S3	2.78	0.09	U3	1.13	0.04	V3	1.11	1.01
T4	0.89	0.03	R4	1.06	0.03	S4	1.85	0.05	U4	1.32	0.04	V4	0.05	0.04
T5	1.56	0.03	R5	1.13	0.03	S5	3.10	0.08	U5	1.31	0.04	V5	1.11	1.01
T6	1.93	0.07	R6	1.31	0.03	S6	1.31	0.03	U6	2.43	0.07	V6	0.05	0.04
T7	1.00	0.03	R7	1.82	0.06	S7	0.96	0.03	U7	1.64	0.06	V7	1.11	1.01
T8	1.28	0.04	R8	2.25	0.07	S8	1.91	0.06	U8	1.32	0.04	V8	0.05	0.04
T9	2.23	0.07	R9	2.21	0.06	S9	1.31	0.03	U9	1.51	0.05	V9	1.11	1.01
T10	2.09	0.06	R10	2.86	0.08	S10	1.57	0.04	U10	1.01	0.03	V10	0.05	0.04
T11	2.55	0.06	R11	2.09	0.05	S11	1.65	0.04	U11	2.19	0.06	V11	1.11	1.01
T12	2.96	0.07	R12	1.08	0.02	S12	1.39	0.03	U12	2.17	0.06	V12	0.05	0.04
T13	2.99	0.07	R13	1.31	0.03	S13	2.80	0.07	U13	1.23	0.03	V13	1.11	1.01
T14	2.01	0.04	R14	1.01	0.02	S14	1.37	0.03	U14	1.21	0.03	V14	0.05	0.04
T15	1.85	0.04	R15	2.52	0.06	S15	0.80	0.02	U15	1.22	0.03	V15	1.11	1.01
-	-	-	R16	0.53	0.01	S16	2.16	0.04	U16	1.15	0.03	V16	0.05	0.04
-	-	-	R17	1.56	0.03	S17	1.22	0.02	U17	2.51	0.06	V17	1.11	1.01
-	-	-	R18	1.08	0.02	S18	2.08	0.04	U18	1.04	0.02	V18	0.05	0.04

Unit of SD (standard deviation) is mm.

4.3.3 Shrinkage

The drying shrinkage with time (for 365 days) for waste rubber concrete without SF is shown in Figs. 4.14-4.16 for w/c ratios considered in the present study. The maximum and minimum drying shrinkage strain was observed at w/c ratios of 0.55 and 0.35.

It can be observed that the drying shrinkage increased with the increase in the waste rubber content. It may be noted that, earlier also, upto 95% increase in drying shrinkage was reported by Yung *et al.* (2013) on 20% replacement of FA by rubber powder. The increase in shrinkage in the present study may be due to: (i) the increase in porosity due to rubber particles (Uygunoglu and Topcu 2010); (ii) the lower internal restraint (from lack of FA) (Sukontasukkul and Tiamlom 2012); (iii) the presence of more flexible material (Sukontasukkul and Tiamlom 2012); and (iv) low modulus of elasticity and capability of deformation of rubber waste (Yung *et al.* 2013).

The drying shrinkage curves for rubber fiber concrete (0%, 10% and 25% rubber fibers) with 5% and 10% SF for w/c ratios 0.35, 0.45 and 0.55 are shown in Figs. 4.17-4.19 respectively. It may be observed from Figs. that drying shrinkage decreased with the increase of SF in concrete. This may be due to filling of voids by the fine SF. A similar trend was reported by Bentur and Goldman (1989). According to Feldman and Cheng-Yi (1985), the smaller drying shrinkage in SF concrete may be associated with its finer pore structure which leads to low diffusibility and considerably slows down rate of drying shrinkage.

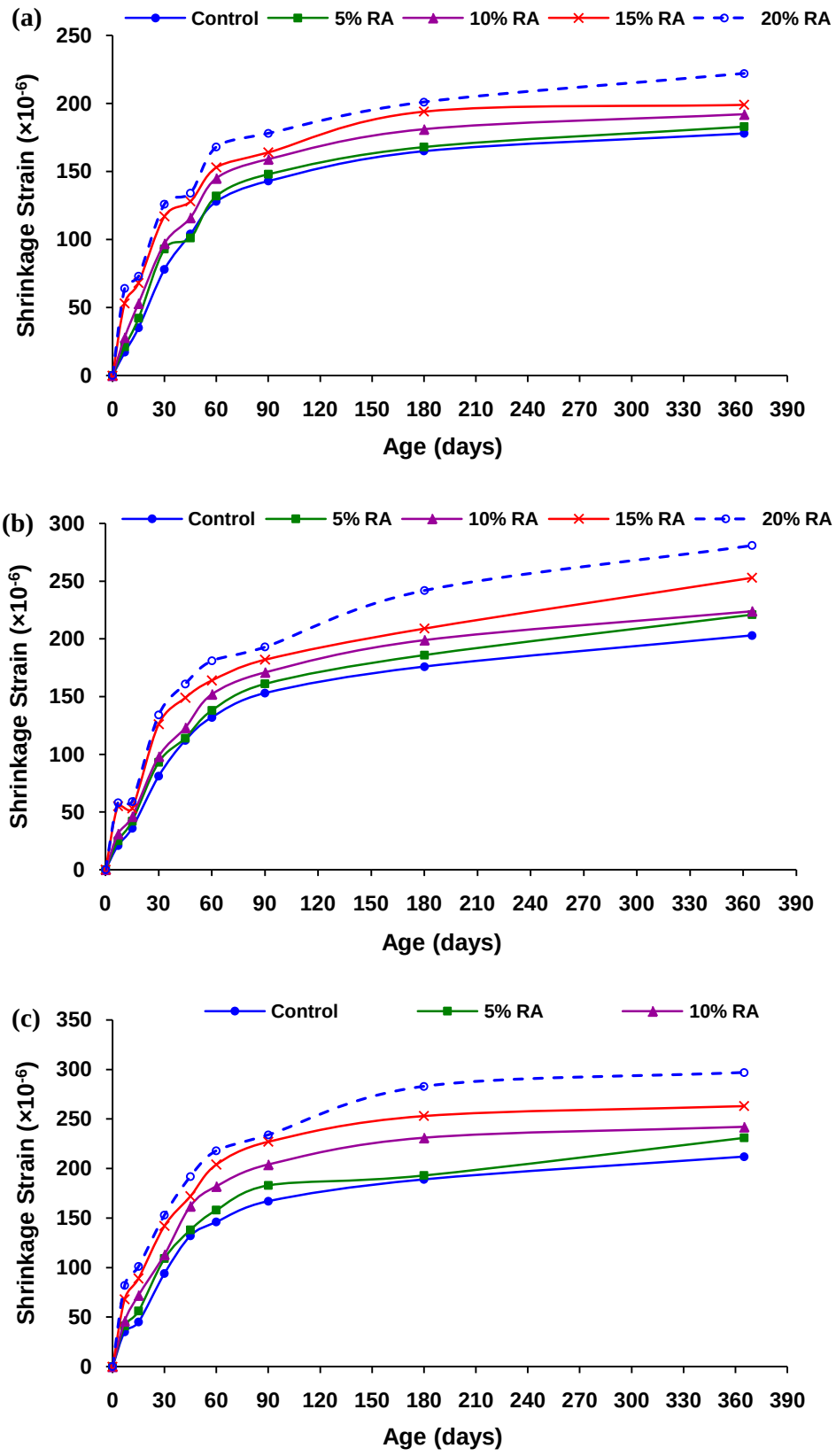

Fig. 4.14 Drying Shrinkage of rubber ash concrete for w/c ratio (a) 0.35; (b) 0.45; and (c) 0.55

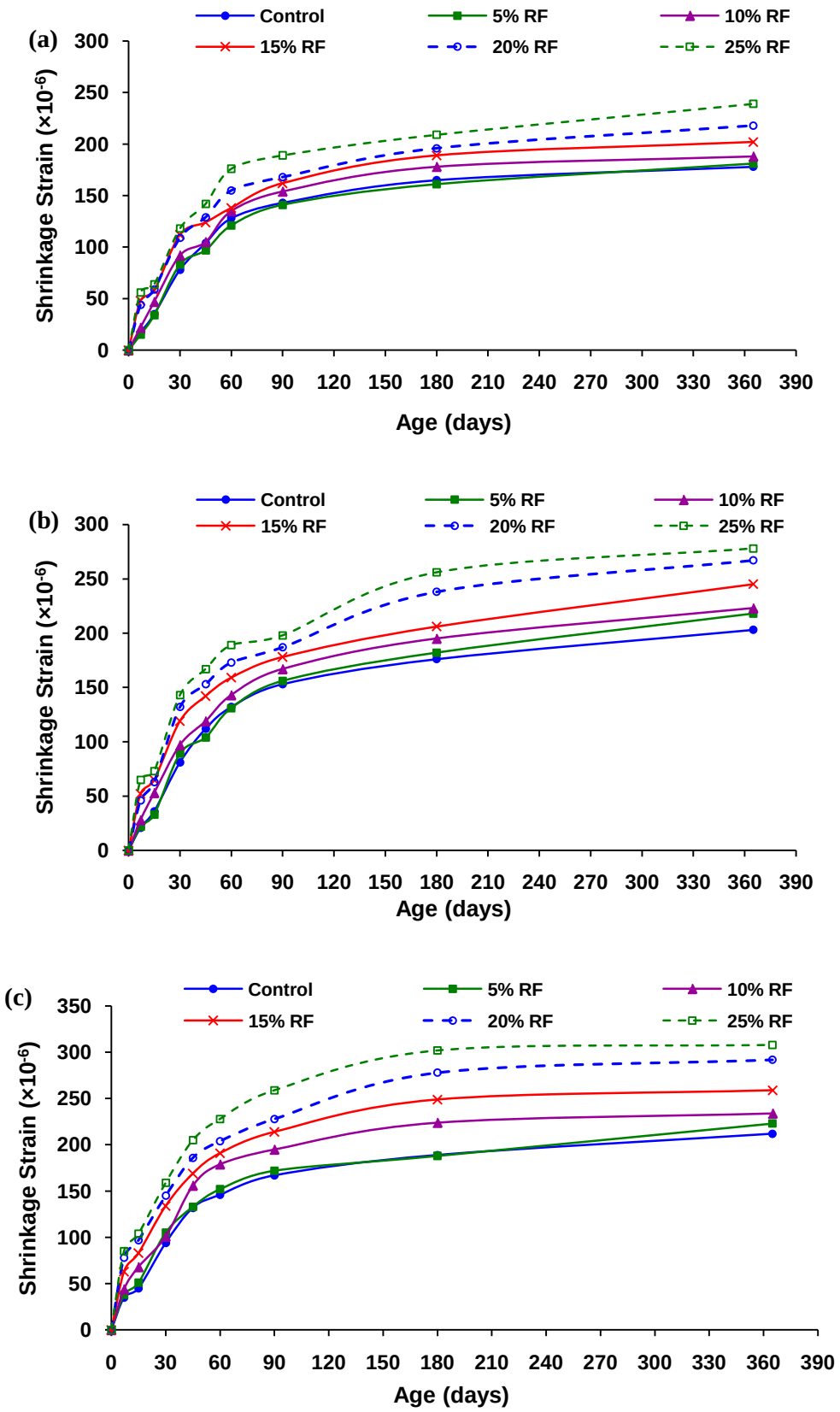

Fig. 4.15 Drying Shrinkage of rubber fiber concrete without silica fume for w/c ratio (a) 0.35; (b) 0.45; and (c) 0.55

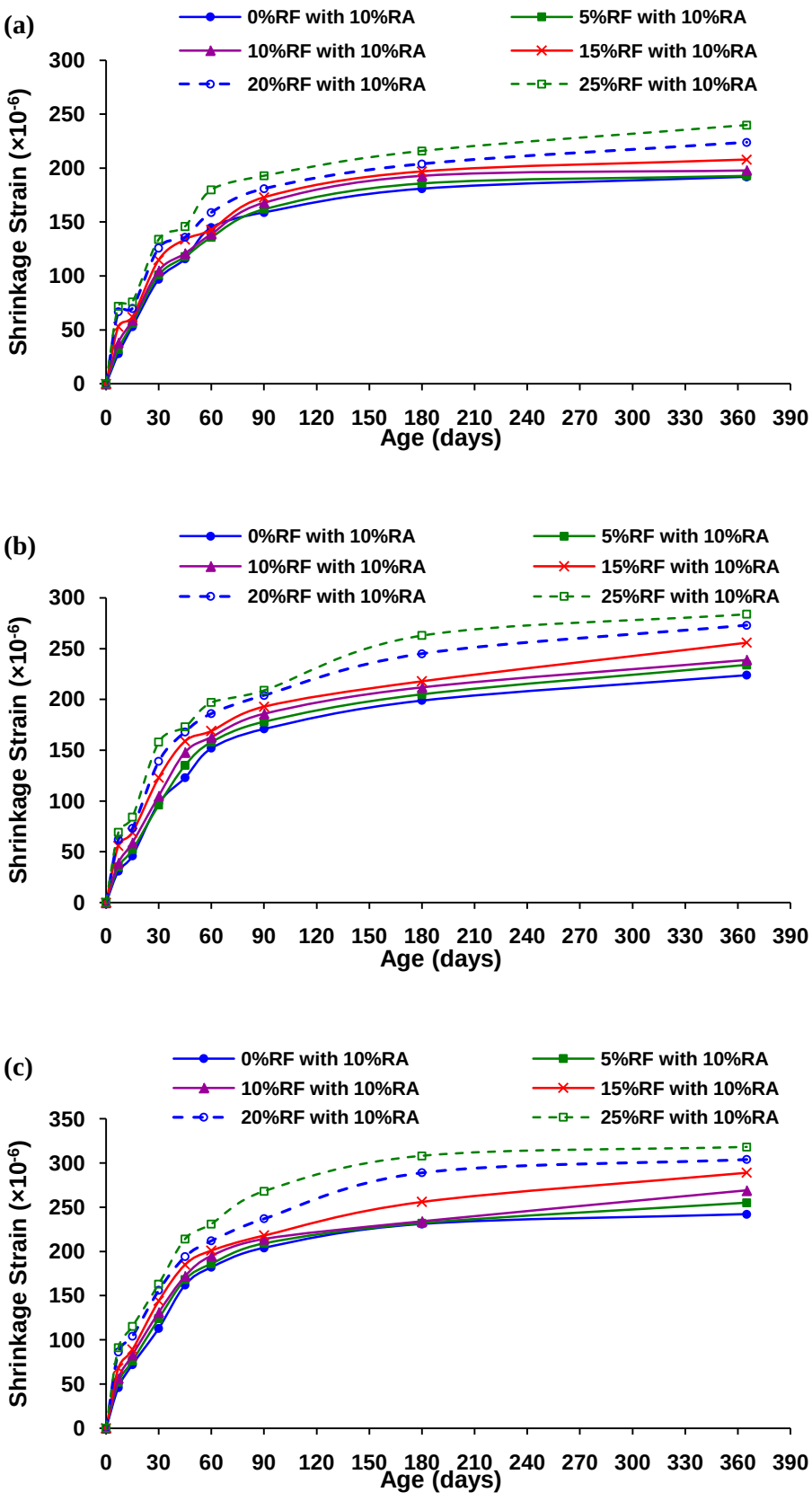

Fig. 4.16 Drying Shrinkage of hybrid concrete for w/c ratio (a) 0.35; (b) 0.45; and (c) 0.55

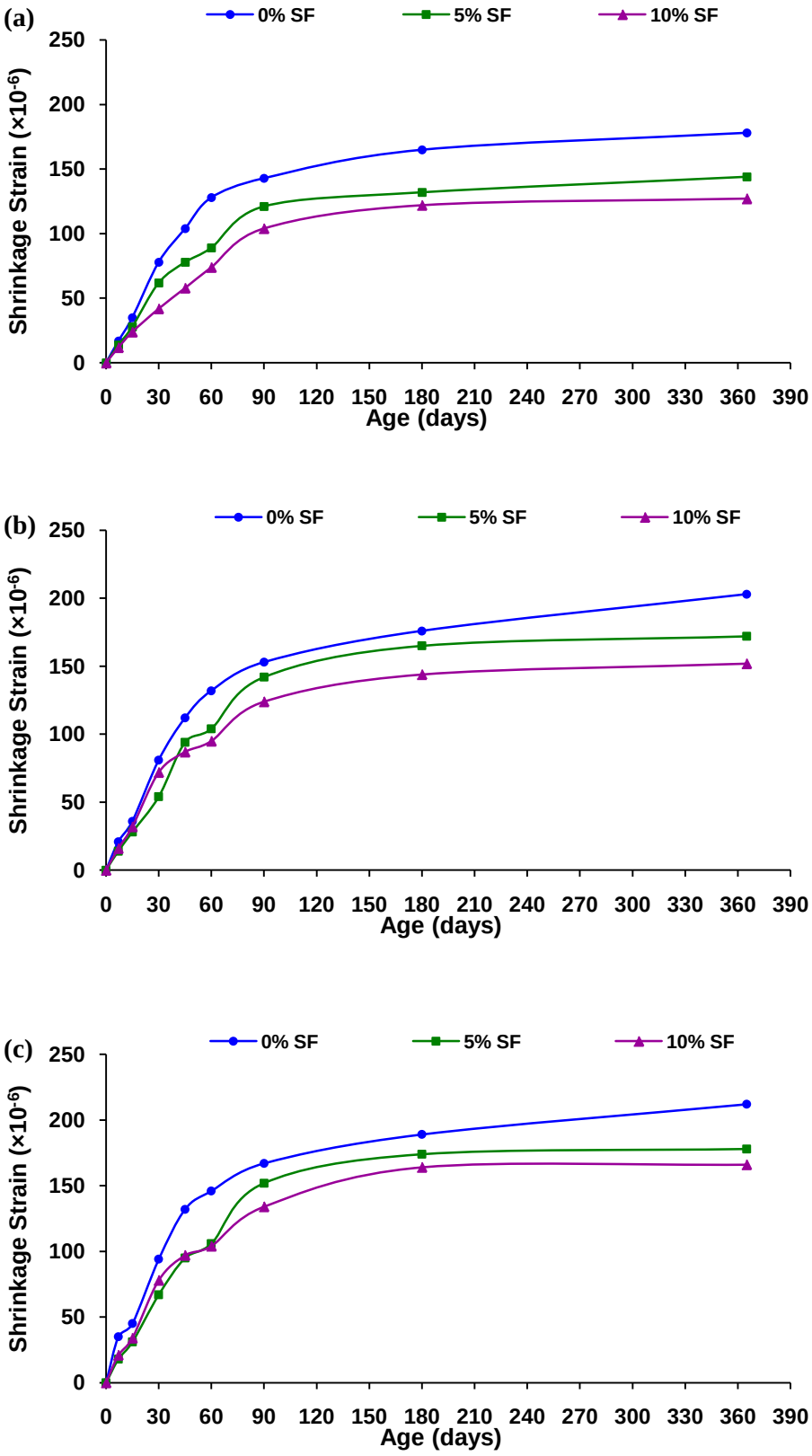

Fig. 4.17 Drying Shrinkage of 0% rubber fiber concrete with silica fume for w/c ratio (a) 0.35; (b) 0.45; and (c) 0.55

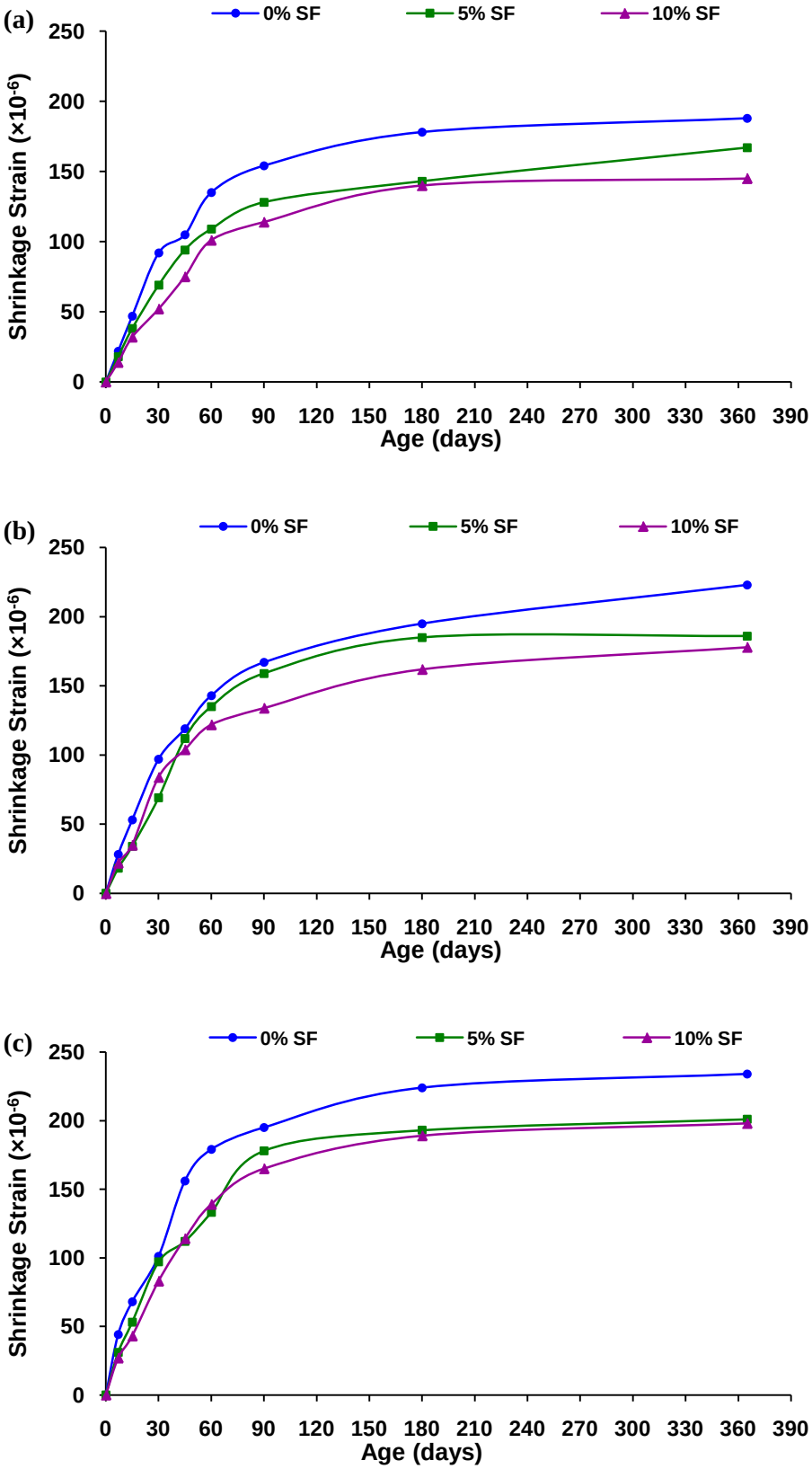

Fig. 4.18 Drying Shrinkage of 10% rubber fiber concrete with silica fume for w/c ratio (a) 0.35; (b) 0.45; and (c) 0.55

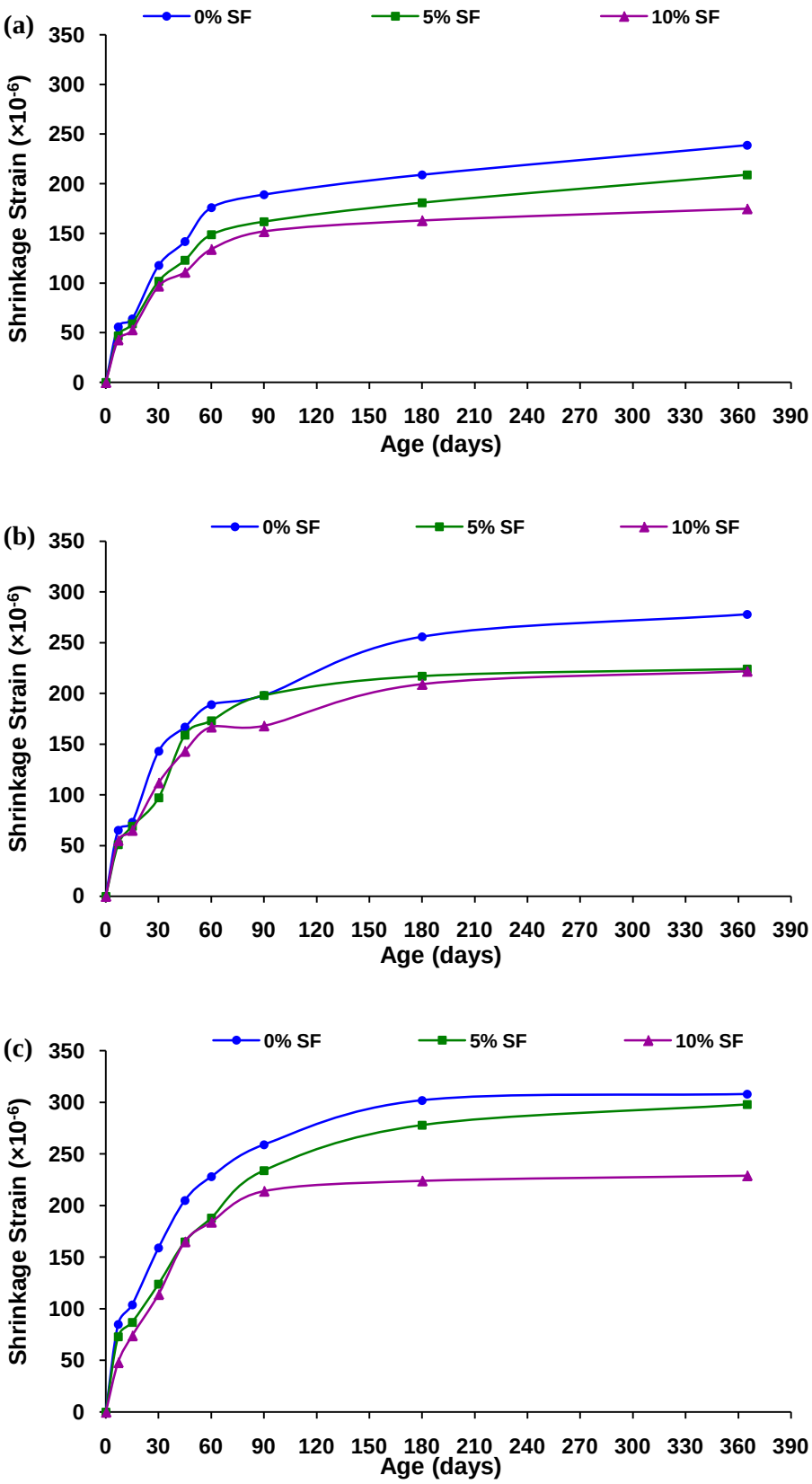

Fig. 4.19 Drying Shrinkage of 25% rubber fiber concrete with silica fume for w/c ratio (a) 0.35; (b) 0.45; and (c) 0.55

4.3.4 Carbonation

The depth of carbonation for concrete mix with w/c ratio 0.35 and varied rubber ash ratio is shown in Fig. 4.20 (a) for 14, 21, 28, 35, 42, 56 and 90 days duration (5% CO_2 exposure). Similarly, Figs. 4.20 (b) and 4.20 (c) show the depth of carbonation for concrete mix with w/c ratios 0.45 and 0.55 respectively. It can be observed that the carbonation depth increased with the increase of CO_2 exposure duration for all the selected w/c ratios and replacement levels (0% to 25%).

It can be further observed from Fig. 4.20 (a) that carbonation depth suddenly increased for the mix with 20% replacement level at 0.35 w/c ratio. This sudden increase may be due to improper compaction/workability. In the case of mix T5 (w/c ratio 0.35 and 20% replacement level of rubber ash), the compaction factor of 0.87 only was possible to be achieved at very high percentage of super plasticizer (2.6%). This reduction in workability resulted in lesser density (due to more voids) as compared to the control mix having compaction factor more than 0.92. This improper compaction of mix T5 resulted into increased carbonation depth. It may be noted that, earlier also, upto 6% increase in carbonation depth at 91 days was reported by Bravo and Brito (2012) on 15% replacement of FA by fine tyre aggregate.

The effect of partial replacement of FA by waste rubber fibers (0% to 25%) on carbonation of concrete mixes was studied. The depth of carbonation for concrete mix with w/c ratio 0.35 and varied rubber fibers ratio is shown in Fig. 4.21 (a) for CO_2 exposure of duration 14, 21, 28, 35, 42, 56 and 90 days. Similarly, Figs. 4.21 (b) and 4.21 (c) show the depth of carbonation for concrete mixes with 0.45 and 0.55 w/c ratio, respectively. It can be seen from Figs. that carbonation depth increased with the increase of CO_2 exposure duration and replacement level.

It may be noted that, earlier also, up to 46% increase in carbonation depth at 91 days was reported by Bravo and Brito (2012) on 15% replacement of coarse aggregate by tyre aggregate for which increase in water absorption was discussed as the reason. The depth of carbonation was observed to be 8.35 mm for 0.35 w/c ratio with 25% replacement level whereas at the same replacement level, the carbonation depth was observed to be 11.92 mm for 0.55 w/c ratio.

It is observed from the present study that the carbonation depth for large replacement level (25%) and high CO_2 concentration (5% for 90 days) was less than the minimum cover required (15 mm).

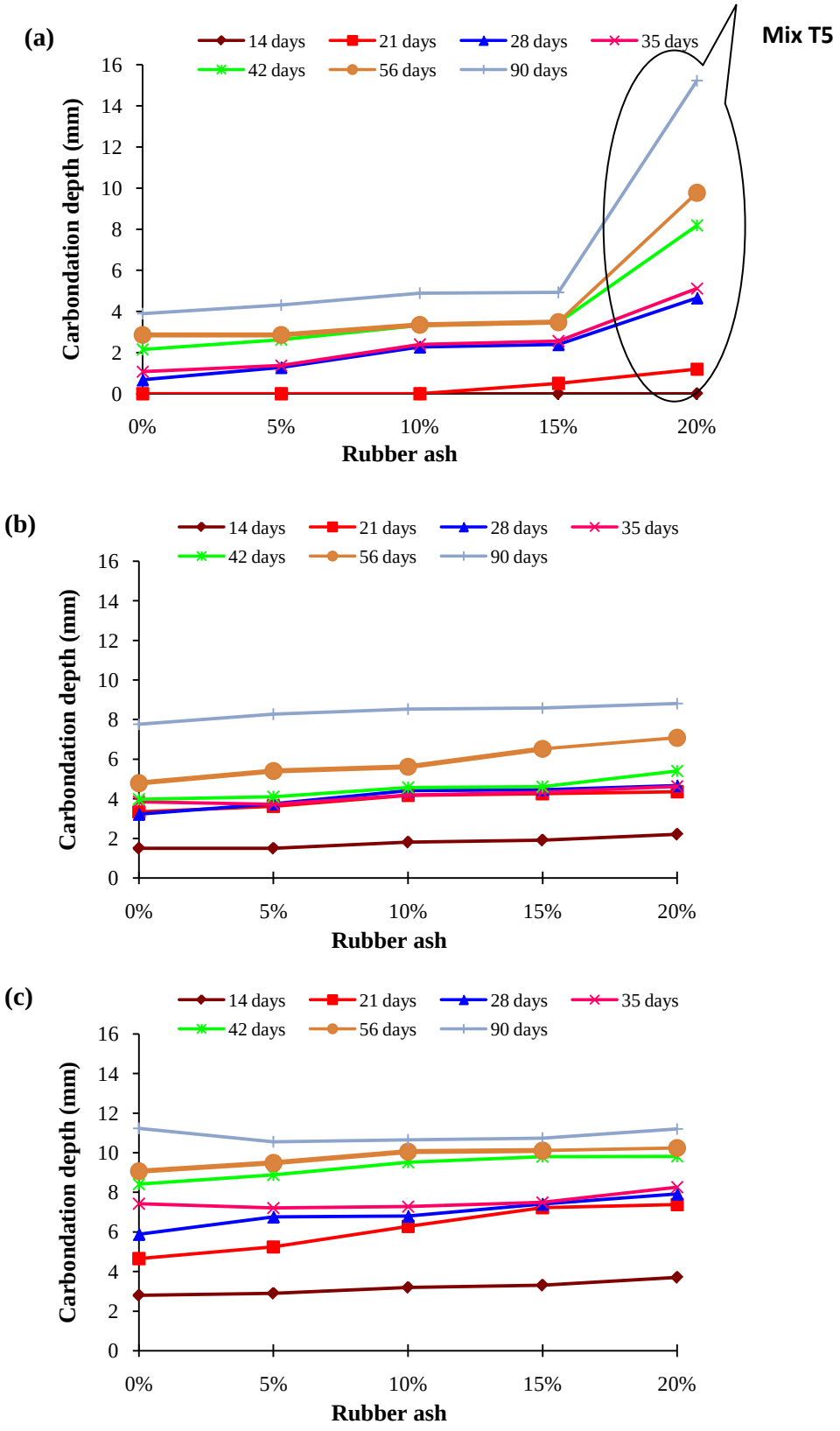

Fig. 4.20 Carbonation depth of rubber ash concrete for (a) w/c ratio 0.35; (b) w/c ratio 0.45; and (c) w/c ratio 0.55

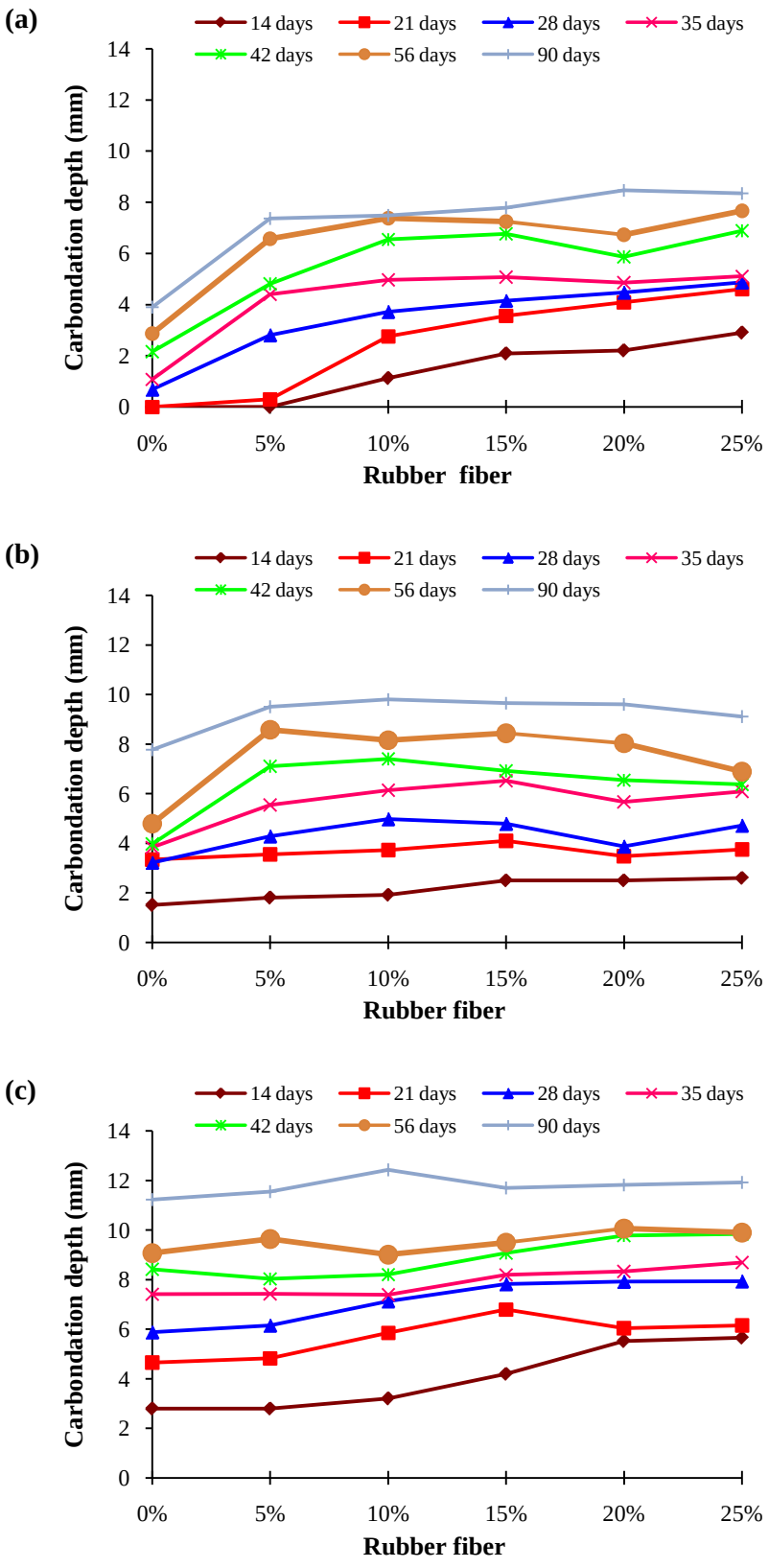

Fig. 4.21 Carbonation depth of rubber fiber concrete for w/c ratio (a) 0.35; (b) 0.45; and (c) 0.55

The effect of partial replacement of FA by combination of 10% rubber ash and varied percentage of rubber fibers (0% to 25%) on carbonation was also studied. The depth of carbonation of hybrid concrete for 0.35 w/c ratio is shown in Fig. 4.22 (a) for duration of 14, 21, 28, 35, 42, 56 and 90 days. Similarly, Figs. 4.22 (b) and 4.22 (c) shows the depth of carbonation for the hybrid concrete with w/c ratios 0.45 and 0.55 respectively.

It can be seen from the Figs. that the carbonation depth in hybrid concrete increased with increase in rubber fiber content. The carbonation depth of 10.65 mm was observed for concrete at 0.55 w/c ratio whereas at the same w/c ratio, carbonation depth of 14.0 mm was observed at 25% replacement level of FA by rubber fibers.

It may be noted from the above reported results that the carbonation depth observed in the most adverse conditions (w/c ratio 0.55, replacement level 25% and high CO_2 concentration; 5% for 90 days) is less than the minimum cover required for any reinforced cement concrete (RCC) member. Minimum concrete cover for any type of RCC member should not be less than 15 mm as per BIS 456 (2000).

The influence of SF (5% and 10%) on carbonation of concrete mixes for rubber fiber concrete (0%, 10% and 25%) for varied w/c has also been studied. The depth of carbonation for concrete mix with 0% rubber fibers for w/c ratio 0.35 and varied SF (0%, 5% and 10%) is shown in Fig. 4.23 (a) for CO_2 exposure of duration 14, 21, 28, 35, 42, 56 and 90 days. Similarly, Figs. 4.23 (b) and 4.23 (c) show the depth of carbonation for concrete mix with w/c ratios 0.45 and 0.55 respectively.

It can be observed that carbonation depth increased with the increase of CO_2 exposure duration. It can also be seen from the Figs. that the carbonation depth for any replacement level of SF by cement decreased with increase in SF content at 0% rubber fibers. The decrease in carbonation depth may be due to decrease in water absorption and water permeability as earlier observed in the present study and also due to increase in particles packing due to SF in the concrete mixture (Xue and Shinozuka 2013; Sohrabi and Karbalaie 2011). A carbonation depth of 1.8 mm was observed for 0.35 w/c ratio with 10% replacement level of SF whereas at the same replacement level, carbonation depth of 3.3 mm was observed for 0.55 w/c ratio at 90 days exposure.

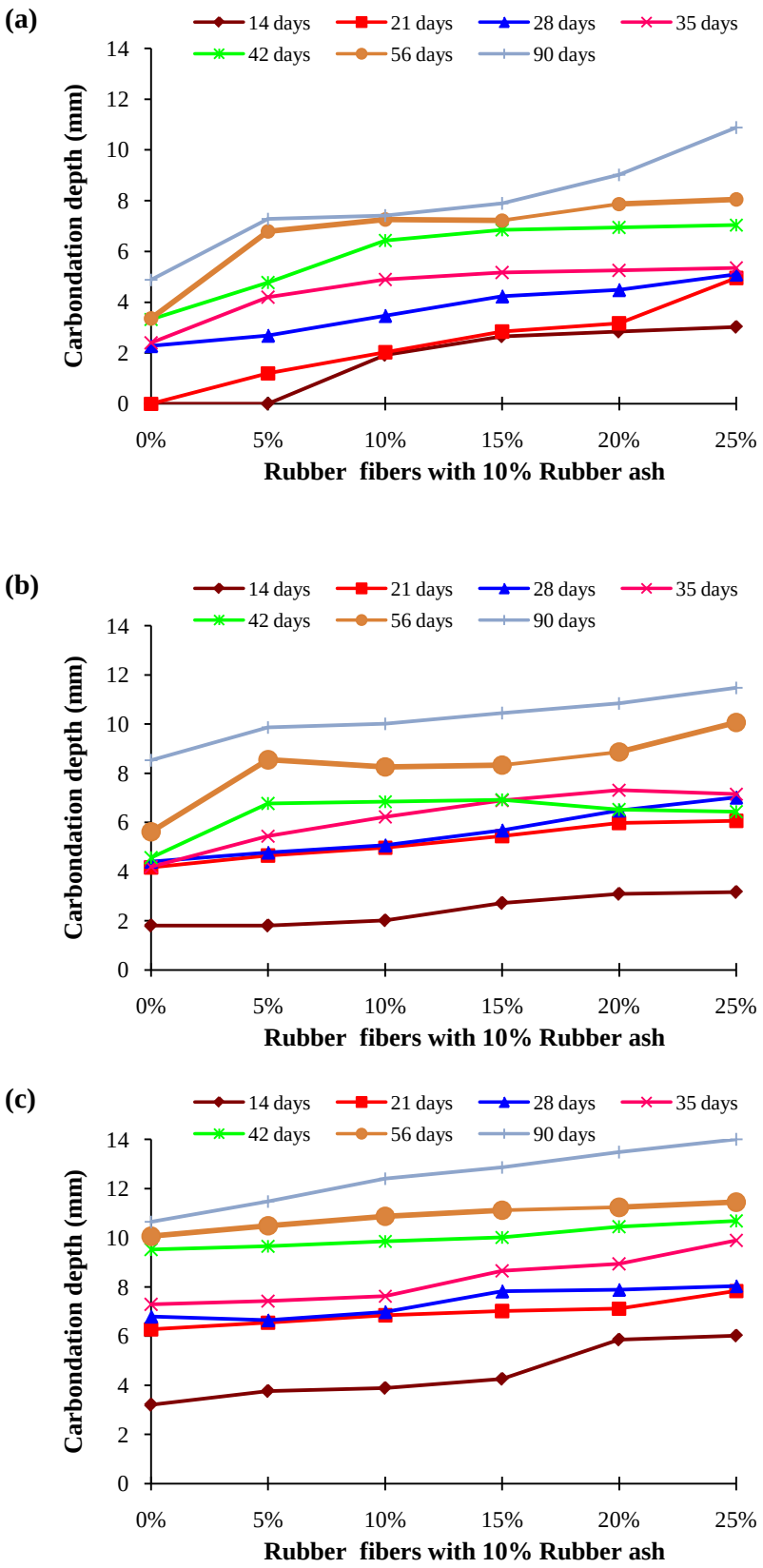

Fig. 4.22 Carbonation depth of hybrid concrete for w/c ratio (a) 0.35; (b) 0.45; and (c) 0.55

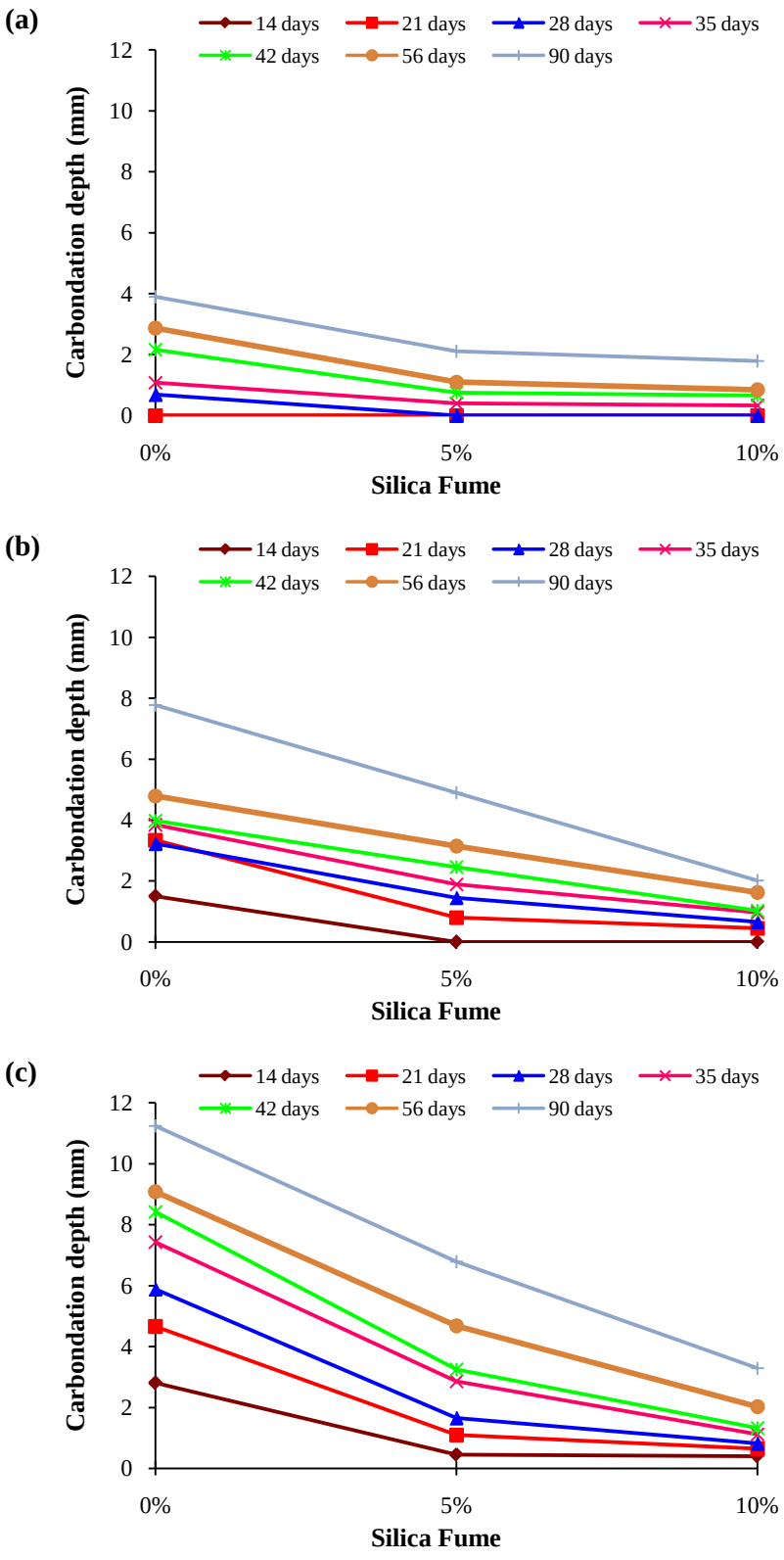

Fig. 4.23 Carbonation depth of 0% rubber fiber concrete with silica fume for w/c ratio (a) 0.35; (b) 0.45; and (c) 0.55

The depth of carbonation for concrete mix with 10% rubber fibers for w/c ratio 0.35 and varied SF (0%, 5% and 10%) is shown in Fig. 4.24 (a) for CO_2 exposure of duration 14, 21, 28, 35, 42, 56 and 90 days. Similarly, Figs. 4.24 (b) and 4.24 (c) show the depth of carbonation for concrete mix with w/c ratios 0.45 and 0.55 respectively. It can be seen from the Figs. that the carbonation depth, for 10% rubber fiber concrete, decreased with increase in SF content. The carbonation depth of 3.1 mm has been observed for 0.35 w/c ratio with 10% replacement level of SF whereas at the same replacement level, carbonation depth of 5.1 mm was observed for 0.55 w/c ratio at 90 days exposures.

The depth of carbonation for concrete mix with 25% rubber fibers for w/c ratio 0.35 and varied SF (0%, 5% and 10%) is shown in Fig. 4.25 (a) for CO_2 exposure of duration 14, 21, 28, 35, 42, 56 and 90 days. Similarly, Figs. 4.25 (b) and 4.25 (c) show the depth of carbonation for concrete mix with w/c ratios 0.45 and 0.55 respectively. It can be seen from the Figs. that the carbonation depth, for 25% rubber fiber concrete, decreased with increase in SF content. The carbonation depth of 5.6 mm has been observed for 0.35 w/c ratio with 10% replacement level of SF whereas at the same replacement level, carbonation depth of 9.0 mm was observed for 0.55 w/c ratio at 90 days exposures. The decrease in carbonation depth may be due to increase in particles packing due to SF in the concrete mixture (Xue and Shinozuka 2013; Sohrabi and Karbalaie 2011).

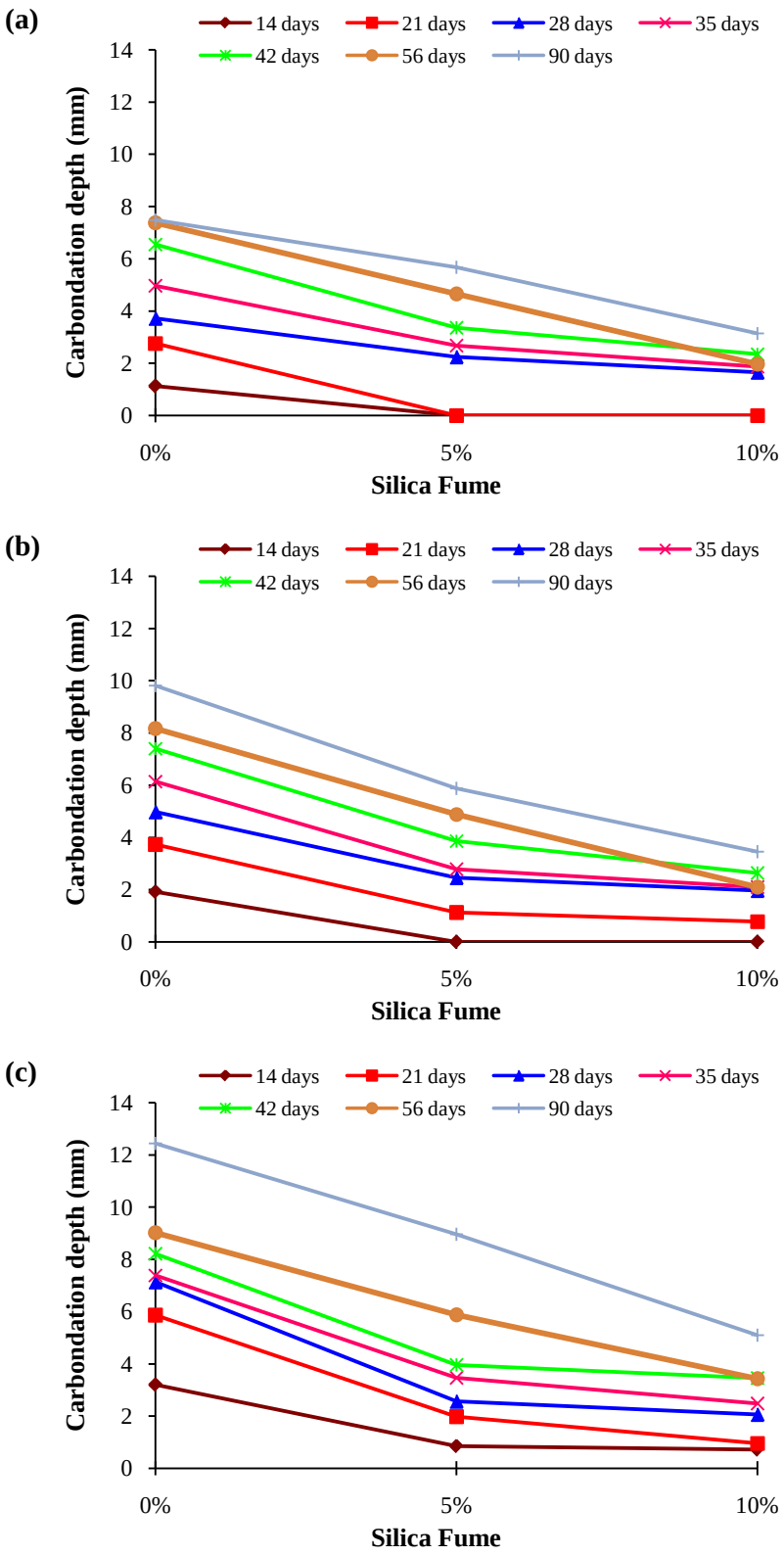

Fig. 4.24 Carbonation depth of 10% rubber fiber concrete with silica fume for w/c ratio (a) 0.35; (b) 0.45; and (c) 0.55

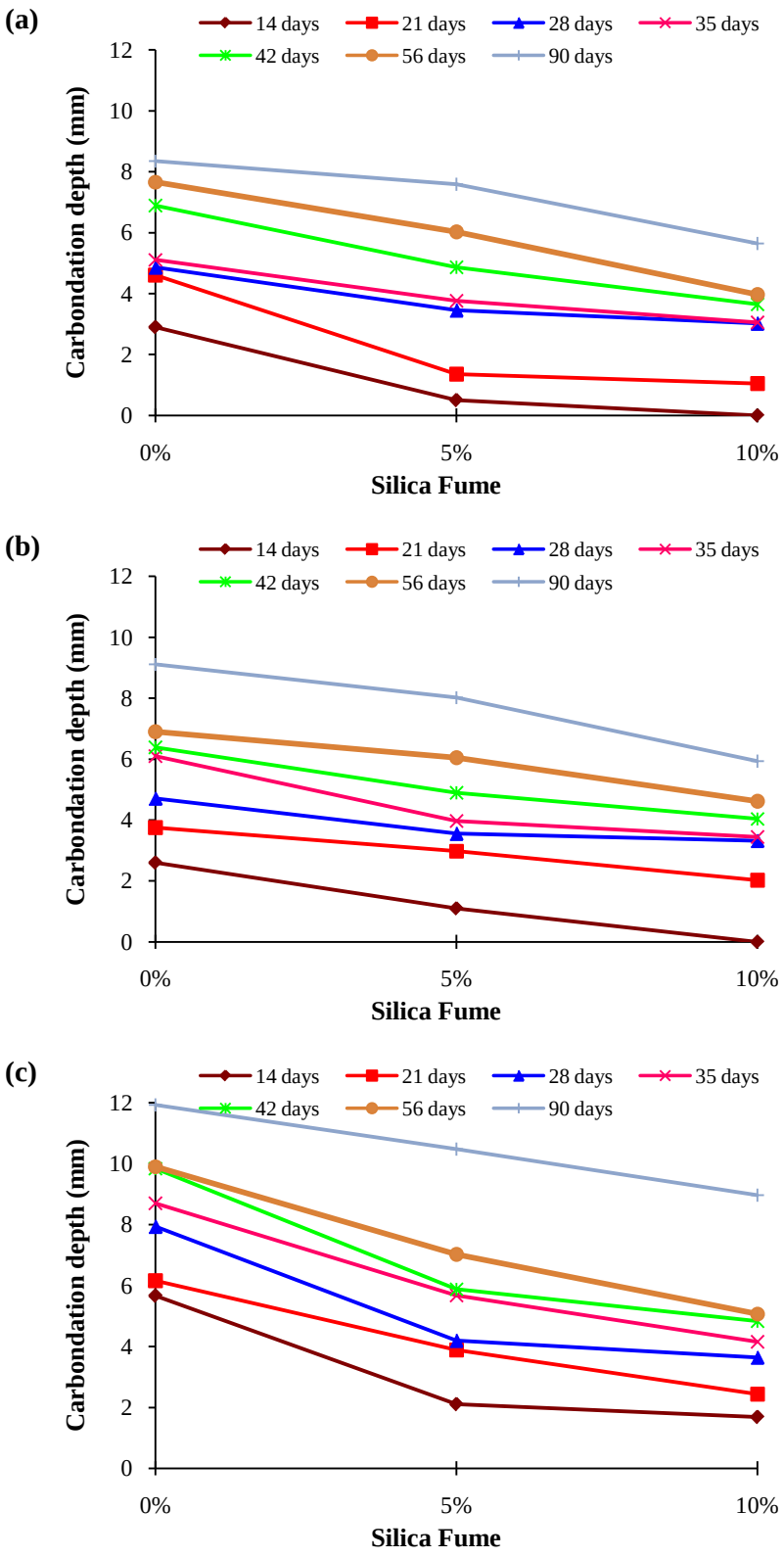

Fig. 4.25 Carbonation depth of 25% rubber fiber concrete with silica fume for w/c ratio (a) 0.35; (b) 0.45; and (c) 0.55

4.3.5 Chloride diffusion

The influence of varying rubber ash content and rubber fiber contents, with and without silica fume (SF) on the chloride diffusion is shown in Figs. 4.26-4.28. Statistical variances of results for chloride diffusion coefficient are shown in Tables 4.2.

The chloride diffusion coefficient is found to change with the increase in rubber ash and rubber fiber content. The chloride diffusion coefficient of control concrete (without rubber fiber and silica fume) decreased by 29.2%, 24.5% and 11.6% for w/c ratios 0.35, 0.45 and 0.55 respectively on 20% replacement of FA by rubber ash.

The chloride diffusion coefficient of concrete (without rubber ash and silica fume) changed by -19.6%, 18.6% and -0.8% for w/c ratios 0.35, 0.45 and 0.55 respectively on 25% replacement of FA by rubber fiber. The observed decrease for concrete (without SF) was 21.6%, 21.8% and 17.5% respectively on 10% replacement of FA by rubber ash along with 25% replacement of FA by rubber fibers. The chloride diffusion coefficient of rubber ash concrete and hybrid concrete decreased with increase in waste rubber content, however no trend of variation in diffusion coefficient are observed with change in rubber fiber content or w/c.

The diffusion coefficient was found to increase in some cases and decrease in other cases. It may be noted that Al-Akhras and Smadi (2004) reported a decrease in chloride-ion penetration on partial replacement of FA by rubber ash. The higher resistance to chloride-ion penetration was attributed to the effect of rubber ash filler packing. In the present study, rubber fibers have also been used, where the packing effect is expected to be lesser as compared to rubber ash concrete. No clear trend is therefore, observed for chloride ion penetration resistance of the rubber fiber concrete in the present study.

It may be further noted that the results of chloride permeability are not in agreement with the water permeability results. Bjegović *et al.* (2011) also observed inconsistent results for water permeability and chloride diffusion properties of rubberized concrete containing SF and fly ash as replacement of cement. According to them, the pressure applied during water permeability test neutralizes initial water repel by rubber and the lack of proper bonding allows water to flow into concrete. On the other hand, better filing of voids present between rubber and natural aggregate, causes higher homogeneity and uniform distribution of ingredients in concrete microstructure, which lowers permeability for chloride ions (Bjegović *et al.* 2011).

It is also observed from Figs. 4.26-4.28 that on replacement of cement by SF, the chloride diffusion coefficient decreased for control concrete (without rubber ash, rubber fiber and silica fume) as well as for the rubber fiber concrete. The chloride diffusion coefficient for concrete (without rubber ash and rubber fiber) decreased by 82.9%, 83.9% and 88.0% for w/c ratios 0.35, 0.45 and 0.55 respectively on 10% replacement of cement by SF. The observed decrease for rubber fiber concrete (25% rubber fiber) was 77.5%, 85.0% and 87.1% respectively. The decrease in chloride diffusion coefficient may be because of the filling of the voids, in the cement paste and between the cement paste and aggregate particles (aggregate-paste transition zones), by the SF leading to a denser microstructure (Gesoglu and Guneyisi 2007).

It is further observed from Figs. 4.26-4.28 that the chloride ion permeability of the waste rubber fiber concrete containing 10% SF is much lower than that of waste rubber fiber concrete containing 5% SF. The drastic reduction may be due to very small amount of OH^- ions in 10% SF concrete. It was observed by Torii and Kawamura (1994) that OH^- ions reduce drastically for mortar containing 10% SF in comparison to mortar containing 5% SF. The decrease in OH^- ions decreases the chloride permeability due to increase in the chloride binding capacity of concrete (Byfors 1986). Similar observations of drastic reduction in chloride permeability were made by Bentz *et al.* (2000) for the cement paste containing 6% or more SF. The increase in the fraction of the pozzolonic CSH gel (with very low diffusivity) in comparison to conventional CSH gel was cited as the reason for same, by the authors.

The control mix of w/c ratio 0.55 showed the highest value of chloride diffusion coefficient of 7.6×10^{-12} m^2/s at 28 days whereas for w/c ratio 0.35, the highest value of chloride diffusion coefficient was 3.43×10^{-12} m^2/s (indicating high resistance to chloride-ion penetration). It can also be observed that whereas the depth of water penetration increased with the increase in rubber fibers content for all three w/c ratio, the chloride diffusion coefficient was found to increase in some cases and decrease in other cases. This may be due to different locations of samples for water permeability and chloride diffusion. The water permeability was measured for the outer surface of concrete specimen, whereas the chloride diffusion coefficient test was carried out on the inner surface of the sample (a 50 mm long core from the inner side of concrete).

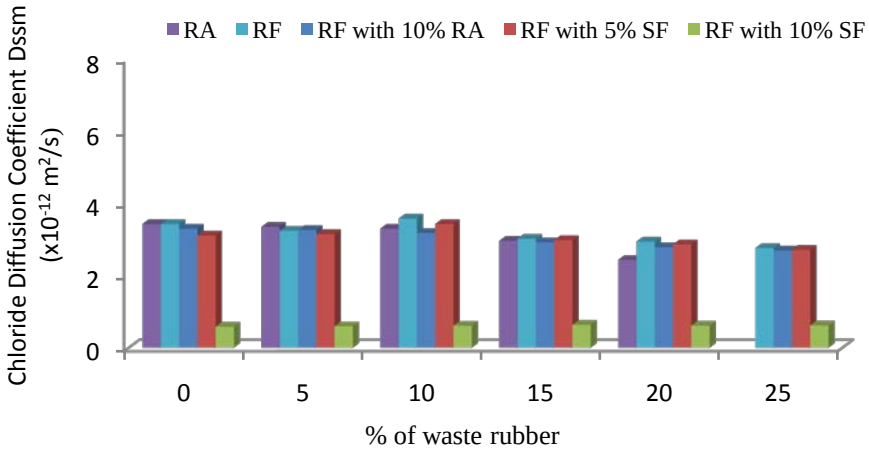

Fig. 4.26 Chloride diffusion coefficient of waste rubber concrete for 0.35 w/c ratio

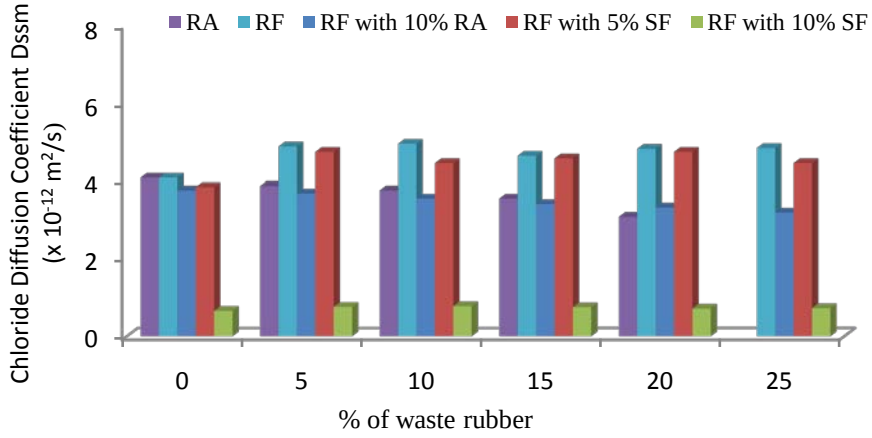

Fig. 4.27 Chloride diffusion coefficient of waste rubber concrete for 0.45 w/c ratio

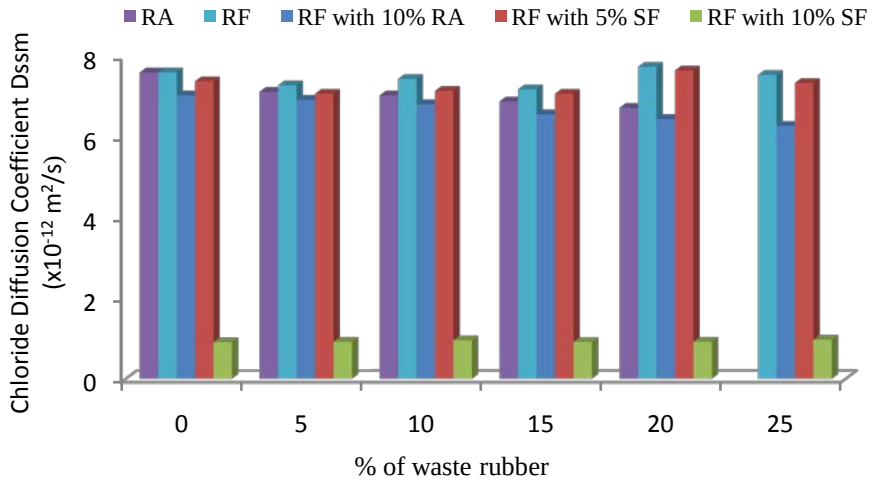

Fig. 4.28 Chloride diffusion coefficient of waste rubber concrete for 0.55 w/c ratio

Table 4.2 Statistical variances of chloride diffusion test results for waste rubber concrete

Mix No.	SD	COV	Mix No.	SD	COV	Mix No.	SD	COV	Mix No.	SD	COV	Mix No.	SD	COV
T1	0.34	0.09	R1	0.23	0.07	S1	0.24	0.07	U1	0.28	0.10	V1	0.04	0.07
T2	0.35	0.09	R2	0.08	0.02	S2	0.09	0.03	U2	0.20	0.07	V2	0.05	0.09
T3	0.10	0.03	R3	0.09	0.02	S3	0.11	0.03	U3	0.12	0.04	V3	0.03	0.05
T4	0.10	0.04	R4	0.13	0.04	S4	0.04	0.01	U4	0.12	0.04	V4	0.05	0.08
T5	0.09	0.04	R5	0.17	0.06	S5	0.16	0.06	U5	0.27	0.09	V5	0.05	0.09
T6	0.10	0.02	R6	0.09	0.03	S6	0.18	0.06	U6	0.21	0.08	V6	0.03	0.05
T7	0.03	0.01	R7	0.11	0.03	S7	0.12	0.03	U7	0.15	0.04	V7	0.06	0.09
T8	0.05	0.01	R8	0.14	0.03	S8	0.37	0.09	U8	0.04	0.01	V8	0.04	0.05
T9	0.11	0.03	R9	0.08	0.02	S9	0.19	0.06	U9	0.42	0.11	V9	0.07	0.09
T10	0.10	0.03	R10	0.10	0.02	S10	0.26	0.08	U10	0.30	0.06	V10	0.06	0.09
T11	0.18	0.02	R11	0.17	0.04	S11	0.09	0.03	U11	0.07	0.01	V11	0.08	0.11
T12	0.11	0.02	R12	0.13	0.03	S12	0.11	0.04	U12	0.19	0.04	V12	0.06	0.09
T13	0.15	0.02	R13	0.32	0.04	S13	0.21	0.03	U13	0.42	0.06	V13	0.05	0.05
T14	0.25	0.04	R14	0.10	0.01	S14	0.72	0.10	U14	0.63	0.10	V14	0.05	0.05
T15	0.15	0.02	R15	0.23	0.03	S15	0.17	0.03	U15	0.12	0.02	V15	0.06	0.06
-	-	-	R16	0.19	0.03	S16	0.17	0.03	U16	0.11	0.02	V16	0.06	0.06
-	-	-	R17	0.13	0.02	S17	0.07	0.01	U17	0.12	0.02	V17	0.05	0.05
-	-	-	R18	0.26	0.04	S18	0.14	0.02	U18	0.13	0.02	V18	0.12	0.11

Unit of SD (standard deviation) is m^2/s.

4.3.6 Corrosion

4.3.6.1 *Corrosion assessment*

a) Macrocell

The Macrocell current was measured in accordance with ASTM G109 (2005) across the 100-Ohm resistance. Positive macrocell current shows that corrosion is in progress. A minimum value of 10 μA has been considered to ensure the presence of sufficient corrosion (ASTM 2005). For control concrete (without rubber ash, rubber fiber and silica fume), the macrocell current was less than 10 μA, at all the ages (18 months) at w/c ratio 0.35 (Fig. 4.29 a). Whereas, more than 10 μA macrocell current was recorded at 16^{th} and 12^{th} month for w/c ratios 0.45 and 0.55 respectively (Figs. 4.29b-c).

Waste rubber ash concrete

The variation of macrocell current with time for waste rubber ash concrete is shown in Figs. 4.29 (a)-(c) for w/c ratios 0.35, 0.45 and 0.55 respectively. The macrocell current of waste rubber ash concrete was higher than that for the mix without rubber ash at all the ages for w/c ratio 0.35 (Fig. 4.29 a).

With the replacement of 5% and 20% FA by waste rubber ash at w/c ratio 0.35, a value of more than the 10 μA was recorded for current at 14^{th} month and 12^{th} month respectively. Similarly, for w/c ratio 0.55, a value of more than 10 μA was recorded at 8^{th} month and 10^{th} month for 5% and 20% replacement level respectively. The maximum anodic current for control mix was measured as 6.4 μA, 14.2 μA and 15.1 μA for w/c ratios 0.35, 0.45 and 0.55 respectively at 18^{th} month whereas the maximum current for 20% waste rubber ash concrete was measured as 25.4 μA, 30.8 μA and 34.5 μA respectively. From the above results, it can be reported that the inclusion of waste rubber ash leads to early initiation of corrosion.

Waste rubber fiber concrete

The variation of macrocell current with time for waste rubber fiber concrete (without silica fume) is shown in Fig. 4.30. The macrocell current for waste rubber fibers mixes was more than that for the mix without rubber fiber at all the ages for w/c ratio 0.35 (Fig. 4.30 a).

With the replacement of 5% and 25% FA by waste rubber fibers at w/c ratio 0.35, current exceeded 10 μA at 13^{th} month and 11^{th} month respectively. Similarly, for w/c ratio 0.55, current exceeded 10 μA at 10^{th} month and 9^{th} month for 5% and 25% replacement level respectively. The maximum anodic current for control mix was measured as 6.4 μA, 14.2 μA and 15.1 μA for w/c ratios 0.35, 0.45 and 0.55 respectively at 18^{th} month whereas the maximum current for 25% waste rubber fiber concrete was measured as 22.3 μA, 22.9 μA and 24.1 μA respectively . From the above results, it can be reported that the inclusion of waste rubber fiber increases the probability of early initiation of corrosion.

Hybrid concrete

The variation of macrocell current with time for hybrid concrete (10% FA replaced by rubber ash with varying percentage of FA replaced by rubber fiber) is shown in Fig. 4.31. The macrocell current of hybrid concrete was more than that of the mix without rubber fiber and rubber ash at all the ages for w/c ratio 0.35 (Fig. 4.31 a).

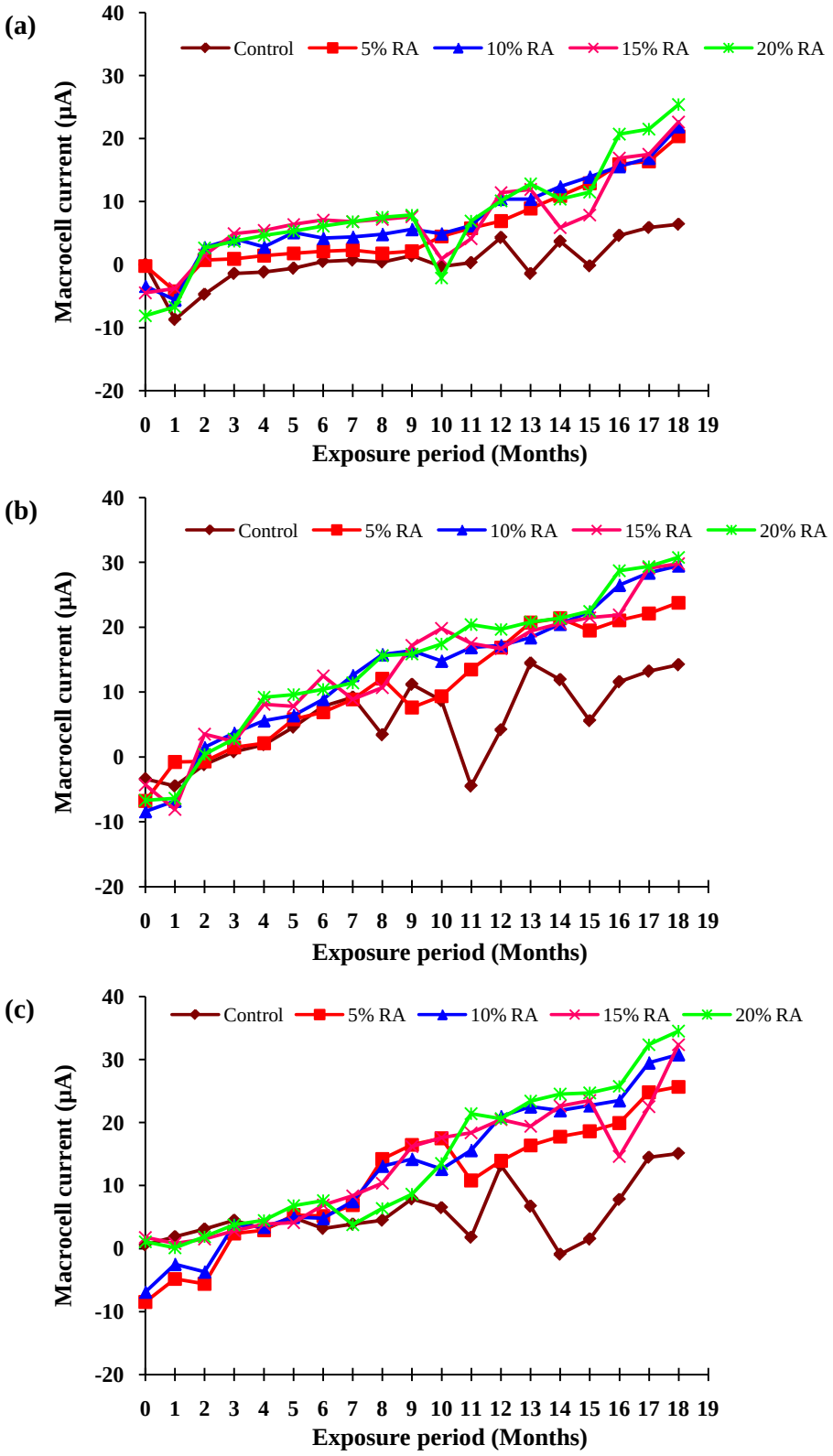

Fig. 4.29 Macrocell current of rubber ash concrete for w/c ratio (a) 0.35; (b) 0.45; and (c) 0.55

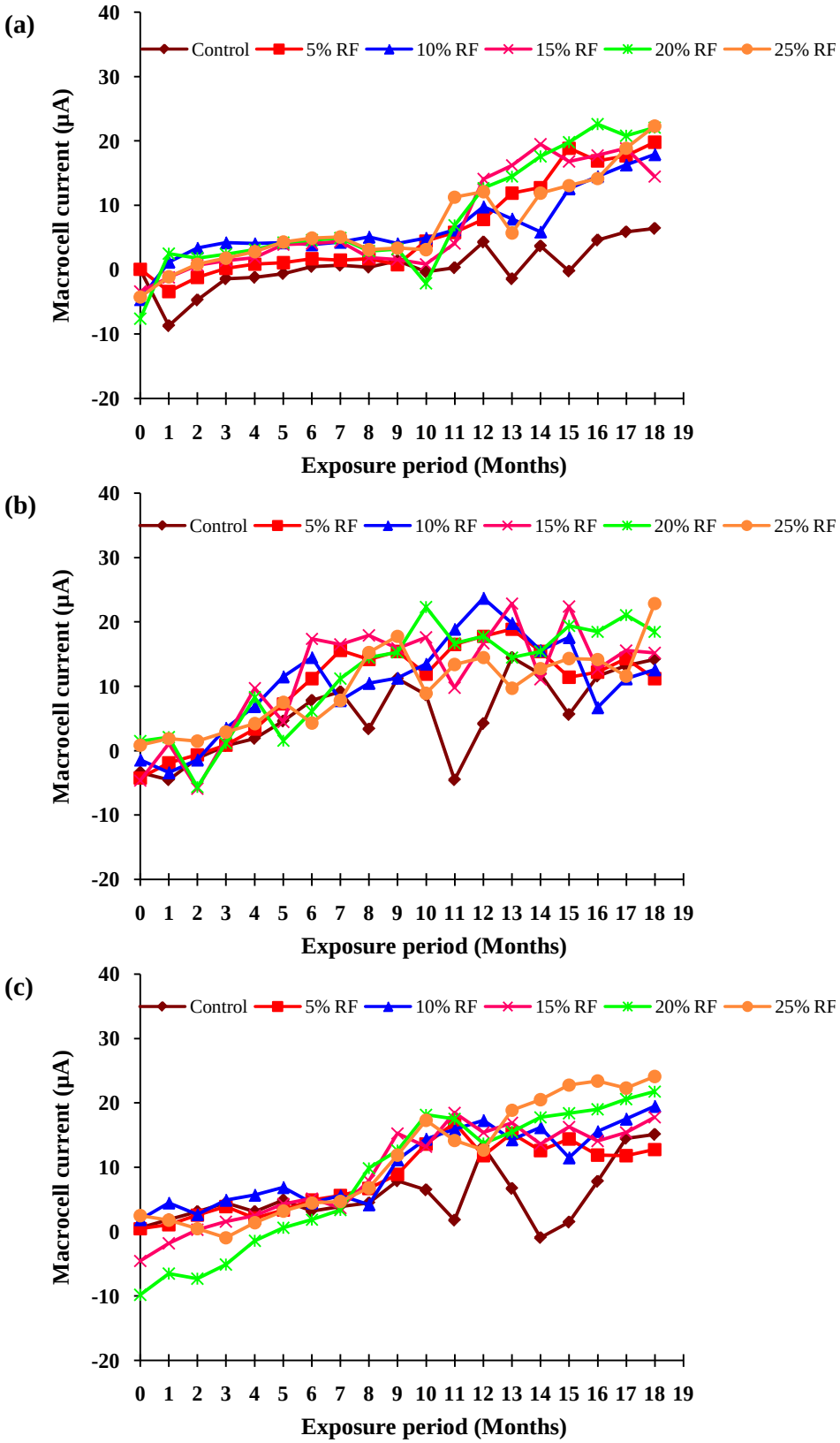

Fig. 4.30 Macrocell current of rubber fiber concrete without silica fume for w/c ratio (a) 0.35; (b) 0.45; and (c) 0.55

With the replacement of 5% and 25% FA by waste rubber fibers in hybrid concrete at w/c ratio 0.35, the current exceeded 10 μA at 12th month and 7th month respectively. Similarly, for w/c ratio 0.55, the current exceeded 10 μA at 10th month and 9th month for 5% and 25% replacement level respectively. The maximum anodic current for concrete (without SF) was measured as 6.4 μA, 14.2 μA and 15.1 μA for w/c ratios 0.35, 0.45 and 0.55 respectively at 18th month whereas the maximum current for hybrid concrete (10% FA replaced by rubber ash along with 25% FA replaced by rubber fiber) was measured as 26.7 μA, 32.9 μA and 36.4 μA respectively. From the above results, it can be reported that the inclusion of waste rubber ash and rubber fiber increases the probability of early initiation of corrosion.

Silica fume concrete with 0% rubber fibers

The variation of macrocell current with time for silica fume concrete containing no rubber fibers is shown in Figs. 4.32(a)-(c). First, consider the case of 0% SF. The macrocell current was less than 10 μA at all the ages (18 months) for w/c ratio 0.35 (Fig. 4.32a). However, more than 10 μA macrocell current was recorded at 9th and 12th month for w/c ratios 0.45 and 0.55 respectively (Figs. 4.32b-c). Next, consider 5% silica fume concrete. The macrocell current was less than 10 μA at all the ages (18 months) for w/c ratio 0.35 (Fig. 4.32a). However, more than 10 μA macrocell current was recorded at 13th and 12th month for w/c ratios 0.45 and 0.55 respectively (Figs. 4.32b-c). Next, consider 10% silica fume concrete. The macrocell current was less than 10 μA at all the ages (18 months) for w/c ratio 0.35 (Fig. 4.32a). However, more than 10 μA macrocell current was recorded at 18th month for both the w/c ratios 0.45 and 0.55 (Figs. 4.32b-c). It is observed from the above results that corrosion initiation in SF concrete takes place at later age as compared to concrete without SF.

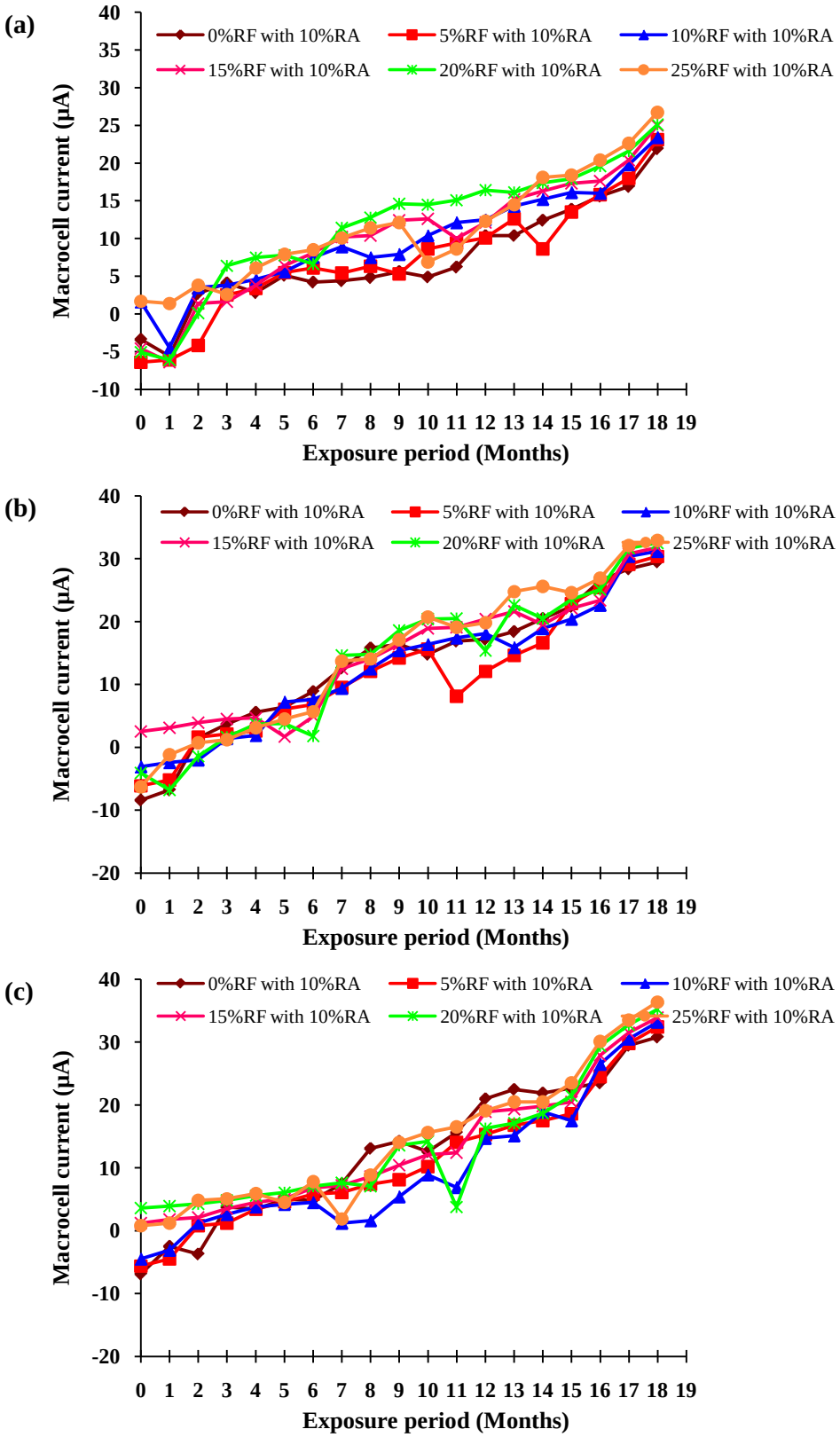

Fig. 4.31 Macrocell current of hybrid concrete for w/c ratio (a) 0.35; (b) 0.45; and (c) 0.55

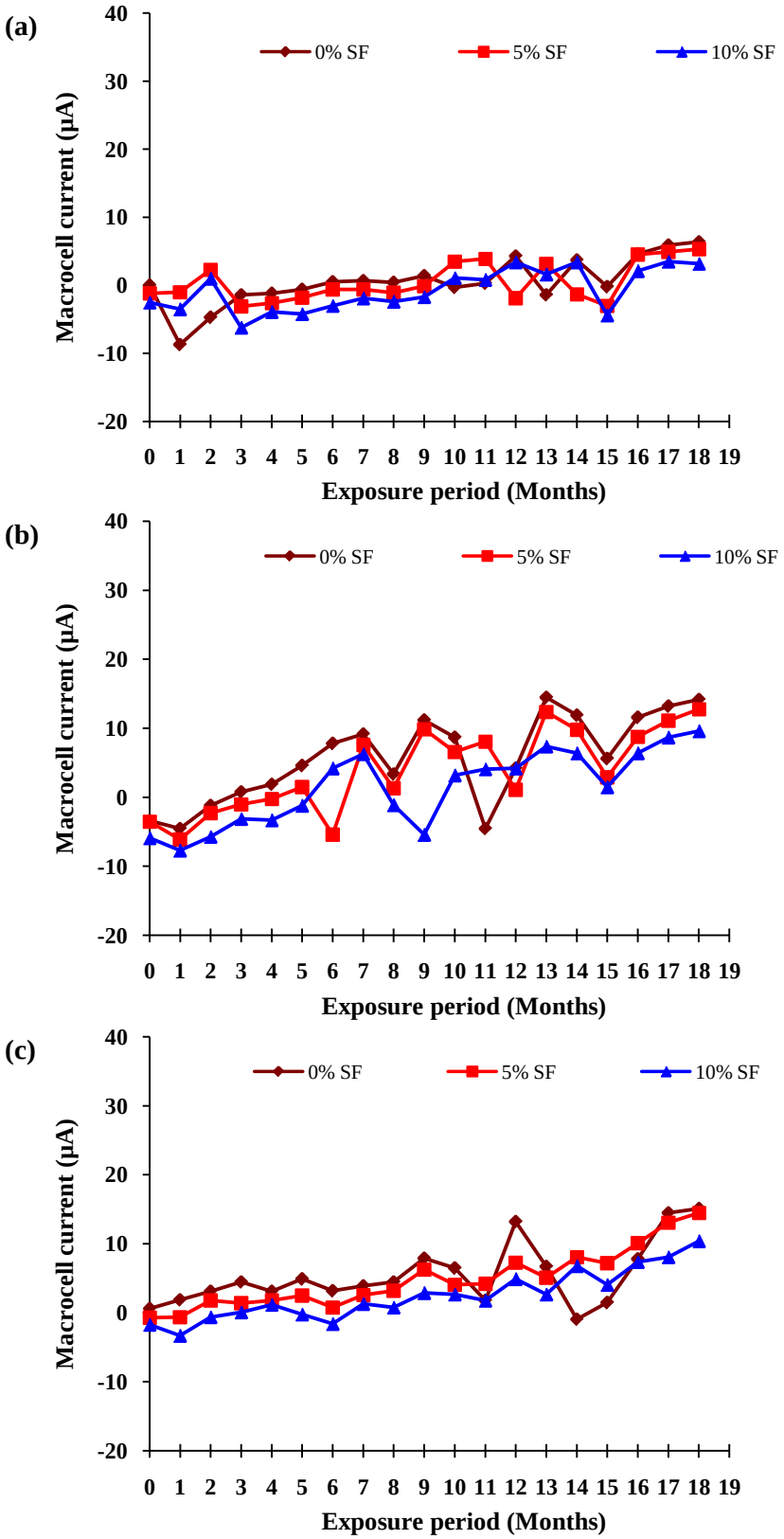

Fig. 4.32 Macrocell current of 0% rubber fiber concrete with silica fume for w/c ratio (a) 0.35; (b) 0.45; and (c) 0.55

Silica fume concrete with 10% rubber fibers

The variation of macrocell current with time for silica fume concrete containing 10% rubber fibers is shown in Figs. 4.33(a)-(c).

First, consider the case of 0% SF. The macrocell current was more than 10 μA at 15th month for w/c ratio 0.35 (Fig. 4.33a). However, more than 10 μA macrocell current was recorded at 5th and 9th month for w/c ratios 0.45 and 0.55 respectively (Figs. 4.33b-c).

Next, consider 5% SF concrete. The macrocell current was more than 10 μA at 18th month for w/c ratio 0.35 (Fig. 4.33a). However, more than 10 μA macrocell current was recorded at 10th month for both w/c ratios 0.45 and 0.55 respectively (Figs. 4.33b-c).

Next, consider 10% SF concrete. The macrocell current was more than 10 μA at 18th month for w/c ratio 0.35 (Fig. 4.33a). However, more than 10 μA macrocell current was recorded at 17th month for both the w/c ratios 0.45 and 0.55 (Figs. 4.33b-c). It is observed from the above results that corrosion initiation in SF concrete takes place at later age as compared to concrete without SF.

Silica fume concrete with 25% rubber fibers

The variation of macrocell current with time for SF concrete containing 25% rubber fibers is shown in Figs. 4.34(a)-(c).

First, consider the case of 0% SF. The macrocell current was more than 10 μA at 11th month for w/c ratio 0.35 (Fig. 4.34a). However, more than 10 μA macrocell current was recorded at 8th and 9th month for w/c ratios 0.45 and 0.55 respectively (Figs. 4.34b-c).

Next, consider 5% SF concrete. The macrocell current was more than 10 μA at 14th month for w/c ratio 0.35 (Fig. 4.34a). However, more than 10 μA macrocell current was recorded at 8th month and 9th month for w/c ratios 0.45 and 0.55 respectively (Figs. 4.34b-c).

Next, consider 10% SF concrete. The macrocell current was more than 10 μA at 17th month for w/c ratio 0.35 (Fig. 4.34a). However, more than 10 μA macrocell current was recorded at 9th month and 10th for both the w/c ratios 0.45 and 0.55 (Figs. 4.34b-c). It is observed from the above results that corrosion initiation in SF concrete will be stated at later age as compared to concrete without SF.

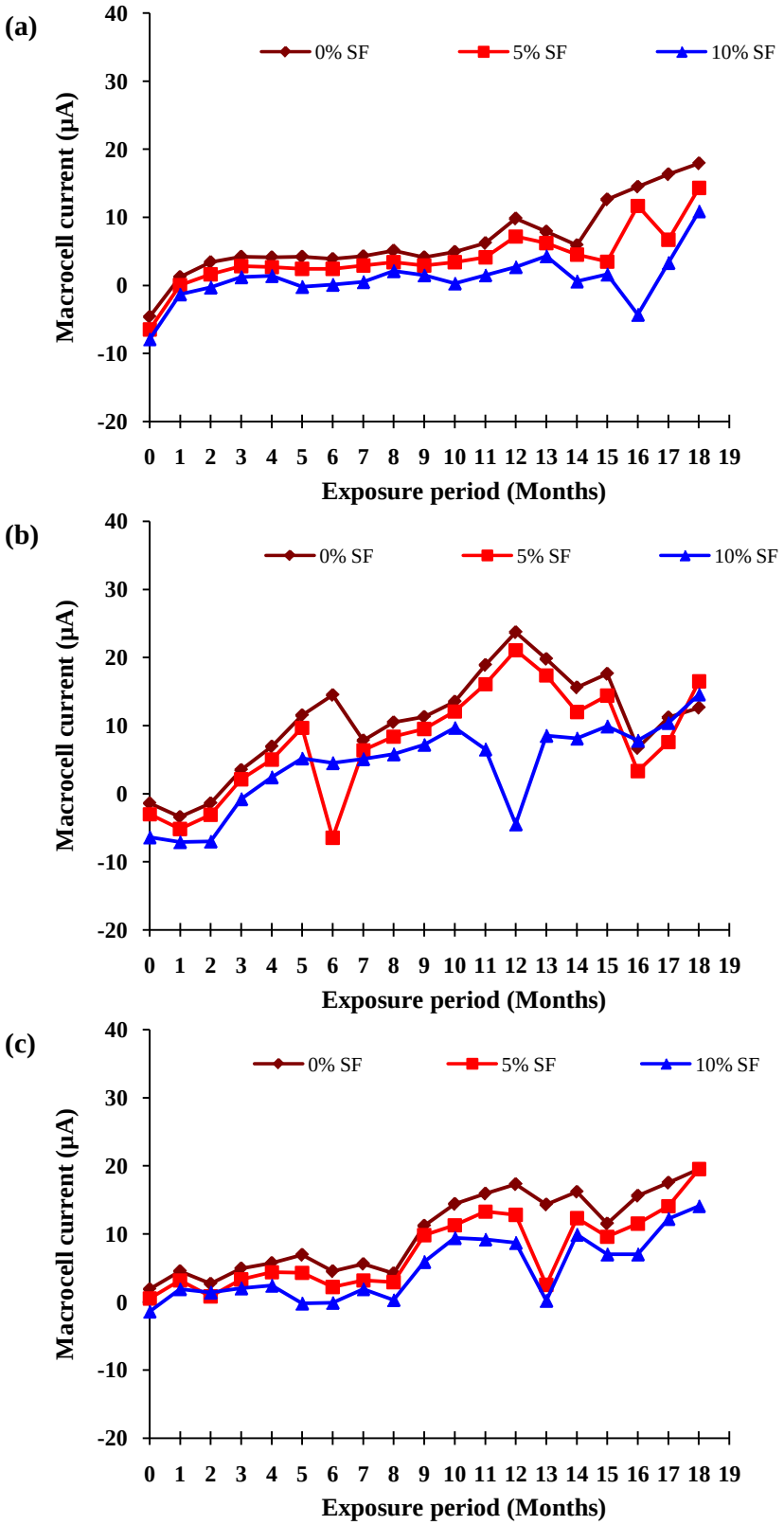

Fig. 4.33 Macrocell current of 10% rubber fiber concrete with silica fume for w/c ratio (a) 0.35; (b) 0.45; and (c) 0.55

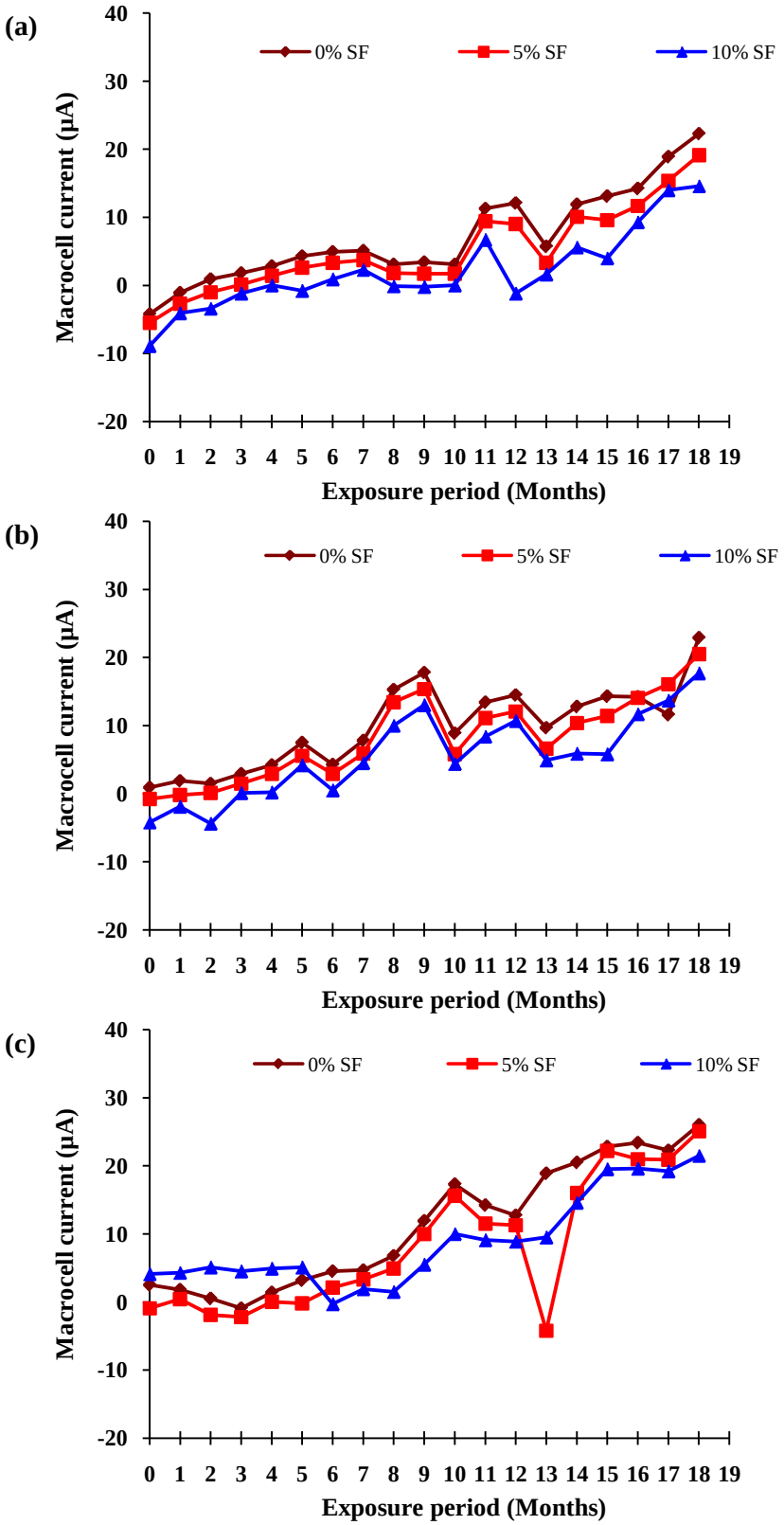

Fig. 4.34 Macrocell current of 25% rubber fiber concrete with silica fume for w/c ratio (a) 0.35; (b) 0.45; and (c) 0.55

b) Half-cell potential measurements

The half-cell potential was measured in accordance with ASTM C876 (ASTM 2009) between top bar and reference electrode. The results of half-cell potential readings with time for waste rubber concrete is shown in Figs. 4.35-4.40 for w/c ratios 0.35, 0.45 and 0.55 respectively. As stated earlier, according to ASTM (2009), there is more than 90% probability that corrosion in reinforcing steel bars will occur where potentials are more negative than -350 mV.

For control concrete (without rubber ash, rubber fiber and SF), the potential was less negative than -350 mV at all the ages (18 months) at w/c ratio 0.35 (Fig. 4.35a). Whereas, more negative than -350 mV potential was recorded at 13^{th} and 12^{th} month for w/c ratios 0.45 and 0.55 respectively (Figs. 4.35b-c).

Waste rubber ash concrete

The variation of half-cell potential with time for waste rubber ash concrete (without SF) is shown in Fig. 4.35. The half-cell potential of waste rubber ash concrete was higher than that for the control mix at all the ages for w/c ratio 0.35 (Fig. 4.35a).

With the replacement of 5% and 20% FA by waste rubber ash at w/c ratio 0.35, more negative than -350 mV potential was recorded at 16^{th} month and 14^{th} month respectively. Similarly, for w/c ratio 0.55, the potential became more negative than -350 mV at 13^{th} month for both 5% and 20% replacement levels. The maximum potential for control mix was measured as -298 mV, -376 mV and -414 mV for w/c ratios 0.35, 0.45 and 0.55 respectively at 18^{th} month whereas the maximum potential for 20% waste rubber ash concrete was measured as -398 mV, -438 mV and -472 mV respectively. It is observed from the above results that the inclusion of waste rubber ash increases the probability of early initiation of corrosion.

Waste rubber fiber concrete

The variation of half-cell potential with time for waste rubber fiber concrete (without SF) is shown in Fig. 4.36. The half cell potential of waste rubber fiber concrete was higher than that for the mix without rubber fiber at all the ages for w/c ratio 0.35 (Fig. 4.36 a).

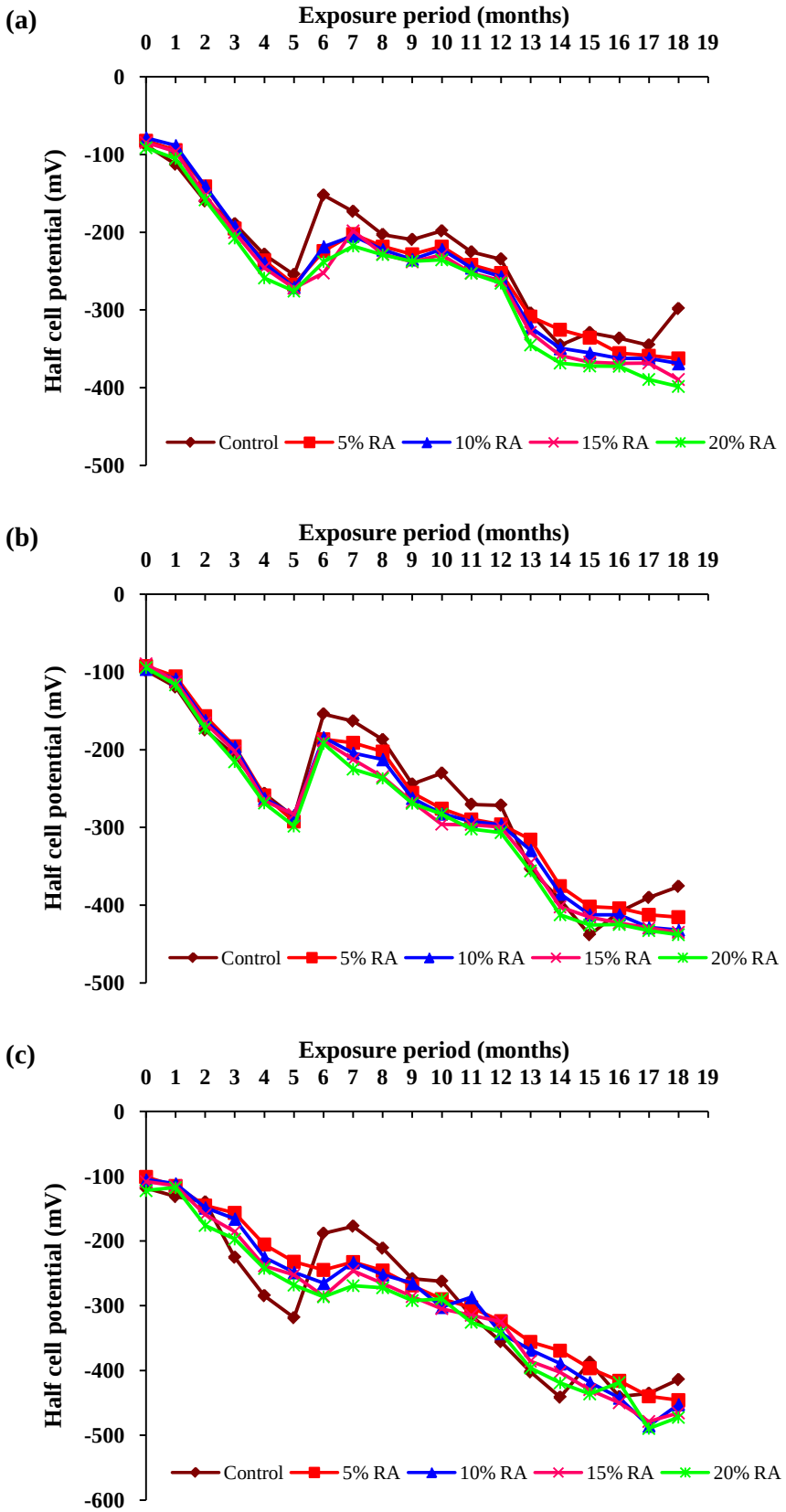

Fig. 4.35 Half-cell potential of rubber ash concrete for w/c ratio (a) 0.35; (b) 0.45; and (c) 0.55

With the replacement of 5% and 25% FA by waste rubber fiber at w/c ratio 0.35, more negative than -350 mV potential was recorded at 14th month and 13th month respectively. Similarly, for w/c ratio 0.55, the potential became more negative than -350 mV at 12th month and 11th month for 5% and 20% replacement level respectively. The maximum potential for control mix was measured as -298 mV, -376 mV and -414 mV for w/c ratios 0.35, 0.45 and 0.55 respectively at 18th month whereas the maximum potential for 25% waste rubber fiber concrete was measured as -391 mV, -455 mV and -482 mV respectively. It is observed from the above results that the inclusion of waste rubber fiber increases the probability of early initiation of corrosion.

Hybrid concrete

The variation of half-cell potential with time for hybrid concrete (10% FA replaced by rubber ash with varying percentage of FA replaced by rubber fiber) is shown in Fig. 4.37. The potential of hybrid concrete was higher than that for the control mix at all the ages for w/c ratio 0.35 (Fig. 4.37 a).

With the replacement of 5% and 25% FA by waste rubber fiber in hybrid concrete at w/c ratio 0.35, more negative than -350 mV potential was recorded at 14th month in both the replacements. Similarly, for w/c ratio 0.55, the potential became more negative than -350 mV at 13th month and 12th month for 5% and 25% replacement level respectively.

The maximum potential for control mix was measured as -298 mV, -376 mV and -414 mV for w/c ratios 0.35, 0.45 and 0.55 respectively at 18th month whereas the maximum potential for hybrid concrete (10% FA replaced by rubber ash along with 25% FA replaced by rubber fiber) was measured as -397 mV, -462 mV and -489 mV respectively. It is observed from the above results that the inclusion of waste rubber ash and rubber fiber increases the probability of early initiation of corrosion.

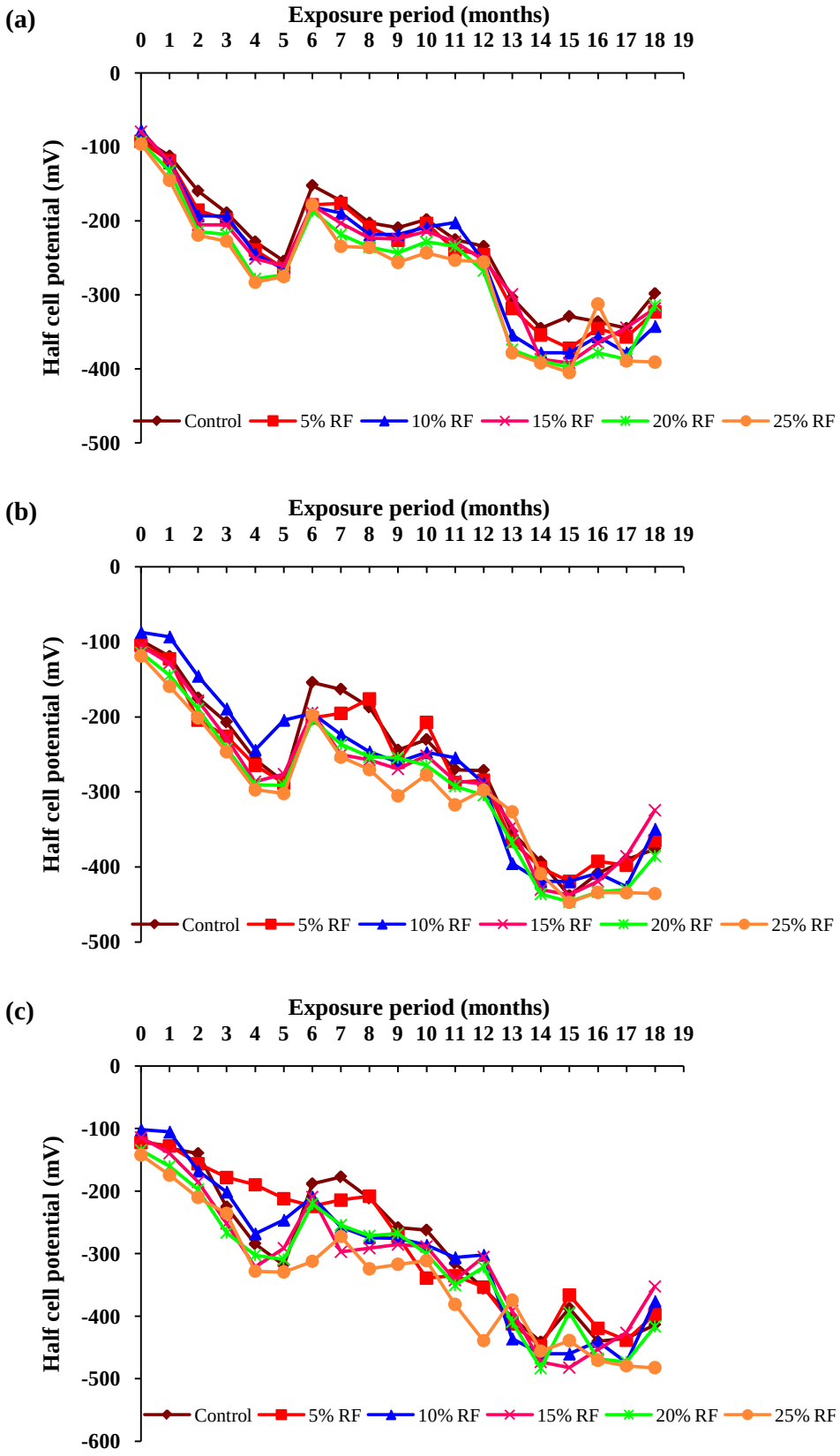

Fig. 4.36 Half-cell potential of rubber fiber concrete without silica fume for w/c ratio (a) 0.35; (b) 0.45; and (c) 0.55

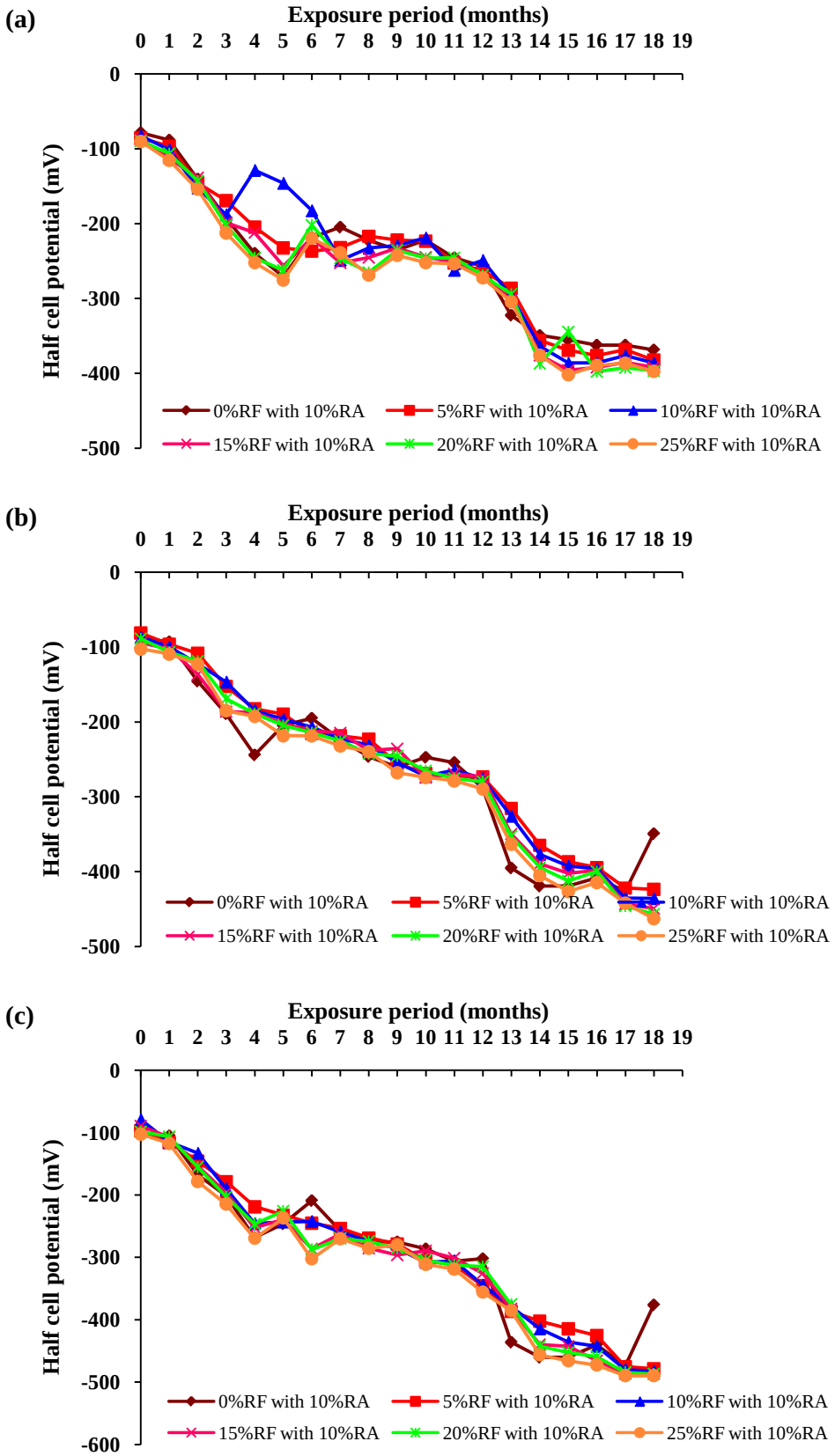

Fig. 4.37 Half-cell potential of hybrid concrete for w/c ratio (a) 0.35; (b) 0.45; and (c) 0.55

Silica fume concrete with 0% rubber fibers

The variation of half-cell potential with time for silica fume concrete containing no rubber fibers is shown in Figs. 4.38(a)-(c). First, consider the case of 0% SF. The potential was less negative than -350 mV at all ages for w/c ratio 0.35 (Fig. 4.38a). However, more negative than -350 mV potential was recorded at 13^{th} and 12^{th} month for w/c ratios 0.45 and 0.55 respectively (Figs. 4.38b-c). Next, consider 5% SF concrete. The potential was less negative than -350 mV at all ages for w/c ratio 0.35 (Fig. 4.38a). However, more negative than -350 mV potential was recorded at 18^{th} and 16^{th} month for w/c ratios 0.45 and 0.55 respectively (Figs. 4.38b-c). Next, consider 10% SF concrete. The potential was less negative than -350 mV at all ages for all three w/c ratios 0.35, 0.45 and 0.55 (Fig. 4.38).

Silica fume concrete with 10% rubber fibers

The variation of half-cell potential with time for silica fume concrete containing 10% rubber fibers is shown in Figs. 4.39(a)-(c). First, consider the case of 0% SF. The half cell potential was found to more negative than -350 mV at 13^{th} month for all three w/c ratios 0.35, 0.45 and 0.55 (Fig. 4.39a-c). Next, consider 5% SF concrete. The half cell potential was less negative than -350 mV at all ages for w/c ratio 0.35 (Fig. 4.39a). However, more negative than -350 mV half cell potential difference was recorded at 17^{th} month for both w/c ratios 0.45 and 0.55 (Figs. 4.39b-c). Next, consider 10% SF concrete. The half cell potential was less negative than -350 mV at all ages for all three w/c ratios 0.35,0.45 and 0.55 (Fig. 4.39).

Silica fume concrete with 25% rubber fibers

The variation of half-cell potential with time for SF concrete containing 25% rubber fibers is shown in Figs. 4.40(a)-(c). First, consider the case of 0% SF. The potential was found to be more negative than -350 mV at 13^{th} month for w/c ratio 0.35 (Fig. 4.40a). However, more negative than -350 mV potential was recorded at 14^{th} and 11^{th} month for w/c ratios 0.45 and 0.55 respectively (Figs. 4.40b-c). Next, consider 5% SF concrete. The potential was found to be more negative than -350 mV at 15^{th} month for w/c ratio 0.35 (Fig. 4.40a). Further, more negative than -350 mV potential, was recorded at 15^{th} and 11^{th} month for w/c ratios 0.45 and 0.55 respectively (Figs. 4.40b-c). Next, consider 10% SF concrete. The potential was less negative than -350 mV at all ages for w/c ratios 0.35 and 0.45 (Fig. 4.40a-b), whereas more negative than -350 mV potential was recorded at 18^{th} month for w/c ratio 0.55 (Fig. 4.40c).

It is clear from the above results that corrosion initiation in SF concrete takes place at a later age as compared to concrete without SF.

The maximum half cell potential for 0% rubber fibers were measured as -376 mV, -354 mV and -275 mV on 0%, 5% and 10% replacement of cement by SF for w/c ratio 0.45 respectively at 18^{th} month whereas the corresponding maximum half cell potential for 25% waste rubber fibers were measured as -435 mV, -372 mV and -323 mV.

A decrease in the macrocell currents as well as the half-cell was observed at some instants which may be due to: (i) the formation of corrosion products on the steel surface, restricting further corrosion (Vedalakshmi *et al.* 2008); and (ii) filling of pores with water resulting in lack of oxygen (Raupach 1996).

4.3.7 Acid attack

a) Visual Observations

A white layer was found to be deposited on cube specimen exposed to sulphuric acid which indicated the formation of Gypsum. The deterioration of the edges of concrete cubes specimen was also found to increase with the increase in duration of immersion in sulphuric acid. The deterioration was more in control mix as compared to rubberised concrete.

Most particles, of FA and cement, on the surface were observed to be dislocated due to effect of hydrochloric acid. The effect of hydrochloric acid on deterioration was almost same for control mix and rubberized concrete. The deterioration was more in case of hydrochloric acid as compared to the sulphuric acid.

The reaction of hydrochloric acid with $Ca(OH)_2$ produces $CaCl_2$ having a high fusibility which might be responsible for more deterioration.

Deterioration decreased with increase in silica fume concrete which may be attributed to the reduced permeability and more dense structure of silica fume concrete.

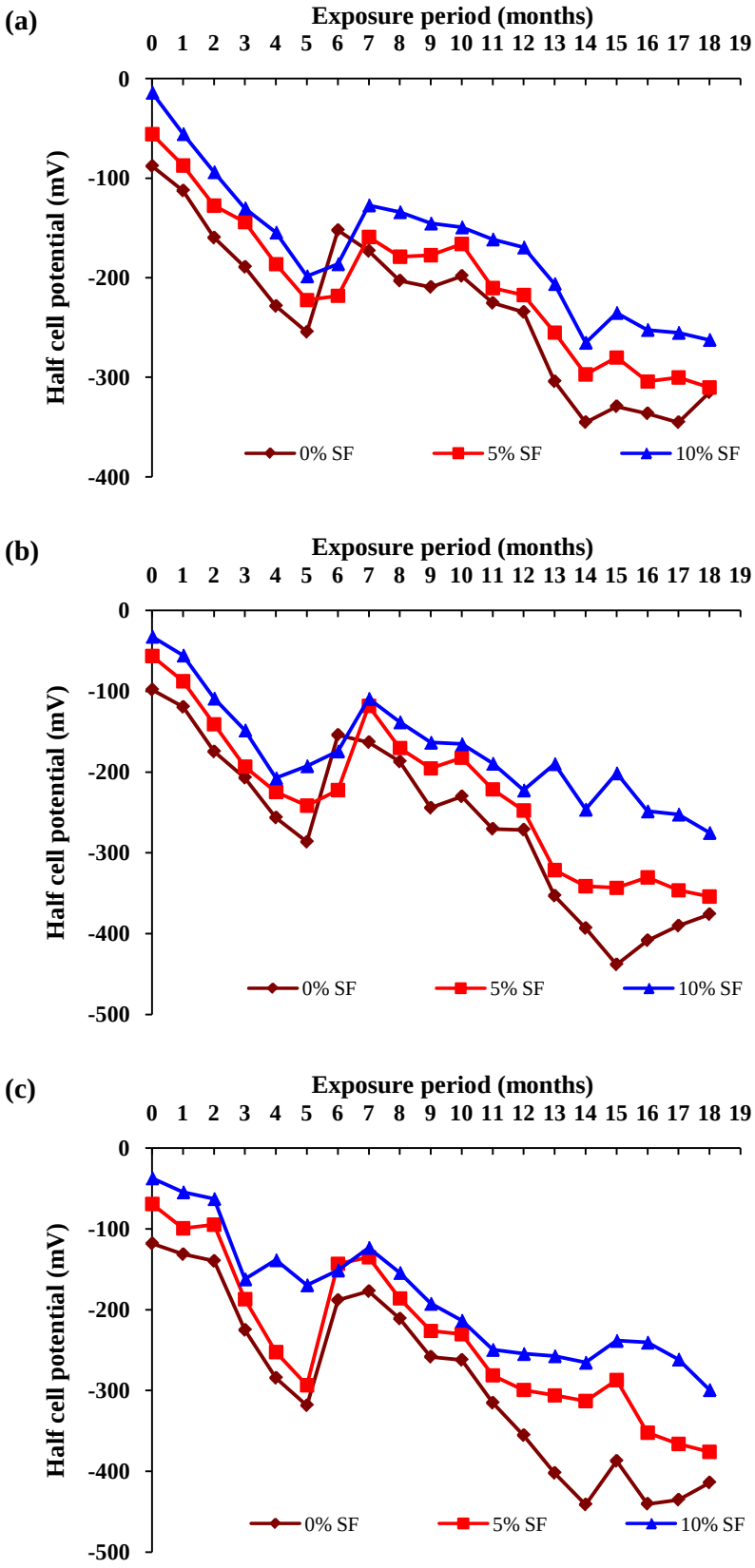

Fig. 4.38 Half-cell potential of 0% rubber fiber concrete with silica fume w/c ratio (a) 0.35; (b) 0.45; and (c) 0.55

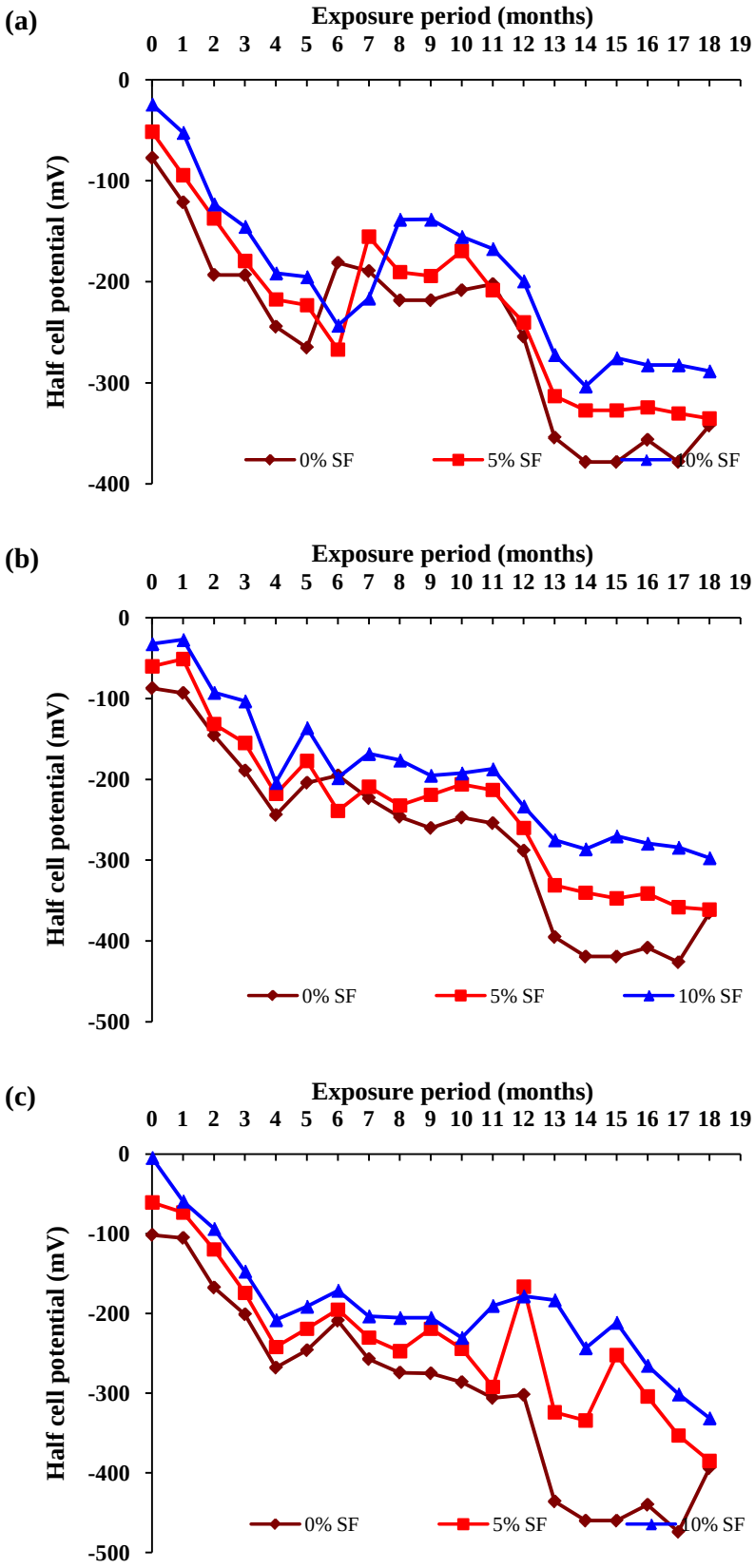

Fig. 4.39 Half-cell potential of 10% rubber fiber concrete with silica fume for w/c ratio (a) 0.35; (b) 0.45; and (c) 0.55

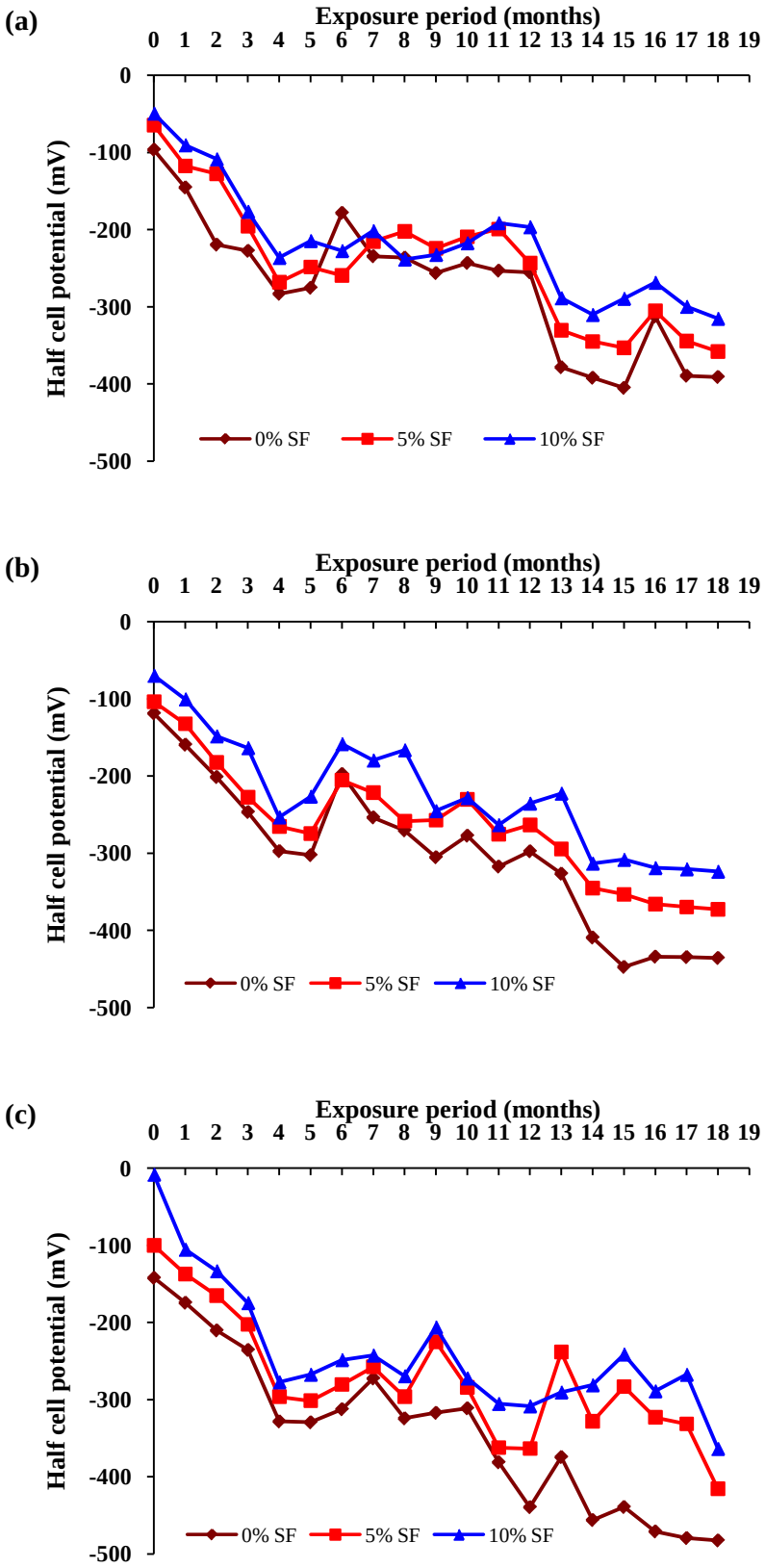

Fig. 4.40 Half-cell potential of 25% rubber fiber concrete with silica fume for w/c ratio (a) 0.35; (b) 0.45; and (c) 0.55

b) Mass loss in sulphuric acid

The change in mass of the waste rubber concrete exposed to sulphuric acid at 28 days is shown in Figs. 4.41-4.46 respectively. It is seen from the Figs. that the mass of concrete specimens decreased with the increase of immersion time in sulphuric acid for all three w/c ratios. The change in mass was almost same for control mix and waste rubber concrete. It is also observed from the Figs. that mass loss of control concrete (without rubber ash, rubber fiber and SF) increased from 4.1%, 4.1% and 5.0% to 14.2%, 16.2% and 18.7% for w/c ratios 0.35, 0.45 and 0.55 respectively on increasing the immersion period from 7 days to 180 days.

It is observed from Fig. 4.41 that mass loss (on 180 days immersion in sulphuric acid) of concrete (without rubber fiber and SF) decreased from 14.2%, 16.2% and 18.7% to 13.7%, 15.8% and 18.5% for w/c ratios 0.35, 0.45 and 0.55 respectively on 20% replacement of FA by rubber ash. Whereas the mass loss (on 180 days immersion in sulphuric acid) of concrete (without rubber ash and SF) increased from 14.2%, 16.2% and 18.7% to 14.4%, 16.6% and 19.6% respectively on 25% replacement of FA by rubber fibers.

It is observed from Fig. 4.43 that mass loss (on 180 days immersion in sulphuric acid) of hybrid concrete decreased from 13.7%, 16.0% and 18.6% to 13.5%, 15.8% and 18.5% for w/c ratios 0.35, 0.45 and 0.55 respectively on 25% replacement of FA by rubber fibers.

It may be noted that, earlier also, upto 35% increase in mass loss was reported by Azevedo *et al.* (2012) on 15% replacement of sand by rubber waste whereas Raghavan *et al.* (1998) reported little effect of alkaline environment on rubber shreds.

It is observed from Fig. 4.44 that mass loss (on 180 days immersion in sulphuric acid) of concrete (without rubber ash and rubber fiber) decreased from 14.2%, 16.2% and 18.7% to 12.1%, 12.3% and 13.0% for w/c ratios 0.35, 0.45 and 0.55 respectively on 10% replacement of cement by SF.

It is observed from Fig. 4.45 that mass loss (on 180 days immersion in sulphuric acid) of 10% rubber fiber concrete decreased from 13.2%, 16.0% and 19.2% to 12.5%, 12.9% and 13.6% for w/c ratios 0.35, 0.45 and 0.55 respectively on 10% replacement of cement by SF. Whereas, the mass loss (on 180 days immersion in sulphuric acid) of 25% rubber fiber concrete decreased from 14.1%, 16.7% and 19.6% to 12.6%, 12.7% and 13.5% for w/c ratios 0.35, 0.45 and 0.55 respectively on 10% replacement of cement by SF (Fig. 4.46).

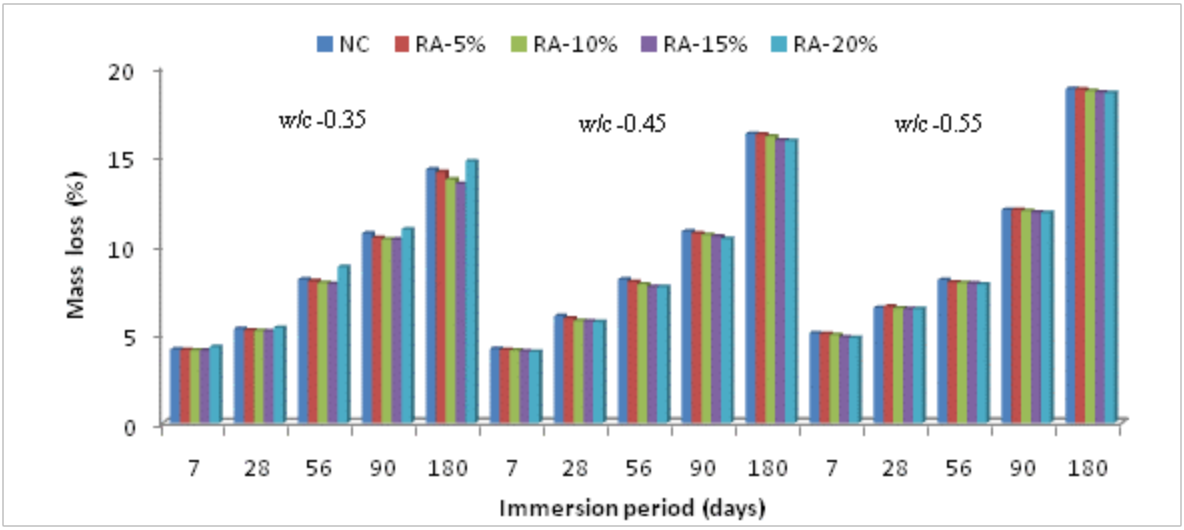

Fig. 4.41 Mass loss of rubber ash concrete in sulphuric acid

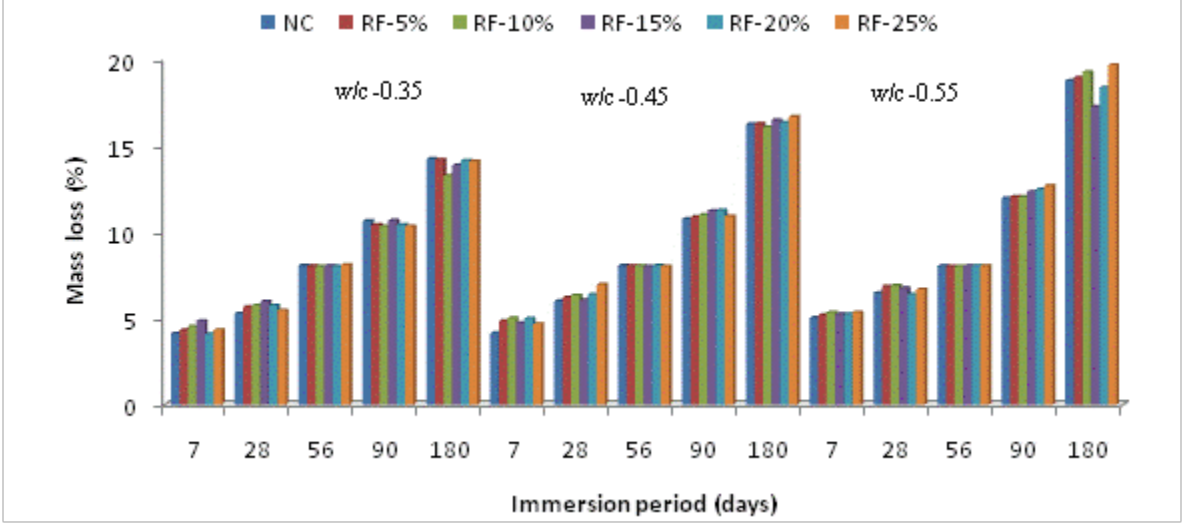

Fig. 4.42 Mass loss of rubber fiber concrete without silica fume in sulphuric acid

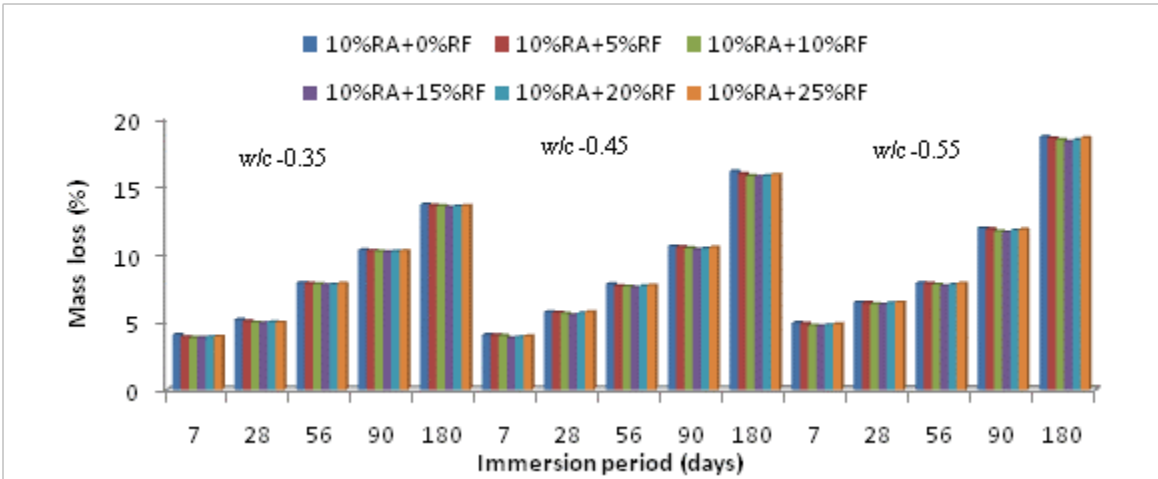

Fig. 4.43 Mass loss of hybrid concrete in sulphuric acid

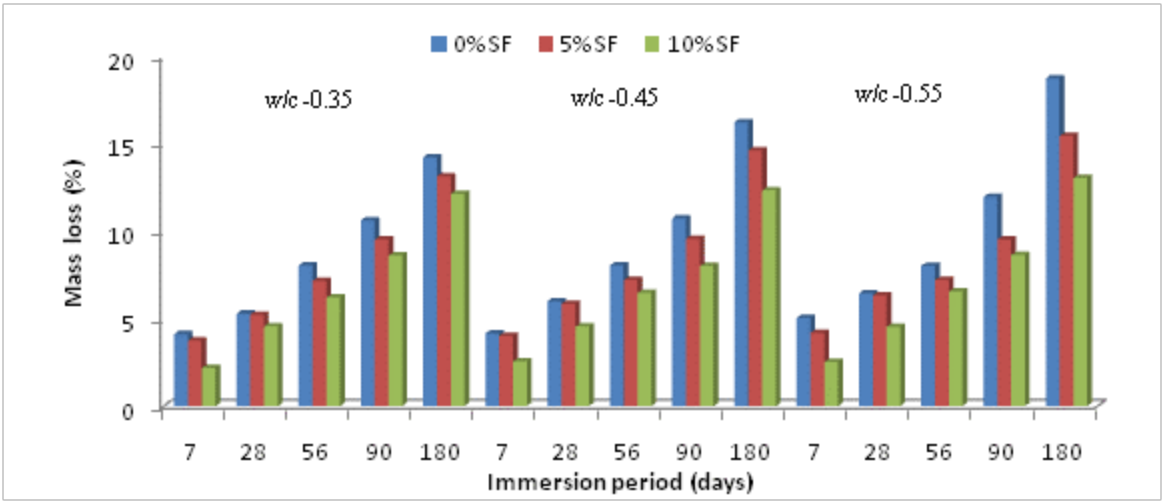

Fig. 4.44 Mass loss of 0% rubber fiber concrete with silica fume in sulphuric acid

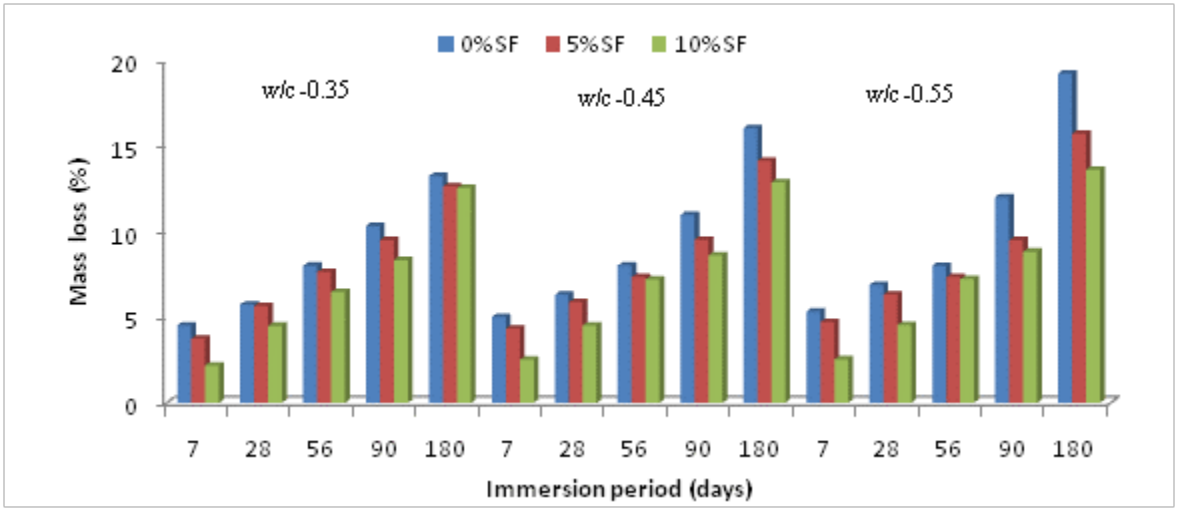

Fig. 4.45 Mass loss of 10% rubber fiber concrete with silica fume in sulphuric acid

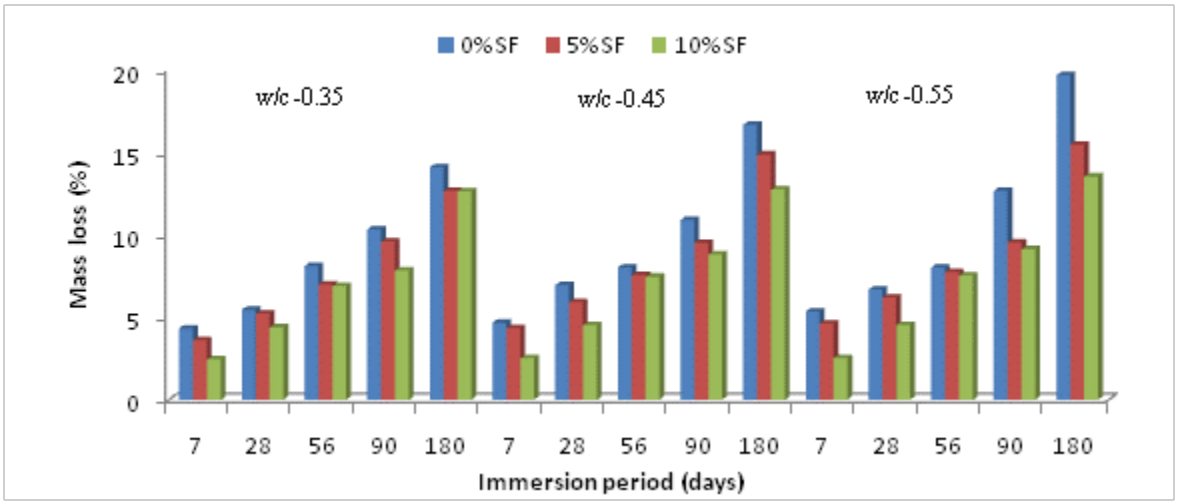

Fig. 4.46 Mass loss of 25% rubber fiber concrete with silica fume in sulphuric acid

c) Mass loss in hydrochloric acid

The change in mass of the waste rubber concrete exposed to hydrochloric acid at 28 days is shown in Figs. 4.47-4.52 respectively. It is seen from the Figs. that the mass of concrete specimens decreased with the increase of immersion time in hydrochloric acid for all three w/c ratios. The change in mass was almost same for control mix and waste rubber concrete. It is also observed from the Figs. that mass loss of control concrete (without rubber ash, rubber fiber and SF) increased from 6.1%, 6.0% and 6.1% to 17.8%, 18.0% and 17.1% for w/c ratios 0.35, 0.45 and 0.55 respectively on increasing the immersion period from 7 days to 180 days.

It is observed from Fig. 4.47 and 4.48 that mass loss (on 180 days immersion in hydrochloric acid) of concrete (without rubber fiber and SF) decreased from 8.8%, 9.0% and 8.1% to 8.7%, 8.7% and 7.8%, on 20% replacement of FA by rubber ash. Whereas the mass loss (on 180 days immersion in hydrochloric acid) of concrete (without rubber ash and SF) increased from 8.8%, 9.0% and 8.1% to 9.0%, 9.1% and 8.6%, on 25% replacement of FA by rubber fibers for w/c ratios 0.35, 0.45 and 0.55 respectively.

It is observed from Fig. 4.49 that mass loss (on 180 days immersion in hydrochloric acid) of hybrid concrete decreased from 8.6%, 8.7% and 8.0% to 8.3%, 8.6% and 7.8%, for w/c ratios 0.35, 0.45 and 0.55 respectively on 25% replacement of FA by rubber fibers.

It is observed from Fig. 4.50 that mass loss (on 180 days immersion in hydrochloric acid) of control concrete decreased from 8.8%, 9.0% and 8.1% to 6.0%, 6.3% and 6.9% for w/c ratios 0.35, 0.45 and 0.55 respectively on 10% replacement of cement by SF.

It is observed from Fig. 4.51 that mass loss (on 180 days immersion in hydrochloric acid) of 10% rubber fiber concrete decreased from 8.4%, 8.4% and 8.9% to 5.7%, 6.6% and 6.9% for w/c ratios 0.35, 0.45 and 0.55 respectively on 10% replacement of cement by SF. Whereas, the mass loss (on 180 days immersion in hydrochloric acid) of 25% rubber fiber concrete decreased from 8.1%, 8.3% and 8.6% to 5.7%, 6.4% and 7.7% for w/c ratios 0.35, 0.45 and 0.55 respectively on 10% replacement of cement by SF (Fig. 4.52).

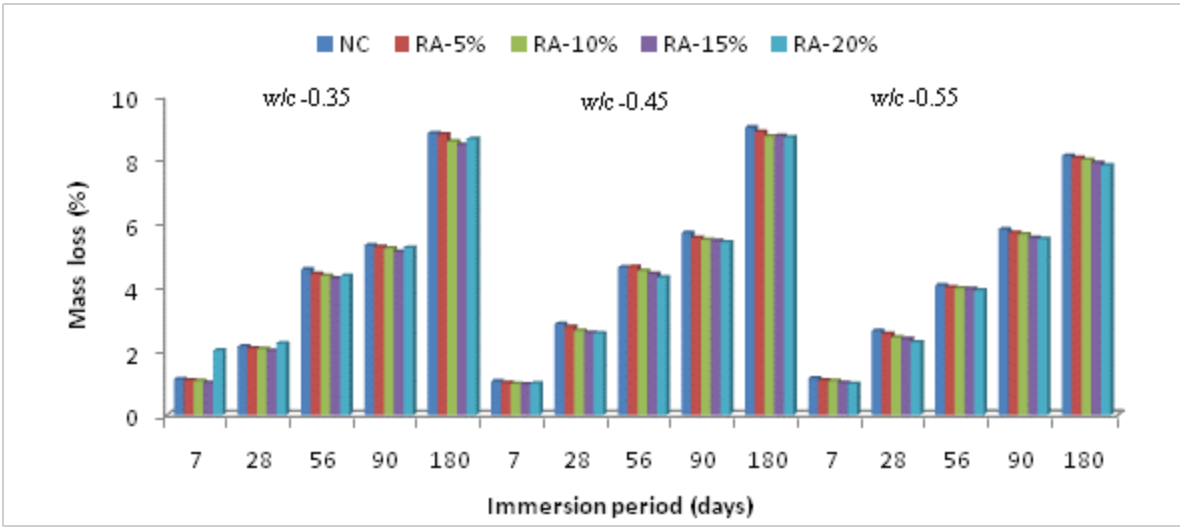

Fig. 4.47 Mass loss of rubber ash concrete in hydrochloric acid

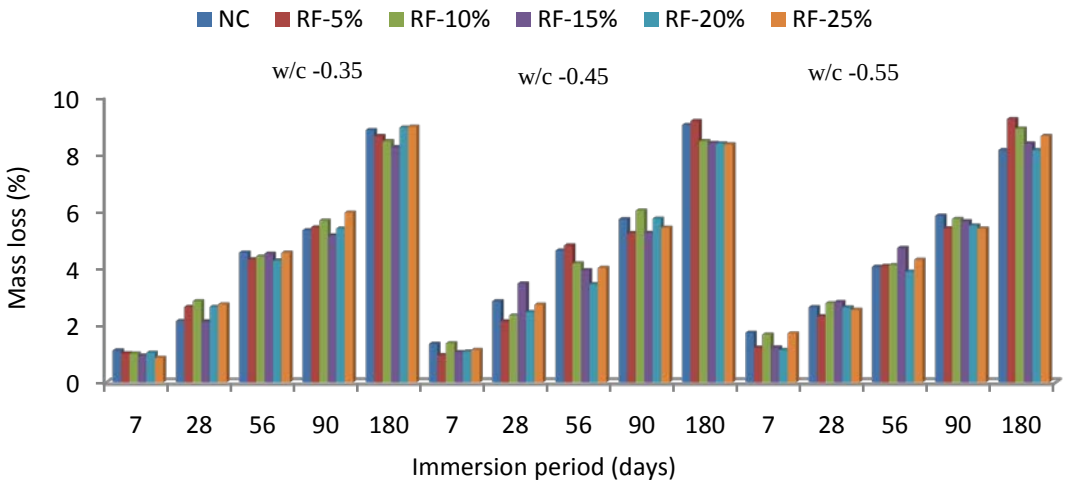

Fig. 4.48 Mass loss of rubber fiber concrete without silica fume in hydrochloric acid

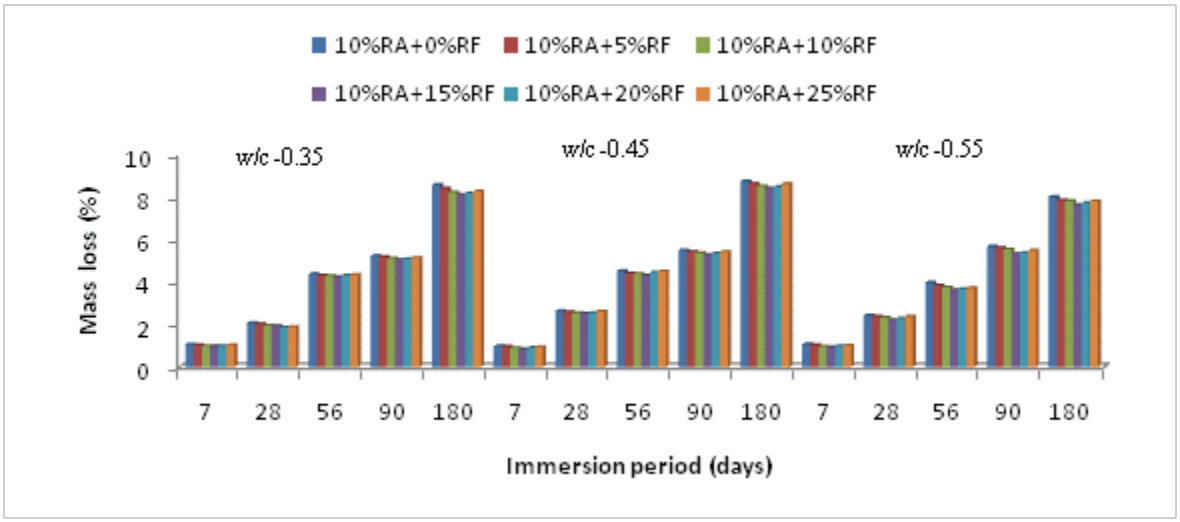

Fig. 4.49 Mass loss of hybrid concrete in hydrochloric acid

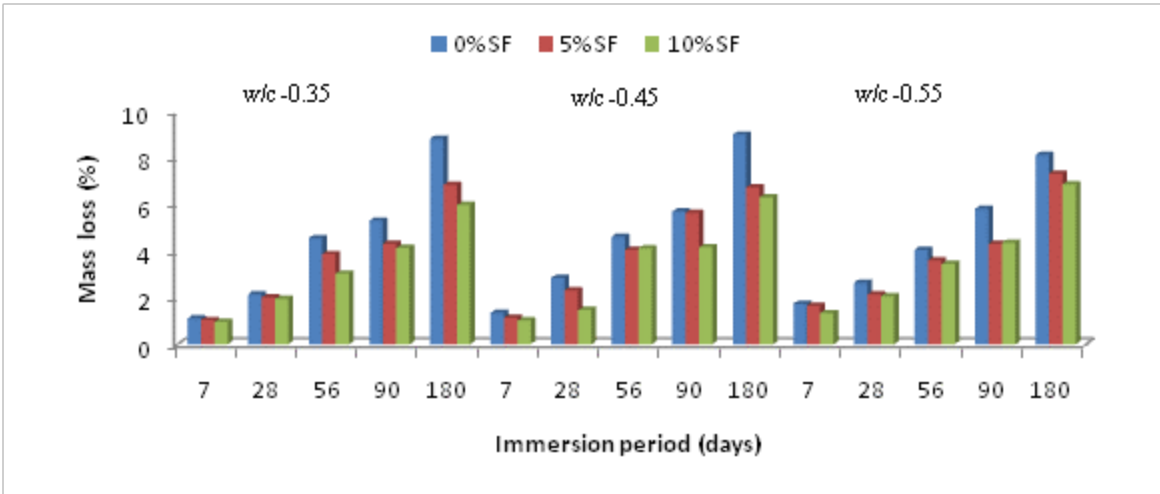

Fig. 4.50 Mass loss of 0% rubber fiber concrete with silica fume in hydrochloric acid

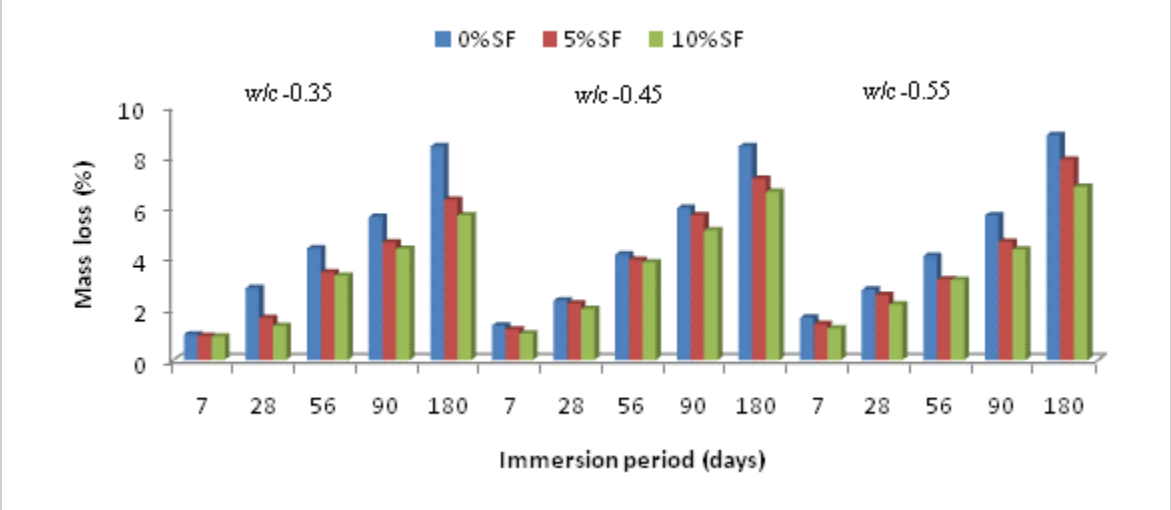

Fig. 4.51 Mass loss of 10% rubber fiber concrete with silica fume in hydrochloric acid

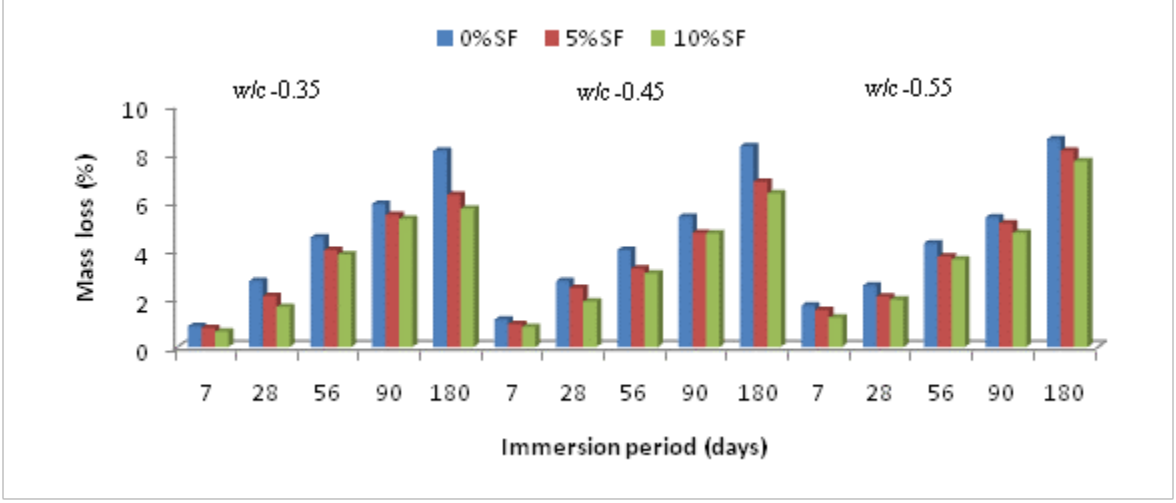

Fig. 4.52 Mass loss of 25% rubber fiber concrete with silica fume in hydrochloric acid

d) Compressive strength of concrete after immersion in sulphuric acid

The compressive strength of the waste rubber concrete at 28 days is shown in Figs. 4.53-4.58 respectively. It is seen from the Figs. that the strength decreased with the increase of immersion time in sulphuric acid and replacement level of waste rubber content for all three w/c ratios.

Compressive strength of control concrete (without rubber ash, rubber fiber and SF) decreased from 58.9 N/mm^2, 50.4 N/mm^2 and 33.7 N/mm^2 to 33.1 N/mm^2, 22.1 N/mm^2 and 11.2 N/mm^2 for w/c ratios 0.35, 0.45 and 0.55 respectively on 180 days immersion in sulphuric acid (Fig. 4.53). Whereas, compressive strength of 20% rubber ash concrete decreased (on 180 days immersion in sulphuric acid) from 42.0 N/mm^2, 45.1 N/mm^2 and 35.6 N/mm^2 to 26.4 N/mm^2, 17.6 N/mm^2 and 8.4 N/mm^2 respectively (Figs. 4.53) and compressive strength of 25% rubber fiber concrete decreased (on 180 days immersion in sulphuric acid) from 28.4 N/mm^2, 23.6 N/mm^2 and 15.3 N/mm^2 to 15.4 N/mm^2, 10.1 N/mm^2 and 5.1 N/mm^2 respectively (Fig. 4.54).

Compressive strength of 10% rubber ash concrete (control mix of hybrid concrete) decreased (on 180 days immersion in sulphuric acid) from 56.7 N/mm^2, 48.5 N/mm^2 and 34.1 N/mm^2 to 30.2 N/mm^2, 19.6 N/mm^2 and 9.8 N/mm^2 for w/c ratios 0.35, 0.45 and 0.55 respectively. Whereas, for replacement of 25% of FA by rubber fiber, compressive strength of hybrid concrete decreased (on 180 days immersion in sulphuric acid) from 31.2 N/mm^2, 28.4 N/mm^2 and 21.2 N/mm^2 to 25.2 N/mm^2, 15.4 N/mm^2 and 6.1 N/mm^2 respectively (Fig. 4.55).

The change in compressive strength of waste rubber fiber concrete, with and without SF, is shown in Figs. 4.56-4.58 for w/c ratios 0.35, 0.45 and 0.55 respectively. It is observed from the Figs. that the compressive strength of concrete specimens decreased with the increase of immersion time in sulphuric acid for all three w/c ratios.

Next, consider the effect of SF on the compressive strength loss of concrete (without rubber ash and rubber fiber) due to sulphuric acid. The strength decreased (on 180 days immersion in sulphuric acid) from 75.2 N/mm^2, 62.7 N/mm^2 and 39.7 N/mm^2 to 44.1 N/mm^2, 28.6 N/mm^2 and 14.8 N/mm^2 respectively (Figs. 4.56) for 10% replacement of cement by SF,.

Next, consider the effect of SF on the compressive strength loss of 10% rubber fiber concrete due to sulphuric acid. Compressive strength of 10% rubber fiber concrete decreased (on 180 days immersion in sulphuric acid) from 45.5 N/mm^2, 35.8 N/mm^2 and 24.9 N/mm^2 to 25.1 N/mm^2, 14.5 N/mm^2 and 8.4 N/mm^2 for w/c ratios 0.35, 0.45 and 0.55 respectively. However, for 10%

replacement of cement by SF, the strength decreased (on 180 days immersion in sulphuric acid) from 59.6 N/mm^2, 45.7 N/mm^2 and 29.4 N/mm^2 to 34.2 N/mm^2, 20.4 N/mm^2 and 10.4 N/mm^2 respectively (Figs. 4.57).

Next, consider the effect of SF on the compressive strength loss of 25% rubber fiber concrete due to sulphuric acid. Compressive strength of 25% rubber fiber concrete decreased (on 180 days immersion in sulphuric acid) from 28.4 N/mm^2, 23.6 N/mm^2 and 15.3 N/mm^2 to 15.4 N/mm^2, 10.1 N/mm^2 and 5.1 N/mm^2 for w/c ratios 0.35, 0.45 and 0.55 respectively. However, for 10% replacement of cement by SF, the strength decreased (on 180 days immersion in sulphuric acid) from 37.9 N/mm^2, 29.9 N/mm^2 and 19.1 N/mm^2 to 21.4 N/mm^2, 13.9 N/mm^2 and 6.9 N/mm^2 respectively (Figs. 4.58).

e) Compressive strength of concrete after immersion in hydrochloric acid

The compressive strength of the waste rubber concrete at 28 days is shown in Figs. 4.59-4.64. The compressive strength was found to decrease with the increase of immersion time in hydrochloric acid and replacement level of waste rubber content for all three w/c ratios.

Compressive strength of control concrete (without rubber ash, rubber fiber and SF) decreased from 58.9 N/mm^2, 50.4 N/mm^2 and 33.7 N/mm^2 to 48.9 N/mm^2, 39.4 N/mm^2 and 24.5 N/mm^2 for w/c ratios 0.35, 0.45 and 0.55 respectively on 180 days immersion in hydrochloric acid (Fig. 4.59). However, compressive strength of 20% rubber ash concrete decreased (on 180 days immersion in hydrochloric acid) from 42.0 N/mm^2, 45.1 N/mm^2 and 35.6 N/mm^2 to 33.2 N/mm^2, 30.4 N/mm^2 and 12.2 N/mm^2 respectively (Figs. 4.59) and strength of 25% rubber fiber concrete decreased (on 180 days immersion in hydrochloric acid) from 28.4 N/mm^2, 23.6 N/mm^2 and 15.3 N/mm^2 to 24.2 N/mm^2, 19.1 N/mm^2 and 11.4 N/mm^2 respectively (Figs. 4.60).

Compressive strength of 10% rubber ash concrete (control mix of hybrid concrete) decreased (on 180 days immersion in hydrochloric acid) from 56.7 N/mm^2, 48.5 N/mm^2 and 34.1 N/mm^2 to 43.2 N/mm^2, 36.5 N/mm^2 and 19.5 N/mm^2 for w/c ratios 0.35, 0.45 and 0.55 respectively (Fig. 4.59). However, compressive strength of hybrid concrete (10% rubber ash and 25% rubber fiber)

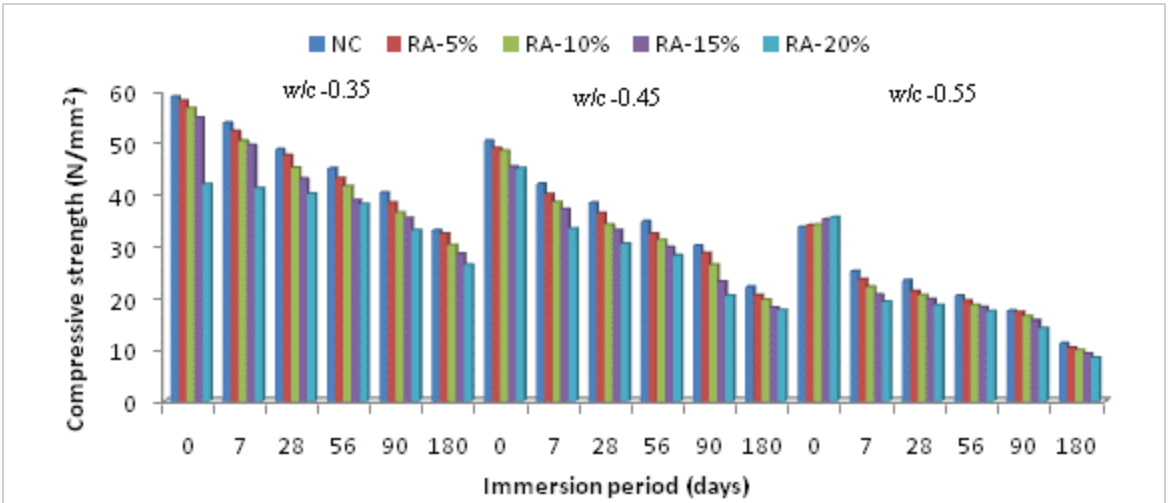

Fig. 4.53 Compressive strength of rubber ash concrete in sulphuric acid

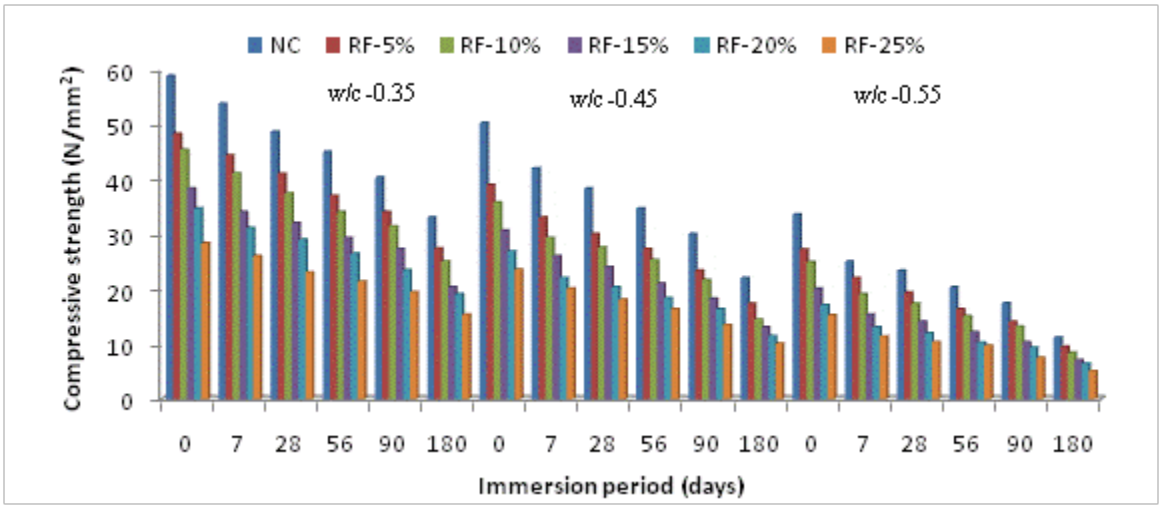

Fig. 4.54 Compressive strength of rubber fiber concrete without silica fume in sulphuric acid

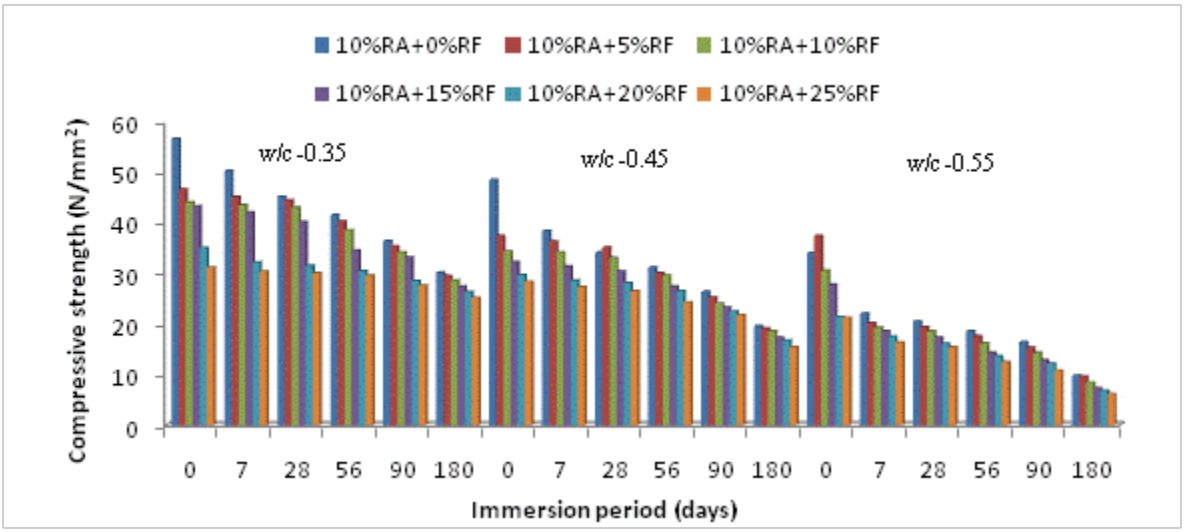

Fig. 4.55 Compressive strength of hybrid concrete in sulphuric acid

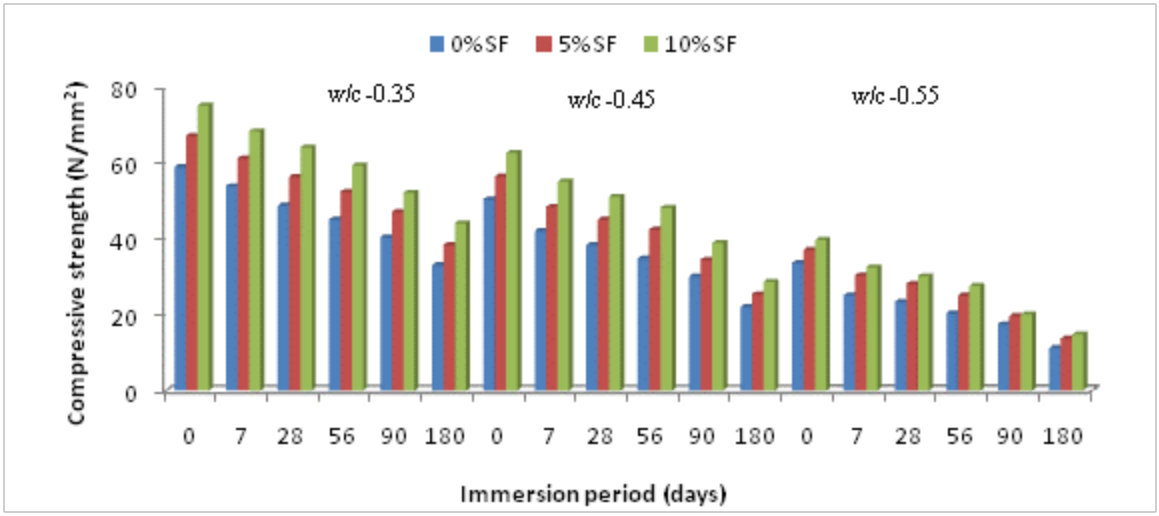

Fig. 4.56 Compressive strength of 0% rubber fiber concrete with silica fume in sulphuric acid

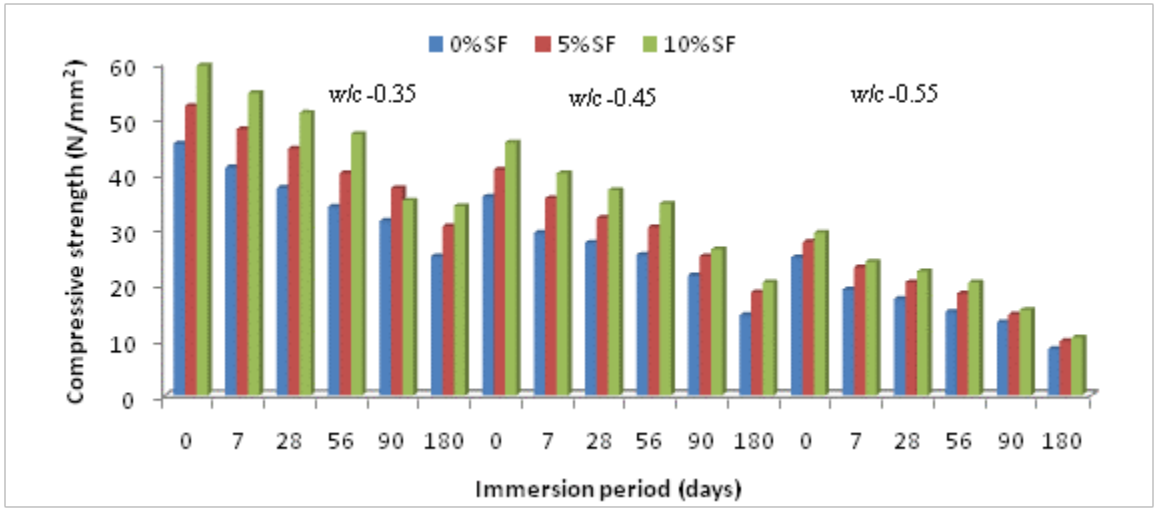

Fig. 4.57 Compressive strength of 10% rubber fiber concrete with silica fume in sulphuric acid

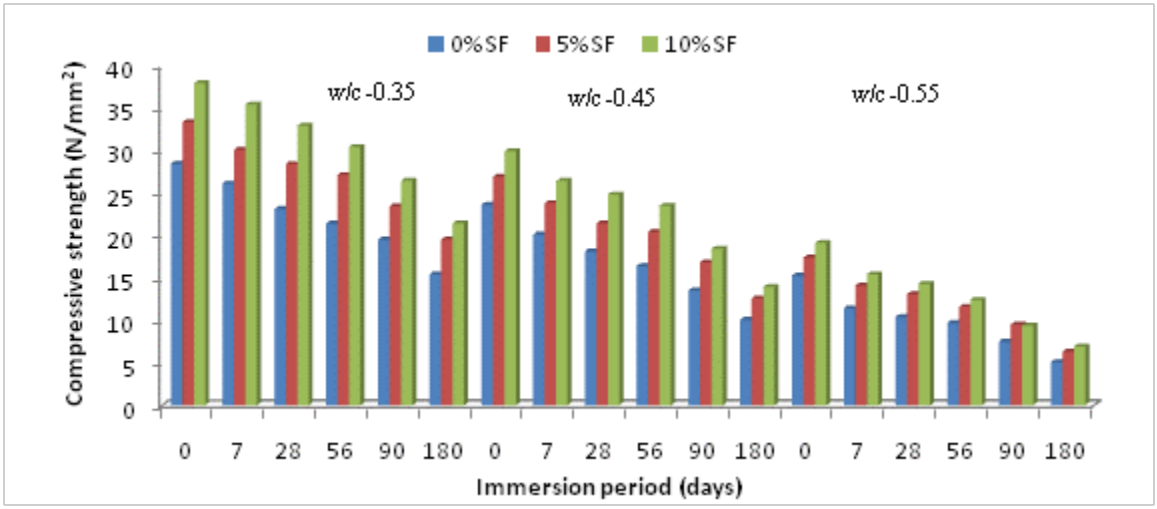

Fig. 4.58 Compressive strength of 25% rubber fiber concrete with silica fume in sulphuric acid

decreased (on 180 days immersion in hydrochloric acid) from 31.2 N/mm^2, 28.4 N/mm^2 and 21.2 N/mm^2 to 27.5 N/mm^2, 22.5 N/mm^2 and 15.4 N/mm^2 respectively (Figs. 4.61).

The change in compressive strength of waste rubber fiber concrete, with and without SF, is shown in Figs. 4.62-4.64 for w/c ratios 0.35, 0.45 and 0.55 respectively. It is observed from the Figs. that the compressive strength of concrete specimens decreased with the increase of immersion time in hydrochloric acid for all three w/c ratios.

Next, consider the effect of SF on the compressive strength loss of control concrete, due to hydrochloric acid. The strength decreased (on 180 days immersion in hydrochloric acid) from 75.2 N/mm^2, 62.7 N/mm^2 and 39.7 N/mm^2 to 66.4 N/mm^2, 54.1 N/mm^2 and 32.9 N/mm^2 at w/c ratios 0.35, 0.45 and 0.55 respectively for 10% replacement of cement by SF (Figs. 4.62).

Next, consider the effect of SF on the compressive strength loss of 10% rubber fiber concrete, due to hydrochloric acid. The strength decreased (on 180 days immersion in hydrochloric acid) from 45.5 N/mm^2, 35.8 N/mm^2 and 24.9 N/mm^2 to 37.8 N/mm^2, 27.9 N/mm^2 and 18.1 N/mm^2 for w/c ratios 0.35, 0.45 and 0.55 respectively (Fig. 4.63). However, for 10% replacement of cement by SF, the strength decreased (on 180 days immersion in hydrochloric acid) from 59.6 N/mm^2, 45.7 N/mm^2 and 29.4 N/mm^2 to 52.7 N/mm^2, 40.1 N/mm^2 and 24.6 N/mm^2 respectively (Figs. 4.63).

Next, consider the effect of SF on the compressive strength loss of 25% rubber fiber concrete, due to hydrochloric acid. The strength decreased (on 180 days immersion in hydrochloric acid) from 28.4 N/mm^2, 23.6 N/mm^2 and 15.3 N/mm^2 to 24.2 N/mm^2, 19.1 N/mm^2 and 11.4 N/mm^2 for w/c ratios 0.35, 0.45 and 0.55 respectively (Fig. 4.64). However, for 10% replacement of cement by SF, the strength decreased (on 180 days immersion in hydrochloric acid) from 37.9 N/mm^2, 29.9 N/mm^2 and 19.1 N/mm^2 to 33.6 N/mm^2, 25.7 N/mm^2 and 15.6 N/mm^2 respectively (Figs. 4.64).

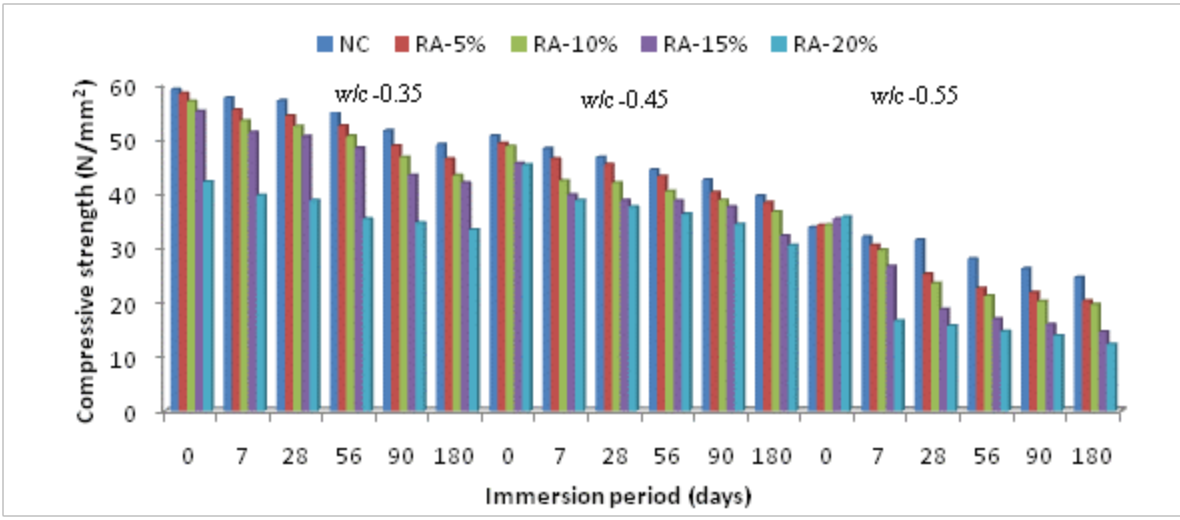

Fig. 4.59 Compressive strength of rubber ash concrete in hydrochloric acid

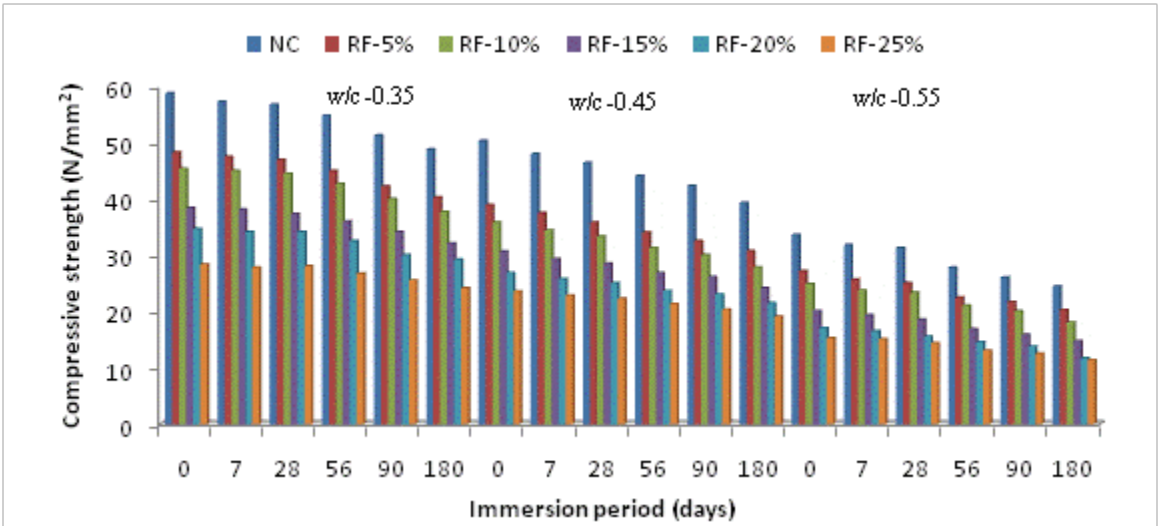

Fig. 4.60 Compressive strength of rubber fiber concrete in hydrochloric acid

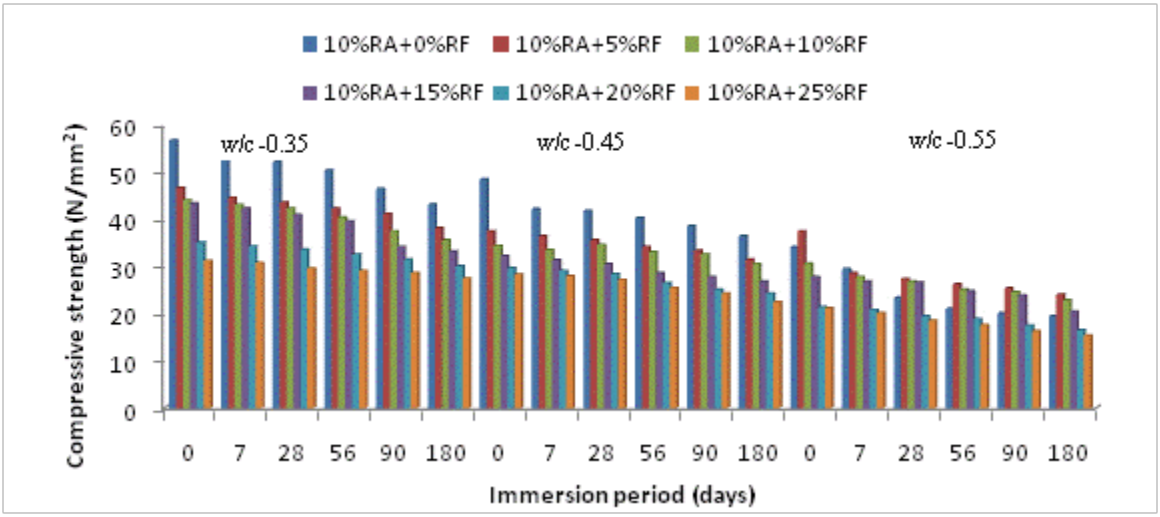

Fig. 4.61 Compressive strength of hybrid concrete in hydrochloric acid

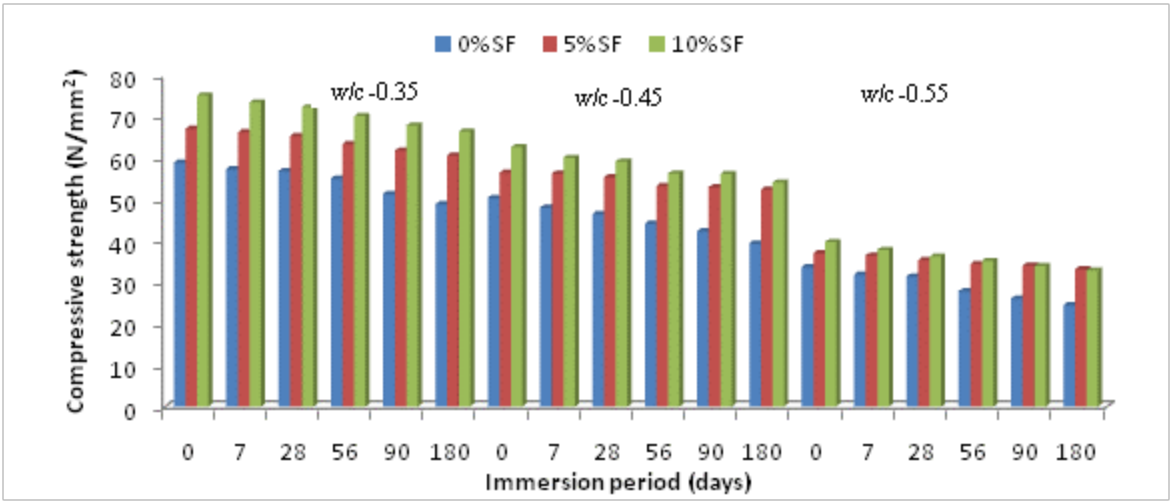

Fig. 4.62 Compressive strength of 0% rubber fiber concrete with silica fume in hydrochloric acid

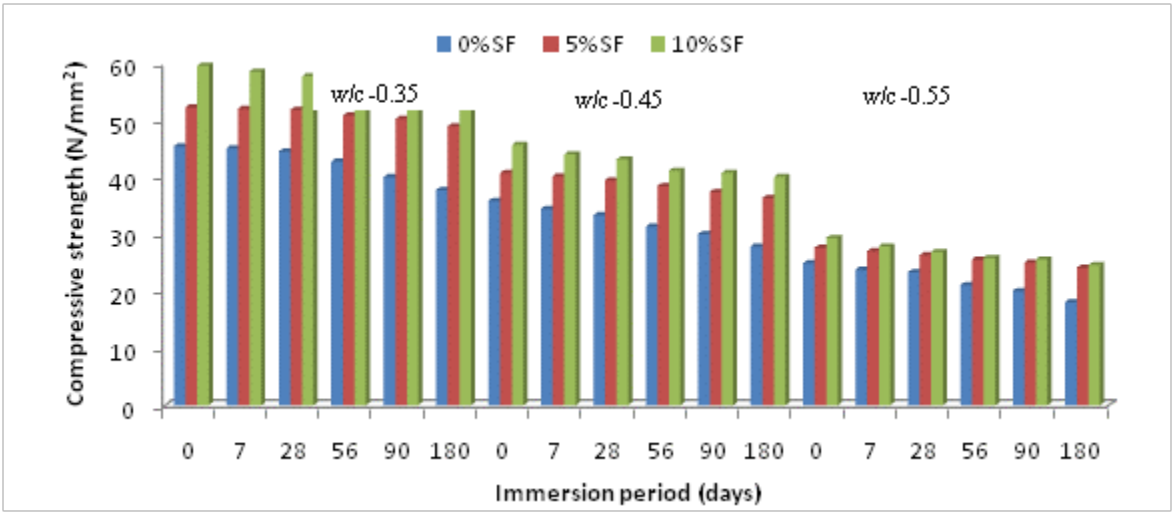

Fig. 4.63 Compressive strength of 10% rubber fiber concrete with silica fume in hydrochloric acid

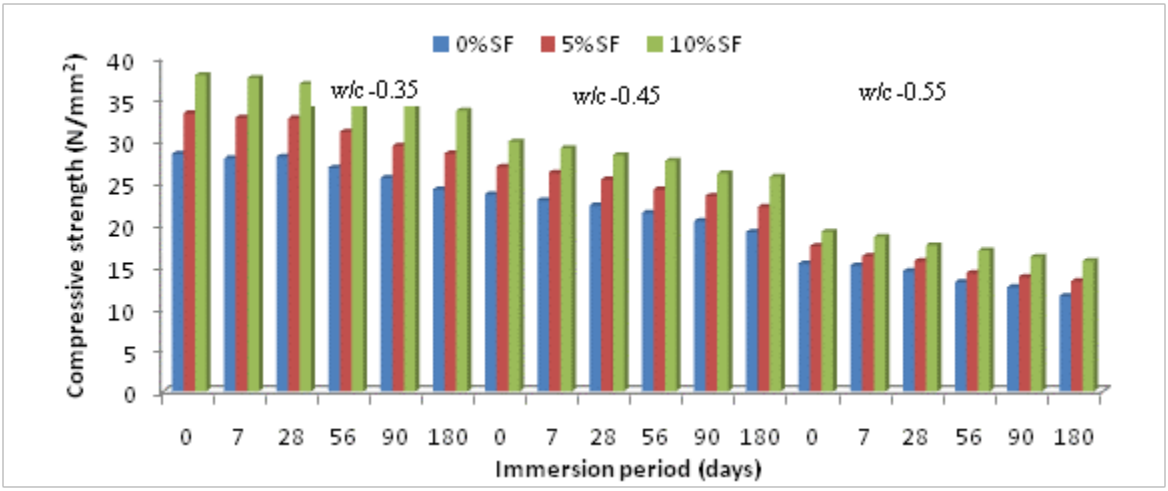

Fig. 4.64 Compressive strength of 25% rubber fiber concrete with silica fume in hydrochloric acid

4.3.8 Micro structural analysis

Micro-structural image of the rubber fiber concrete without exposure to any acid is shown in Fig. 4.65. Gap is observed at the interface of aggregates and cement pate (Fig. 4.65).

Figs. 4.66 and 4.67 show the microstructure of the concrete exposed to sulphuric acid. Gypsum was visible on the concrete surface due to sulphuric acid attack (Figs. 4.66-4.67). Gap at the interface of aggregates and cement paste was found to increase (Fig. 4.66) and the cavity due to separation of FA was also observed (Fig. 4.67).

Figs. 4.68 and 4.69 show the microstructure of the concrete exposed to hydrochloric acid. Brownish belts were observed when concrete specimens were exposed to hydrochloric acid (Figs. 4.68-4.69). Similar observations were made earlier by De Ceukelaire (1992) for cement mortar specimens. Large cavities due to hydrochloric acid attack were observed (Fig. 4.68). Gap at the interface of aggregates and cement paste was also found to increase (Fig. 4.69).

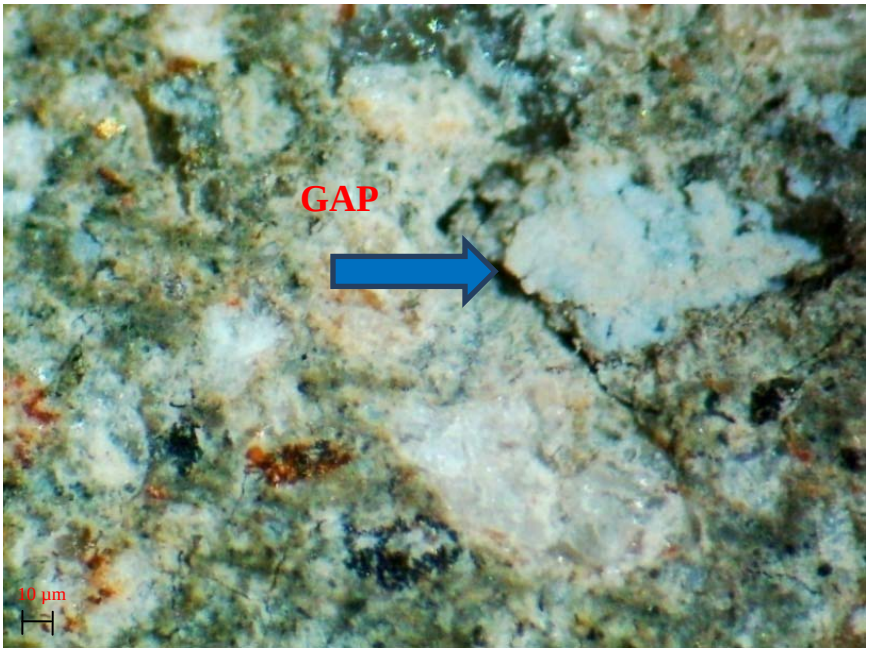

Fig. 4.65 Microstructure of rubber fiber concrete without exposure to any acid at 90x magnification

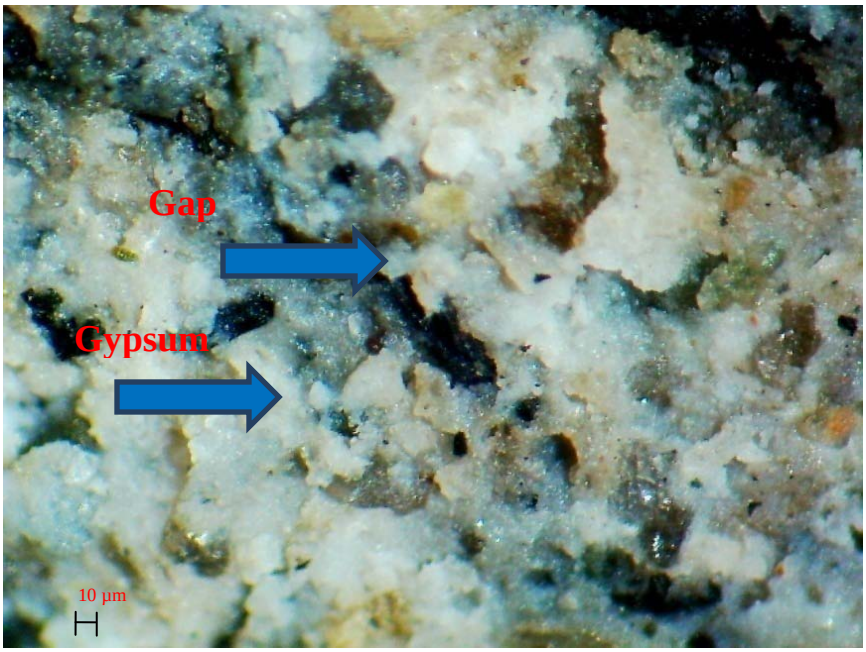

Fig. 4.66 Microstructure of rubber fiber concrete with sulphuric acid attack of 180 days duration at 60x magnification

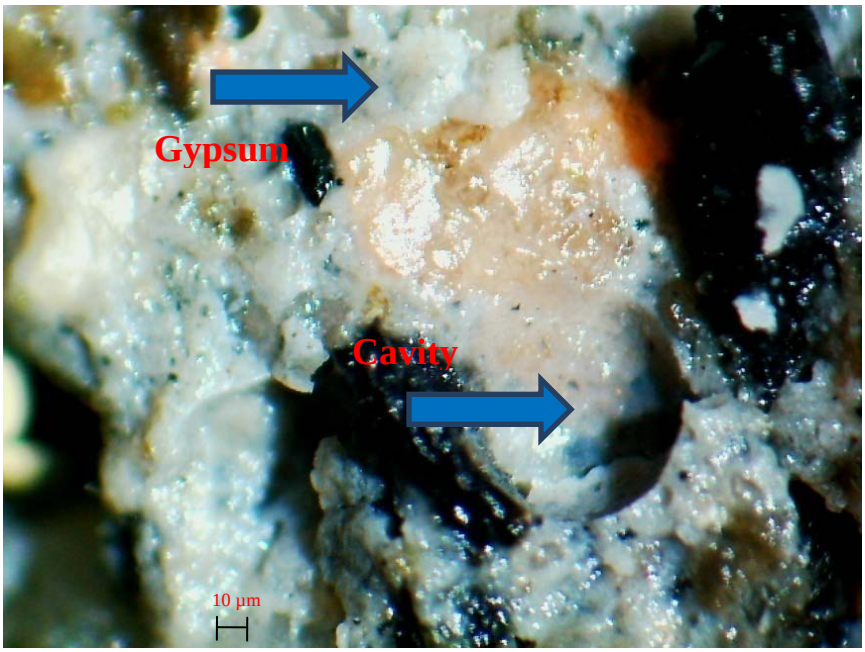

Fig. 4.67 Microstructure of rubber fiber concrete with sulphuric acid attack of 180 days duration at 90x magnification

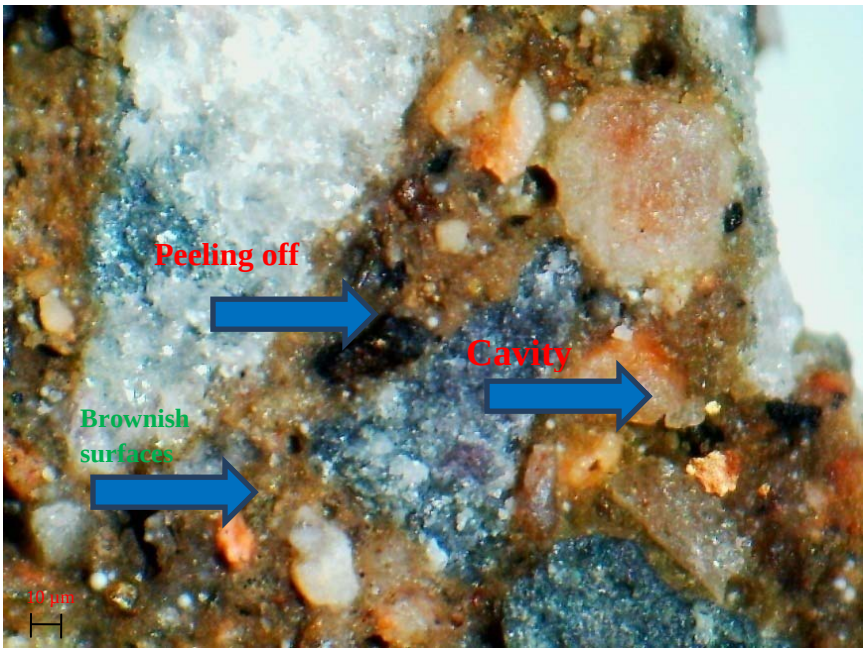

Fig. 4.68 Microstructure of rubber fiber concrete with hydrochloric acid attack of 180 days duration at 60x magnification

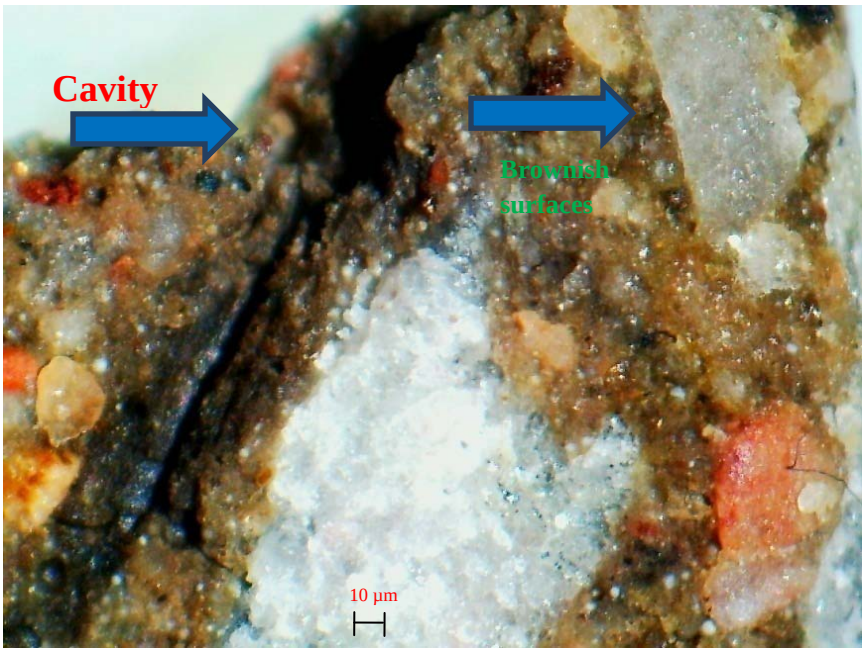

Fig. 4.69 Microstructure of rubber fiber concrete with hydrochloric acid attack of 180 days duration at 90x magnification

4.4 CONCLUSIONS

The durability properties of concrete, which are essential in promoting the use of waste rubber content as fine aggregate, were evaluated in this chapter. Various tests on specimens of waste rubber concrete were performed to study the water absorption, water permeability, shrinkage, carbonation, chloride diffusion, corrosion and acid attack (sulphuric acid and hydrochloric acid). Three water cement ratios, 0.35, 0.45 and 0.55 were considered. As rubber aggregates are a waste product of used rubber tyres, detailed microstructural characteristics of waste rubber concrete was carried out to ensure compatibility of this material with the concrete. Following conclusions are drawn from the studies:

1. Rubber ash and rubber fiber increase the water absorption of concrete for w/c ratios 0.35 and 0.45 and decrease the water absorption of concrete for w/c ratio 0.55.
2. Rubber ash and rubber fiber increase the permeability of the concrete, however the permeability remains in the category of medium permeability defined in the literature. The permeability of rubberized concrete reduces on partial replacement of cement by silica fume.
3. Rubber ash and rubber fiber increase the drying shrinkage of concrete. The drying shrinkage decreases with the increase of silica fume in concrete.
4. Carbonation depth of rubber ash concrete, rubber fiber concrete and hybrid concrete increases with increasing replacement levels of rubber ash and rubber fiber. However, the observed carbonation depth in the most adverse conditions is less than the minimum cover required (15 mm) for RCC member.
5. No trend is observed for the change in chloride ion resistance with the replacement level of rubber ash and rubber fibers. The chloride-ion resistance increases on partial replacement of cement by silica fume.
6. The probability of an early corrosion initiation increases on partial replacement of fine aggregate by rubber ash and rubber fiber. Corrosion initiation is delayed by silica fume concrete in both the control concrete and rubberized concrete.
7. Mass loss due to sulphuric acid and hydrochloric acid increases with the increase in replacement level of rubber ash and rubber fiber. The mass loss decreases for control concrete as well as rubberized concrete on partial replacement of cement by silica fume.

8. The loss in compressive strength due to acid attack is more in case of rubberized concrete.
9. The loss in compressive strength on sulphuric acid attack is more in comparison to loss on hydrochloric acid attack for the control concrete as well as rubberized concrete.
10. Micro structural analysis of rubber fiber concrete shows the increase in gap at the interface of the aggregates and cement paste on exposure to sulphuric acid and hydrochloric acid.

CHAPTER 5

ELASTICITY AND DUCTILITY ASSESSMENT OF RUBBERIZED CONCRETE

5.1 INTRODUCTION

Concrete is a brittle material with high rigidity. High flexibility, impact resistance and fatigue resistance are required in many applications such as shock absorbers, foundation pads of machinery, railway buffers etc. Additional ingredients are required to improve the properties of concrete in some situations where these requirements are not fulfilled. A more ductile concrete is technically better for certain applications and gives sufficient warning time before failure.

In this chapter, the elasticity and ductility properties of concrete containing waste rubber tyre in form of rubber ash, rubber fibers and in combined form with control concrete have been discussed. The elasticity and ductility properties of concrete containing waste rubber fibers with silica fume (SF) have also been discussed.

5.2 ELASTICITY AND DUCTILITY PARAMETERS

Ductility of concrete defines the energy absorption capacity of concrete and therefore it is desirable to assess ductility in depth. The various significant elasticity and ductility parameters studied are as follows:

1. Static modulus which provides the flexibility of concrete and depends on the ingredient materials of concrete.
2. Ultrasonic pulse velocity (UPV) which reflects the quality of hardened concrete and depends upon the voids in the internal structure.
3. Dynamic modulus which shows deformability of concrete and is related to elastic deformation of the aggregate and density of concrete.
4. Impact resistance under drop weight test which describes post-cracking behavior of concrete.
5. Impact resistance under flexural loading test which describes the behavior of concrete under bending due to applied impact loading.
6. Impact resistance under rebound test which reflects the energy absorbed by the concrete due to the rebound of impact load.

7. Fatigue resistance which reflects the ability to withstand repetitive loads without fracture.

In the present study, the above elasticity and ductility properties of waste rubber concrete have been evaluated by using static modulus test, ultrasonic pulse velocity test, dynamic modulus test, impact resistance under drop weight test, impact resistance under flexural test, impact resistance under rebound test and fatigue test.

5.3 EXPERIMENTAL PROCEDURE

5.3.1 Static modulus of elasticity

Cylindrical specimen of 150 mm diameter and 300 mm height were used to determine the modulus of elasticity as per ASTM C469 (2002). Specimens were tested on a compression testing machine of 200 tonne capacity with longitudinal compressometer and lateral extensometer attachments as shown in Fig. 5.1. Load was applied gradually with the rate of travel of machine equivalent to 240±35 kN/m^2/s. The applied load and corresponding strains were measured. The modulus of elasticity was then calculated by the following equation:

$$E_s = (\sigma_2 - \sigma_1)/(\varepsilon_2 - 0.000050) \quad (5.1)$$

where: σ_2 = stress corresponding to 40% of ultimate load, σ_1 = stress corresponding to a longitudinal strain, and ε_2 = longitudinal strain produced by stress σ_2.

Fig. 5.1 Modulus of elasticity apparatus

5.3.2 Ultrasonic pulse velocity

A non-destructive test using an ultrasonic pulse device was conducted on the cube specimens according to ASTM C597 (2002). For this purpose, a commercial UPV measurement

instrument and two ultrasonic transducers with a centre frequency of 54 kHz were utilized to measure the propagation time of a sonic wave through concrete specimen as shown in Fig. 5.2. Sufficient gel was applied between the surfaces of the concrete cube and transducers to ensure proper contact.

Fig. 5.2 Ultrasonic pulse velocity apparatus

5.3.3 Dynamic modulus of elasticity

The measured UPV was utilized to calculate the dynamic modulus. The following equation from Topçu and Bilir (2009) was chosen to evaluate the dynamic modulus.

$$E_d = \left(V^2 \rho / g\right) \times 10^{-2} \tag{5.2}$$

where, E_d = dynamic modulus (kN/mm^2), V = UPV (km/s), ρ = density (kg/m^3) and g = acceleration due to gravity (9.81 m/s^2).

5.3.4 Impact Resistance

5.3.4.1 *Impact resistance under drop weight test*

Drop weight test was performed on cylindrical specimens (150 mm in diameter and 65 mm in height) as per ACI 544 (1999) to estimate the energy absorption capacity of concrete specimens. In this test, repeated impact loading was applied on the specimen from a height. The number of blows was obtained for the prescribed level of distress (occurrence of first crack and failure cracks).

Specimens of 28 days age were tested by the drop weight impact testing machine fabricated in the laboratory as per guidelines of ACI committee 544 (1999). The machine consists of a 4.5 kg hammer ball dropping from 450 mm height on a hardened steel ball of 65 mm diameter (Fig. 5.3a). The steel ball was placed at the centre of specimen and this specimen was placed on the base plate within the positioning lugs as shown in Fig. 5.3(a).

The hammer ball was dropped repeatedly and the number of blows (N_1) required to cause the first visible crack on the top was recorded. Number of blows (N_2) which caused opening of cracks in such a way that the concrete pieces started touching side lugs was also recorded. The values of N_1 and N_2 were designated as initial crack resistance factor and ultimate crack resistance factor respectively.

The impact energy at initial crack, $E_{p,dwi}$ (where first subscript *p* denotes the type of energy absorbed i.e. potential energy and second subscript *dw* denotes the type of test i.e. drop weight) was calculated by the equation given below:

$$E_{p,dwi} = N_1 mgh \tag{5.3}$$

Similarly, the impact energy at ultimate crack, $E_{p,dwu}$ was calculated by the equation given below:

$$E_{p,dwu} = N_2 mgh \tag{5.4}$$

where, N_1 and N_2 are the number of blows at initial and ultimate crack level, *m* is the mass of drop hammer (4.5 kg), *g* is acceleration due to gravity (9.81 m/s^2) and *h* is the releasing height of drop hammer (450 mm).

5.3.4.2 *Impact resistance under flexural loading test*

Impact test on the beams was performed to determine the potential energy of rubber fiber concrete (Fig. 5.3b). In this test, beams of 100 mm × 100 mm × 500 mm size (three specimens for each mix) were tested with a center to center span of 400 mm. A hammer of 1.0 kg weight was dropped on the mid span of the beam from a height of 450 mm. Number of drops up to failure, N_f was measured and energy absorbed by the specimen, $E_{p,fl}$ (subscript *fl* denotes flexural loading) was calculated by the following equation:

$$E_{p,fl} = \sum_{i=1}^{N_f} m_i g h_i \tag{5.5}$$

where, m_i is the mass of drop hammer (1.0 kg) and h_i is the drop height (450 mm).

5.3.4.3 *Impact resistance under rebound test*

Rebound test was performed on cubes of 150 mm size to determine the impact resistance of waste rubber fiber concrete (Fig 5.3c). A steel ball of 0.5 kg weight was dropped on the specimens (three for each mix) from a standard height of 1.0 m. The rebound height of steel

ball was recorded by a sensitive camera. Initial potential energy before rebound, $E_{p,ri}$ and final potential energy after rebound, $E_{p,rf}$ were calculated using following equations:

$$E_{p,ri} = mgh_i \quad (5.6)$$

$$E_{p,rf} = mgh_f \quad (5.7)$$

where, m is mass of steel ball (0.5 kg), h_i is the initial height of steel ball (1.0 m) and h_f is height recorded after rebound (varies for different mixes).

The energy absorption capacity of concrete specimen, $E_{p,r}$ was calculated as the difference of the final and initial potential energy ($E_{p,r} = E_{p,ri} - E_{p,rf}$). Loss due to air resistance was ignored.

Fig. 5.3 (a) Drop weight test; (b) Flexural test; and (c) Rebound test

5.3.5 Fatigue strength

Flexural fatigue test was carried out in the laboratory on a servo-hydraulic fatigue testing machine of capacity 20 kN as shown in Fig. 5.4. The loading mode was four points bending with a span of 450 mm and loads were applied at one third of the span as applied in static flexural test. The flexural fatigue test was accomplished with load and frequency control. A constant amplitude load with haversine (sine wave) was applied to the concrete specimen with 5 Hz frequency as shown in Fig. 5.5.

Fig. 5.4 Fatigue testing machine

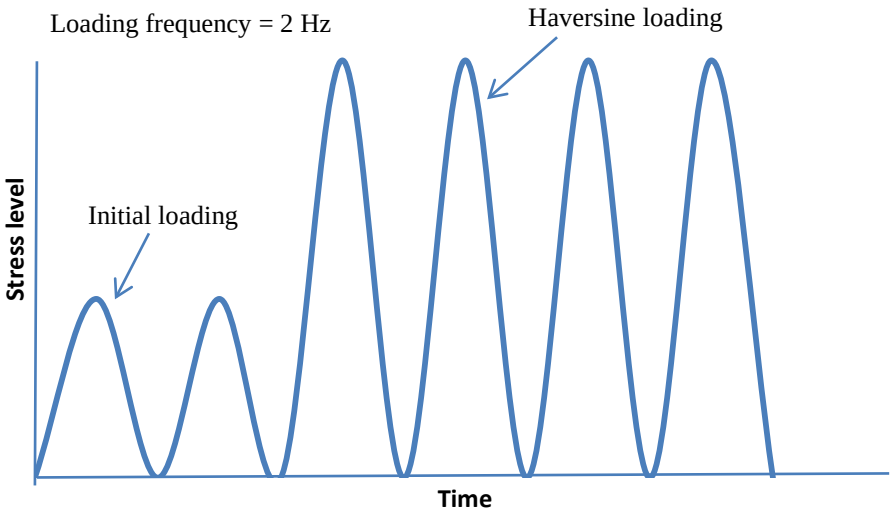

Fig. 5.5 Haversine loading

Waste rubber concrete specimens (rubber ash concrete, rubber fibers concrete, hybrid concrete, rubber fibers with 5% and 10% SF) of 28 days age for all three w/c ratios were tested on fatigue testing machine. Fatigue test were conducted at three different stress levels (the ratio of applied cyclic stress to the average static flexural strength) i.e. 0.7, 0.8 and 0.9. The details about the mean static flexural strength have already been given in Chapter 3. The number of cycles '*N*' to failure of concrete specimen was recorded as fatigue life o the concrete specimen. The test setup used for cycling loading is shown in Fig. 5.4.

5.4 RESULTS AND DISCUSSION

5.4.1 Static modulus of elasticity

The static modulus for rubber ash concrete, rubber fiber concrete, hybrid concrete, rubber fiber concrete with 5% and 10% SF is shown in Figs. 5.6-5.8 alongwith the statistical variances of results in Table 5.1. It can be observed that the rubber concrete decreases the static modulus of concrete.

The static modulus of concrete (without rubber fiber and silica fume) decreased by 24.8% and 10.2% for w/c ratios 0.35 and 0.45 respectively and increased by 4.5% for w/c ratio 0.55 on 20% replacement of FA by rubber ash. The static modulus of concrete (without rubber ash and silica fume) decreased by 32.5%, 34.5% and 24.4% for w/c ratios 0.35, 0.45 and 0.55 respectively on 25% replacement of FA by rubber fiber. The static modulus of control concrete decreased by 37.2%, 15.9% and 40.8% for w/c ratios 0.35, 0.45 and 0.55 respectively on 10% replacement of FA by rubber ash along with 25% replacement of FA by rubber fiber.

It may be noted that, earlier also, upto 83% reduction in static modulus was reported by Gueniyisi *et al.* (2004) on 50% replacement of total volume of aggregate by waste crumb rubber. The lower static modulus may be due to defects in the internal structure of the concrete matrix (Azmi *et al.* 2008).

It is also observed from Figs. 5.6-5.8 that on replacement of cement by SF, the static modulus of concrete (without rubber ash and rubber fiber) increased by 7.9%, 9.4% and 5.6% for w/c ratios 0.35, 0.45 and 0.55 respectively on 10% replacement of cement by SF. Whereas, the observed increase for rubber fiber concrete (25% rubber fiber) was 22.8%, 16.5% and 21.9% respectively. The increase in static modulus with SF may be due to filling of pores between aggregate and cement paste (Guneyisi *et al.* 2004).

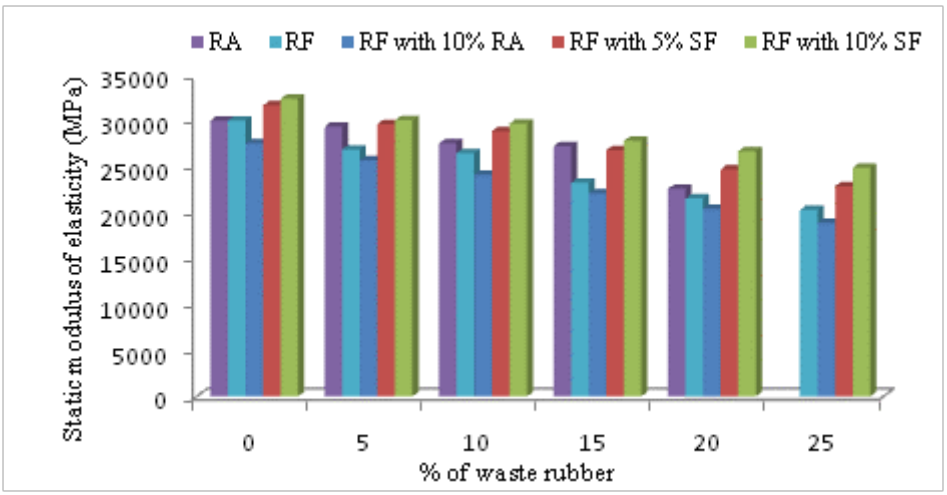

Fig. 5.6 Static modulus of elasticity of waste rubber concrete for 0.35 w/c ratio

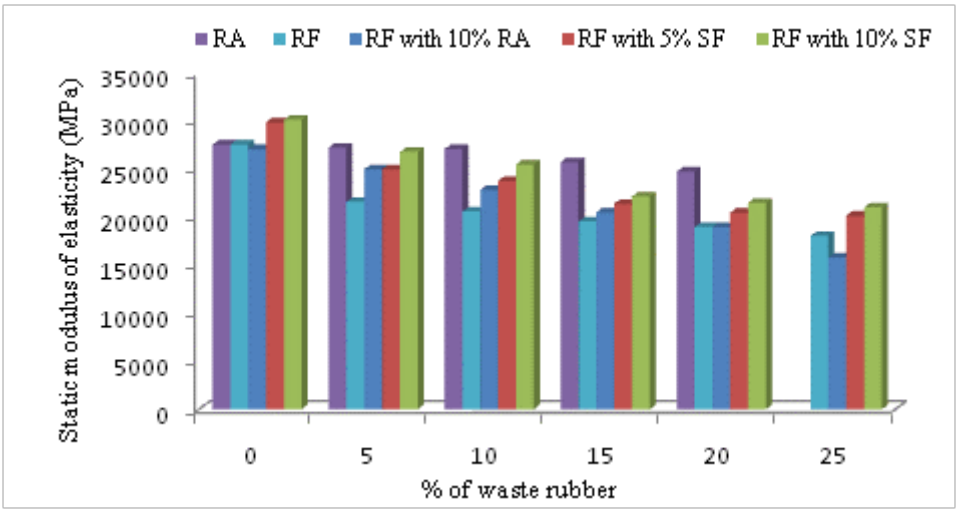

Fig. 5.7 Static modulus of elasticity of waste rubber concrete for 0.45 w/c ratio

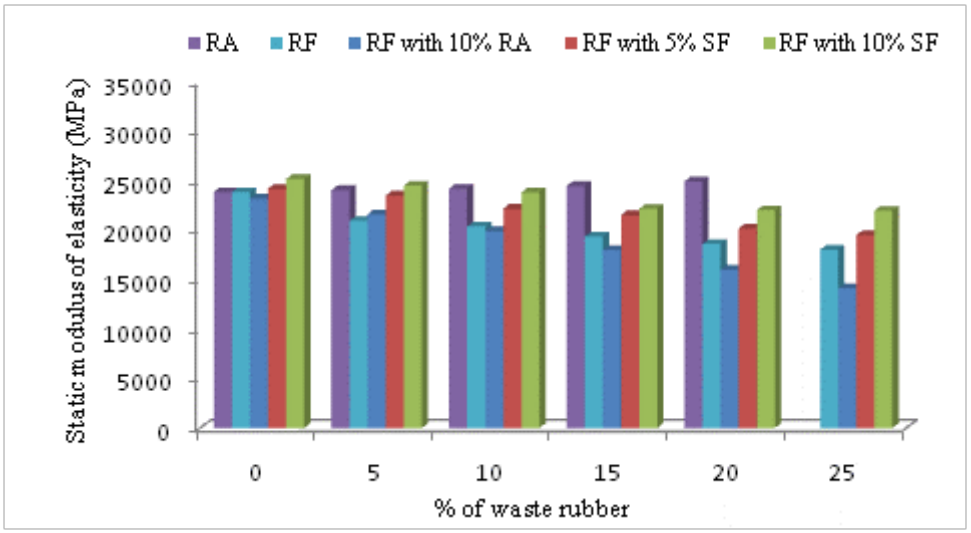

Fig. 5.8 Static modulus of elasticity of waste rubber concrete for 0.55 w/c ratio

Table 5.1 Statistical variances of static modulus test results for waste rubber concrete

Mix No.	SD	COV	Mix No.	SD	COV	Mix No.	SD	COV	Mix No.	SD	COV	Mix No.	SD	COV
T1	1938	0.07	R1	495	0.02	S1	1567	0.06	U1	1194	0.04	V1	1053	0.03
T2	1201	0.04	R2	629	0.02	S2	1183	0.05	U2	732	0.02	V2	1149	0.04
T3	1149	0.04	R3	1079	0.04	S3	1635	0.07	U3	943	0.03	V3	707	0.02
T4	1753	0.07	R4	1067	0.05	S4	1730	0.09	U4	1114	0.04	V4	1856	0.07
T5	1019	0.05	R5	1265	0.06	S5	1648	0.09	U5	1019	0.04	V5	1842	0.07
T6	1350	0.05	R6	1209	0.06	S6	1004	0.06	U6	1306	0.05	V6	1353	0.06
T7	2111	0.08	R7	2172	0.09	S7	2241	0.09	U7	717	0.02	V7	1217	0.04
T8	2025	0.08	R8	1267	0.06	S8	1294	0.06	U8	1120	0.04	V8	1007	0.04
T9	1486	0.06	R9	1645	0.07	S9	1235	0.06	U9	1134	0.05	V9	973	0.04
T10	1322	0.06	R10	901	0.05	S10	1387	0.07	U10	994	0.05	V10	1127	0.05
T11	1260	0.06	R11	964	0.05	S11	1173	0.07	U11	904	0.04	V11	1203	0.06
T12	1443	0.06	R12	508	0.03	S12	619	0.04	U12	1110	0.06	V12	1183	0.06
T13	1924	0.09	R13	2400	0.09	S13	1567	0.07	U13	1613	0.07	V13	2844	0.13
T14	1675	0.07	R14	1108	0.05	S14	969	0.05	U14	1088	0.05	V14	1023	0.04
T15	398	0.02	R15	883	0.04	S15	257	0.01	U15	959	0.04	V15	1142	0.05
-	-	-	R16	763	0.04	S16	967	0.06	U16	120	0.06	V16	1304	0.06
-	-	-	R17	1062	0.06	S17	798	0.05	U17	1109	0.06	V17	589	0.03
-	-	-	R18	885	0.05	S18	648	0.05	U18	774	0.04	V18	1629	0.07

Unit of SD (standard deviation) is MPa.

5.4.2 Ultrasonic pulse velocity

The influence of varying waste rubber content with and without SF on ultrasonic pulse velocity (UPV) is shown in Figs. 5.9-5.11. The ultrasonic pulse velocity is found to decrease with the increase in waste rubber content.

The ultrasonic pulse velocity of concrete (without rubber fiber and SF) decreased by 13.0% and 4.4% for w/c ratios 0.35 and 0.45 and increased by 3.2% for w/c ratio 0.55 on 20% replacement level of FA by rubber ash. The ultrasonic pulse velocity of concrete (without rubber ash and rubber fiber) decreased by 28.9%, 27.5% and 25.7% for w/c ratios 0.35, 0.45 and 0.55 respectively on 25% replacement level of FA by rubber fibers. Whereas, the ultrasonic pulse velocity of concrete (without SF) decreased by 19.5%, 21.5% and 17.3% for w/c ratios 0.35, 0.45 and 0.55 respectively on 10% replacement of FA by rubber ash along with 25% replacement of FA by rubber fiber.

The observed decrease in ultrasonic pulse velocity may be due to the increase in the voids in the specimen which favors the absorption of ultrasonic waves or may be due to presence of low density waste rubber content. It may be noted that, earlier also, upto 34% reduction in ultrasonic pulse velocity was reported by Uygunog˘lu and Topcu (2010) on 50% replacement of FA by rubber particles. The lower ultrasonic pulse velocity may be due to (i) the absorption of ultrasonic waves by rubber particles (Oikonomou and Mavridou 2009); and (ii) higher porosity in the rubberized concrete (Uygunog˘lu and Topcu 2010).

It is also observed from Figs. 5.9-5.11 that the ultrasonic pulse velocity increased on replacement of cement by SF, for control concrete as well as for the rubber fiber concrete. The ultrasonic pulse velocity for control concrete increased by 4.9%, 8.9% and 8.8% for w/c ratios 0.35, 0.45 and 0.55 respectively on 10% replacement of cement by SF, whereas the corresponding increase for rubber fiber concrete (25% rubber fiber) was 13.3%, 17.1% and 14.2% respectively.

5.4.3 Dynamic modulus of elasticity

The influence of varying waste rubber content with and without SF on dynamic modulus is shown in Figs. 5.12-5.14 with the statistical variances in Table 5.2. The Figs. show that the dynamic modulus of elasticity decreased with the increase in waste rubber content.

The dynamic modulus of concrete (without rubber fiber and SF) decreased by 31.4% and 14.3% for w/c ratios 0.35 and 0.45 whereas increased by 3.6% for w/c ratio 0.55 on 20% replacement of FA by rubber ash. Whereas, the dynamic modulus of concrete (without rubber ash and SF) decreased by 52.1%, 50.9% and 47.5% respectively, on 25% replacement of FA by rubber fiber. The observed decrease for concrete (without SF) was 40.8%, 31.1% and 35.3% respectively, on 10% replacement of FA by rubber ash along with 25% replacement of FA by rubber fiber.

As expected, the decrease in density, reported in Section 3.3.2.1, resulted in reduced dynamic modulus of waste rubber fiber concrete. The observed decrease in modulus in the present study may be due to the increase of a porous structure which favors the absorption of ultrasonic waves or may be due to presence of low density rubber (Oikonomou and Mavridou 2009). It may be noted that upto 68% reduction in dynamic modulus was observed by Oikonomou and Mavridou (2009) on 12.5% replacement of FA by crumb rubber.

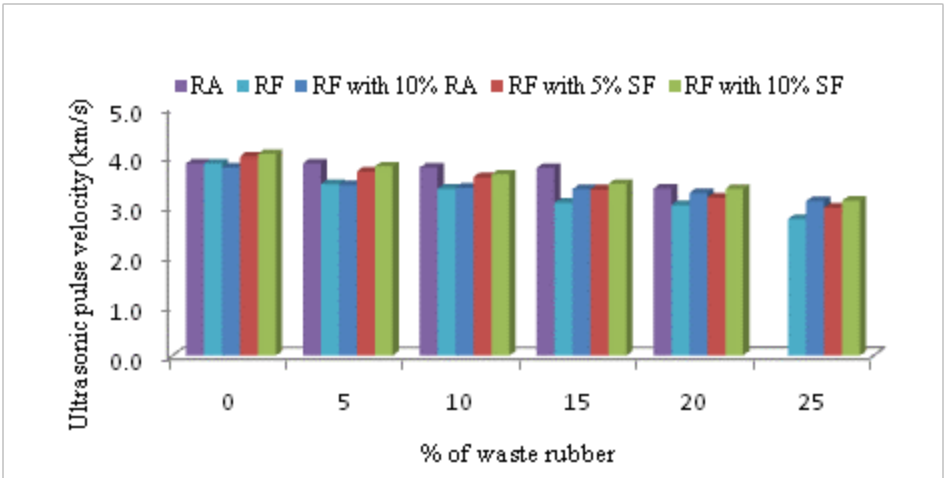

Fig. 5.9 Ultrasonic pulse velocity of waste rubber concrete for 0.35 w/c ratio

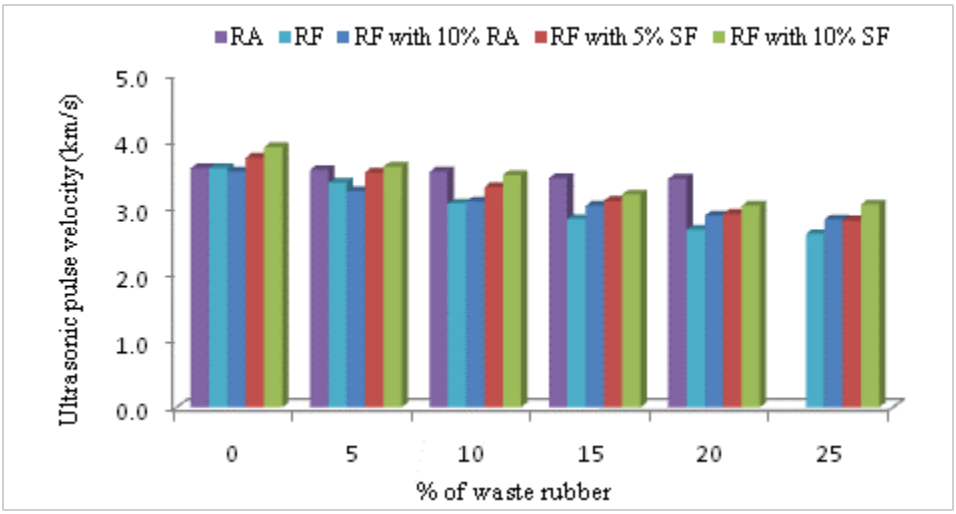

Fig. 5.10 Ultrasonic pulse velocity of waste rubber concrete for 0.45 w/c ratio

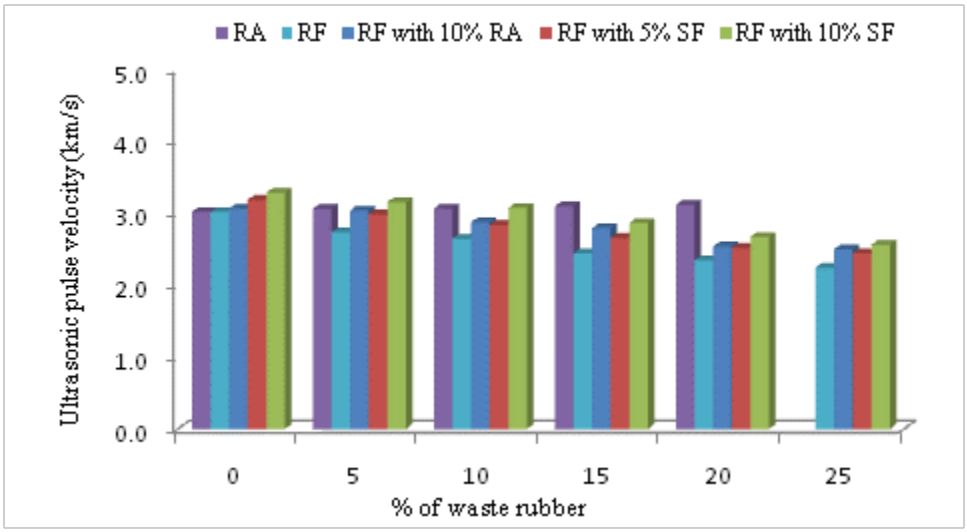

Fig. 5.11 Ultrasonic pulse velocity of waste rubber concrete for 0.55 w/c ratio

It is also observed from Figs. 5.12-5.14 that the dynamic modulus of concrete increased on replacement of cement by SF, for control concrete as well as for the rubber fiber concrete. The dynamic modulus for concrete (without rubber ash and rubber fiber) increased by 11.4%, 20.1% and 20.4% for w/c ratios 0.35, 0.45 and 0.55 respectively on 10% replacement of cement by SF, whereas, the corresponding increase for rubber fiber concrete (25% rubber fiber) was 29.9%, 41.0% and 32.8%. The increase in dynamic modulus with SF may be due to improved bonding and less voids between the rubber and the cement matrix (Gesoglu and Guneyisi 2007).

Table 5.2 Statistical variances of dynamic modulus test results for waste rubber concrete

Mix No.	SD	COV	Mix No.	SD	COV	Mix No.	SD	COV	Mix No.	SD	COV	Mix No.	SD	COV
T1	1.11	0.03	R1	1.13	0.03	S1	3.14	0.10	U1	1.87	0.04	V1	2.09	0.05
T2	3.27	0.10	R2	1.18	0.04	S2	1.54	0.06	U2	1.30	0.04	V2	1.30	0.03
T3	1.82	0.05	R3	0.98	0.03	S3	0.82	0.03	U3	1.23	0.04	V3	0.89	0.03
T4	0.85	0.02	R4	1.14	0.05	S4	1.80	0.07	U4	1.25	0.04	V4	1.31	0.04
T5	1.50	0.06	R5	1.06	0.05	S5	1.22	0.05	U5	1.22	0.05	V5	1.76	0.06
T6	0.85	0.03	R6	1.65	0.1	S6	1.04	0.05	U6	1.05	0.05	V6	1.15	0.05
T7	1.92	0.07	R7	1.39	0.04	S7	1.01	0.03	U7	1.08	0.03	V7	2.35	0.06
T8	1.47	0.05	R8	0.87	0.03	S8	2.84	0.13	U8	1.14	0.04	V8	1.73	0.05
T9	2.65	0.10	R9	0.87	0.04	S9	2.33	0.12	U9	1.65	0.06	V9	2.89	0.11
T10	2.77	0.11	R10	1.20	0.06	S10	2.29	0.12	U10	1.08	0.05	V10	5.14	0.26
T11	2.77	0.15	R11	1.23	0.08	S11	2.26	0.13	U11	1.74	0.09	V11	1.61	0.07
T12	1.06	0.05	R12	1.01	0.06	S12	1.73	0.1	U12	2.61	0.16	V12	1.74	0.07
T13	2.65	0.14	R13	1.49	0.07	S13	2.00	0.1	U13	0.96	0.04	V13	2.36	0.10
T14	1.87	0.09	R14	1.39	0.08	S14	3.58	0.2	U14	1.47	0.07	V14	1.91	0.07
T15	0.72	0.03	R15	1.32	0.07	S15	2.65	0.16	U15	1.57	0.09	V15	2.09	0.09
-	-	-	R16	1.37	0.11	S16	3.03	0.2	U16	0.92	0.05	V16	0.66	0.03
-	-	-	R17	1.15	0.09	S17	2.38	0.2	U17	1.00	0.07	V17	1.48	0.08
-	-	-	R18	1.15	0.10	S18	1.71	0.14	U18	1.57	0.10	V18	1.67	0.11

Unit of SD (standard deviation) is GPa.

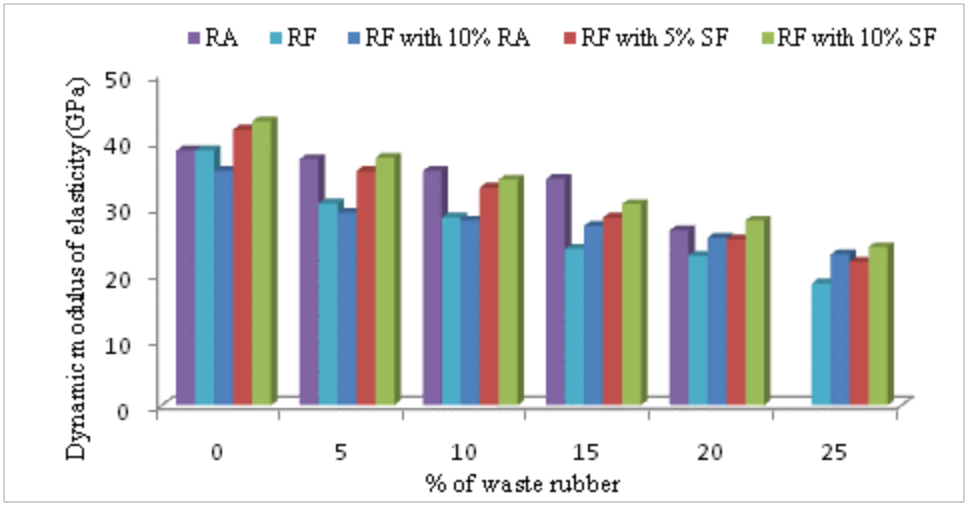

Fig. 5.12 Dynamic modulus of elasticity of waste rubber concrete for 0.35 w/c ratio

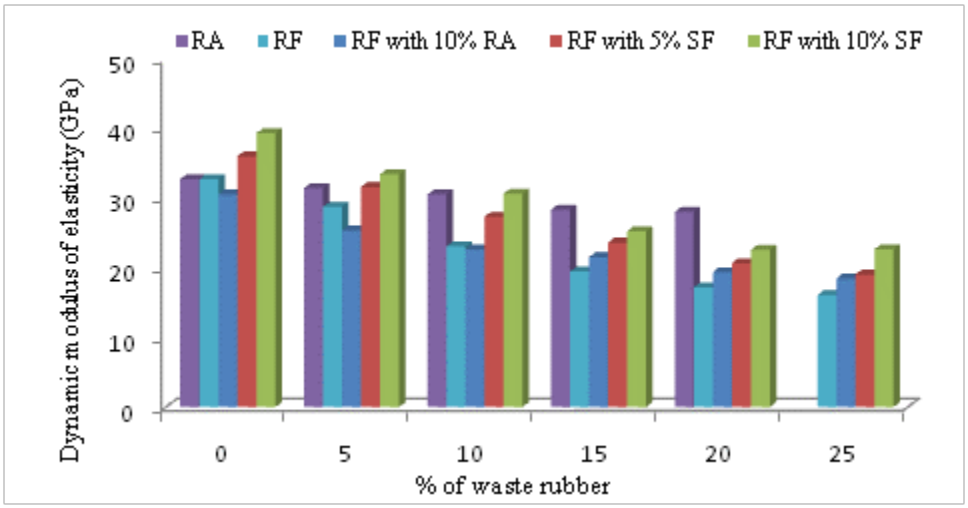

Fig. 5.13 Dynamic modulus of elasticity of waste rubber concrete for 0.45 w/c ratio

Fig. 5.14 Dynamic modulus of elasticity of waste rubber concrete for 0.55 w/c ratio

5.4.4 Impact Resistance

5.4.4.1 *Impact resistance under drop weight test*

The impact resistance of waste rubber concrete for all three different w/c ratios was recorded in terms of numbers of blows required for producing first visible crack (N_1) and ultimate failure (N_2) of the specimen.

The numbers of blows for 0% to 20% replacement of FA by rubber ash at three selected w/c ratios, along with the statistical variances of the results, are listed in Table 5.3. It can be seen from the Table that the number of blows (N_1 and N_2), increased significantly with the increase in rubber ash content. The difference between number of blows for ultimate failure and first crack (N_2-N_1) is also found to increase significantly with the increase in rubber ash content for all three w/c ratios. Typically, for w/c ratio of 0.45, difference increased from 6 on no replacement to 15 on 20% replacement of FA by rubber ash.

The numbers of blows for 0% to 25% replacement of FA by rubber fiber, without any replacement of cement by SF, at three selected w/c ratios are listed in Table 5.4. Statistical variances of results for impact resistance of rubber fiber concrete are also shown in the Table. It can be seen from the Table that the number of blows (N_1 and N_2), increased significantly with the increase in rubber fiber content. The difference between number of blows for ultimate failure and first crack (N_2-N_1) is also found to increase significantly with the increase in rubber fiber content for all three w/c ratios. Typically, for w/c ratio of 0.45, difference increased from 6 on replacement to 32 on 25% replacement of FA by rubber fibers.

The numbers of blows for hybrid concrete (10% rubber ash and 0% to 25% replacement of FA by rubber fiber), at three selected w/c ratios are listed in Table 5.5 alongwith the statistical variances of results. It can be seen from the Table that the number of blows (N_1 and N_2), increased significantly with the increase in rubber fiber content. The difference between number of blows for ultimate failure and first crack (N_2-N_1) is also found to increase significantly with the increase of replacement level of rubber fibers. Typically, for w/c ratio of 0.45, difference increased from 10 on no replacement to 28 on 10% replacement of FA by rubber ash along with 25% replacement of FA by rubber fiber.

.

It may be noted that, earlier also, upto 160% increase in impact resistance was reported by Atahan *et al.* (2012) on 100% replacement of FA by crumb rubber. Increase in impact resistance may be due to the (i) less brittleness and much lower elastic modulus of the rubber aggregate which increased the impact resistance (Atahan *et al.* 2012); and (ii) ability of rubber to absorb energy (Al-Tayeb *et al.* 2013).

The number of blows for rubber fiber concrete, with 5% and 10% replacement of cement by SF, are shown in Tables 5.6 and 5.7 respectively. Statistical variances of results for impact resistance of rubber fiber concrete with 5% and 10% SF are also shown in the Tables. An increase in number of blows is observed with the increase in rubber fiber content as observed earlier in Table 5.13 for concrete without SF. The values of N_1 and N_2, for all three water cement ratios, increase by about five times on incorporation of 25% rubber fiber for both 5% SF concrete and 10% SF concrete.

Table 5.3 Impact resistance results for rubber ash concrete

Mix	N_1			N_2			N_2-N_1	Impact Energy (J)		N_2/N_1
	Mean	SD	COV (%)	Mean	SD	COV (%)		First crack	Ultimate failure	
T1	58	5.29	10.17	65	3.61	5.23	7	1152	1291	1.12
T2	67	9.64	13.58	77	2.65	2.82	10	1331	1530	1.15
T3	88	6.93	6.79	102	7.00	5.88	14	1748	2026	1.16
T4	105	9.64	5.16	120	23.39	9.51	15	2086	2384	1.14
T5	118	24.33	8.88	138	4.00	1.13	20	2344	2741	1.17
T6	47	1.73	3.53	53	2.00	3.64	6	934	1053	1.13
T7	52	6.08	9.81	60	5.29	7.35	8	1033	1192	1.15
T8	63	9.54	12.55	73	7.81	8.40	10	1252	1450	1.16
T9	88	11.53	8.73	98	10.82	6.98	10	1748	1947	1.11
T10	94	4.36	2.09	109	2.65	1.09	15	1867	2165	1.16
T11	39	3.61	9.03	44	2.65	6.46	5	775	874	1.13
T12	43	3.61	7.68	50	5.29	10.17	7	854	993	1.16
T13	52	1.73	2.75	61	2.65	3.63	9	1033	1212	1.17
T14	67	9.64	12.36	78	7.94	8.19	11	1331	1549	1.16
T15	72	3.61	1.95	86	2.65	1.20	14	1430	1708	1.19

SD = Standard deviation; COV = coefficient of variation

Table 5.4 Impact resistance results for rubber fiber concrete without silica fume

Mix	N_1			N_2			N_2-N_1	Impact Energy (J)		N_2/N_1
	Mean	SD	COV (%)	Mean	SD	COV (%)		First crack	Ultimate failure	
R1	58	5.29	10.17	65	3.61	5.23	7	1152	1291	1.12
R2	82	9.64	13.58	95	2.65	2.82	13	1629	1887	1.16
R3	106	6.93	6.79	124	7.00	5.88	18	2106	2463	1.17
R4	198	9.64	5.16	219	23.39	9.51	21	3933	4350	1.11
R5	242	6.08	2.47	278	7.81	2.90	36	4807	5523	1.15
R6	302	24.33	8.88	349	4.00	1.13	47	5999	6933	1.16
R7	47	1.73	3.53	53	2.00	3.64	6	934	1053	1.13
R8	69	6.08	9.81	78	5.29	7.35	9	1371	1549	1.13
R9	87	9.54	12.55	102	7.81	8.40	15	1728	2026	1.17
R10	145	11.53	8.73	167	10.82	6.98	22	2880	3317	1.15
R11	197	8.66	4.63	221	16.64	6.93	24	3913	4390	1.12
R12	214	4.36	2.09	246	2.65	1.09	32	4251	4887	1.15
R13	39	3.61	9.03	44	2.65	6.46	5	775	874	1.13
R14	48	3.61	7.68	56	5.29	10.17	8	954	1112	1.17
R15	65	1.73	2.75	76	2.65	3.63	11	1291	1510	1.17
R16	89	9.64	12.36	106	7.94	8.19	17	1768	2106	1.19
R17	118	4.58	3.75	144	6.24	4.55	26	2344	2861	1.22
R18	189	3.61	1.95	224	2.65	1.20	35	3755	4450	1.19

Table 5.5 Impact resistance results for hybrid concrete

Mix	N_1			N_2			N_2-N_1	Impact Energy (J)		N_2/N_1
	Mean	SD	COV (%)	Mean	SD	COV (%)		First crack	Ultimate failure	
S1	88	5.29	10.17	102	3.61	5.23	14	1748	2026	1.16
S2	96	9.64	13.58	111	2.65	2.82	15	1907	2205	1.16
S3	118	6.93	6.79	138	7.00	5.88	20	2344	2741	1.17
S4	205	9.64	5.16	228	23.39	9.51	23	4072	4529	1.11
S5	256	6.08	2.47	286	7.81	2.90	30	5086	5681	1.12
S6	314	24.33	8.88	359	4.00	1.13	45	6238	7132	1.14
S7	63	1.73	3.53	73	2.00	3.64	10	1252	1450	1.16
S8	73	6.08	9.81	84	5.29	7.35	11	1450	1669	1.15
S9	92	9.54	12.55	106	7.81	8.40	14	1828	2106	1.15
S10	156	11.53	8.73	173	10.82	6.98	17	3099	3437	1.11
S11	204	8.66	4.63	226	16.64	6.93	22	4053	4490	1.11
S12	226	4.36	2.09	254	2.65	1.09	28	4490	5046	1.12
S13	52	3.61	9.03	61	2.65	6.46	9	1033	1212	1.17
S14	59	3.61	7.68	73	5.29	10.17	14	1172	1450	1.24
S15	72	1.73	2.75	89	2.65	3.63	17	1430	1768	1.24
S16	96	9.64	12.36	117	7.94	8.19	21	1907	2324	1.22
S17	132	4.58	3.75	159	6.24	4.55	27	2622	3159	1.20
S18	196	3.61	1.95	228	2.65	1.20	32	3894	4529	1.16

Table 5.6 Impact resistance results for rubber fiber concrete with 5% silica fume

Mix	N_1			N_2			N_2-N_1	Impact Energy (J)		N_2/N_1
	Mean	SD	COV (%)	Mean	SD	COV (%)		First crack	Ultimate failure	
U1	61	2.65	4.14	67	2.65	3.79	6	1212	1331	1.10
U2	84	2.00	2.38	96	4.36	4.32	12	1669	1907	1.14
U3	115	1.73	1.52	135	1.73	1.29	20	2285	2682	1.17
U4	209	7.94	3.97	233	7.94	3.54	24	4152	4629	1.11
U5	245	13.23	5.51	279	9.64	3.60	34	4867	5542	1.14
U6	309	2.65	0.86	355	8.54	2.35	46	6138	7052	1.15
U7	49	3.00	6.12	56	3.61	6.94	7	973	1112	1.14
U8	75	1.73	2.37	83	3.61	4.57	8	1490	1649	1.11
U9	89	1.73	1.99	108	6.56	6.50	19	1768	2145	1.21
U10	153	3.61	2.42	178	4.36	2.41	25	3039	3536	1.16
U11	214	10.54	5.19	251	13.11	5.53	37	4251	4986	1.17
U12	221	1.73	0.79	261	3.46	1.32	40	4390	5185	1.18
U13	43	2.65	6.46	49	3.61	8.02	6	854	973	1.14
U14	52	1.73	3.46	62	2.65	4.49	10	1033	1232	1.19
U15	71	6.24	9.75	83	4.36	5.59	12	1410	1649	1.17
U16	97	1.73	1.75	112	2.65	2.43	15	1927	2225	1.15
U17	128	7.00	5.60	162	6.56	4.23	34	2543	3218	1.27
U18	197	11.36	6.17	236	2.65	1.13	39	3913	4688	1.20

Table 5.7 Impact resistance results for rubber fiber concrete with 10% silica fume

Mix	N_1			N_2			N_2-N_1	Impact Energy (J)		N_2/N_1
	Mean	SD	COV (%)	Mean	SD	COV (%)		First crack	Ultimate failure	
V1	64	3.61	6.02	72	6.08	9.35	8	1271	1430	1.13
V2	89	1.73	1.92	101	6.08	6.47	12	1768	2006	1.13
V3	124	1.00	0.81	143	3.00	2.14	19	2463	2841	1.15
V4	214	2.00	0.94	240	3.61	1.53	26	4251	4768	1.12
V5	251	8.19	3.38	289	6.08	2.13	38	4986	5741	1.15
V6	322	6.08	1.93	372	6.08	1.67	50	6397	7390	1.16
V7	54	4.58	9.35	59	4.36	8.07	5	1073	1172	1.09
V8	84	3.46	4.33	91	6.24	7.43	7	1669	1808	1.08
V9	94	3.00	3.30	112	4.36	4.07	18	1867	2225	1.19
V10	158	6.00	3.66	184	3.46	1.92	26	3139	3655	1.16
V11	223	2.65	1.20	265	12.49	4.98	42	4430	5264	1.19
V12	229	8.89	4.06	274	5.57	2.08	45	4549	5443	1.20
V13	49	4.36	9.91	54	6.56	10.75	5	973	1073	1.10
V14	58	2.65	4.82	67	5.57	9.13	9	1152	1331	1.16
V15	74	4.36	6.32	89	6.08	7.41	15	1470	1768	1.20
V16	101	7.00	7.53	121	6.24	5.47	20	2006	2404	1.20
V17	132	6.08	4.86	164	15.13	10.29	32	2622	3258	1.24
V18	204	11.14	5.80	244	5.57	2.34	40	4053	4847	1.20

In general, it can be concluded that the impact resistance, for first crack as well as for ultimate failure, increased with the increase in rubber ash and rubber fiber content. Similar observations were made by Mohammadi *et al.* (2009) for steel fibers and the increase in impact resistance was attributed to long fibers which are expected to arrest the cracks due to their superior bond resistance. As the replacement level of rubber ash or rubber fibers will increase, rubber-cement composite will have higher flexibility.

Tables 5.6-5.7 reveal that although the impact energy is enhanced by SF, however, no definite pattern is observed for effect of SF on N_2-N_1.

The number of blows required for the first crack in concrete, for three different w/c ratios, is shown in Fig. 5.3-5.7. It can be observed that the number of blows is more for the waste rubber concrete as compared to the corresponding case of non waste rubber concrete. The fracture pattern of cylindrical specimen for control concrete and rubber fiber concrete (25% rubber fibers) without SF is shown in Figs. 5.18(a) and 5.18(b) respectively.

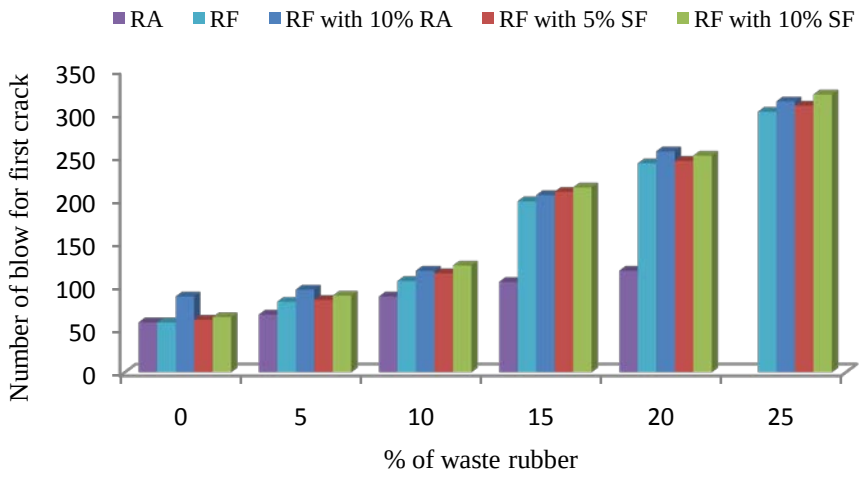

Fig. 5.15 Number of blows for first crack (N_1) for w/c ratio 0.35

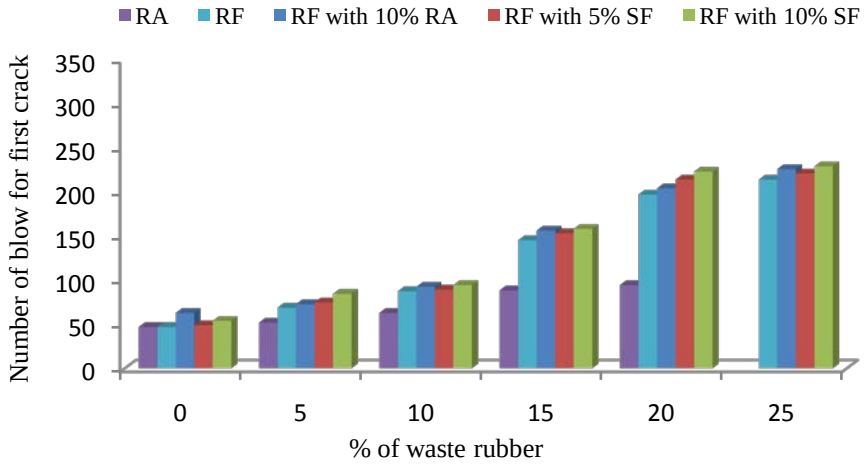

Fig. 5.16 Number of blows for first crack (N_1) for w/c ratio 0.45

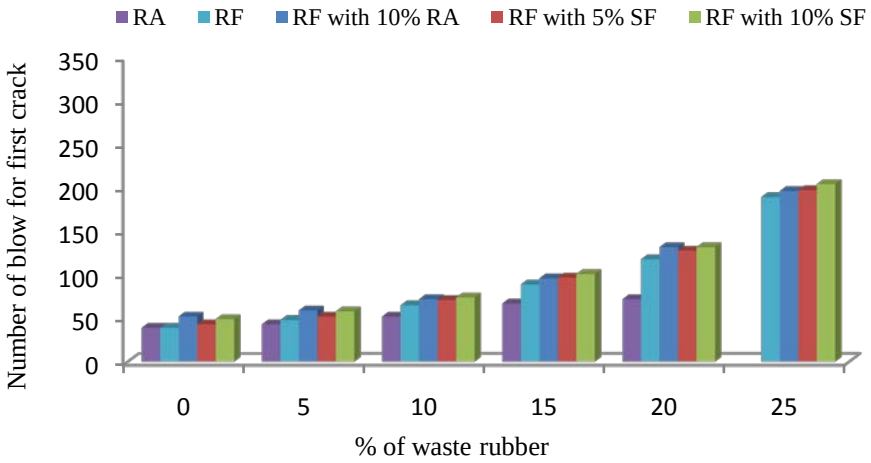

Fig. 5.17 Number of blows for first crack (N_1) for w/c ratio 0.55

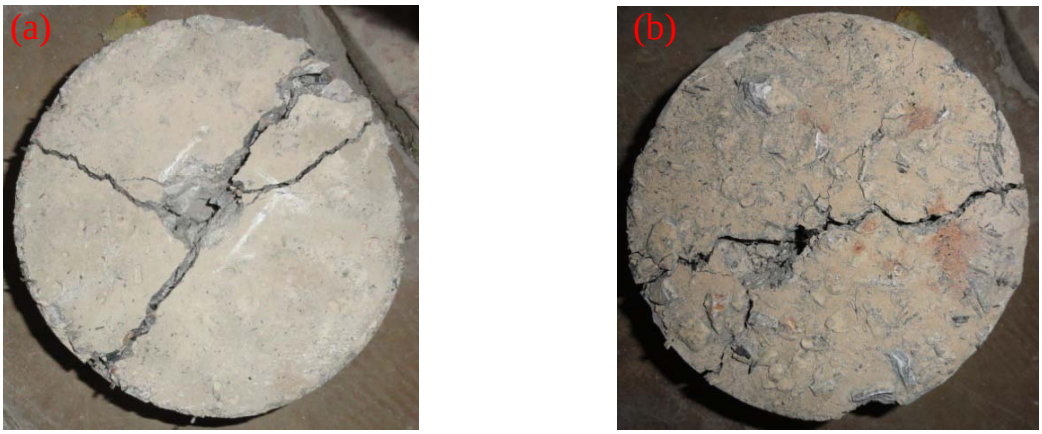

Fig. 5.18 Fracture pattern of concrete with different rubber fiber volume: (a) control concrete; and (b) rubber fiber concrete (25% rubber fibers)

5.4.4.2 *Regression analysis for drop weight test*

Linear relationship between number of blows for first crack and ultimate failure crack for rubber ash concrete, rubber fiber concrete, hybrid concrete, rubber fiber concrete with 5% and 10% SF, was established. Based on the test results, the relationship between N_1 and N_2 may be expressed as:

$$N_2 = 1.161\,N_1 - 0.626 \text{ for rubber ash concrete} \quad (5.8)$$

$$N_2 = 1.145\,N_1 + 1.037 \text{ for rubber fiber concrete without silica fume} \quad (5.9)$$

$$N_2 = 1.107\,N_1 + 5.6 \text{ for hybrid concrete} \quad (5.10)$$

$$N_2 = 1.155\,N_1 + 1.108 \text{ for rubber fiber concrete with 5\% silica fume} \quad (5.11)$$

$$N_2 = 1.171\,N_1 - 0.884 \text{ for rubber fiber concrete with 10\% silica fume} \quad (5.12)$$

Coefficient of determination (R^2) for rubber ash concrete, rubber fiber concrete, hybrid concrete, rubber fiber concrete with 5% SF and 10% SF are 0.996, 0.998, 0.997, 0.996 and 0.997 respectively. According to Rahmani *et al.* (2012), a coefficient of determination of 0.7 or higher is sufficient for a reasonable model, hence above equations can be successfully used to represent the relationship between N_1 and N_2 for rubber ash concrete, rubber fiber concrete, hybrid concrete, rubber fiber concrete with 5% SF and 10% SF.

5.4.4.3 *Impact resistance under flexural loading test*

Fig. 5.19 shows the impact energy at failure, under flexural loading test, for waste rubber concrete for w/c ratio 0.35. It can be seen from the Fig. that the increase in the replacement level of waste rubber content significantly improves the impact energy for types of concrete. Figs. 5.20 and 5.21 show the impact energy at failure under flexural loading test for waste rubber concrete for w/c ratios 0.45 and 0.55 respectively. It is again observed that the impact energy increased with the increase in waste rubber content.

It is observed from the Figs. that the impact energy of concrete (without rubber fiber and SF) increased from 36.0 N.m to 63.0 N.m, 27.0 N.m to 54.0 N.m and 22.5 N.m to 50.0 N.m for w/c ratios 0.35, 0.45 and 0.55 respectively, on 20% replacement of FA by rubber ash. Whereas the impact energy of concrete (without rubber fiber and SF) increased from 36.0 N.m to 108.0 N.m, 27.0 N.m to 90.0 N.m and 22.5 N.m to 81.0 N.m respectively on 25% replacement of FA by rubber fibers. Similarly, the impact energy of concrete (without SF) increased from 41.0 N.m to 95.0 N.m, 32.0 N.m to 85.5 N.m and 27.0 N.m to 81.0 N.m respectively, on 10% replacement of FA by rubber ash along with 25% replacement of FA by rubber fiber.

It may be noted that, earlier also, upto 171% increase in impact resistance was reported by Reda Taha *et al.* (2008) on 50% replacement of coarse aggregate by rubber chipped and 37% increased in impact energy on 50% replacement of FA by crumb rubber. Increase in impact resistance may be due to the relatively high flexibility of low stiffness particles at low to medium replacement and thus absorb a considerable amount of energy (Reda Taha *et al.* 2008).

It can be observed from Figs. 5.19-5.21 that the impact energy increased with the increase of SF in concrete. It is also observed from the Figs. that on 10% replacement of cement by SF, the impact energy of concrete (without rubber ash and rubber fiber) increased from 36.0 N.m to 50.0 N.m, 27.0 N.m to 41.0 N.m and 22.5 N.m to 32.0 N.m for w/c ratios 0.35, 0.45 and 0.55 respectively. Similarly, the impact energy of rubber fiber concrete (25% rubber fiber) increased from 108.0 N.m to 131.0 N.m, 90.0 N.m to 117.0 N.m and 81.0 N.m to 113.0 N.m for w/c ratios 0.35, 0.45 and 0.55 respectively, on 10% replacement of cement by SF.

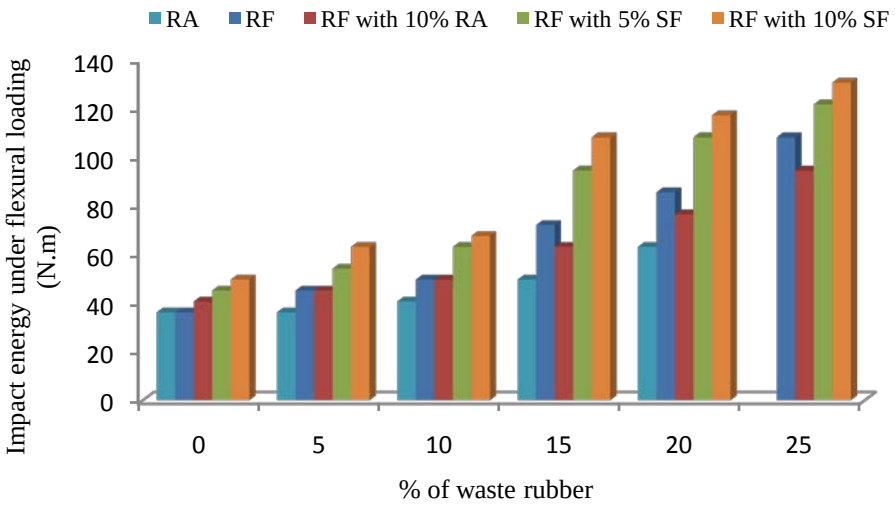

Fig. 5.19 Impact energy under flexural loading test of waste rubber concrete for w/c ratio 0.35

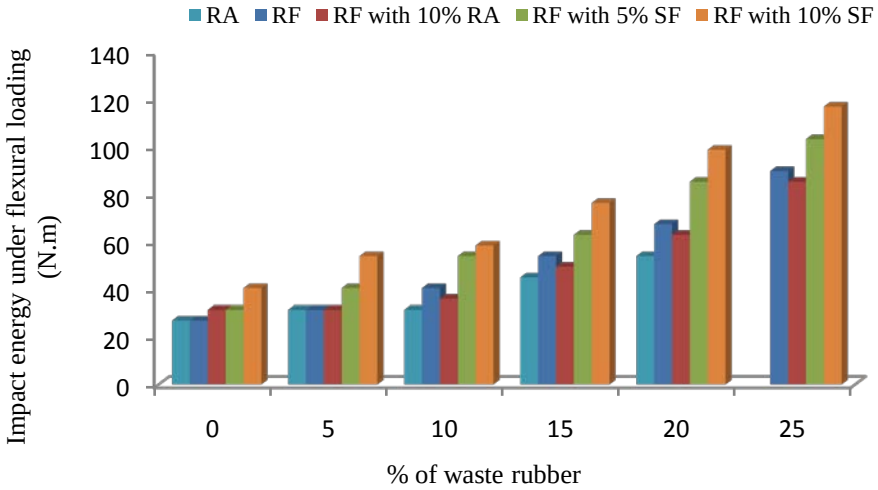

Fig. 5.20 Impact energy under flexural loading test of waste rubber concrete for w/c ratio 0.45

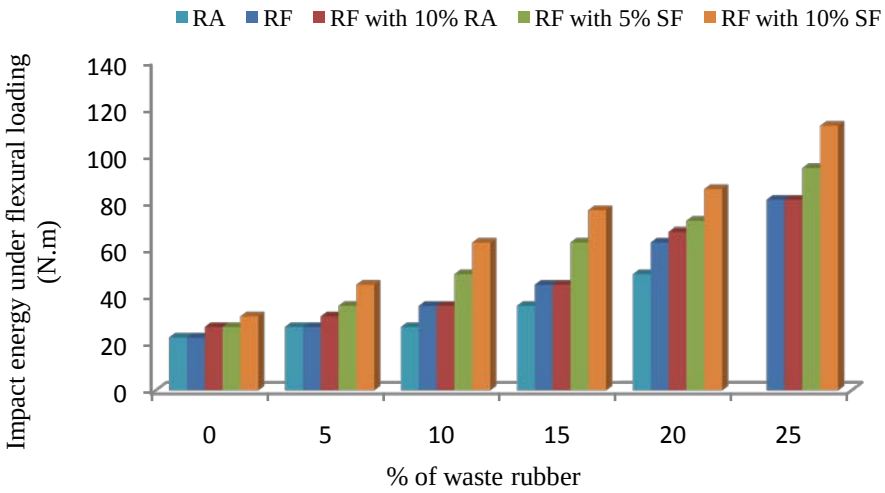

Fig. 5.21 Impact energy under flexural loading test of waste rubber concrete for w/c ratio 0.55

5.4.4.4 *Impact resistance under rebound test*

Fig. 5.22 shows the impact energy absorbed in rebound test, for waste rubber concrete for w/c ratio 0.35. It can be seen from the Fig. that the increase in the replacement level of rubber ash and rubber fibers significantly improves the impact energy absorbed for all waste rubber content. Figs. 5.23-5.24 show the impact energy absorbed under rebound test for waste rubber concrete for w/c ratios 0.45 and 0.55 respectively. It is again observed that the impact energy absorbed increased with the increase of replacement level of rubber ash and rubber fiber. Similar observations were made by Obzay *et al.* (2011) for the crumb rubber concrete.

It is observed from the Figs. that on 20% replacement of FA by rubber ash, the impact energy absorbed by concrete increased from 1.79 N.m to 1.93 N.m, 1.77 N.m to 1.90 N.m and 1.74 N.m to 1.85 N.m for w/c ratios 0.35, 0.45 and 0.55 respectively, whereas, on 25% replacement of FA by rubber fibers, the impact energy absorbed by concrete increased from 1.79 N.m to 1.99 N.m, 1.77 N.m to 1.96 N.m and 1.74 N.m to 1.94 N.m respectively.

It is further observed from the Figs. that on replacement of FA by 10% rubber ash and 0% to 25% rubber fibers, the impact energy absorbed by concrete increased from 1.84 N.m to 2.00 N.m, 1.81 N.m to 1.98 N.m and 1.81 N.m to 1.96 N.m for w/c ratios 0.35, 0.45 and 0.55 respectively.

It may be noted that, earlier also, upto 24% increased in energy absorption capacity was reported by Ozbay *et al.* (2011) on 25% replacement of FA by crumb rubber. Increase in impact resistance may be due to the absorption capacity of rubber particles and therefore the rubber concrete can absorb more energy than control mix (Ozbay *et al.* 2011).

It can be observed from Figs. 5.22-5.24, that there is a minor effect of replacement of cement by SF on the impact energy absorbed. It is also observed from the Figs. that on 10% replacement of cement by SF, the impact energy absorbed by concrete (without rubber ash and rubber fiber) increased marginally from 1.79 N.m to 1.80 N.m, 1.77 N.m to 1.79 N.m and 1.74 N.m to 1.76 N.m for w/c ratios 0.35, 0.45 and 0.55 respectively. Similarly, impact energy absorbed by rubber fiber concrete (25% rubber fiber) increased marginally from 1.99 N.m to 2.01 N.m, 1.96 N.m to 1.98 N.m and 1.94 N.m to 1.97 N.m respectively on 10% replacement of cement by SF.

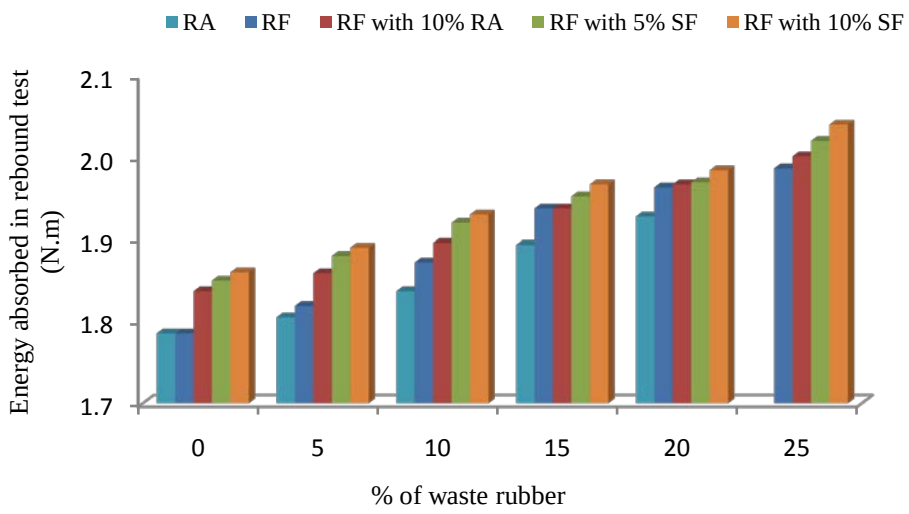

Fig. 5.22 Impact energy absorbed in rebound test of waste rubber concrete for w/c ratio 0.35

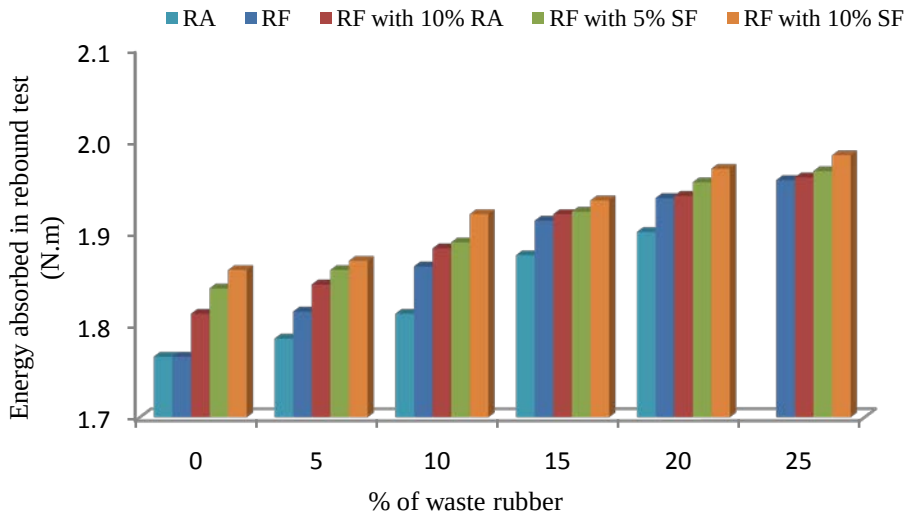

Fig. 5.23 Impact energy absorbed in rebound test of waste rubber concrete for w/c ratio 0.45

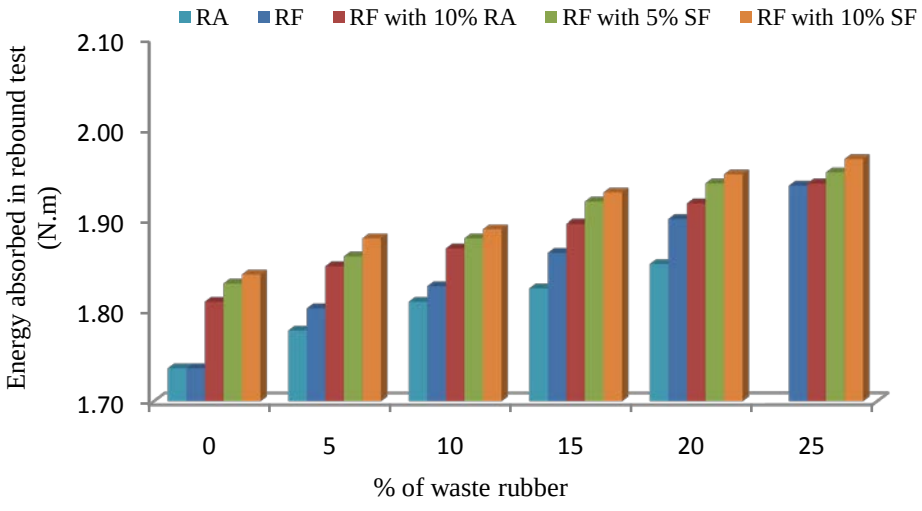

Fig. 5.24 Impact energy absorbed in rebound test of waste rubber concrete for w/c ratio 0.55

5.4.4.5 *Relationship between Impact Energy under drop weight and flexural loading test*

A relationship was developed in form of an equation for evaluating the impact energy under drop weight test from the impact energy under flexural loading or the impact energy under rebound test and vice-versa. Table 5.8 shows the logarithmic relationship between impact energy under drop weight, $E_{p,dwi}$ and impact energy under flexural loading, $E_{p,fl}$. Correlation coefficient (R^2) values show good relationship between $E_{p,dwi}$ and $E_{p,fl}$. Similarly, Table 5.9 shows the logarithmic relationship between impact energy under drop weight, $E_{p,dwi}$ and impact energy under rebound test, $E_{p,r}$. Correlation coefficient (R^2) values show good relationship between $E_{p,dwi}$ and $E_{p,r}$.

Table 5.8 Relationship between Impact Energy under drop weight test $E_{p,dwi}$ and flexural loading $E_{p,fl}$.

Silica fume (%)	w/c ratio	Equation	correlation coefficient (R^2)
Rubber ash concrete	0.35	$E_{p,dwi} = 1985.\ln E_{p,fl} - 5778$	0.909
	0.45	$E_{p,dwi} = 1425.\ln E_{p,fl} - 3763$	0.951
	0.55	$E_{p,dwi} = 881.\ln E_{p,fl} - 1946$	0.894
Rubber fiber concrete	0.35	$E_{p,dwi} = 4589.\ln E_{p,fl} - 15621$	0.988
	0.45	$E_{p,dwi} = 2954.\ln E_{p,fl} - 8886$	0.972
	0.55	$E_{p,dwi} = 2374.\ln E_{p,fl} - 7098$	0.930
Hybrid concrete	0.35	$E_{p,dwi} = 5626.\ln E_{p,fl} - 19351$	0.989
	0.45	$E_{p,dwi} = 3505.\ln E_{p,fl} - 10699$	0.985
	0.55	$E_{p,dwi} = 2351.\ln E_{p,fl} - 6924$	0.946
Rubber fiber concrete with 5% SF	0.35	$E_{p,dwi} = 4783.\ln E_{p,fl} - 17318$	0.972
	0.45	$E_{p,dwi} = 3165.\ln E_{p,fl} - 10208$	0.938
	0.55	$E_{p,dwi} = 2291.\ln E_{p,fl} - 7122$	0.856
Rubber fiber concrete with 10% SF	0.35	$E_{p,dwi} = 4967.\ln E_{p,fl} - 18478$	0.949
	0.45	$E_{p,dwi} = 3666.\ln E_{p,fl} - 12768$	0.969
	0.55	$E_{p,dwi} = 2240.\ln E_{p,fl} - 7255$	0.801

$E_{p,dwi}$ and $E_{p,fl}$ are in N.m.

Table 5.9 Relationship between Impact Energy under drop weight test $E_{p,dwi}$ and rebound test $E_{p,r}$.

Type of Concrete	w/c ratio	Equation	correlation coefficient (R^2)
Rubber ash concrete	0.35	$E_{p,dwi} = 15378.\ln E_{p,r} - 7718$	0.982
	0.45	$E_{p,dwi} = 13243.\ln E_{p,r} - 6617$	0.996
	0.55	$E_{p,dwi} = 10899.\ln E_{p,r} - 5319$	0.880
Rubber fiber concrete	0.35	$E_{p,dwi} = 43444.\ln E_{p,r} - 24441$	0.937
	0.45	$E_{p,dwi} = 33013.\ln E_{p,r} - 18223$	0.915
	0.55	$E_{p,dwi} = 25782.\ln E_{p,r} - 13956$	0.832
Hybrid concrete	0.35	$E_{p,dwi} = 54743.\ln E_{p,r} - 32011$	0.956
	0.45	$E_{p,dwi} = 47020.\ln E_{p,r} - 27172$	0.893
	0.55	$E_{p,dwi} = 39560.\ln E_{p,r} - 22933$	0.785
Rubber fiber concrete with 5% SF	0.35	$E_{p,dwi} = 44957.\ln E_{p,r} - 25558$	0.921
	0.45	$E_{p,dwi} = 35073.\ln E_{p,r} - 19607$	0.914
	0.55	$E_{p,dwi} = 26567.\ln E_{p,r} - 14485$	0.854
Rubber fiber concrete with 10% SF	0.35	$E_{p,dwi} = 46458.\ln E_{p,r} - 26798$	0.900
	0.45	$E_{p,dwi} = 34887.\ln E_{p,r} - 19578$	0.923
	0.55	$E_{p,dwi} = 25809.\ln E_{p,r} - 14143$	0.809

$E_{p,dwi}$ and $E_{p,r}$ are in N.m.

5.4.4.6 *Weibull distribution analysis of drop weight test*

The statistical analysis of impact test data of concrete has been described in literature by different mathematical probability models (Xiang-yu *et al.* 2011; Nataraja *et al.* 1999; Song *et al.* 2004; Atef *et al.* 2006). In this study, a number of blows were required in drop weight test making the mechanism similar to the fatigue test. Thus, Weibull distribution function (Xiang-yu *et al.* 2011) has been adopted as a method for statistical analysis of impact test data since this function has been widely used for statistical description of fatigue test data (Li *et al.* 2007; Raif and Irfan 2008). The Weibull distribution provides reasonably accurate forecast with small number of samples (Pasha et al. 2006) so it has been adopted in the present study.

Weibull distribution function is characterized by a probability distribution function $f(n)$ and is given below (Xiang-yu *et al.* 2011):

$$f(n) = \frac{\alpha}{u}\left(\frac{n}{u}\right)^{\alpha-1} e^{-\left(\frac{n}{u}\right)^{\alpha}} \tag{5.13}$$

where, α is Weibull slope or shape parameter; u is scale parameter; and n is specific value of random variable N (=N_1 and N_2 for the present study).

Cumulative density function is obtained by integration of probability distribution function and expressed as

$$F_N(n) = e^{-\left(\frac{n}{u}\right)^{\alpha}} \tag{5.14}$$

The probability of survivorship function is given by (Xiang-yu *et al.* 2011)

$$L_N(n) = 1 - F_N(n) = e^{-\left(\frac{n}{u}\right)^{\alpha}} \tag{5.15}$$

Following relation is obtained by taking natural logarithms of both sides of equation (5.15).

$$\ln\left[\ln\left(\frac{1}{L_N}\right)\right] = \alpha\ln(n) - \alpha\ln(u) \tag{5.16}$$

The relation expressed in equation (5.14) is used to verify the number of blows for first crack resistance and failure resistance. The data of impact resistance (N_1 and N_2) is arranged in ascending order and the empirical survivorship functions for N_1 and N_2 are obtained as (Xiang-yu *et al.* 2011)

$$L_N = 1 - \frac{j}{s+1} \tag{5.17}$$

where, j = failure order number and s = total number of specimen.

The relationship between $\ln\left[\ln\left[1/L_N\right]\right]$ and $\ln n$ should be linear for the application of two parameter Weibull distribution to statistical data of impact resistance (Xiang-yu *et al.* 2011). The variation of $\ln\left[\ln\left[1/L_N\right]\right]$ with $\ln N_1$ for rubber ash concrete, rubber fiber concrete, hybrid concrete, rubber fiber concrete with 5% SF and 10% SF is shown in Figs. 5.25-5.29 respectively.

Similarly, the variation of $\ln\left[\ln\left[1/L_N\right]\right]$ with $\ln N_2$ for rubber ash concrete, rubber fiber concrete, hybrid concrete, rubber fiber concrete with 5% SF and 10% SF is shown in Figs. 5.30-5.34 respectively.

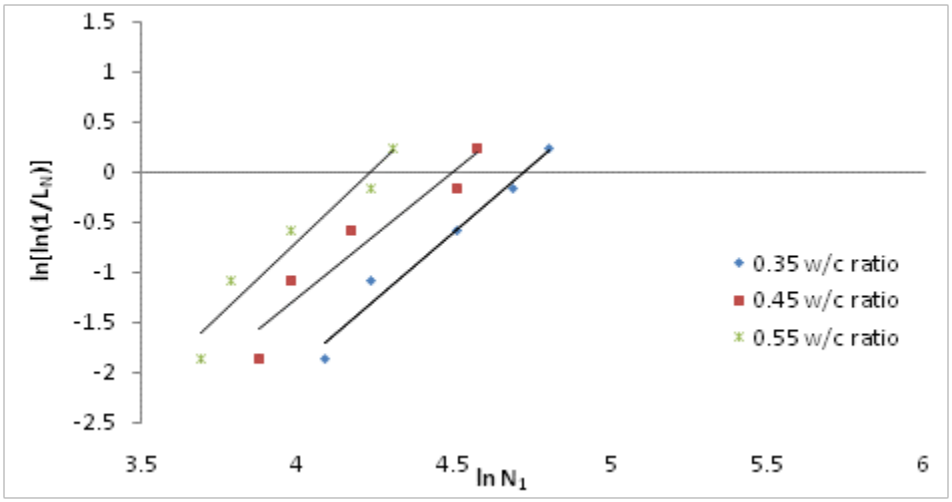

Fig. 5.25 Weibull distribution of N_1 for rubber ash concrete

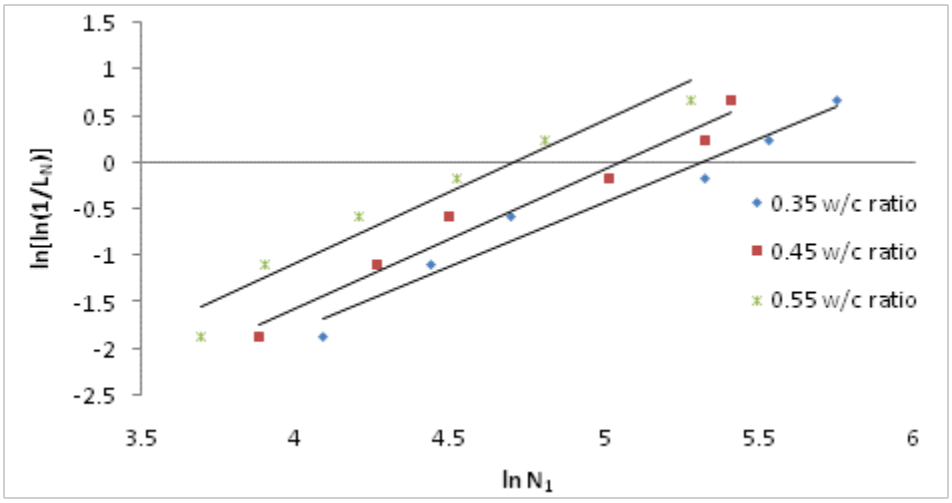

Fig. 5.26 Weibull distribution of N_1 for rubber fiber concrete without silica fume

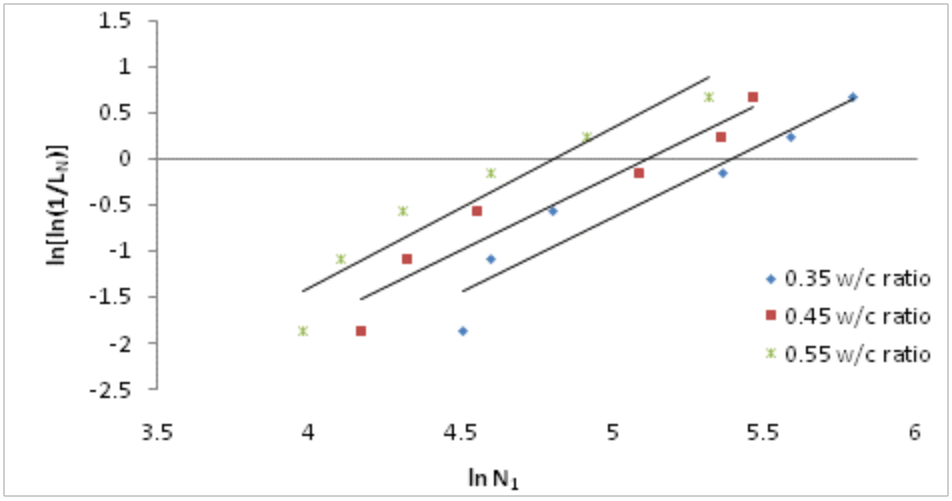

Fig. 5.27 Weibull distribution of N_1 for hybrid concrete

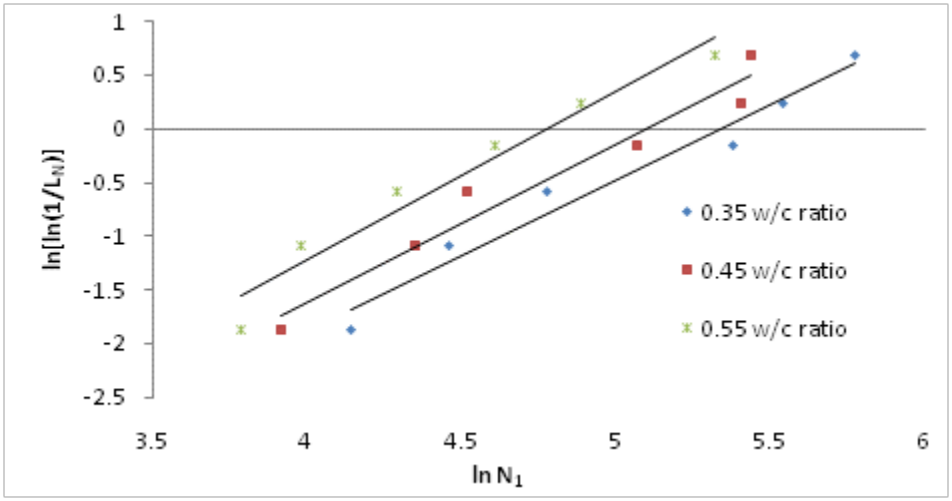

Fig. 5.28 Weibull distribution of N_1 for rubber fiber concrete with 5% silica fume

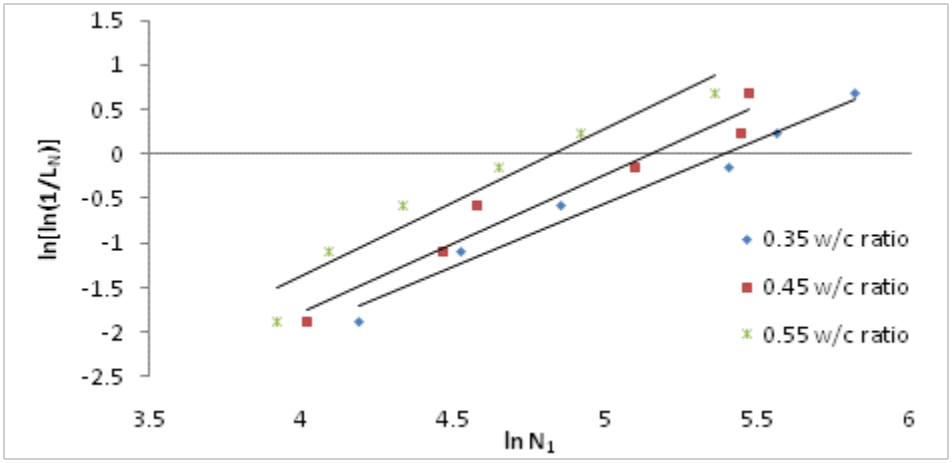

Fig. 5.29 Weibull distribution of N_1 for rubber fiber concrete with 10% silica fume

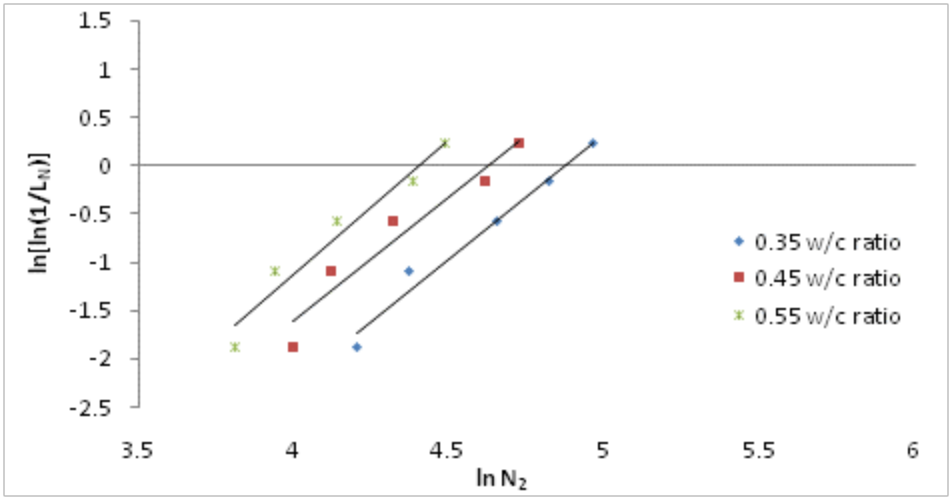

Fig. 5.30 Weibull distribution of N_2 for rubber ash concrete

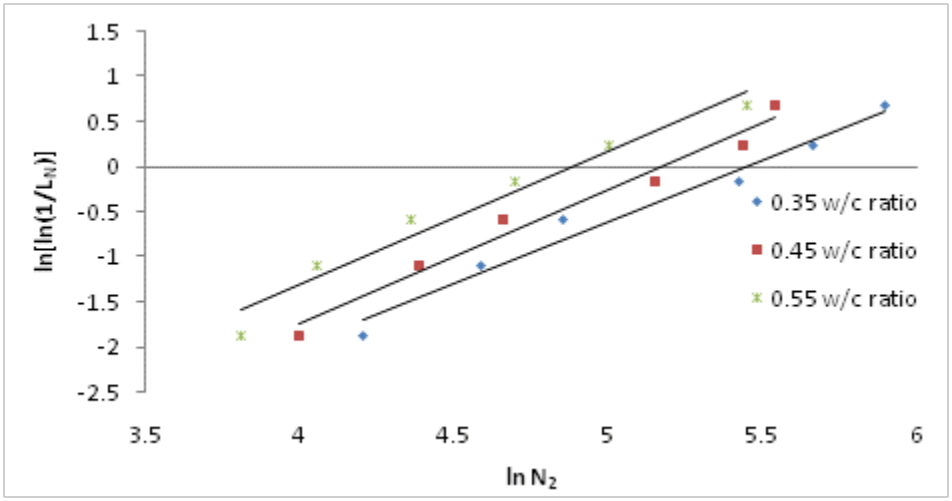

Fig. 5.31 Weibull distribution of N_2 for rubber fiber concrete without silica fume

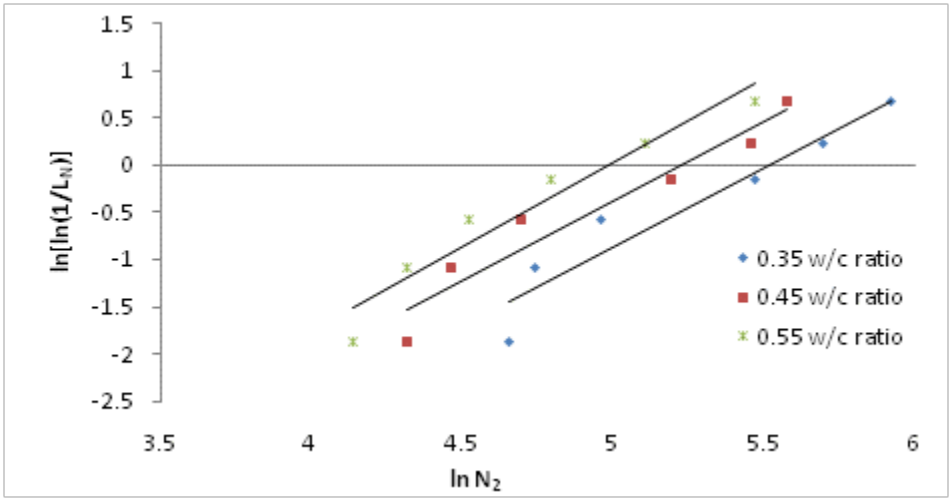

Fig. 5.32 Weibull distribution of N_2 for hybrid concrete

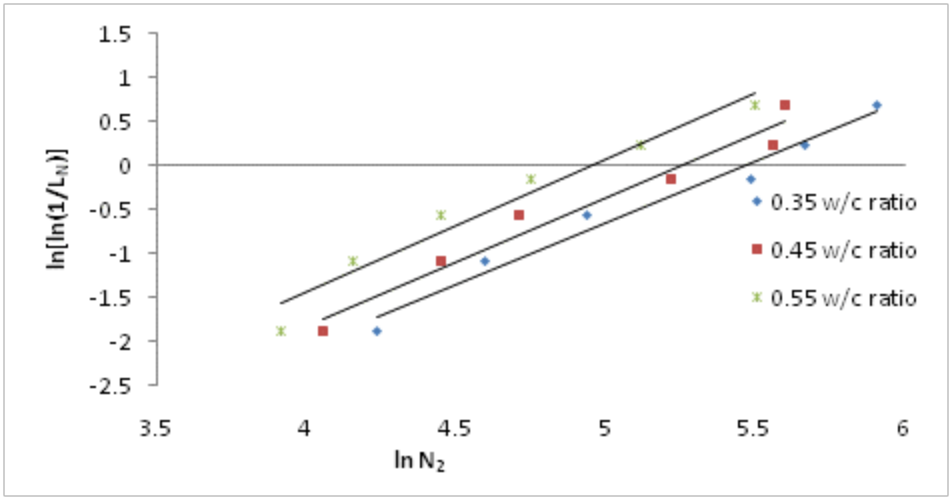

Fig. 5.33 Weibull distribution of N_2 for rubber fiber concrete with 5% silica fume

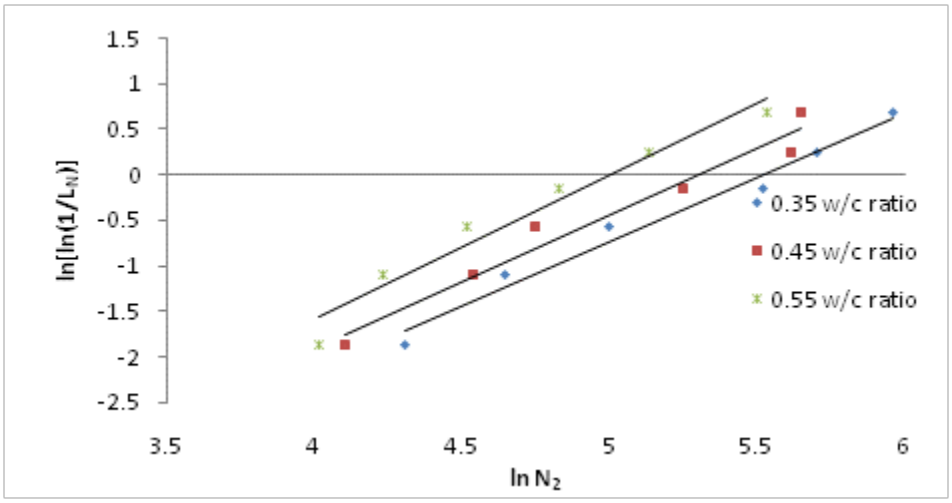

Fig. 5.34 Weibull distribution of N_2 for rubber fiber concrete with 10% silica fume

The regression coefficients of α, $\alpha \ln u$ and the correlation coefficient R^2 corresponding to all the concrete samples for linear regression are shown in Table 5.10. The correlation coefficient R^2 is more than 0.95 in all the cases. Therefore a two parameter Weibull distribution can be assumed to apply to statistical distribution of N_1 and N_2 for waste rubber concrete. Similar observation has been made earlier by Xiang-yu *et al.* (2011) for the concrete containing steel fibers.

Table 5.10 Statistical parameters of Weibull distribution

Failure crack blow	Type of Concrete	w/c ratio	Regression coefficient (α)	Regression coefficient (α *ln u*)	correlation coefficient (R^2)
N_1	Rubber ash concrete	0.35	2.7	12.74	0.969
		0.45	2.526	11.36	0.911
		0.55	2.95	12.49	0.933
	Rubber fiber concrete	0.35	1.373	7.293	0.961
		0.45	1.483	7.477	0.966
		0.55	1.525	7.172	0.948
	Hybrid concrete	0.35	1.626	8.769	0.907
		0.45	1.622	8.288	0.924
		0.55	1.73	8.312	0.911
	Rubber fiber concrete with 5% SF	0.35	1.397	7.469	0.963
		0.45	1.469	7.49	0.956
		0.55	1.569	7.492	0.95
	Rubber fiber concrete with 10% SF	0.35	1.429	7.692	0.971
		0.45	1.539	7.92	0.953
		0.55	1.661	8.013	0.935
N_2	Rubber ash concrete	0.35	2.604	12.67	0.977
		0.45	2.561	11.85	0.936
		0.55	2.805	12.34	0.952
	Rubber fiber concrete	0.35	1.378	7.501	0.972
		0.45	1.483	7.675	0.972
		0.55	1.482	7.227	0.957
	Hybrid concrete	0.35	1.676	9.251	0.914
		0.45	1.681	8.787	0.929
		0.55	1.791	8.928	0.936
	Rubber fiber concrete with 5% SF	0.35	1.39	7.613	0.975
		0.45	1.442	7.581	0.964
		0.55	1.516	7.516	0.955
	Rubber fiber concrete with 10% SF	0.35	1.417	7.82	0.976
		0.45	1.457	7.734	0.963
		0.55	1.588	7.95	0.955

5.4.5 Fatigue strength

The fatigue strength of waste rubber concrete for three different w/c ratios (0.35, 0.45 and 0.55) was recorded in terms of numbers of cycles to ultimate failure of the specimen, N_{ft} .

The numbers of cycles to failure N_{ft} for 0% to 20% replacement of FA by rubber ash at three stress levels (0.9, 0.8 and 0.7) for three selected w/c ratios are listed in Table 5.11 where it is

seen that the number of cycles required for causing the ultimate failure, increased significantly with the increase in rubber ash content for all three w/c ratios. Typically, for w/c ratio of 0.45, number of cycles increased from 264 (mix T6) to 302 (mix T10) for 0.9 stress level; 13,657 (mix T6) to 15,874 (mix T10) for 0.8 stress level; and 207,415 (mix T6) to 214,287 (mix T10) for 0.7 stress level on 20% replacement of FA by rubber ash.

Table 5.11 Fatigue life of rubber ash concrete

Mix*	RA	w/c ratio	Stress level					
			0.9		0.8		0.7	
			No. of Cycles	COV (%)	No. of Cycles	COV (%)	No. of Cycles	COV (%)
T1	0%	0.35	307	6.6	15,714	8.0	221,475	3.2
T2	5%	0.35	327	8.3	15,899	9.5	231,474	1.6
T3	10%	0.35	335	8.8	16,704	4.9	234,741	1.6
T4	15%	0.35	342	9.3	16,987	8.8	236,547	1.3
T5	20%	0.35	358	9.7	17,122	9.9	238,967	1.3
T6	0%	0.45	264	9.6	13,657	8.9	207,415	5.2
T7	5%	0.45	272	9.0	14,174	7.5	209,147	5.4
T8	10%	0.45	279	4.2	14,756	9.5	211,740	4.2
T9	15%	0.45	298	8.4	15,027	8.5	212,147	5.3
T10	20%	0.45	302	5.1	15,874	9.3	214,287	1.4
T11	0%	0.55	249	8.2	11,875	9.5	178,957	6.3
T12	5%	0.55	254	8.4	12,514	9.3	182,547	3.7
T13	10%	0.55	259	4.1	12,874	9.3	187,456	1.8
T14	15%	0.55	271	5.3	13,147	9.0	189,657	1.9
T15	20%	0.55	278	5.2	13,474	2.0	191,578	1.2

*Mixes defined in Table 2.2 COV-Coefficient of variance

The numbers of cycles to failure for 0% to 25% replacement of FA by rubber fiber, without any replacement of cement by SF, at three selected w/c ratios (0.35, 045 and 0.55) are listed in Table 5.12 where it is seen that the number of cycles to failure, required for causing the ultimate failure, increase significantly with the increase in rubber content for all three w/c ratios. Typically, for w/c ratio of 0.45, the number of cycles increased from 264 (mix R7) to 356 (mix R12) for 0.9 stress level; 13,657 (mix R7) to 25,987 (mix R12) for 0.8 stress level; and 207,415 (mix R7) to 304,719 (mix R12) for 0.7 stress level up to 25% replacement of FA by rubber fibers.

Table 5.12 Fatigue life of rubber fiber concrete without silica fume

Mix*	RF	w/c ratio	Stress level					
			0.9		0.8		0.7	
			No. of Cycles	COV (%)	No. of Cycles	COV (%)	No. of Cycles	COV (%)
R1	0%	0.35	307	9.5	15,714	7.7	221,475	1.2
R2	5%	0.35	412	7.7	18,726	8.7	297,854	3.2
R3	10%	0.35	428	3.0	22,344	9.0	348,562	1.8
R4	15%	0.35	434	8.2	23,577	7.7	368,957	2.2
R5	20%	0.35	452	6.2	26,785	5.2	396,578	1.8
R6	25%	0.35	488	4.6	28,755	7.7	402,184	3.2
R7	0%	0.45	264	8.3	13,657	9.4	207,415	1.2
R8	5%	0.45	312	5.2	17,865	6.5	234,789	1.1
R9	10%	0.45	328	4.9	19,245	9.3	252,367	5.2
R10	15%	0.45	332	5.1	21,578	7.2	268,957	3.7
R11	20%	0.45	344	9.9	24,589	9.7	283,785	4.5
R12	25%	0.45	356	7.7	25,987	8.5	304,719	1.4
R13	0%	0.55	249	9.9	11,875	6.9	178,957	1.1
R14	5%	0.55	287	7.3	15,478	6.5	204,587	1.2
R15	10%	0.55	296	4.1	16,974	8.4	216,987	5.7
R16	15%	0.55	318	3.7	19,574	5.4	235,169	6.1
R17	20%	0.55	328	6.1	22,547	9.3	264,712	1.8
R18	25%	0.55	334	9.5	23,147	9.4	284,753	1.8

*Mixes defined in Table 2.3 COV-Coefficient of variance

The numbers of cycles to failure for hybrid concrete (FA replaced by 10% rubber ash and 0% to 25% rubber fiber), at three selected w/c ratios are listed in Table 5.13 where it is seen that the number of cycles to failure, required for causing the ultimate failure, increased significantly with the increase in rubber content for all three w/c ratios. Typically, for w/c ratio of 0.45, number of cycles increased from 279 (mix S7) to 339 (mix S12) for 0.9 stress level; 14,756 (mix S7) to 22,478 (mix S12) for 0.8 stress level; and 211,740 (mix S7) to 271,254 (mix S12) for 0.7 stress level on 10% replacement of FA by rubber ash along with 25% replacement of FA by rubber fiber.

Table 5.13 Fatigue life of hybrid concrete

Mix*	RA	RF	w/c ratio	Stress level					
				0.9		0.8		0.7	
				No. of Cycles	COV (%)	No. of Cycles	COV (%)	No. of Cycles	COV (%)
S1	10%	0%	0.35	335	9.0	16,704	5.9	234,741	5.0
S2	10%	5%	0.35	347	8.1	16,942	3.6	239,750	5.2
S3	10%	10%	0.35	354	9.4	17,896	9.8	249,875	3.7
S4	10%	15%	0.35	364	3.5	19,675	2.6	268,745	2.0
S5	10%	20%	0.35	378	4.7	23,027	9.6	280,247	1.1
S6	10%	25%	0.35	385	2.1	24,569	6.3	286,987	3.6
S7	10%	0%	0.45	279	8.4	14,756	5.9	211,740	1.0
S8	10%	5%	0.45	287	3.8	15,698	7.6	214,598	1.1
S9	10%	10%	0.45	296	8.9	17,896	7.8	236,574	4.9
S10	10%	15%	0.45	314	3.8	19,874	6.9	247,565	2.5
S11	10%	20%	0.45	327	3.2	21,587	6.2	253,698	2.1
S12	10%	25%	0.45	339	9.8	22,478	8.3	271,254	1.2
S13	10%	0%	0.55	259	6.6	12,874	8.7	187,456	1.7
S14	10%	5%	0.55	264	7.0	14,789	5.2	189,875	4.7
S15	10%	10%	0.55	272	5.9	15,657	9.6	195,478	1.3
S16	10%	15%	0.55	287	9.5	17,987	8.7	202,587	3.1
S17	10%	20%	0.55	298	8.5	19,574	7.8	214,789	2.5
S18	10%	25%	0.55	307	9.4	20,156	9.9	232,574	1.2

*Mixes defined in Table 2.4 COV-Coefficient of variance

The numbers of cycles to failure for rubber fiber concrete with 5% replacement of cement by SF are shown in Table 5.14. An increase in the number of cycles to failure is observed with the increase in replacement level of rubber fiber as was observed earlier for concrete without SF. It is also observed that with the increase in SF, the fatigue life of waste rubber concrete increased for all three w/c ratios. Typically, for w/c ratio of 0.45, number of cycles increased from 324 (mix U7) to 374 (mix U12) for 0.9 stress level; 16,452 (mix U7) to 30,252 (mix U12) for 0.8 stress level; and 234,743 (mix U7) to 312,475 (mix U12) for 0.7 stress level on 25% replacement of FA by rubber fibers and 5% replacement of cement by SF.

Table 5.14 Fatigue life of rubber fiber concrete with 5% silica fume

Mix*	RF	w/c ratio	Stress level					
			0.9		0.8		0.7	
			No. of Cycles	COV (%)	No. of Cycles	COV (%)	No. of Cycles	COV (%)
U1	0%	0.35	387	4.2	18,698	6.3	254,789	4.9
U2	5%	0.35	436	6.4	21,478	9.7	314,752	1.7
U3	10%	0.35	455	9.6	25,369	5.2	356,987	3.5
U4	15%	0.35	478	5.9	28,975	2.0	379,622	3.2
U5	20%	0.35	508	4.6	32,471	5.2	414,537	2.8
U6	25%	0.35	517	5.8	33,149	9.1	419,874	2.9
U7	0%	0.45	324	6.7	16,452	7.1	234,743	5.1
U8	5%	0.45	335	9.0	19,247	9.0	249,874	6.8
U9	10%	0.45	347	8.8	22,014	8.2	268,746	4.1
U10	15%	0.45	359	9.7	24,587	7.0	272,644	4.8
U11	20%	0.45	369	6.6	27,416	9.7	289,637	3.2
U12	25%	0.45	374	7.9	30,252	7.2	312,475	7.8
U13	0%	0.55	307	8.8	14,697	9.2	206,569	6.5
U14	5%	0.55	317	8.5	16,987	9.2	218,957	1.6
U15	10%	0.55	331	9.9	19,874	2.4	232,475	1.2
U16	15%	0.55	342	7.4	20,478	8.4	242,580	3.3
U17	20%	0.55	364	9.5	22,581	8.3	272,641	2.4
U18	25%	0.55	371	9.3	25,697	9.3	289,654	1.8

*Mixes defined in Table 2.5 COV-Coefficient of variance

The numbers of cycles to failure for rubber fiber concrete with 10% replacement of cement by SF are shown in Table 5.15. An increase in number of cycles to failure is observed with the increase in rubber fiber content, as was observed earlier in Table 5.12 for concrete without SF. It is also observed that with the increase in SF, the fatigue life of waste rubber concrete increased for all three w/c ratios. Typically, for w/c ratio of 0.45, number of cycles increased from 331 (mix V7) to 385 (mix V12) for 0.9 stress level; 17,896 (mix V7) to 32,147 (mix V12) for 0.8 stress level; and 245,875 (mix V7) to 326,547 (mix V12) for 0.7 stress level on 25% replacement of FA by rubber fibers and 10% replacement of cement by SF.

Table 5.15 Fatigue life of rubber fiber concrete with 10% silica fume

Mix*	RF	w/c ratio	Stress level					
			0.9		0.8		0.7	
			No. of Cycles	COV (%)	No. of Cycles	COV (%)	No. of Cycles	COV (%)
V1	0%	0.35	402	3.8	19,647	6.2	265,478	1.3
V2	5%	0.35	442	3.4	22,547	5.5	325,741	3.4
V3	10%	0.35	467	3.6	25,967	5.1	369,582	3.5
V4	15%	0.35	485	9.2	29,671	7.5	392,147	1.9
V5	20%	0.35	518	7.9	33,541	3.3	425,870	1.0
V6	25%	0.35	524	7.2	35,178	4.8	428,147	2.9
V7	0%	0.45	331	6.8	17,896	4.2	245,875	1.1
V8	5%	0.45	347	7.9	20,141	8.7	259,647	3.6
V9	10%	0.45	349	5.9	23,551	7.3	278,962	3.7
V10	15%	0.45	367	7.5	25,874	1.5	292,547	2.7
V11	20%	0.45	379	7.8	28,963	4.2	301,450	2.4
V12	25%	0.45	385	9.7	32,147	5.4	326,547	1.0
V13	0%	0.55	319	8.6	15,951	4.6	214,562	6.1
V14	5%	0.55	322	7.7	17,985	7.6	225,417	6.0
V15	10%	0.55	348	3.0	20,145	8.8	246,321	5.7
V16	15%	0.55	358	8.9	22,365	8.1	256,985	8.6
V17	20%	0.55	369	8.6	24,562	3.6	289,674	8.8
V18	25%	0.55	379	9.4	26,981	6.1	296,541	1.1

*Mixes defined in Table 2.6 COV-Coefficient of variance

In general, it can be concluded that the fatigue strength increased with the increase in waste rubber content. Similar observations were made by Ganesan *et al.* (2013) for self compacting rubberized concrete containing shredded rubber and the increase in fatigue strength was attributed to the crack arresting property of rubber particles resulting from superior bond resistance. As the replacement level of waste rubber content will increase, rubber-cement composite will have higher flexibility and this increase in flexibility level will lead to more energy absorption as compared to the control mix.

It may be noted that, earlier also, increase in fatigue life was reported by Liu *et al.* (2013) on 15% replacement of FA by rubber grains for w/c ratio 0.31.

5.5 CONCLUSIONS

The ductility properties of concrete, which are essential in promoting the use of waste rubber content as fine aggregate, were evaluated in this chapter. Various tests i.e. static modulus test, ultrasonic pulse velocity test, dynamic modulus test, impact resistance under drop weight test, impact resistance under flexural test, impact resistance under rebound test and fatigue test were performed on waste rubber concrete to assess ductility. In view of large variation of impact values, a two-parameter Weibull distribution was adopted to analyze the experimental data of drop weight test. Following conclusions are drawn:

1. The reduction in static and dynamic modulus on partial replacement of the fine aggregate by waste rubber indicates higher flexibility. The waste rubber concrete can therefore be used in building as an earthquake shock-wave absorber, foundation pad of machinery, construction of highway pavement, airport runways and crash barriers.
2. The impact resistance of concrete improves on replacement of fine aggregate by waste rubber content and on replacement of cement by silica fume.
3. The difference between number of blows for ultimate failure and first crack increases significantly with the increase in replacement level of rubber ash and rubber fibers, which indicate the reduction in brittleness of concrete or increase in ductility of waste rubber fiber concrete.
4. Linear relationship exists between number of blows for first crack and ultimate failure cracks for waste rubber concrete.
5. A good correlation exists between the results of drop weight test, flexural loading and rebound test for control mix as well as rubberized concrete.
6. The impact resistance data for drop weight test follows the two-parameter Weibull distribution function.
7. Fatigue strength of concrete improves on replacement of fine aggregate by waste rubber content and on replacement of cement by silica fume.
8. Difference between the numbers of cycles to failure significantly increases with the increase in replacement level of rubber ash and rubber fibers, which indicates the reduction in brittleness of concrete or increase in ductility of waste rubber concrete.

CHAPTER 6

PROPERTIES OF RUBBERIZED CONCRETE AT ELEVATED TEMPERATURE

6.1 INTRODUCTION

The concrete structures can be affected greatly by the exposure to elevated temperatures. In this chapter, the mechanical and durability properties of waste rubber fiber concrete and control concrete subjected to elevated temperature have been discussed. Detailed experimental investigations have been carried out for the effect of elevated temperature on mass loss and change in compressive strength, density, ultrasonic pulse velocity, static modulus, dynamic modulus, water permeability and chloride ion permeability in control mix (no replacement) and waste rubber fiber concrete. The microstructure of waste rubber fiber concrete subjected to elevated temperature has also been investigated. The study is undertaken for varying percentage of waste rubber fibers (0% to 25%) as fine aggregate (FA) for w/c ratio 0.35, 0.45 and 0.55. Two types of cooling, normal cooling and fast cooling have been considered for the effect of elevated temperature on compressive strength of control mix as well as waste rubber fiber concrete. All the specimens are exposed to six level of temperature (27 ^{0}C – 750 ^{0}C) and three different exposure durations (30, 60 and 120 minutes).

6.2 EXPERIMENTAL PROCEDURE

6.2.1 Compressive strength

Mechanical strength of rubber fiber concrete was measured by conducting compression strength test at a loading rate of 0.25 N/mm^2/s. Compressive strength of hardened concrete was performed on 100 mm × 100 mm × 100 mm concrete cubes at 28 days as per BIS 516 (1959). The concrete cubes were left for one week in the free environment after 28 days water curing. Three concrete specimens were then tested at room temperature (27 ^{0}C) and other specimens were exposed to different elevated temperatures (150 ^{0}C, 300 ^{0}C, 450 ^{0}C, 600 ^{0}C and 750 ^{0}C) and three exposure times (30 minutes, 60 minutes and 120 minutes) using an electrical furnace (Fig. 6.1).

Fig. 6.1 Electric Furnace

The specimens were cooled in two regimes. For each combination of elevated temperature and exposure time, three specimens were left in the laboratory condition for normal cooling in air (NC) and other three specimens were submerged in the water for 10 minutes at room temperature for fast cooling (FC) and then placed in natural condition. The method of fast cooling of concrete cubes simulates the practical aspect of fire fighting. Concrete cubes were submerged in the water for 10 minutes to avoid possible rehydration of the cement paste (Nadeem *et al.* 2014). The compressive strength test was carried out on all the specimens after 24 hours and the average of measurements (three in number) of each cooling regime is presented in this study.

6.2.2 Mass Loss

Cube specimens were weighed on an electronics scale before and after conducting the test for compressive strength. The least count of the machine was 100 mg.

6.2.3 Ultrasonic pulse velocity

A non-destructive test using an ultrasonic pulse device was conducted on air cooled cube specimen according to ASTM C597 (1991) to obtain the ultrasonic pulse velocity of the hardened concrete subjected to elevated temperature. Sufficient amount of gel was applied between the surface of the concrete cube and the transducer to ensure proper contact.

6.2.4 Static modulus of elasticity

Air cooled cylindrical specimen of 150 mm dia and 300 mm in height (three for each mix) were used to determine the static modulus as per ASTM C469 (1994). Specimens were tested on the automatic CTM of 300 tonne capacity with longitudinal compressometer and lateral extensometer attachments. Load was applied gradually with the rate of travel of machine for 240±35 kN/m^2/s. The applied load and corresponding strains were measured. The static modulus was then calculated by equation given in Chapter 5 as equation 5.1.

6.2.5 Dynamic modulus of elasticity

The measured Ultrasonic Pulse Velocity (UPV) was utilized to calculate the dynamic modulus of the hardened concrete subjected to elevated temperature. Equation of Topçu and Bilir (2009) was chosen to evaluate the dynamic modulus and given in Chapter 5 as equation 5.2.

6.2.6 Water permeability

Water permeability test on specimen of rubber fiber concrete was carried out as per German standard DIN 1048 (1991). 24 hours air cooled concrete cube of 150 mm × 150 mm × 150 mm size were used for this study. The specimen were tested for 3 days at a pressure of 0.5 N/mm^2 (5 bar) pressure. After 3 days, specimen was split into two halves on compression testing machine. Depth of water penetration was reported as average of 3 cubes and this depth was measured to the nearest 0.1 mm.

6.2.7 Chloride diffusion

Chloride diffusion test in steady state was adopted to evaluate the chloride ion permeability. The test requires very long duration; however it gives more accurate results as compared to rapid chloride permeability test. Cylindrical samples of 50 mm thickness and 65 mm nominal diameter, cured for 28 days, were used to measure the chloride diffusion coefficient of control mix and waste rubber fiber concrete subjected to elevated temperature. Upstream cell of instrument was filled with 3% sodium chloride (NaCl) solution (anode) while downstream cell of instrument was filled with distilled water (cathode). The amount of chloride concentration passed through was measured over a period of 72 hours maintaining the 30 V DC potential differences.

Initial chloride concentration of upstream cell (3% NaCl) was calculated by titration method. Similarly, chloride concentration of downstream cell (distilled water) was also calculated by titration method at every four hours interval depending upon rate of travel of chloride ion into downstream cell. For titration purpose, 10 ml sample was used and potassium chromate (KCr) drops were added as indicator. Quantity of silver nitrate ($AgNO_3$) was measured when the colour of the sample changed to reddish brown.

The chloride diffusion coefficient (D_{smm}) in m^2/s was evaluated by Nernest-Planck's equation suggested by Andrade (1993) and given in Chapter 4 as equation 4.1.

6.3 RESULTS AND DISCUSSION

6.3.1 Compressive strength at normal cooling

The compressive strength of the control mix and waste rubber fiber concrete exposed to different elevated temperatures for 30, 60 and 120 minutes followed by normal (air) cooling is shown in Figs. 6.2-6.10 respectively. The maximum standard deviation and coefficient of variance anywhere for the experimental results shown in these Figs. are 3.21 N/mm^2 and 0.07 respectively (Fig. 6.2, 0% rubber fibers and 150 ^{0}C temperature). It is seen from the Figs, for both the control concrete and waste rubber fiber concrete, that the compressive strength increased marginally up to 150 ^{0}C for all exposures and then there was reduction in the strength with the increase in temperature. The increase in compressive strength upto 150 ^{0}C may be attributed to the drop in calcium hydroxide and unhydrated part (Nadeem *et al.* 2014).

The percentage reduction in compressive strength on 30 minutes exposure of elevated temperature was similar for both control concrete and waste rubber fiber concrete (Figs. 6.2-6.10). The reduction increased with increase in the exposure time for both normal concrete and waste rubber fiber concrete. However, the increase in reduction with the increase in exposure time was more for waste rubber fiber concrete than control concrete. The specimen containing more than 10% rubber fiber content, when exposed to 750 ^{0}C for 120 minutes, were not in position for compressive test due to deterioration. This may be due to decomposition of C-S-H gels (Demirel and Kelestemur 2010).

The increase in rubber fiber content in waste rubber fiber concrete decreased the percentage reduction in compressive strength for elevated temperature upto 300 ^{0}C with 30 minute and 60 minute exposure.

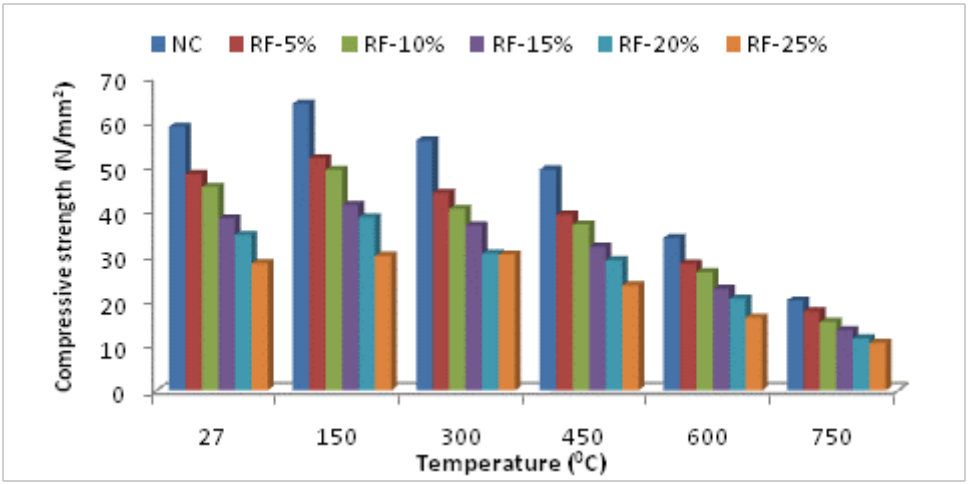

Fig. 6.2 Compressive strength of rubber fiber concrete (w/c ratio 0.35) after exposure to elevated temperature for 30 minutes followed by normal cooling

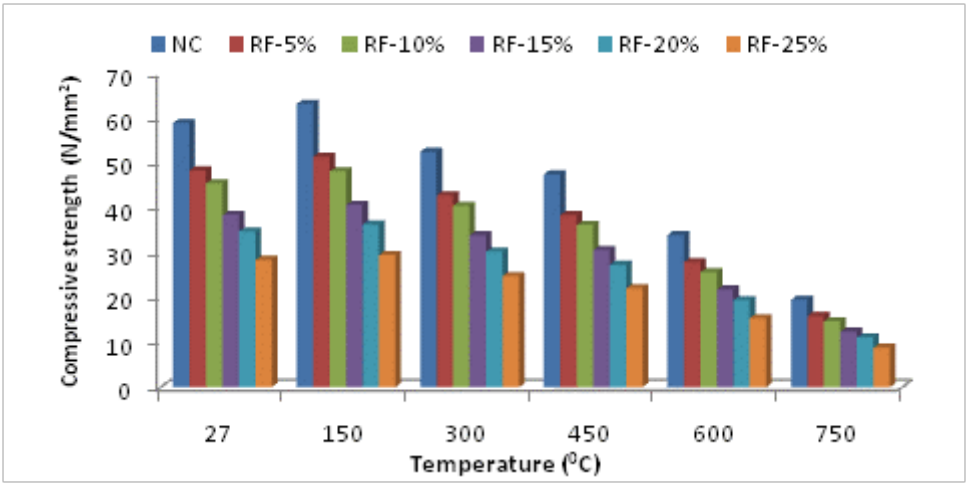

Fig. 6.3 Compressive strength of rubber fiber concrete (w/c ratio 0.35) after exposure to elevated temperature for 60 minutes followed by normal cooling

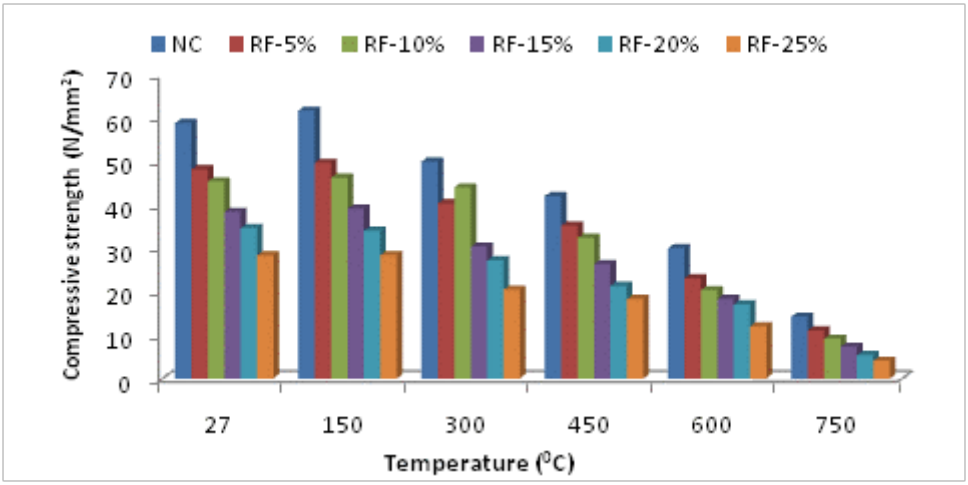

Fig. 6.4 Compressive strength of rubber fiber concrete (w/c ratio 0.35) after exposure to elevated temperature for 120 minutes followed by normal cooling

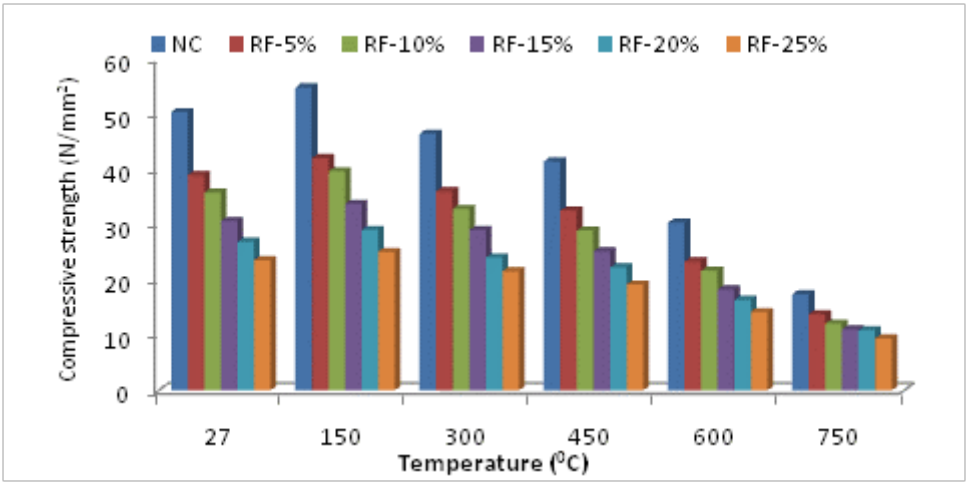

Fig. 6.5 Compressive strength of rubber fiber concrete (w/c ratio 0.45) after exposure to elevated temperature for 30 minutes followed by normal cooling

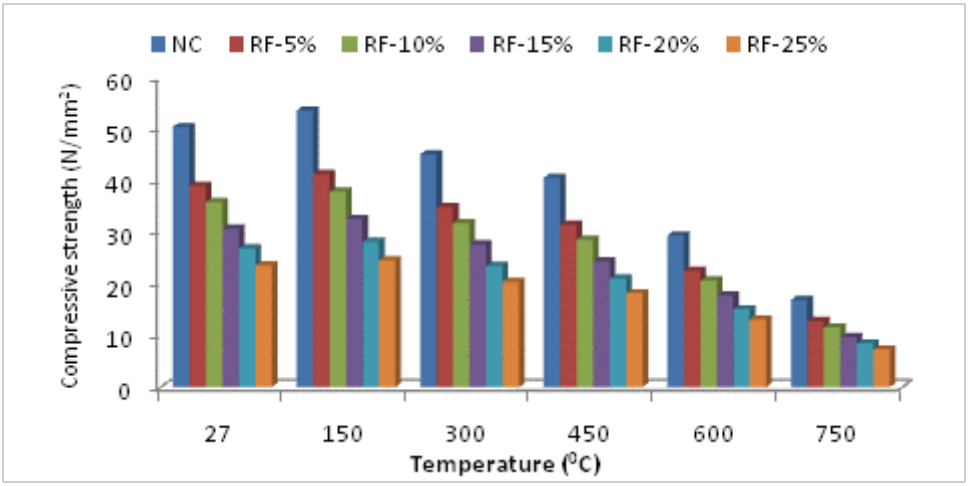

Fig. 6.6 Compressive strength of rubber fiber concrete (w/c ratio 0.45) after exposure to elevated temperature for 60 minutes followed by under normal cooling

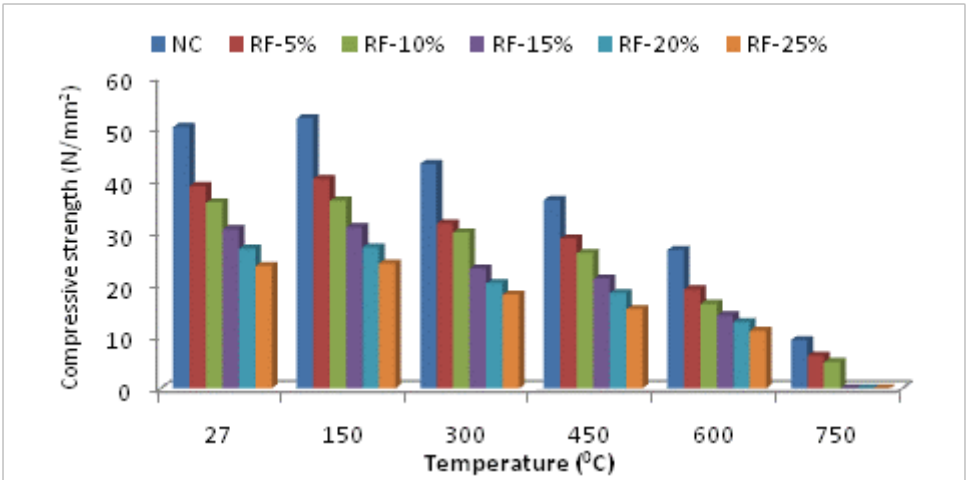

Fig. 6.7 Compressive strength of rubber fiber concrete (w/c ratio 0.45) after exposure to elevated temperature for 120 minutes followed by normal cooling

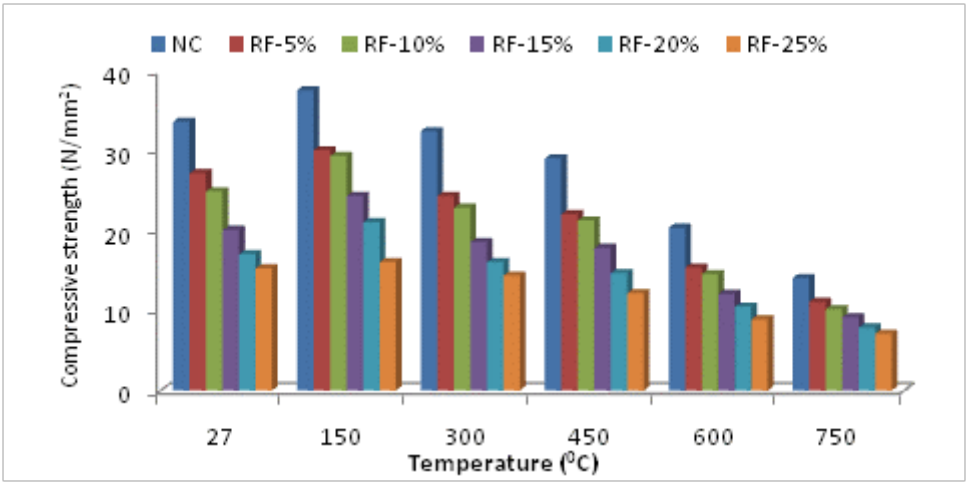

Fig. 6.8 Compressive strength of rubber fiber concrete (w/c ratio 0.55) after exposure to elevated temperature for 30 minutes followed by normal cooling

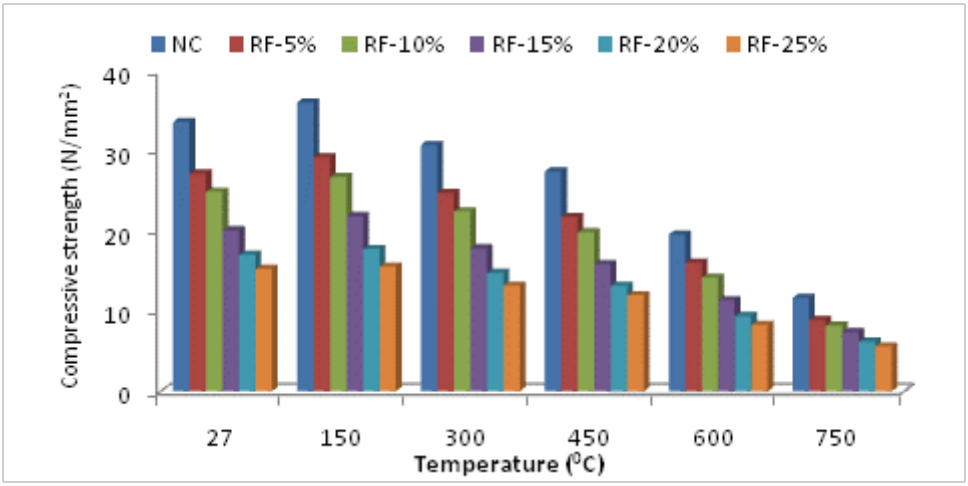

Fig. 6.9 Compressive strength of rubber fiber concrete (w/c ratio 0.55) after exposure to elevated temperature for 60 minutes followed by normal cooling

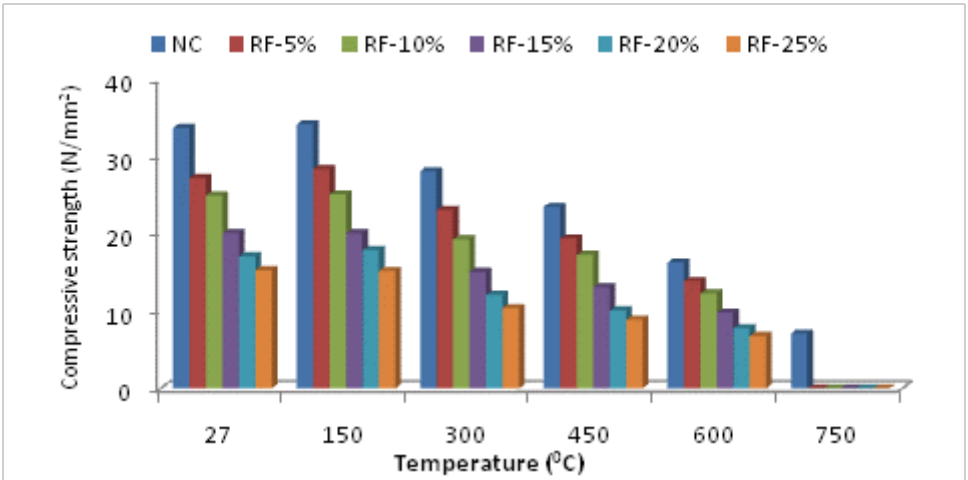

Fig. 6.10 Compressive strength of rubber fiber concrete (w/c ratio 0.55) after exposure to elevated temperature for 120 minutes followed by normal cooling

6.3.2 Compressive strength at fast cooling

The compressive strength of the control mix and waste rubber fiber concrete exposed to different elevated temperatures for 30, 60 and 120 minutes followed by fast (water) cooling is shown in Figs. 6.11-6.19 respectively. The maximum standard deviation and coefficient of variance anywhere for the experimental results shown in these Figs. are 3.12 N/mm^2 and 0.06 respectively (Fig. 6.11, 0% rubber fibers and 150 ^0C temperature). It is seen from the Figs. that, for 30 minutes and 60 minutes exposure, the compressive strength was maximum at 150 ^0C for control concrete as well as waste rubber fiber concrete (except 25% replacement). In case of 120 minutes exposure, the maximum compressive strength was observed at 27 ^0C temperature.

The percentage reduction in compressive strength for 30 minutes exposure of elevated temperature was similar for both normal concrete and waste rubber fiber concrete. The reduction increased in both the cases with the increase in the exposure time. However, the increase in reduction with the increase in exposure time (120 minutes exposure) was more for waste rubber fiber concrete than that of control concrete.

The reduction in compressive strength was more for all the cases of fast cooling as compared to the corresponding cases of normal cooling. This may be due to thermal shock provided by water under elevated temperature. Fast cooling produces residual stresses between outer and inner core of the concrete. This induces tensile stresses in the outer core which in turn are responsible for increase in micro-cracks (Nadeem *et al.* 2014). Similar observations were made by Peng *et al.* (2008). According to another study by Yuzer *et al.* (2004), CaO turns into $Ca(OH)_2$, at the time of fast cooling, and flows through the pore which leads to increase in volume and results in major cracks in concrete.

The increase in rubber fiber content in waste rubber fiber concrete decreased the percentage reduction in compressive strength for elevated temperature upto 300 ^0C with 30 minute exposure followed by fast cooling and for elevated temperature upto 150 ^0C with 120 minute exposure.

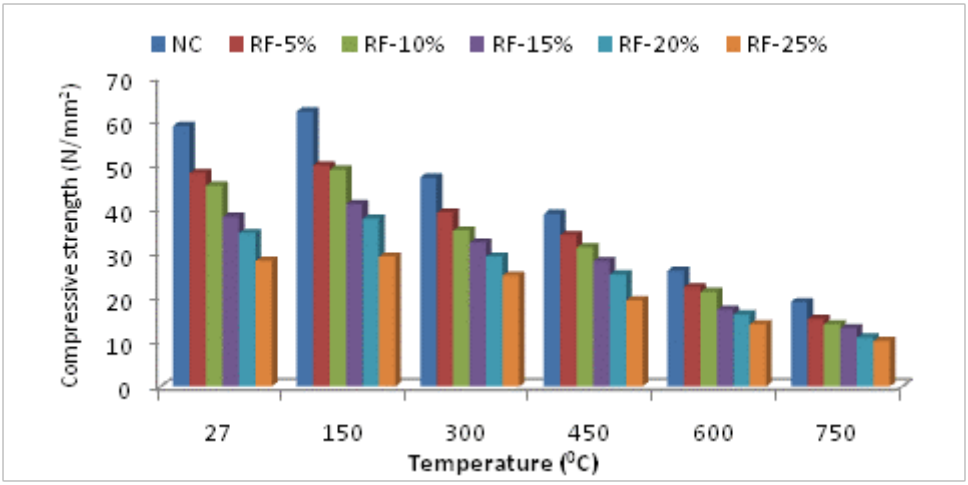

Fig. 6.11 Compressive strength of rubber fiber concrete (w/c ratio 0.35) after exposure to elevated temperature for 30 minutes followed by fast cooling

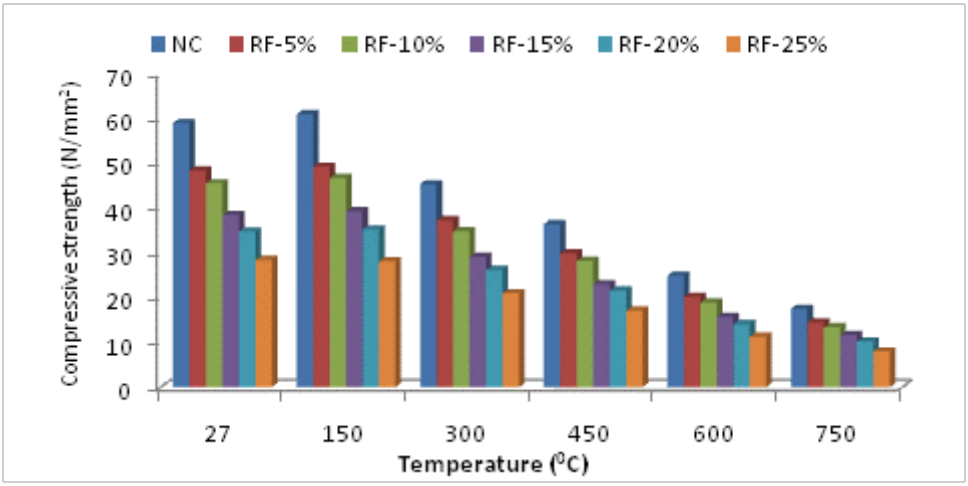

Fig. 6.12 Compressive strength of rubber fiber concrete (w/c ratio 0.35) after exposure to elevated temperature for 60 minutes followed by fast cooling

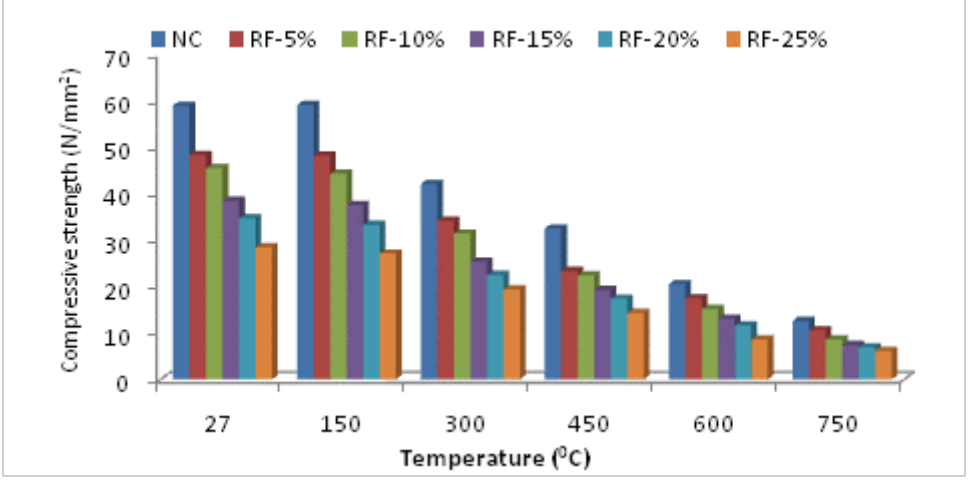

Fig. 6.13 Compressive strength of rubber fiber concrete (w/c ratio 0.35) after exposure to elevated temperature for 120 minutes followed by fast cooling

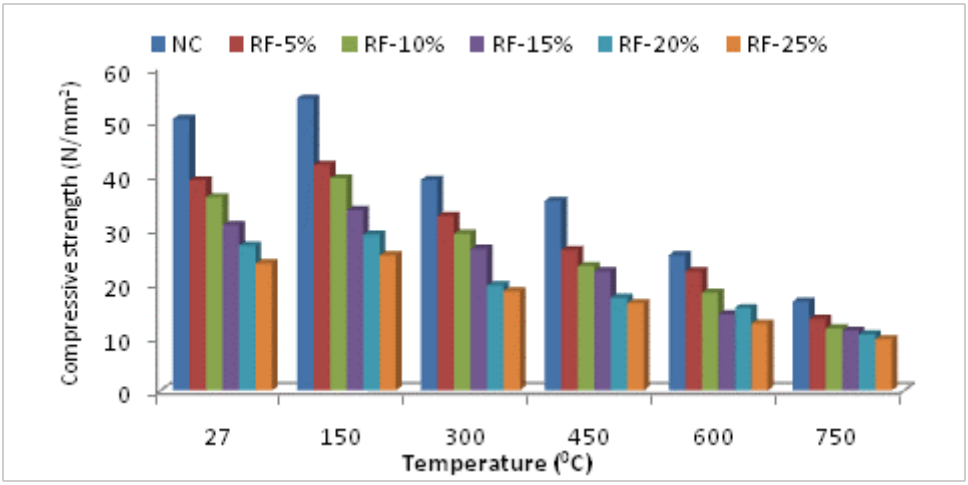

Fig. 6.14 Compressive strength of rubber fiber concrete (w/c ratio 0.45) after exposure to elevated temperature for 30 minutes followed by fast cooling

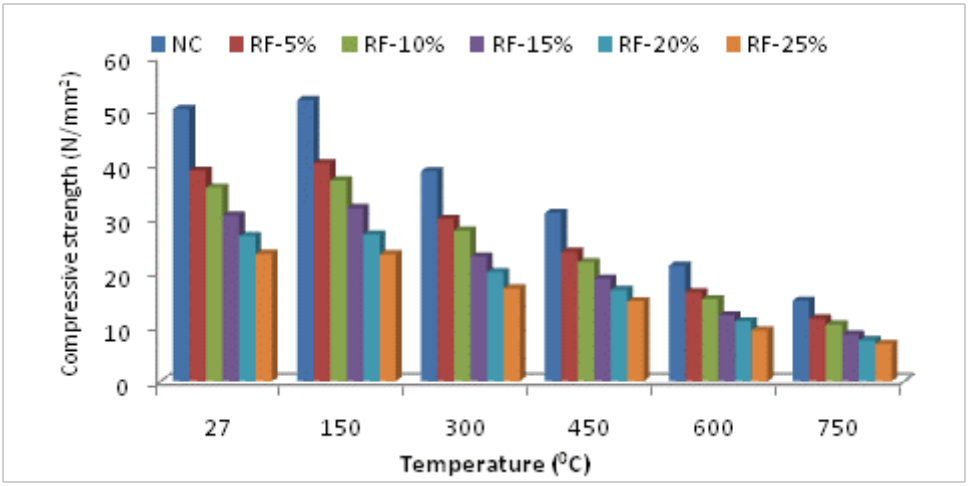

Fig. 6.15 Compressive strength of rubber fiber concrete (w/c ratio 0.45) after exposure to elevated temperature for 60 minutes followed by fast cooling

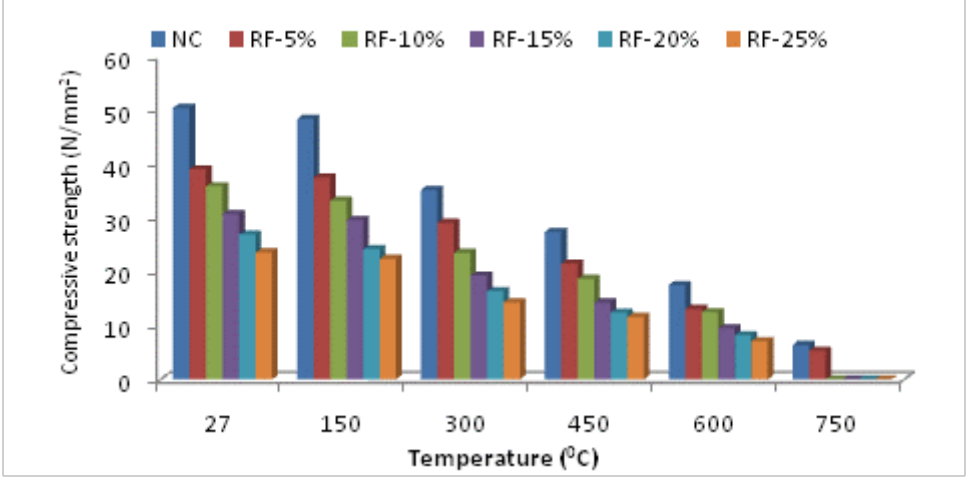

Fig. 6.16 Compressive strength of rubber fiber concrete (w/c ratio 0.45) after exposure to elevated temperature for 120 minutes followed by fast cooling

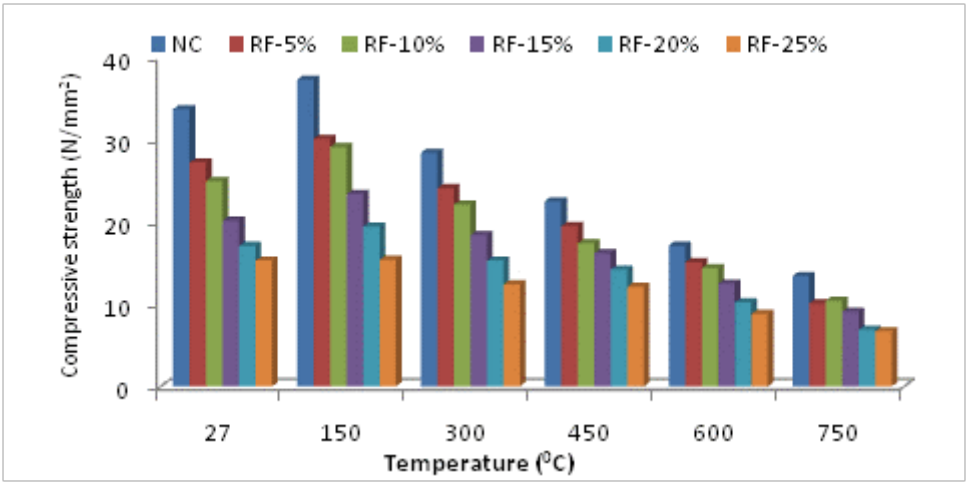

Fig. 6.17 Compressive strength of rubber fiber concrete (w/c ratio 0.55) after exposure to elevated temperature for 30 minutes followed by fast cooling

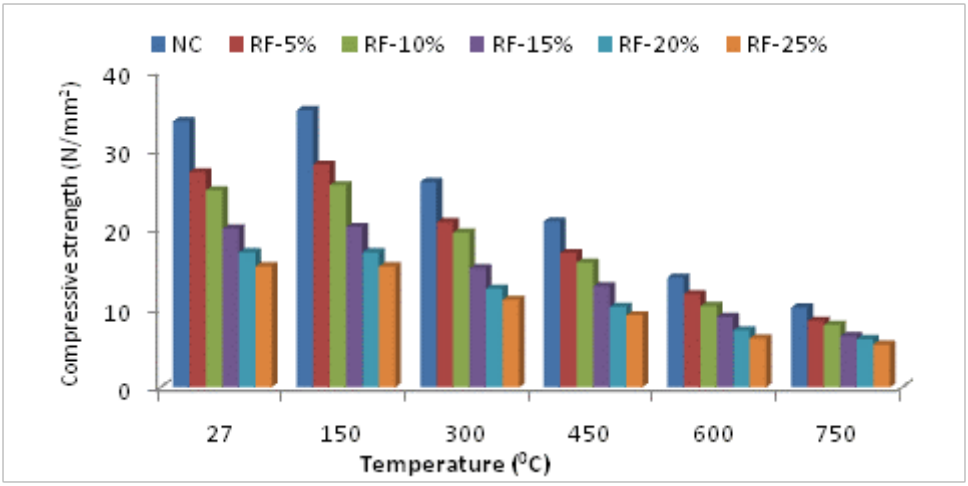

Fig. 6.18 Compressive strength of rubber fiber concrete (w/c ratio 0.55) after exposure to elevated temperature for 60 minutes followed by fast cooling

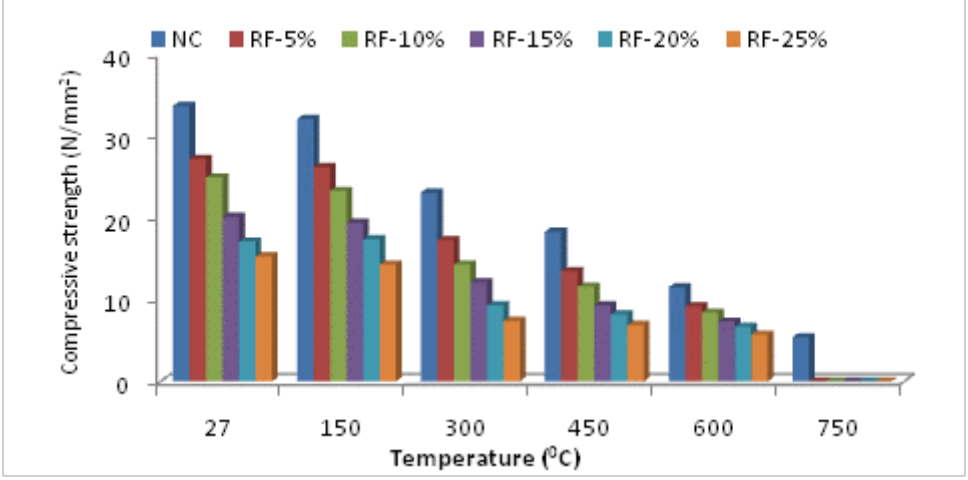

Fig. 6.19 Compressive strength of rubber fiber concrete (w/c ratio 0.55) after exposure to elevated temperature for 120 minutes followed by fast cooling

6.3.3 Mass Loss

The mass loss in control mix and waste rubber fiber concrete exposed to five different elevated temperatures for 30, 60 and 120 minutes followed by normal (air) cooling is shown in Figs. 6.20-6.28 respectively. The maximum standard deviation and coefficient of variance anywhere for the experimental results shown in these Figs. are 0.24% and 0.07 respectively (Fig. 6.22, 25% rubber fibers and 750 ^{0}C temperature). It is seen from the Figs. that there was a mass loss in all the cases of concrete subjected to elevated temperature. The percentage mass loss increased with the increase of elevated temperature and exposure duration for all the cases. Further, for all replacement levels, the mass loss in case of waste rubber fiber concrete was similar to the corresponding case of control concrete.

The mass loss at lower temperatures may be due to evaporation of the capillary water and subsequent release of absorbed and interlayer water (Ramachandran *et al.* 1981) and the mass loss at higher temperature may be due to release of chemically combined water (Nadeem *et al.* 2014, Ismail *et al.* 2011).

6.3.4 Density

The density is required for obtaining the dynamic modulus of concrete.

The density of control mix and waste rubber fiber concrete, before and after exposure to five different elevated temperatures for 30, 60 and 120 minutes, followed by normal (air) cooling is shown in Figs. 6.29-6.37 respectively. The maximum standard deviation and coefficient of variance anywhere for the experimental results shown in these Figs. are 62.57 kg/m^3 and 0.11 respectively (Fig. 6.30, 5% rubber fibers and 27 ^{0}C temperature).

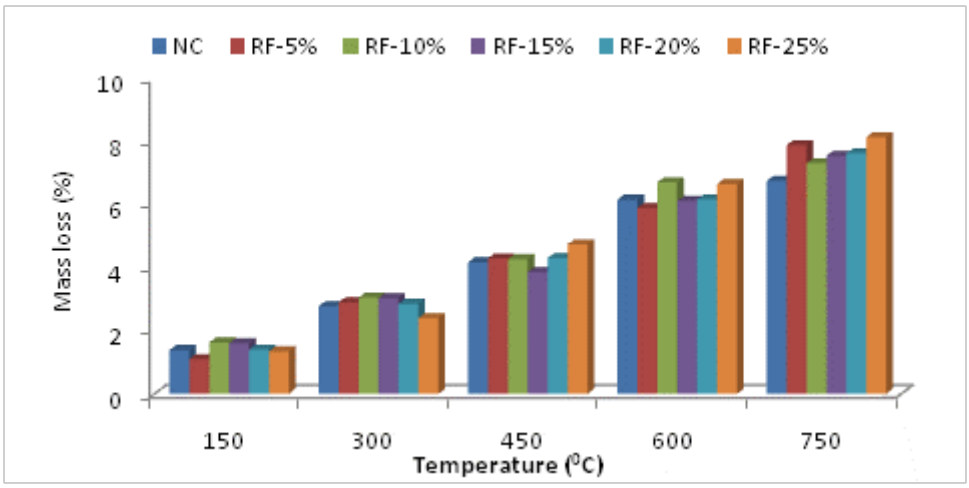

Fig. 6.20 Mass loss of rubber fiber concrete (w/c ratio 0.35) after exposure to elevated temperature for 30 minutes

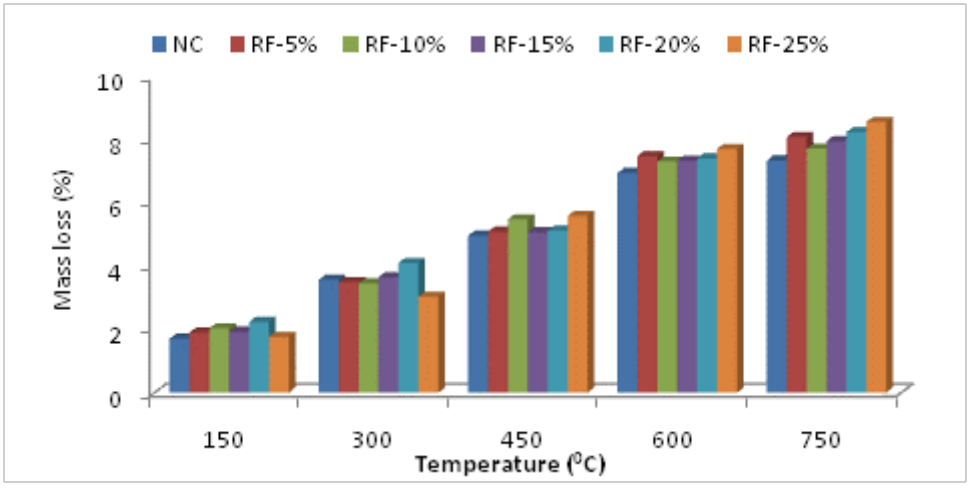

Fig. 6.21 Mass loss of rubber fiber concrete (w/c ratio 0.35) after exposure to elevated temperature for 60 minutes

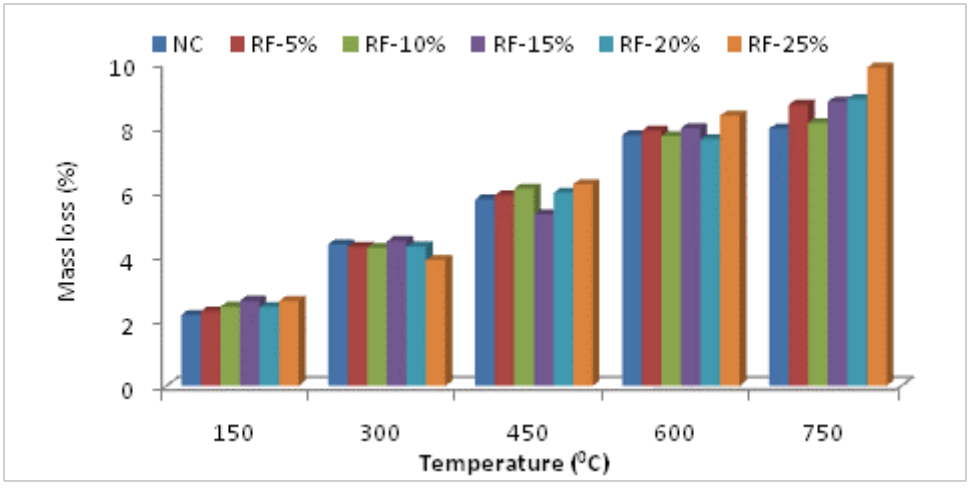

Fig. 6.22 Mass loss of rubber fiber concrete (w/c ratio 0.35) after exposure to elevated temperature for 120 minutes

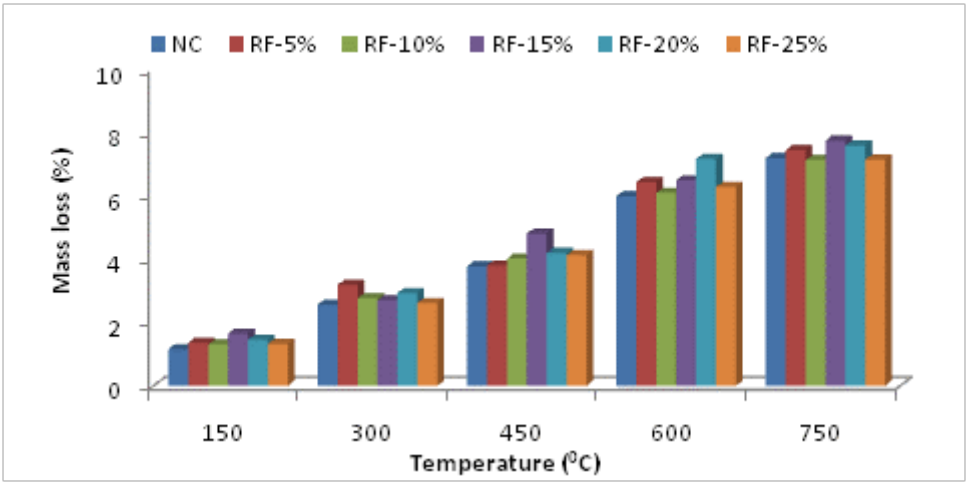

Fig. 6.23 Mass loss of rubber fiber concrete (w/c ratio 0.45) after exposure to elevated temperature for 30 minutes

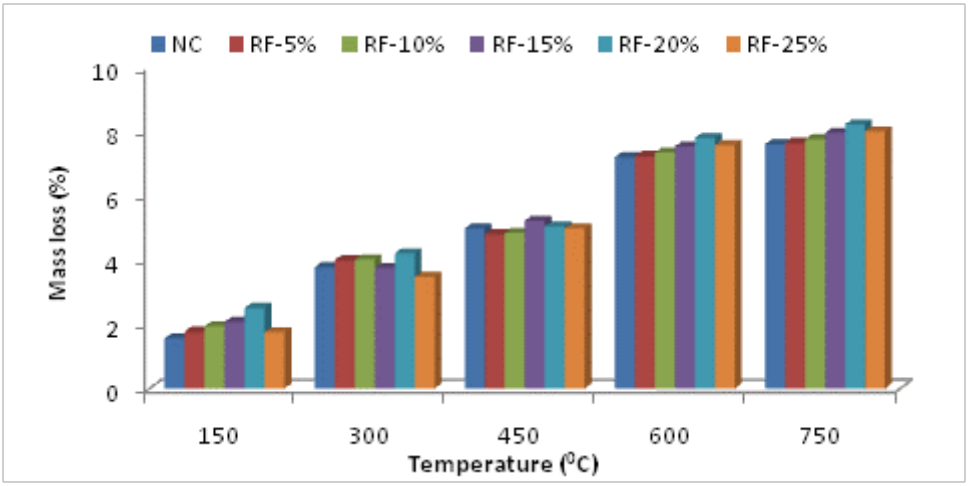

Fig. 6.24 Mass loss of rubber fiber concrete (w/c ratio 0.45) after exposure to elevated temperature for 60 minutes

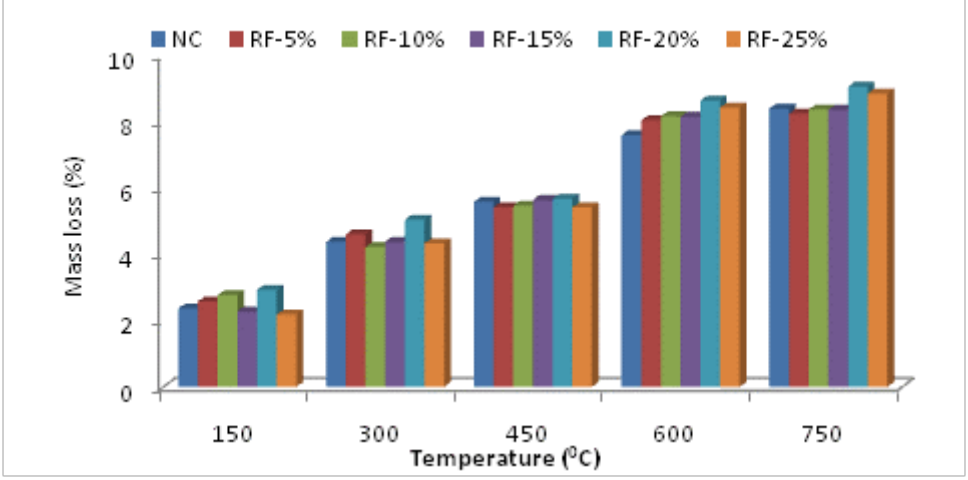

Fig. 6.25 Mass loss of rubber fiber concrete (w/c ratio 0.45) after exposure to elevated temperature for 120 minutes

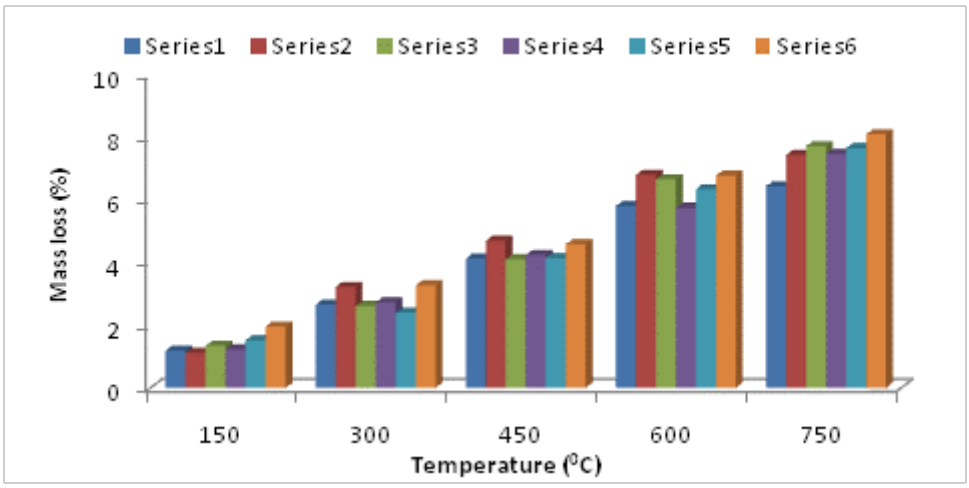

Fig. 6.26 Mass loss of rubber fiber concrete (w/c ratio 0.55) after exposure to elevated temperature for 30 minutes

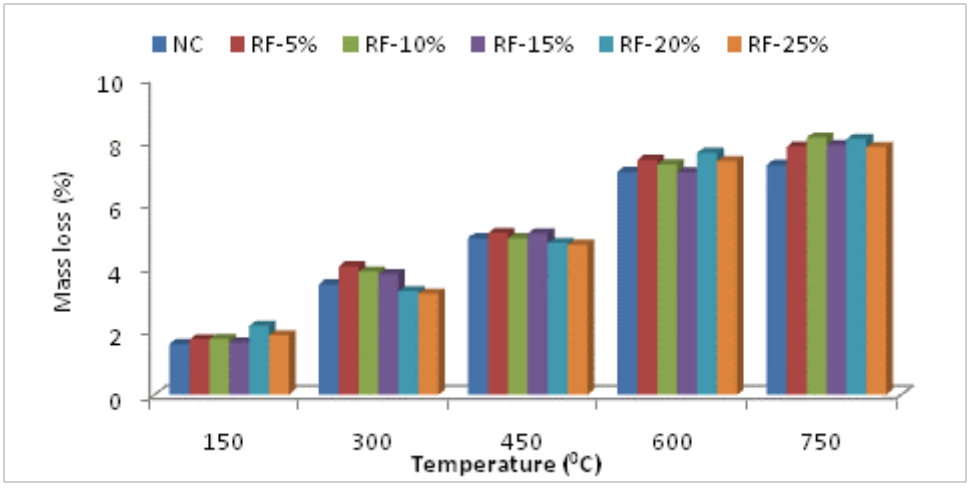

Fig. 6.27 Mass loss of rubber fiber concrete (w/c ratio 0.55) after exposure to elevated temperature for 60 minutes

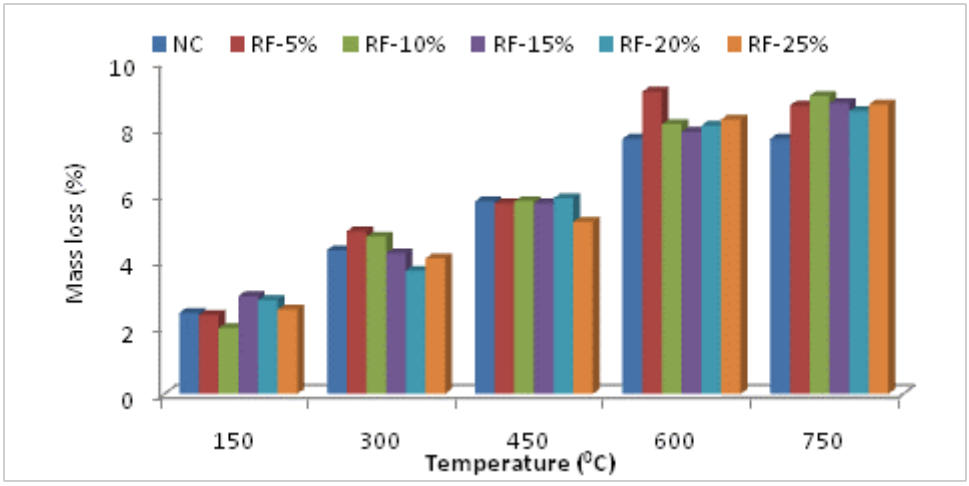

Fig. 6.28 Mass loss of rubber fiber concrete (w/c ratio 0.55) after exposure to elevated temperature for 120 minutes

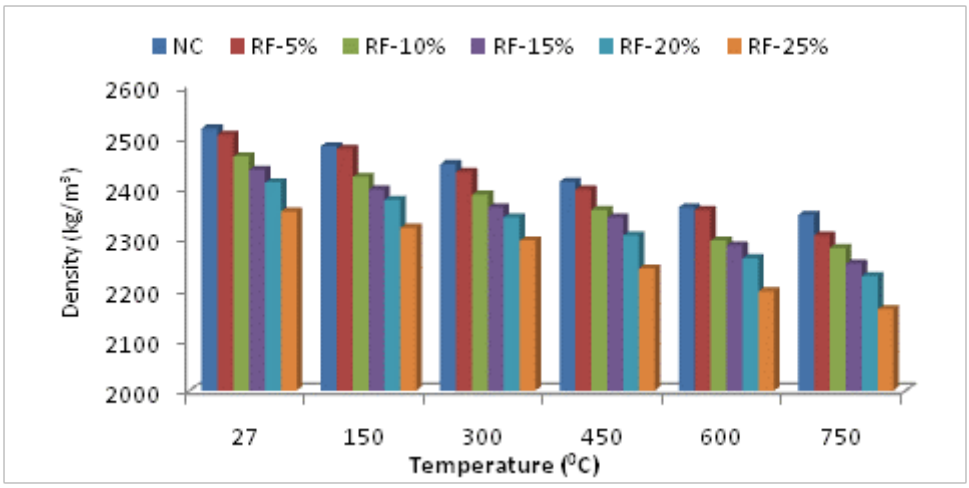

Fig. 6.29 Density of rubber fiber concrete (w/c ratio 0.35) after exposure to elevated temperature for 30 minutes

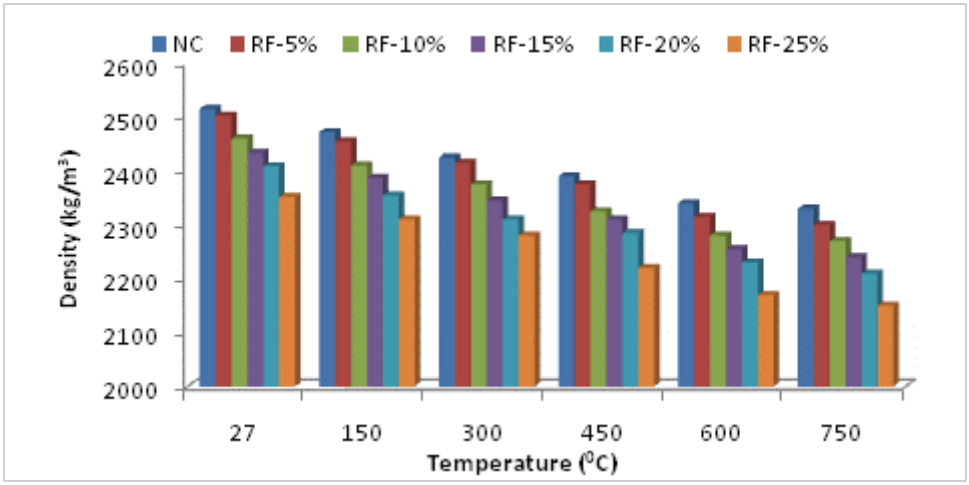

Fig. 6.30 Density of rubber fiber concrete (w/c ratio 0.35) after exposure to elevated temperature for 60 minutes

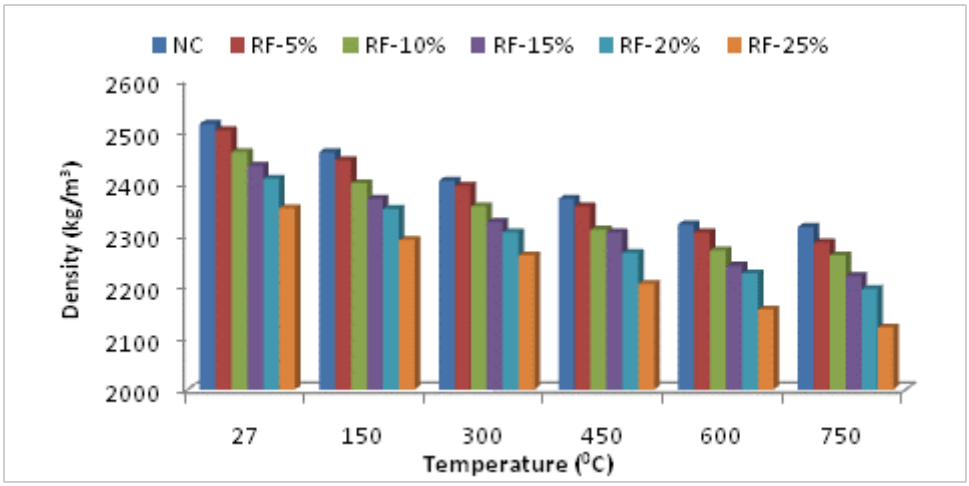

Fig. 6.31 Density of rubber fiber concrete (w/c ratio 0.35) after exposure to elevated temperature for 120 minutes

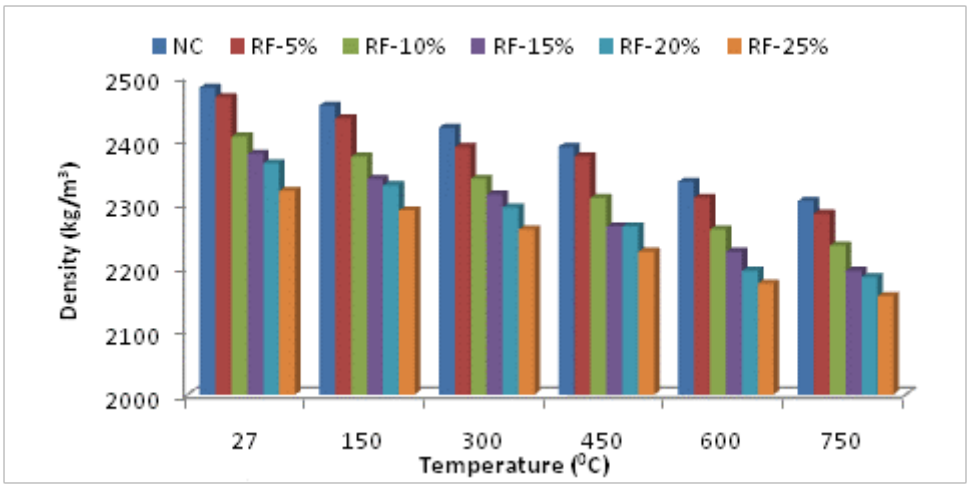

Fig. 6.32 Density of rubber fiber concrete (w/c ratio 0.45) after exposure to elevated temperature for 30 minutes

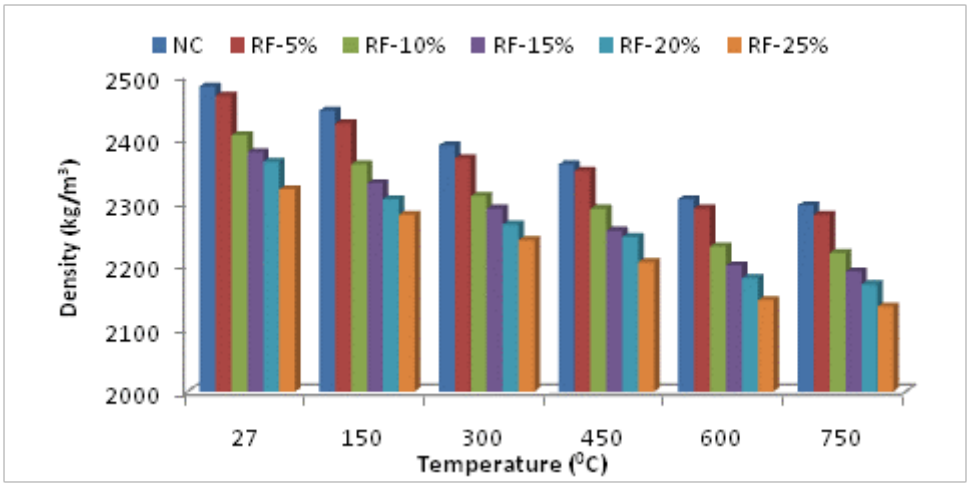

Fig. 6.33 Density of rubber fiber concrete (w/c ratio 0.45) after exposure to elevated temperature for 60 minutes

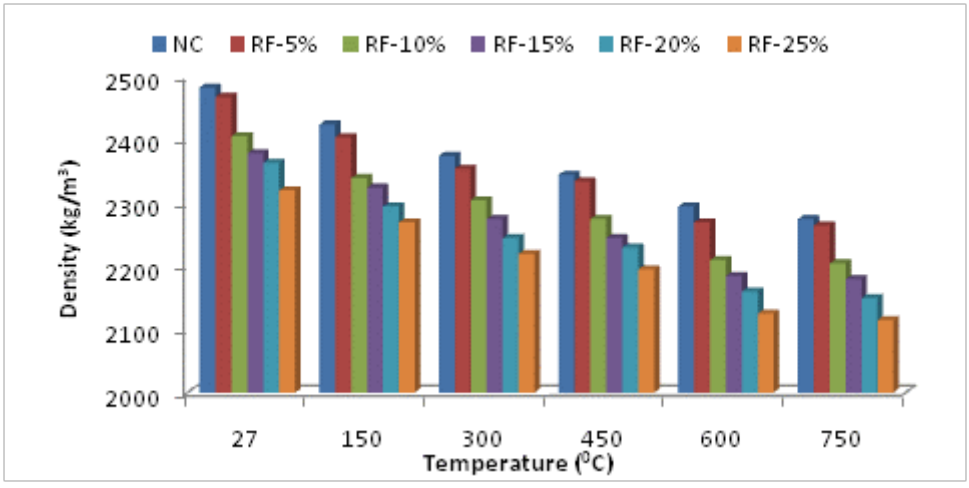

Fig. 6.34 Density of rubber fiber concrete (w/c ratio 0.45) after exposure to elevated temperature for 120 minutes

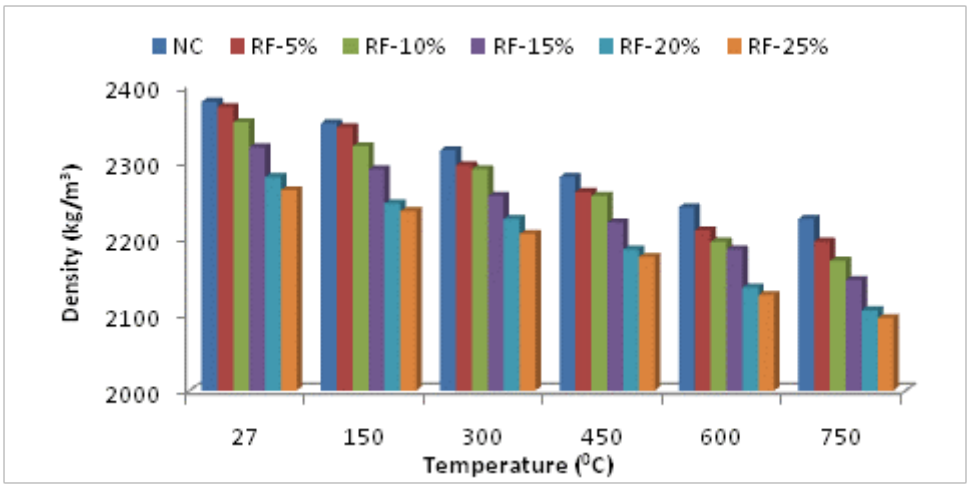

Fig. 6.35 Density of rubber fiber concrete (w/c ratio 0.55) after exposure to elevated temperature for 30 minutes

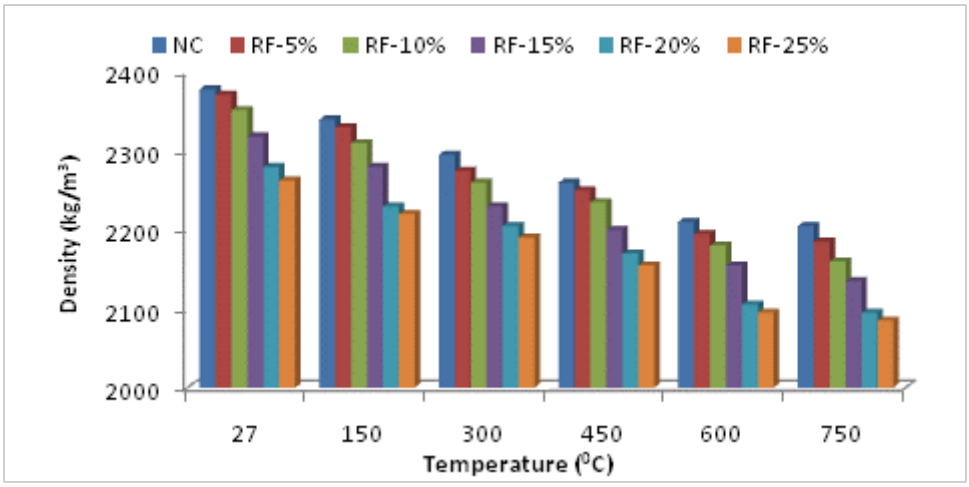

Fig. 6.36 Density of rubber fiber concrete (w/c ratio 0.55) after exposure to elevated temperature for 60 minutes

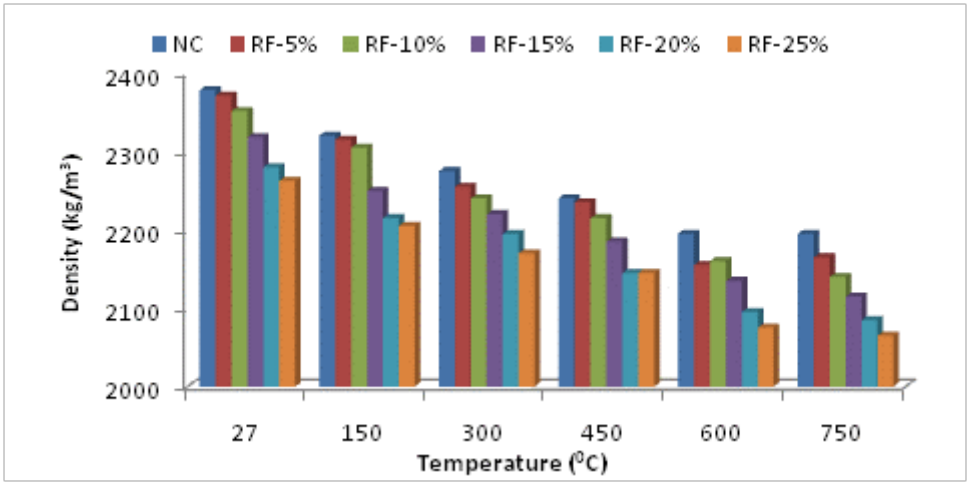

Fig. 6.37 Density of rubber fiber concrete (w/c ratio 0.55) after exposure to elevated temperature for 120 minutes

6.3.5 Ultrasonic pulse velocity

The ultrasonic pulse velocity test was conducted to obtain the effect of elevated temperature on porosity of the concrete. The ultrasonic pulse velocity of the control mix and waste rubber fiber concrete exposed to five different elevated temperatures for 30, 60 and 120 minutes followed by normal (air) cooling is shown in Figs. 6.38-6.46 respectively. The maximum standard deviation and coefficient of variance anywhere for the experimental results shown in these Figs. are 69.14 m/s and 0.14 respectively (Fig. 6.38, 5% rubber fibers and 27 ^{0}C temperature).

The ultrasonic pulse velocity decreased with the increase of elevated temperature and exposure duration for all the cases The observed decrease in ultrasonic pulse velocity indicates the increase in porosity of concrete on exposure to elevated temperature. Further, the percentage decrease in ultrasonic pulse velocity in case of waste rubber fiber concrete was similar to the corresponding case of control concrete upto 60 minute exposure. The percentage decrease in case of 120 minute exposure was higher for the waste rubber fiber concrete in comparison to the control concrete. The percentage reduction in ultrasonic pulse velocity, in waste rubber fiber concrete, was similar for all replacement level of rubber fiber content in concrete at 30 and 60 minute exposure duration whereas for 120 minute exposure duration, the % reduction increased with increase in replacement level of rubber fibers.

6.3.6 Static modulus of elasticity

The static modulus test was carried out to obtain the effect of elevated temperature on the deformation behaviour of concrete. The static modulus of the control mix and waste rubber tyre fiber concrete exposed to five different elevated temperatures for 30, 60 and 120 minutes followed by normal (air) cooling is shown in Figs. 6.47-6.55 respectively. The maximum standard deviation and coefficient of variance anywhere for the experimental results shown in these Figs. are 411.7 MPa and 0.19 respectively (Fig. 6.47, 5% rubber fibers and 27 ^{0}C temperature). It is seen from the Figs. that there was a decrease in static modulus in all the cases of concrete subjected to elevated temperature.

The decrease in static modulus increased with the increment in elevated temperature and exposure duration for all the cases. Further, for all replacement levels of rubber fibers, the decrease in static modulus of waste rubber fiber concrete was similar to the corresponding cases of control concrete. The static modulus decreased up to 88% in case of waste rubber fiber concrete (25% FA replaced by fiber) subjected to elevated temperature of 750 ^{0}C for 120 minutes duration whereas the decrease in the corresponding case of control concrete was

about 87% for w/c ratio 0.45. Similar observations have been made earlier by Yuksel *et al.* (2011).

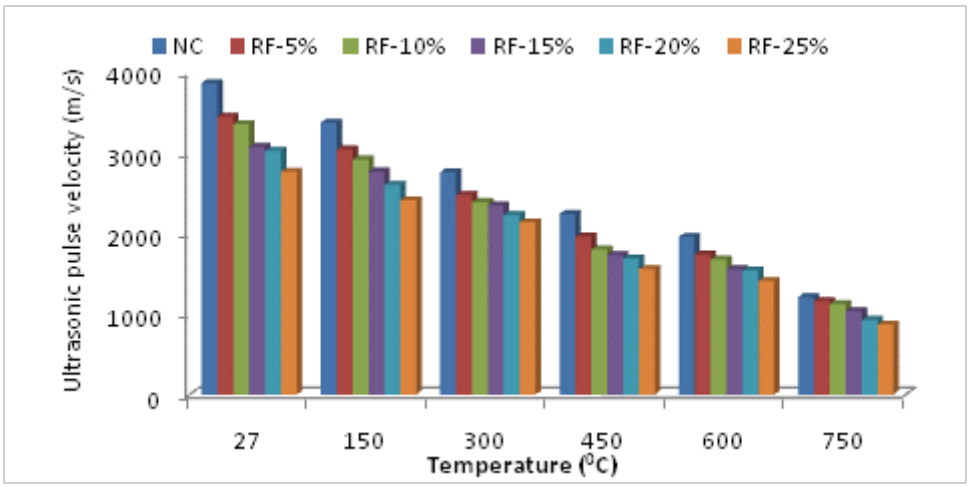

Fig. 6.38 Ultrasonic pulse velocity of rubber fiber concrete (w/c ratio 0.35) after exposure to elevated temperature for 30 minutes

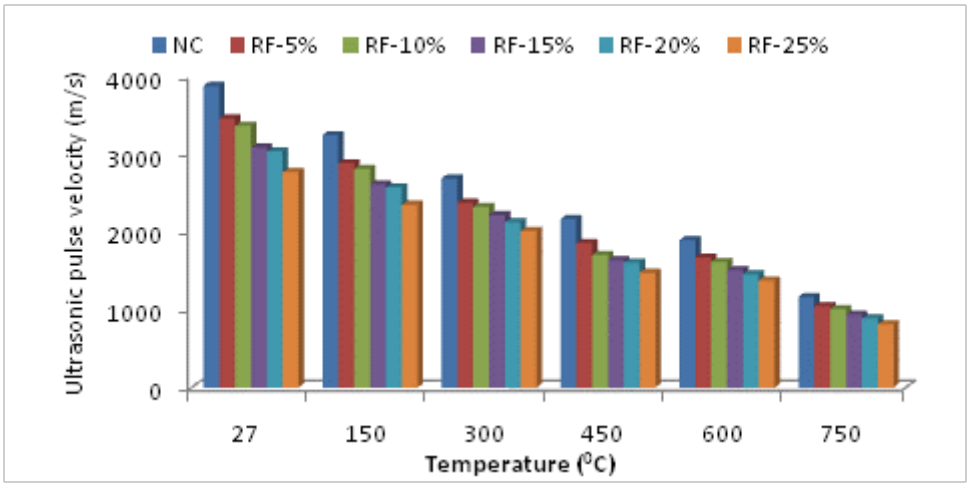

Fig. 6.39 Ultrasonic pulse velocity of rubber fiber concrete (w/c ratio 0.35) after exposure to elevated temperature for 60 minutes

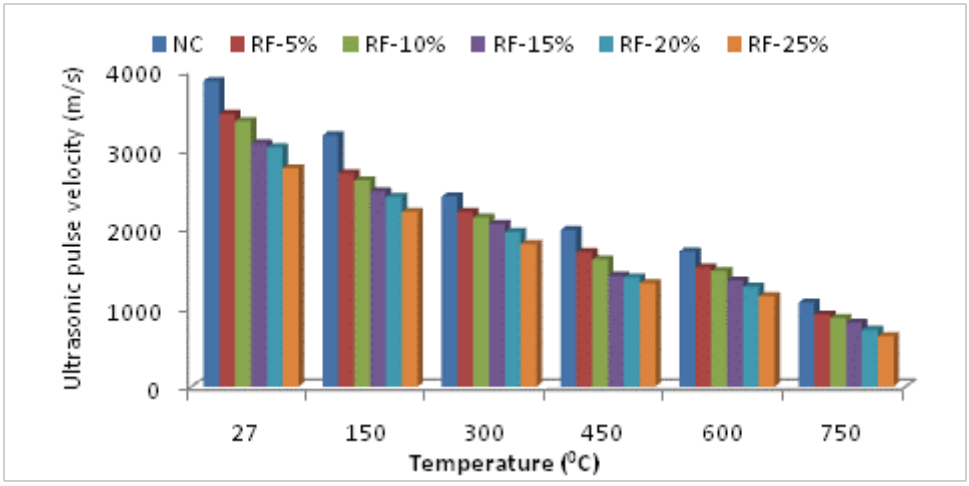

Fig. 6.40 Ultrasonic pulse velocity of rubber fiber concrete (w/c ratio 0.35) after exposure to elevated temperature for 120 minutes

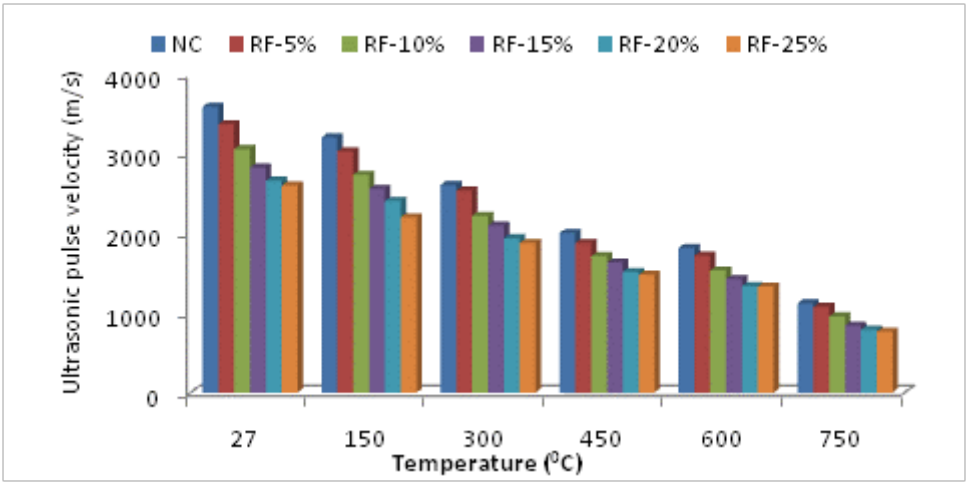

Fig. 6.41 Ultrasonic pulse velocity of rubber fiber concrete (w/c ratio 0.45) after exposure to elevated temperature for 30 minutes

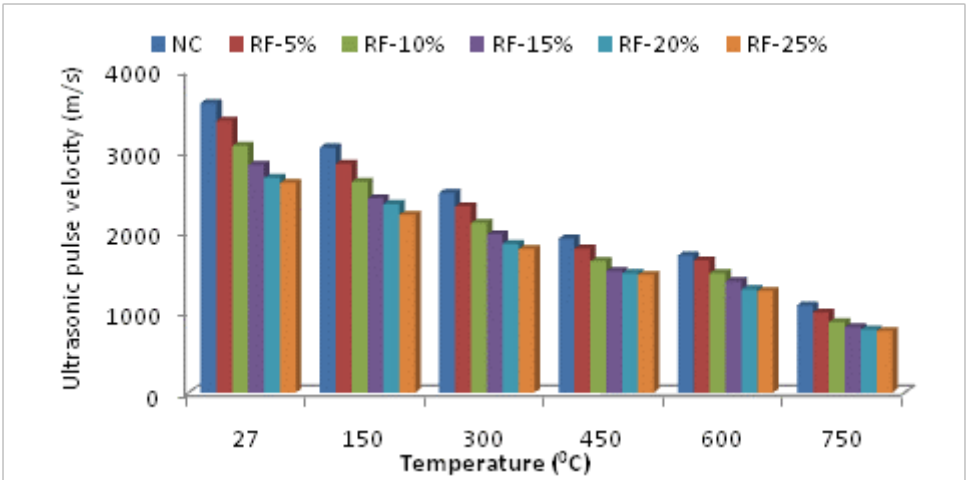

Fig. 6.42 Ultrasonic pulse velocity of rubber fiber concrete (w/c ratio 0.45) after exposure to elevated temperature for 60 minutes

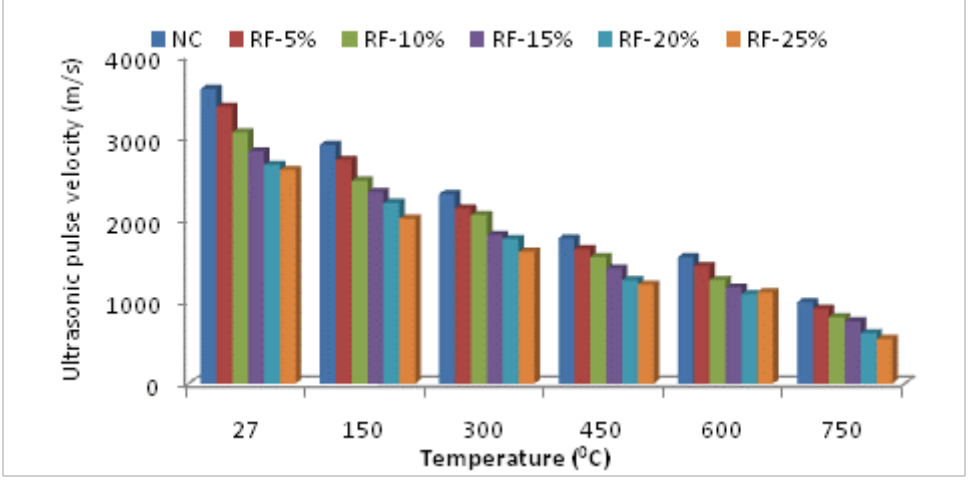

Fig. 6.43 Ultrasonic pulse velocity of rubber fiber concrete (w/c ratio 0.45) after exposure to elevated temperature for 120 minutes

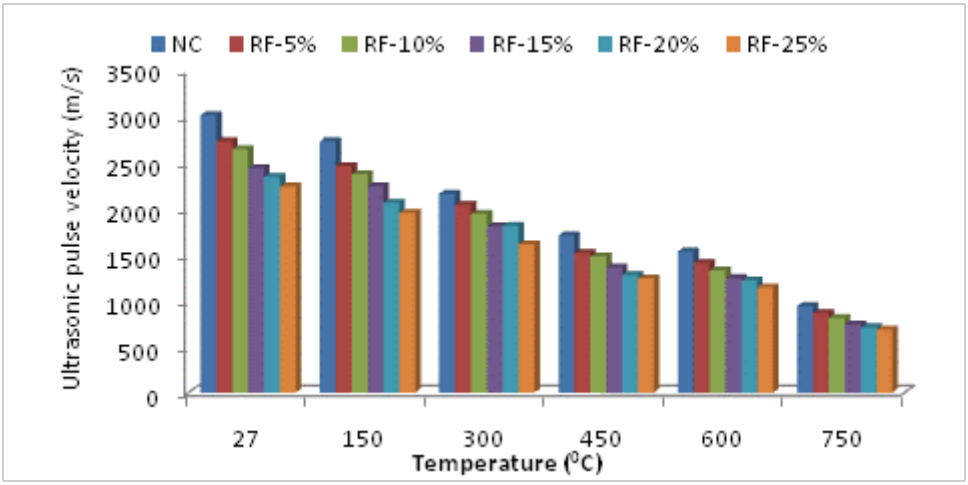

Fig. 6.44 Ultrasonic pulse velocity of rubber fiber concrete (w/c ratio 0.55) after exposure to elevated temperature for 30 minutes

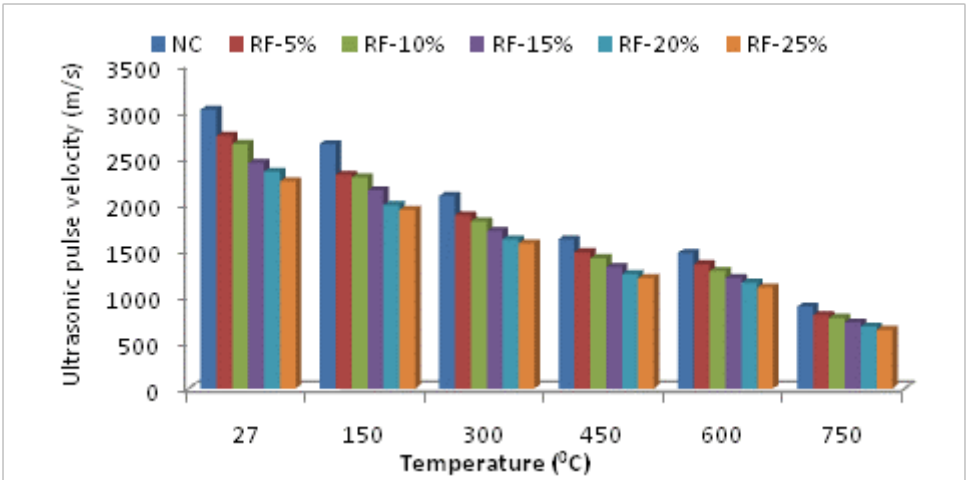

Fig. 6.45 Ultrasonic pulse velocity of rubber fiber concrete (w/c ratio 0.55) after exposure to elevated temperature for 60 minutes

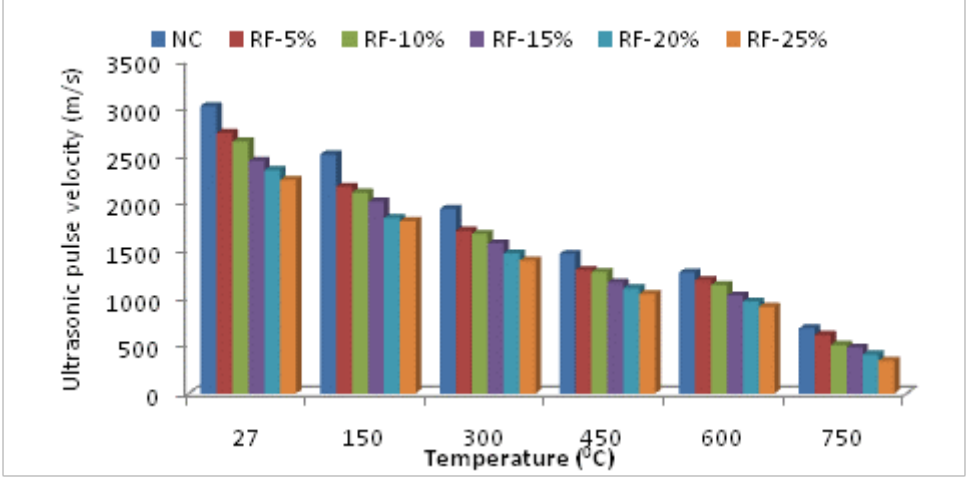

Fig. 6.46 Ultrasonic pulse velocity of rubber fiber concrete (w/c ratio 0.55) after exposure to elevated temperature for 120 minutes

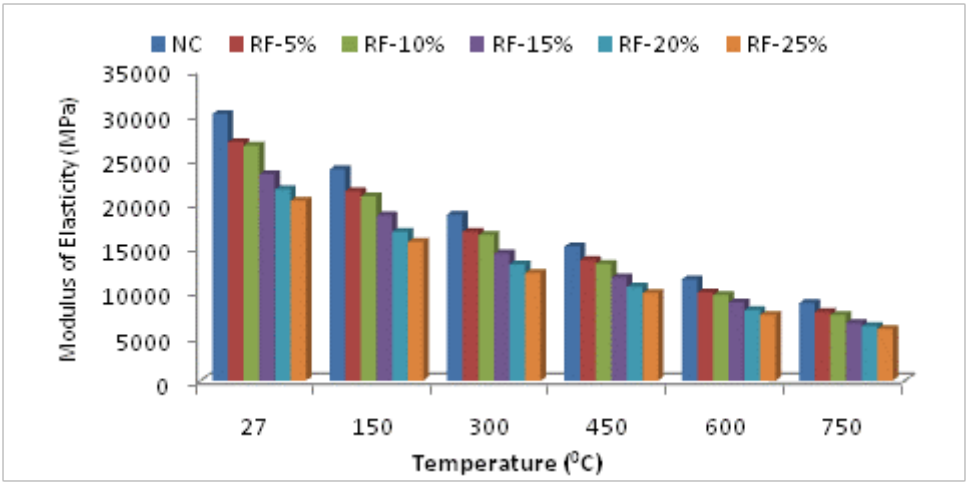

Fig. 6.47 Static modulus of rubber fiber concrete (w/c ratio 0.35) after exposure to elevated temperature for 30 minutes

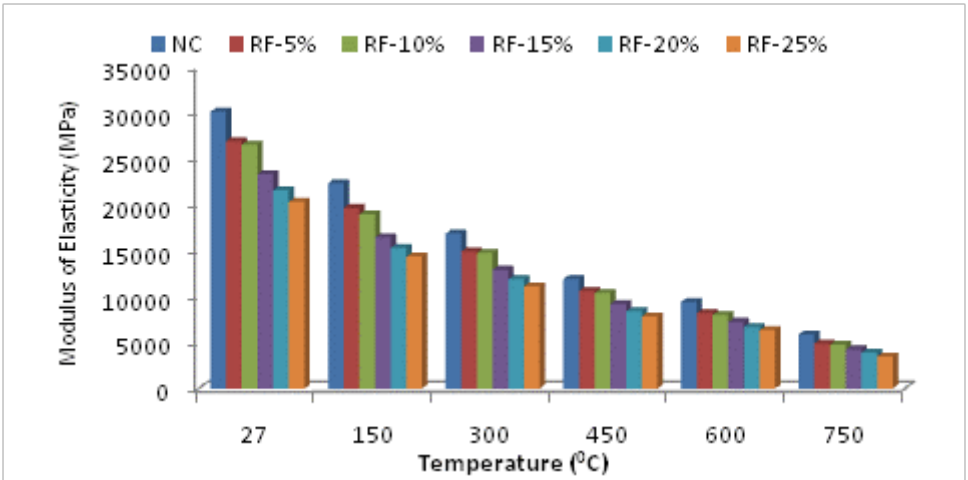

Fig. 6.48 Static modulus of rubber fiber concrete (w/c ratio 0.35) after exposure to elevated temperature for 60 minutes

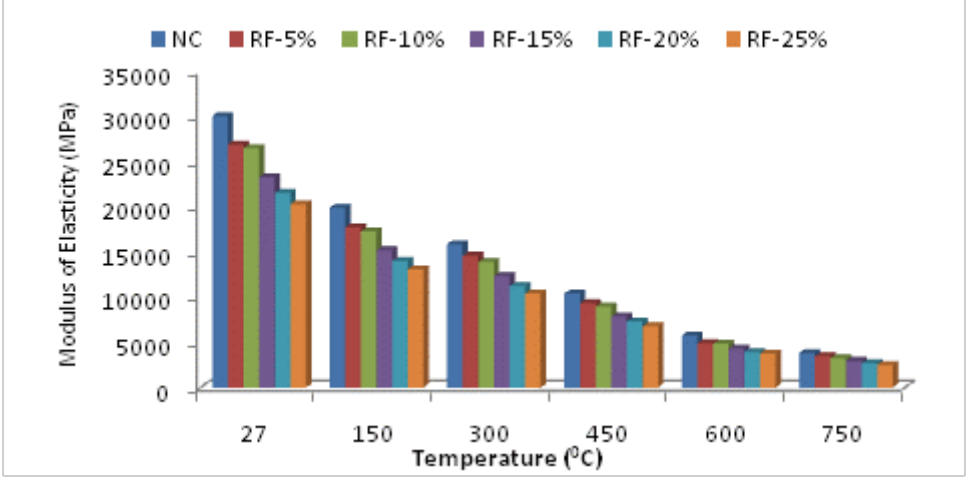

Fig. 6.49 Static modulus of rubber fiber concrete (w/c ratio 0.35) after exposure to elevated temperature for 120 minutes

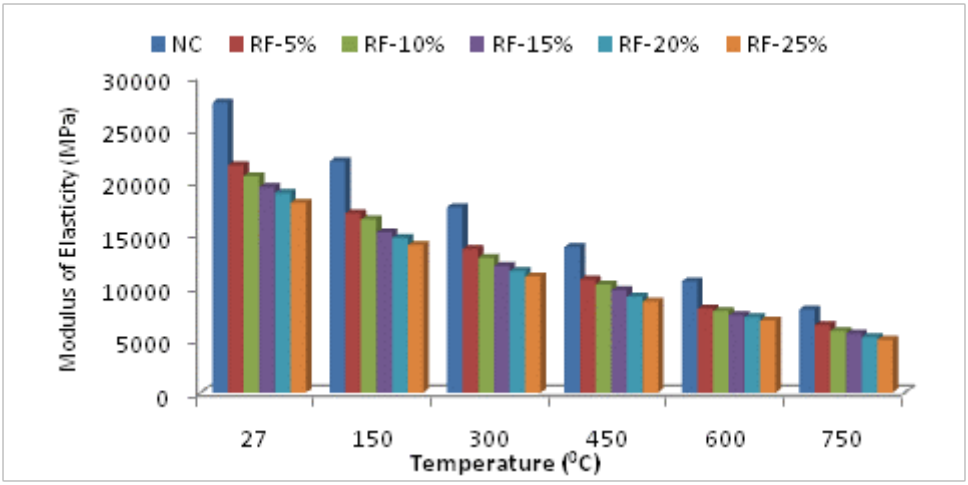

Fig. 6.50 Static modulus of rubber fiber concrete (w/c ratio 0.45) after exposure to elevated temperature for 30 minutes

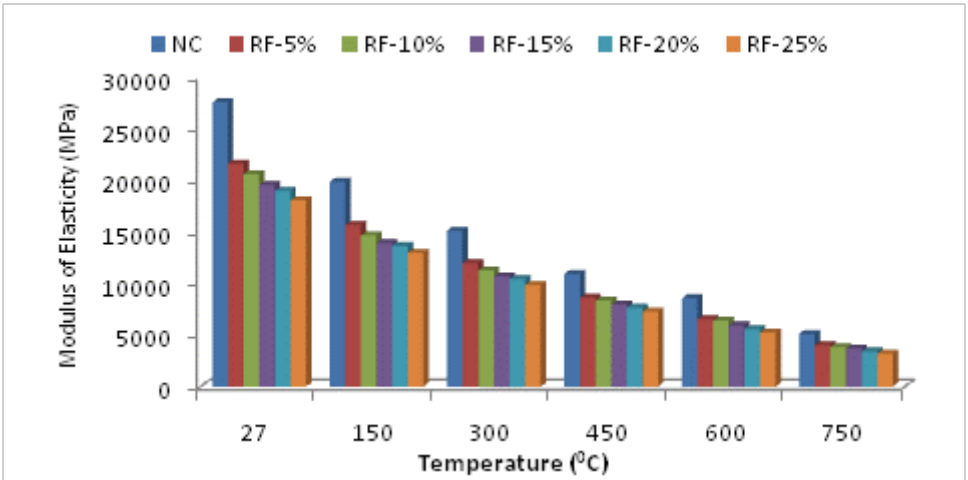

Fig. 6.51 Static modulus of rubber fiber concrete (w/c ratio 0.45) after exposure to elevated temperature for 60 minutes

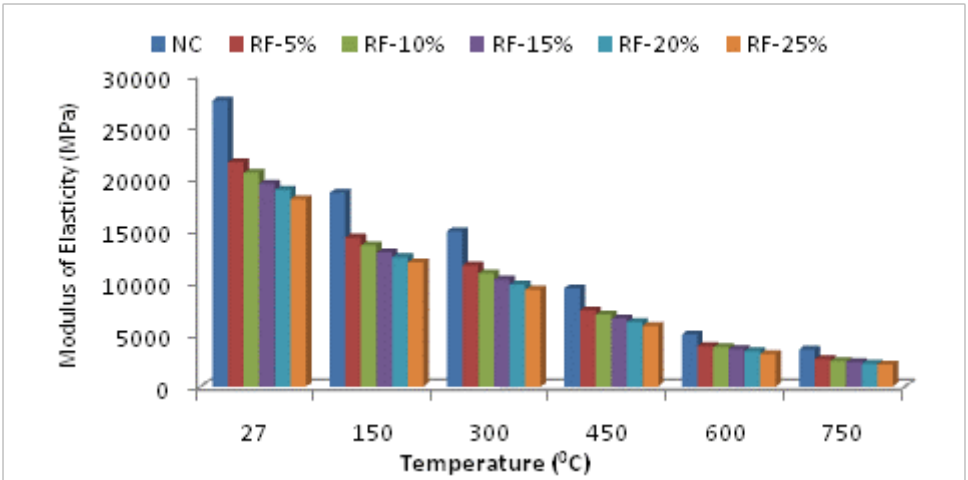

Fig. 6.52 Static modulus of rubber fiber concrete (w/c ratio 0.45) after exposure to elevated temperature for 120 minutes

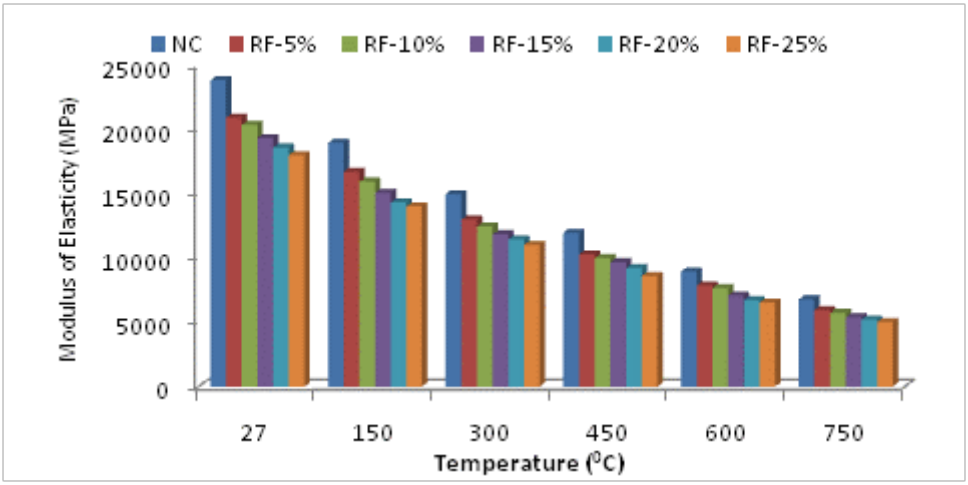

Fig. 6.53 Static modulus of rubber fiber concrete (w/c ratio 0.55) after exposure to elevated temperature for 30 minutes

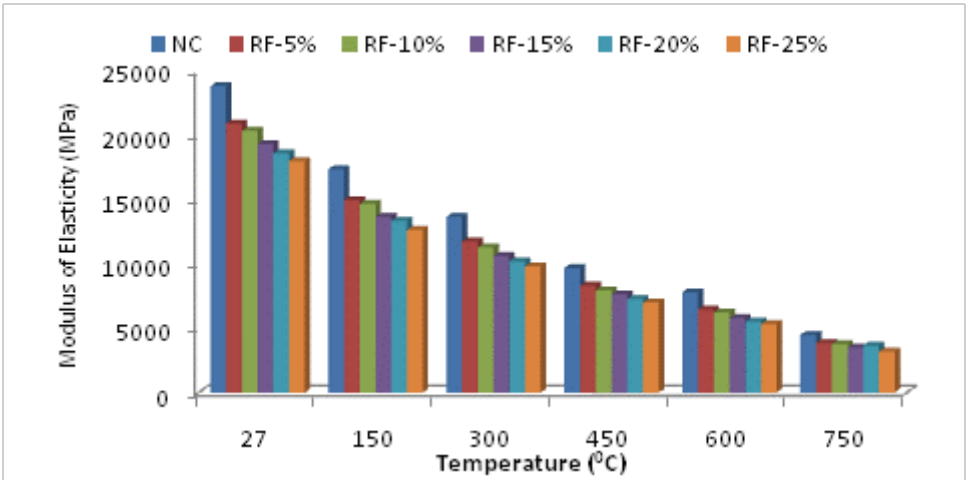

Fig. 6.54 Static modulus of rubber fiber concrete (w/c ratio 0.55) after exposure to elevated temperature for 60 minutes

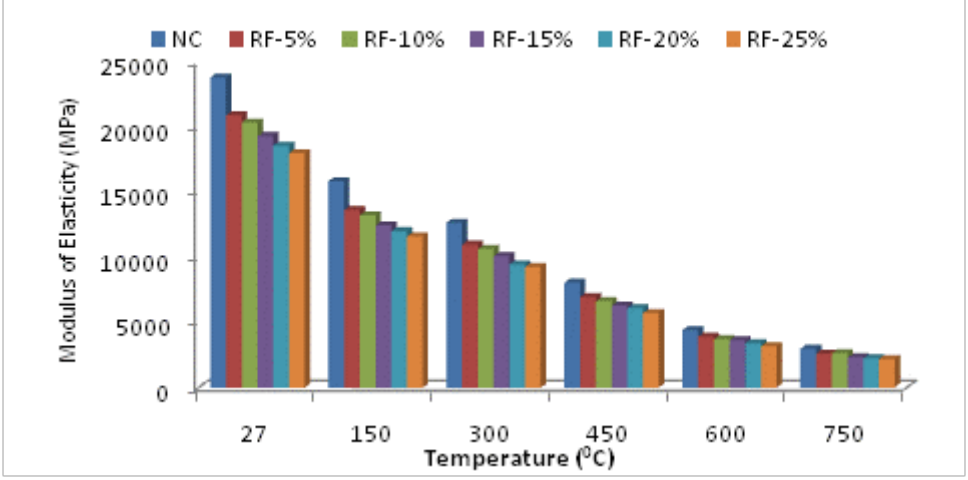

Fig. 6.55 Static modulus of rubber fiber concrete (w/c ratio 0.55) after exposure to elevated temperature for 120 minutes

6.3.7 Dynamic modulus of elasticity

The dynamic modulus was obtained to observe the change in behavior of deformation capacity of the waste rubber fiber concrete. The dynamic modulus of the control mix and waste rubber tyre fiber concrete exposed to five different elevated temperatures for 30, 60 and 120 minutes followed by normal (air) cooling is shown in Figs. 6.56-6.64 respectively. The maximum standard deviation and coefficient of variance anywhere for the experimental results shown in these Figs. are 1.54 GPa and 0.08 respectively (Fig. 6.57, 5% rubber fibers and 27 ^{0}C temperature). It is seen from the Figs. that there was a decrease in dynamic modulus in all the cases of concrete subjected to elevated temperature.

The decrease in dynamic modulus increased with the increment in elevated temperature and exposure duration for all the cases. Further, for all replacement levels of rubber fibers, the decrease in dynamic modulus of waste rubber fiber concrete was similar to the corresponding cases of control concrete. The dynamic modulus decreased by upto 96% when waste rubber fiber concrete (w/c ratio 0.45, 25% FA replaced by fiber) was subjected to elevated temperature of 750 ^{0}C for 120 minute duration whereas the decrease in the corresponding case of control concrete was about 93%. Similar observations have been made earlier by Demir *et al*. (2011) for crushed tile concretes citing the huge change in microstructure of concrete as the reason for the same.

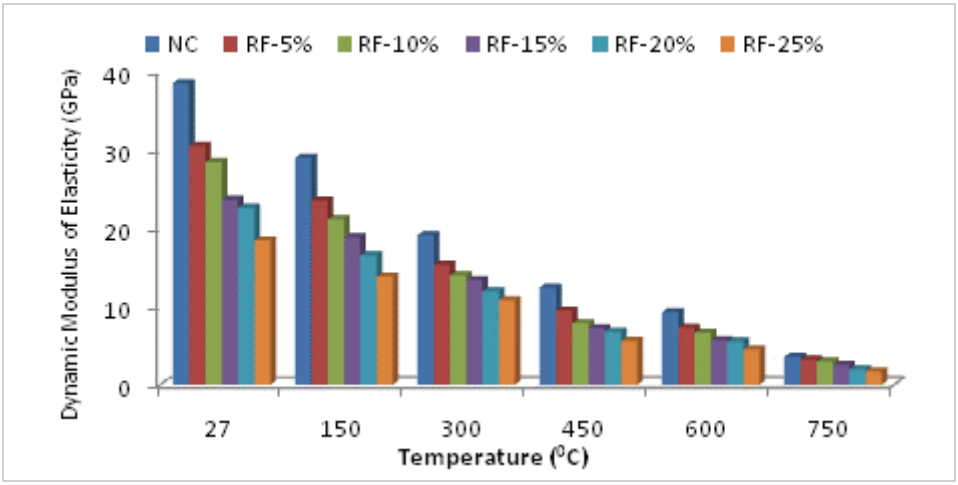

Fig. 6.56 Dynamic modulus of rubber fiber concrete (w/c ratio 0.35) after exposure to elevated temperature for 30 minutes

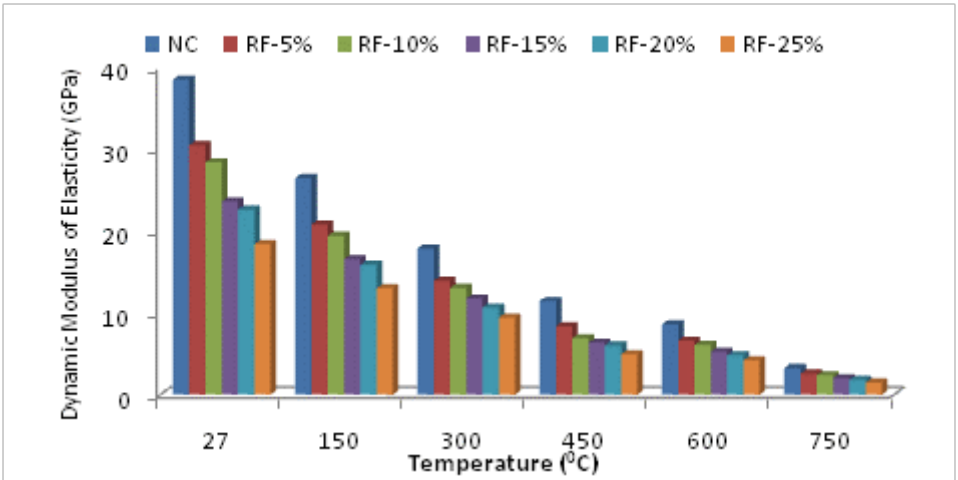

Fig. 6.57 Dynamic modulus of rubber fiber concrete (w/c ratio 0.35) after exposure to elevated temperature for 60 minutes

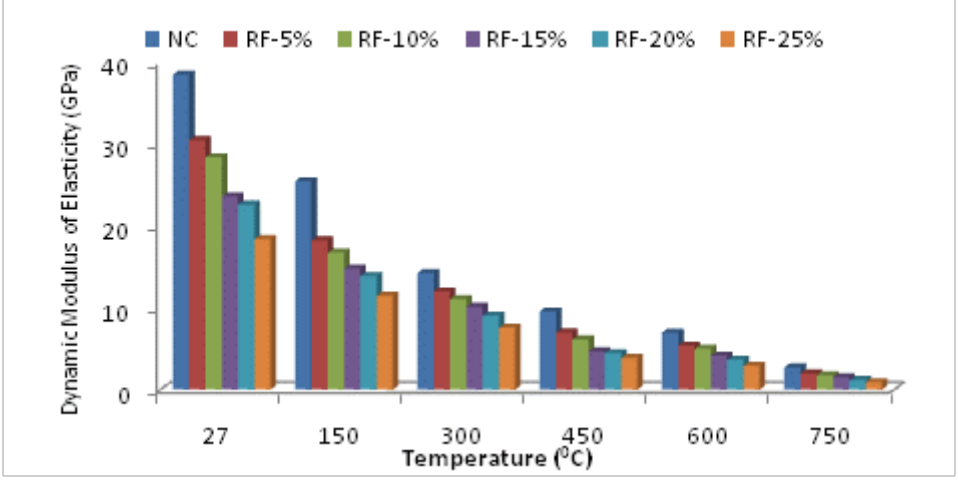

Fig. 6.58 Dynamic modulus of rubber fiber concrete (w/c ratio 0.35) after exposure to elevated temperature for 120 minutes

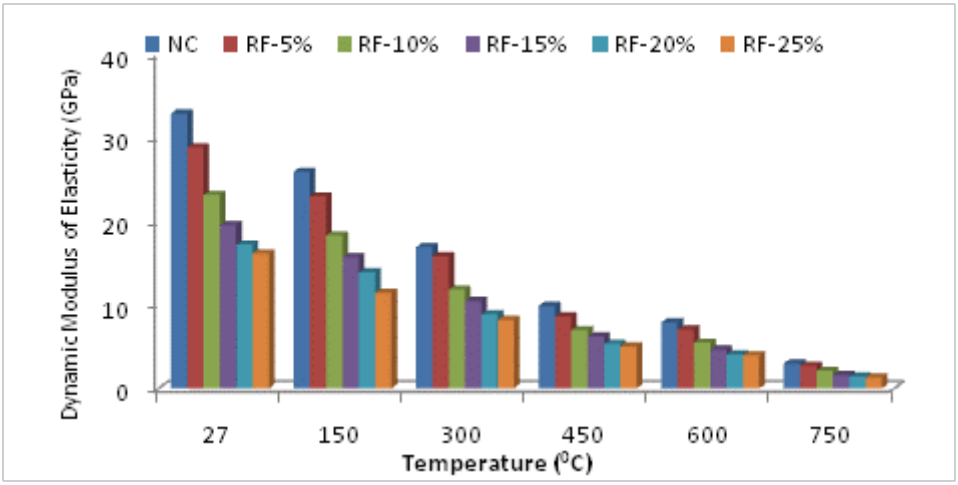

Fig. 6.59 Dynamic modulus of rubber fiber concrete (w/c ratio 0.45) after exposure to elevated temperature for 30 minutes

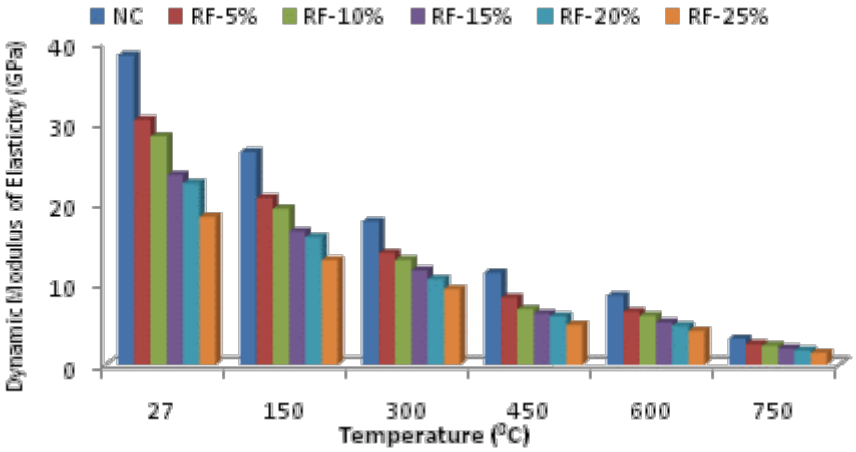

Fig. 6.60 Dynamic modulus of rubber fiber concrete (w/c ratio 0.45) after exposure to elevated temperature for 60 minutes

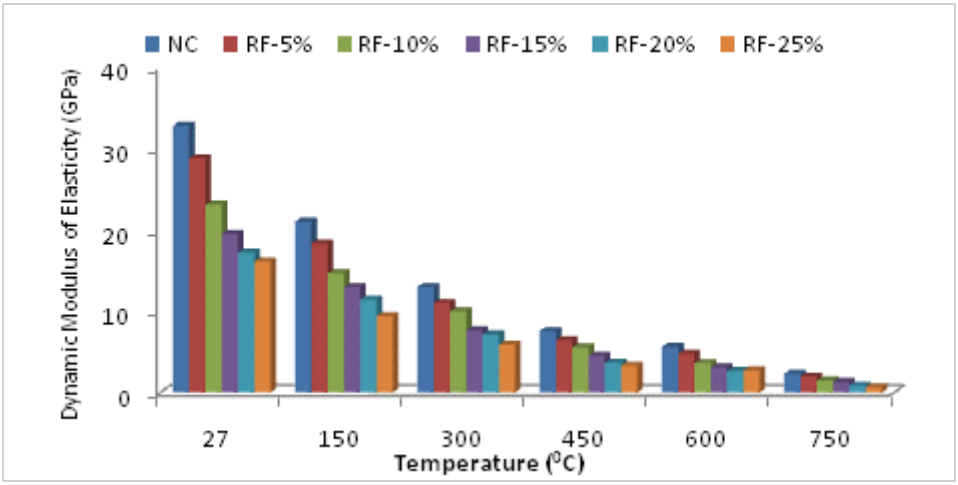

Fig. 6.61 Dynamic modulus of rubber fiber concrete (w/c ratio 0.45) after exposure to elevated temperature for 120 minutes

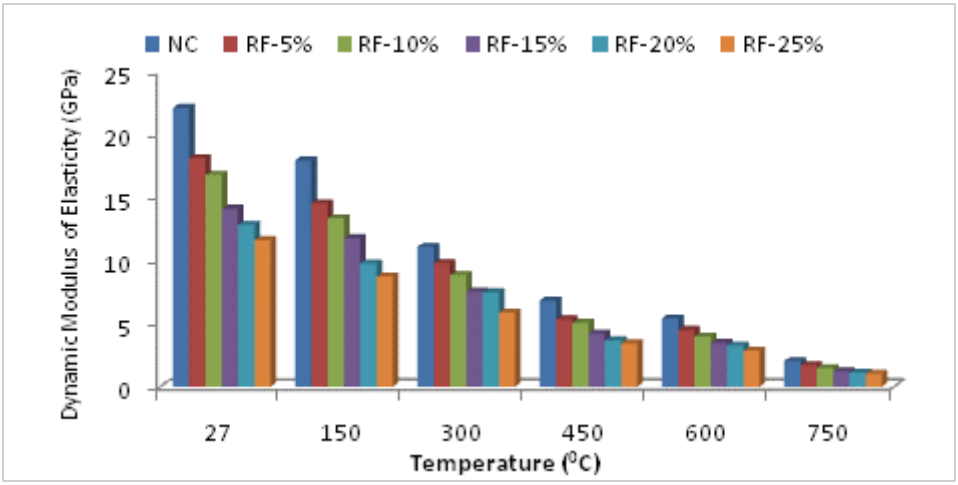

Fig. 6.62 Dynamic modulus of rubber fiber concrete (w/c ratio 0.55) after exposure to elevated temperature for 30 minutes

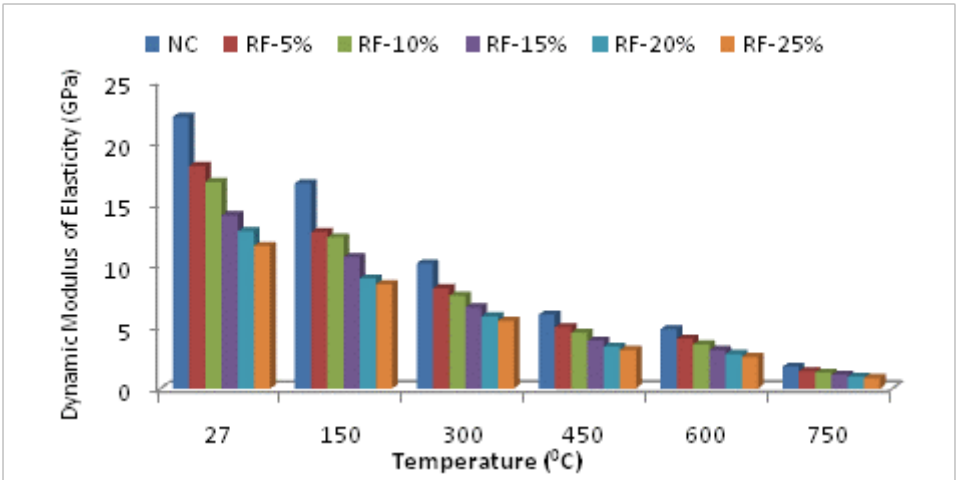

Fig. 6.63 Dynamic modulus of rubber fiber concrete (w/c ratio 0.55) after exposure to elevated temperature for 60 minutes

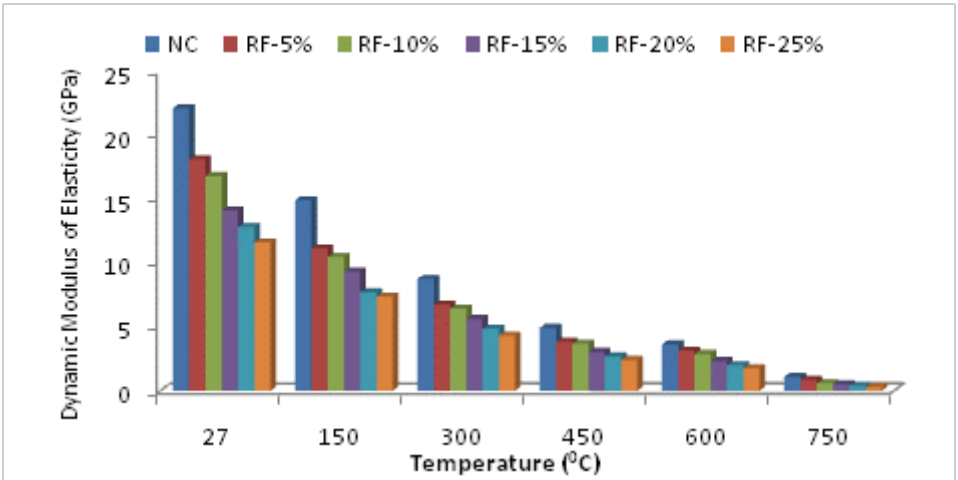

Fig. 6.64 Dynamic modulus of rubber fiber concrete (w/c ratio 0.55) after exposure to elevated temperature for 120 minutes

6.3.8 Water permeability

Depth of water penetration was measured immediately after splitting the specimen as per DIN 1048 (1991). The depth of water penetration of the control mix and waste rubber fiber concrete exposed to five different elevated temperatures for 30, 60 and 120 minutes followed by normal (air) cooling is shown in Figs. 6.65-6.73 respectively. The maximum standard deviation and coefficient of variance anywhere for the experimental results shown in these Figs. are 3.89 mm and 0.06 respectively (Fig. 6.73, 20% rubber fibers and 750 ^{0}C temperature). It is seen from the Figs. that there was an increase in penetration depth in all the cases of concrete subjected to elevated temperature. A similar observation was made by Nadeem *et al.* (2014) on the sorptivity of fly ash and metakaolin concrete subjected to elevated temperature.

The penetration depth increased with the increase of elevated temperature and exposure duration for all the cases. Further, for all replacement levels of rubber fiber, the percentage increase in penetration in case of waste rubber fiber concrete was similar to the corresponding cases of control concrete. However, the absolute values of water penetration depth were always higher for rubber fiber concrete, including at room temperature, than the corresponding control concrete.

The waste rubber fiber concrete at 25% replacement level showed the highest value of water penetration of 83.4 mm (indicating low resistance to water penetration) on 120 minute exposure to a temperature of 750 ^{0}C for w/c ratio 0.55. Ganjian *et al.* (2009) has classified the depth of water permeability (after 72 h) into three category as low (less than 30 mm), medium permeability (30-60 mm) and high permeability (greater than 60 mm). Rubber fiber concrete shows medium permeability in most of the cases and the high permeability is observed only at 750 ^{0}C, 120 minute exposure for 15%, 20% and 25% replacement of FA by fiber.

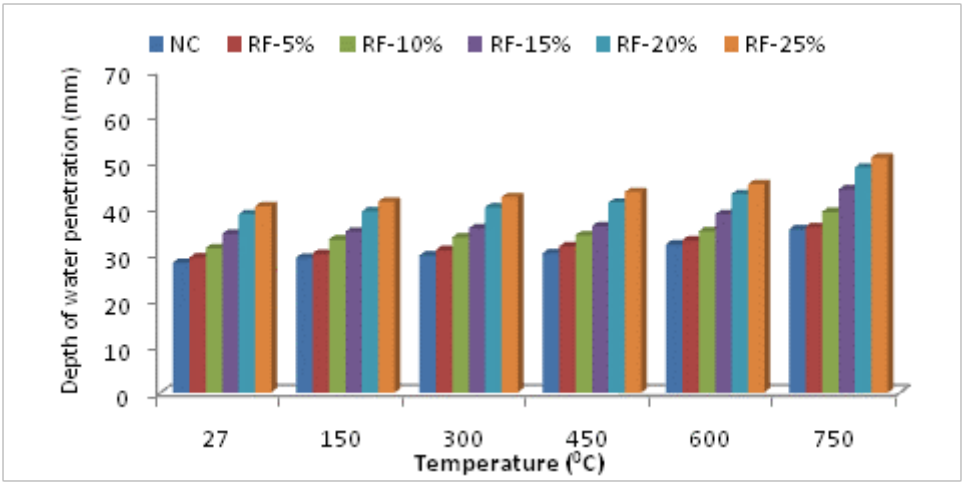

Fig. 6.65 Depth of water penetration in rubber fiber concrete (w/c ratio 0.35) after exposure to elevated temperature for 30 minutes

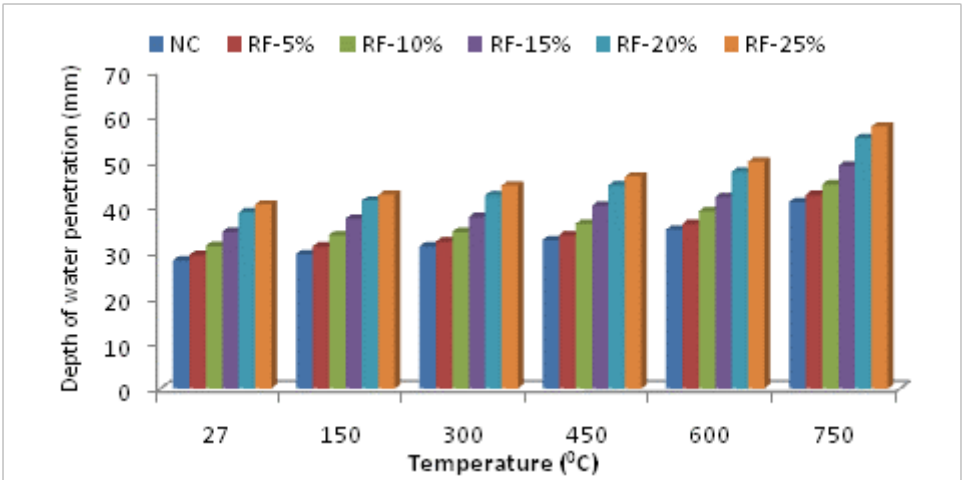

Fig. 6.66 Depth of water penetration in rubber fiber concrete (w/c ratio 0.35) after exposure to elevated temperature for 60 minutes

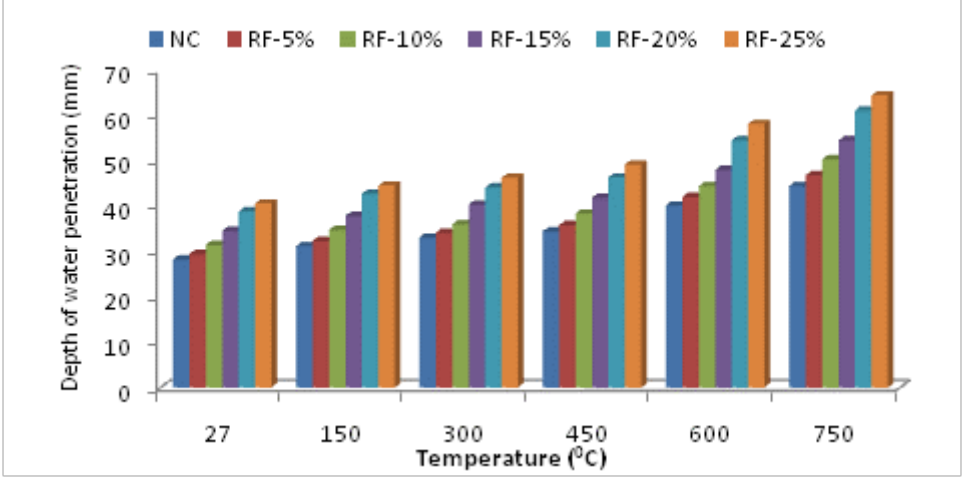

Fig. 6.67 Depth of water penetration in rubber fiber concrete (w/c ratio 0.35) after exposure to elevated temperature for 120 minutes

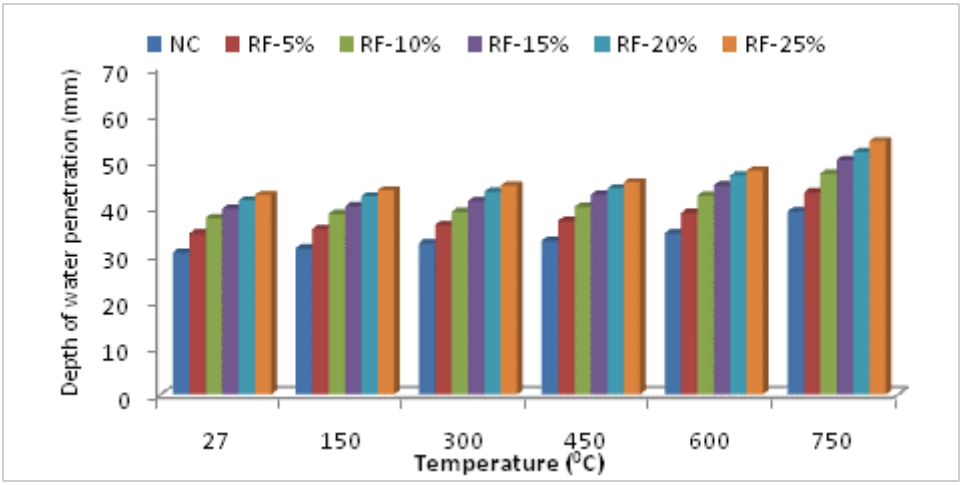

Fig. 6.68 Depth of water penetration in rubber fiber concrete (w/c ratio 0.45) after exposure to elevated temperature for 30 minutes

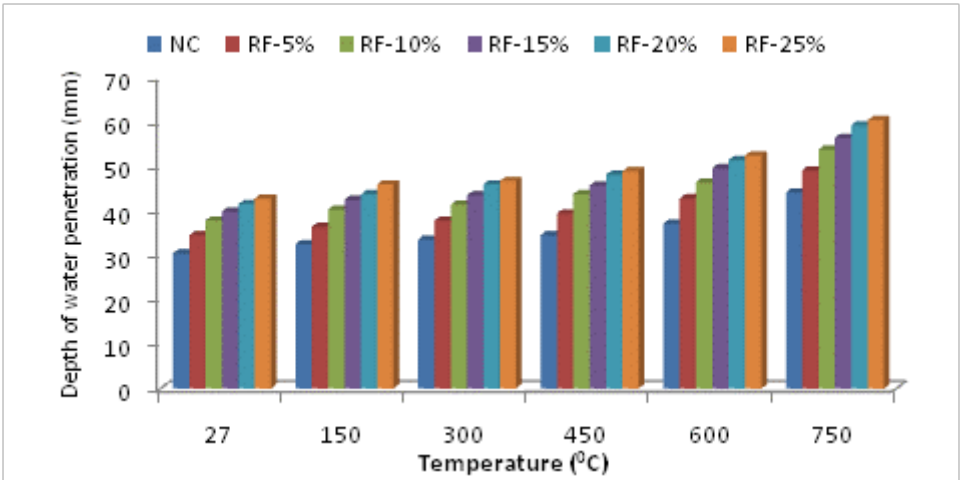

Fig. 6.69 Depth of water penetration in rubber fiber concrete (w/c ratio 0.45) after exposure to elevated temperature for 60 minutes

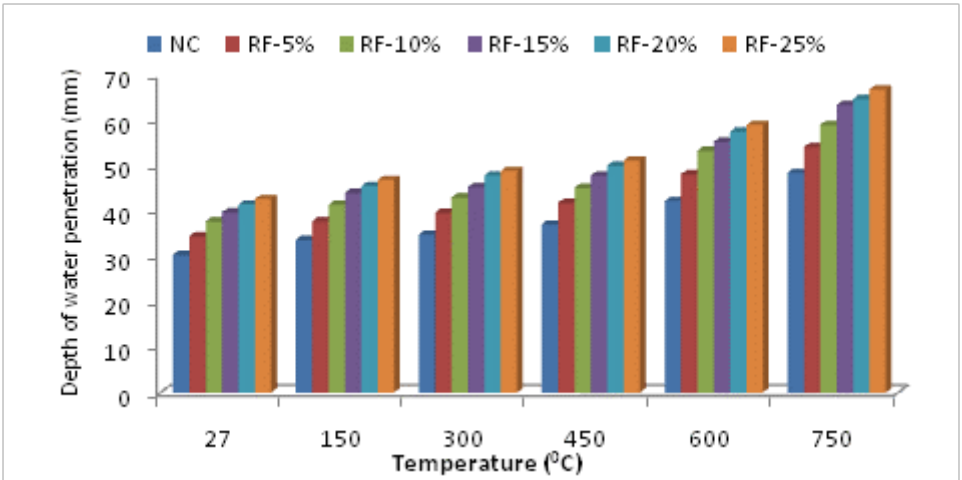

Fig. 6.70 Depth of water penetration in rubber fiber concrete (w/c ratio 0.45) after exposure to elevated temperature for 120 minutes

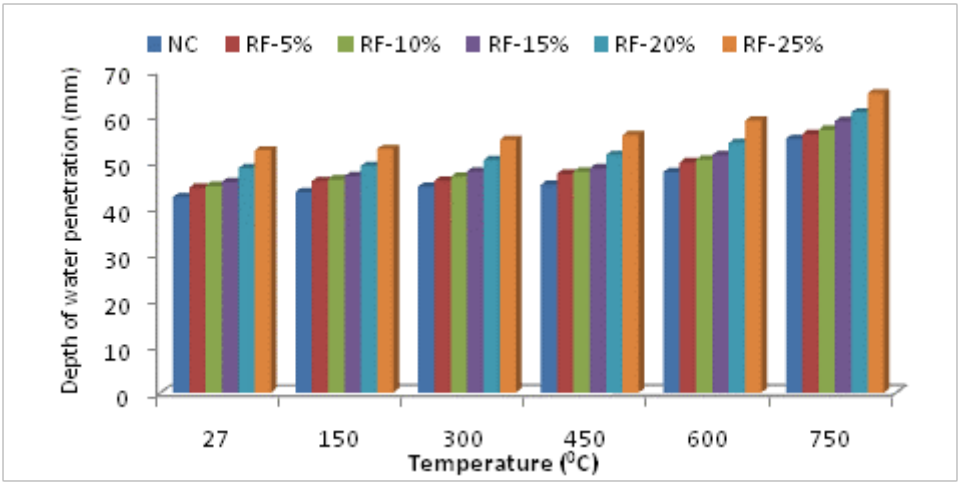

Fig. 6.71 Depth of water penetration in rubber fiber concrete (w/c ratio 0.55) after exposure to elevated temperature for 30 minutes

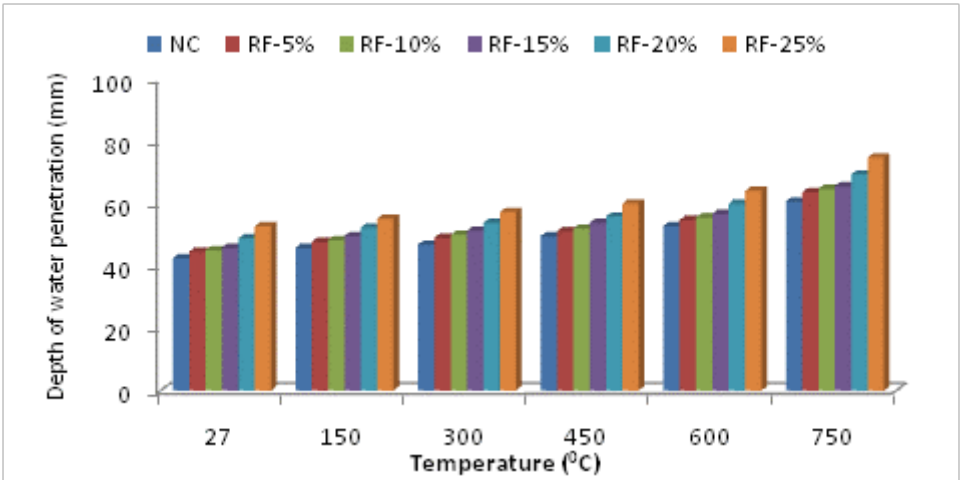

Fig. 6.72 Depth of water penetration in rubber fiber concrete (w/c ratio 0.55) after exposure to elevated temperature for 60 minutes

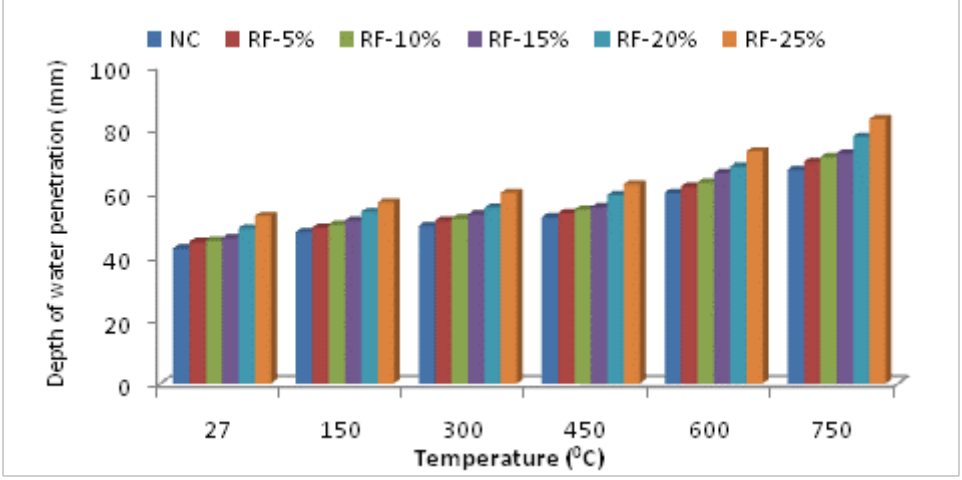

Fig. 6.73 Depth of water penetration in rubber fiber concrete (w/c ratio 0.55) after exposure to elevated temperature for 120 minutes

6.3.9 Chloride diffusion

In this test, a thin slice of concrete (65 mm diameter and 50 mm thick) was used so that the results can be obtained within 72 h from starting of test. The chloride diffusion coefficient of the control mix and waste rubber tyre fiber concrete exposed to five different elevated temperatures for 30, 60 and 120 minutes followed by normal (air) cooling is shown in Figs. 6.74-6.82 respectively. The maximum standard deviation and coefficient of variance anywhere for the experimental results shown in these Figs. are $1.4x10^{-11}$ m^2/s and 0.012 respectively (Fig. 6.82, 25% rubber fibers and 750 ^{0}C temperature). It is seen from the Figs. that there was an increase in chloride diffusion coefficient in all the cases of concrete subjected to elevated temperature. A similar observation was made by Nadeem *et al.* (2014) on the chloride permeability of fly ash and metakaolin concrete subjected to elevated temperature.

The chloride diffusion coefficient increased with the increase of elevated temperature and exposure duration for all the cases. Further, for all replacement levels of rubber fiber, the percentage increase in chloride permeability in case of waste rubber fiber concrete was similar to the corresponding cases of control concrete. The absolute values of chloride diffusion coefficient were always higher, including at room temperature, than the corresponding control concrete. The waste rubber fiber concrete at 25% replacement level showed the highest chloride diffusion coefficient value (2.71×10^{-6} m^2/s), indicating low resistance to chloride permeability, on 120 minute exposure to a temperature of 750 ^{0}C for w/c ratio 0.55.

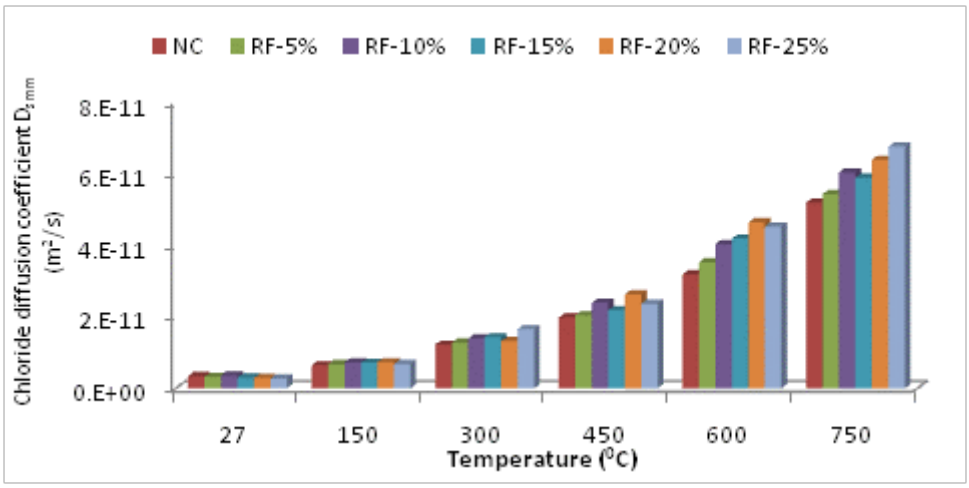

Fig. 6.74 Chloride diffusion coefficient of rubber fiber concrete (w/c ratio 0.35) after exposure to elevated temperature for 30 minutes

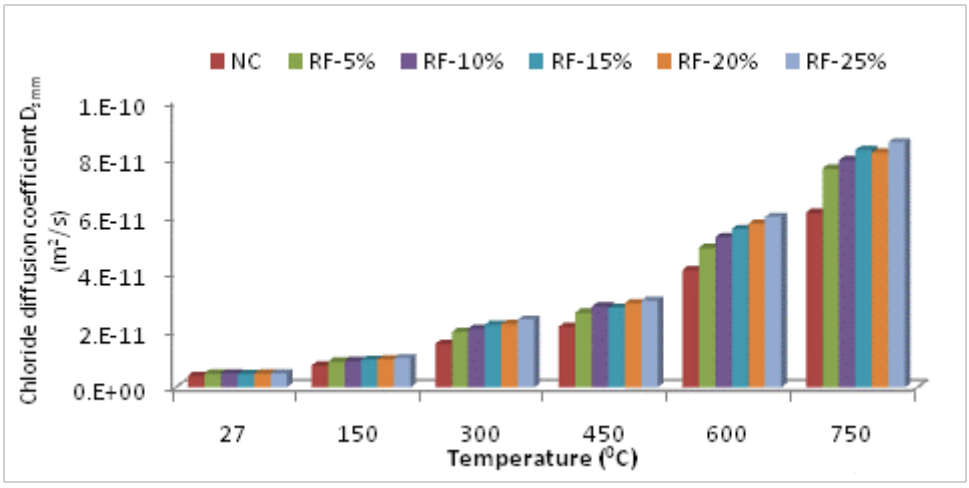

Fig. 6.75 Chloride diffusion coefficient of rubber fiber concrete (w/c ratio 0.35) after exposure to elevated temperature for 60 minutes

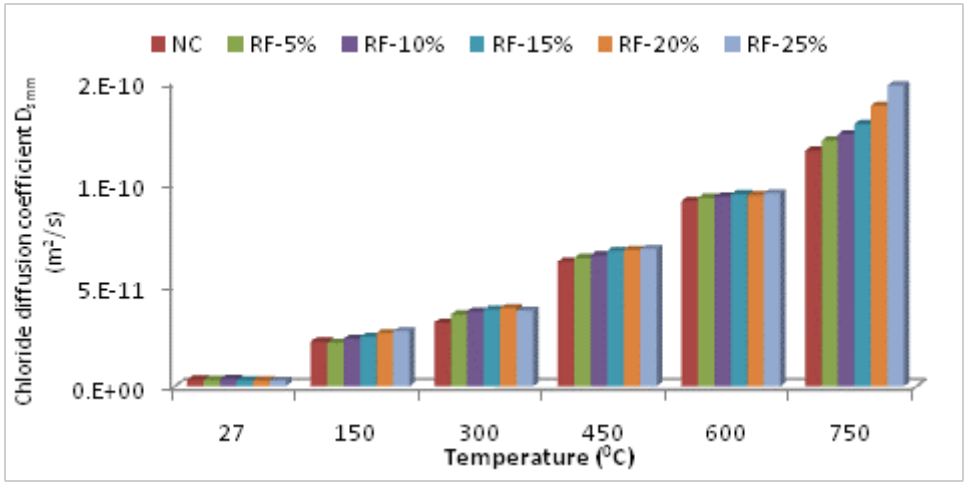

Fig. 6.76 Chloride diffusion coefficient of rubber fiber concrete (w/c ratio 0.35) after exposure to elevated temperature for 120 minutes

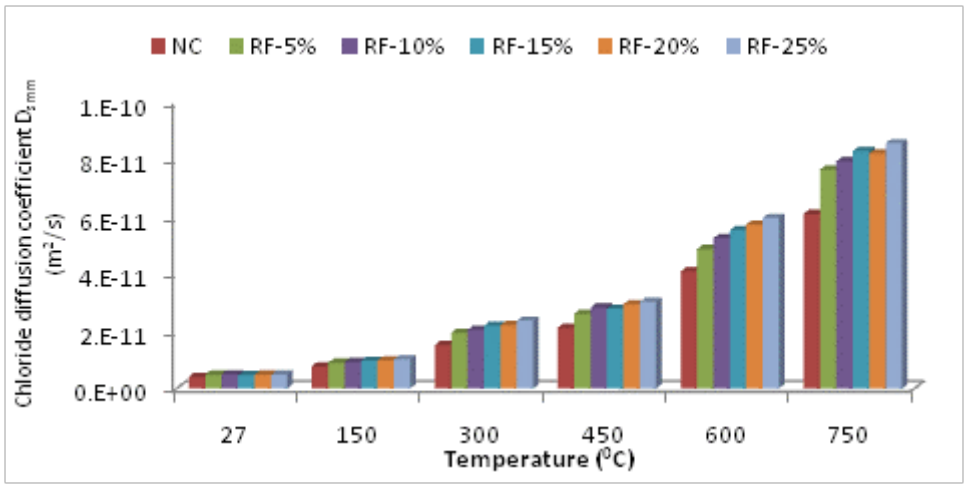

Fig. 6.77 Chloride diffusion coefficient of rubber fiber concrete (w/c ratio 0.45) after exposure to elevated temperature for 30 minutes

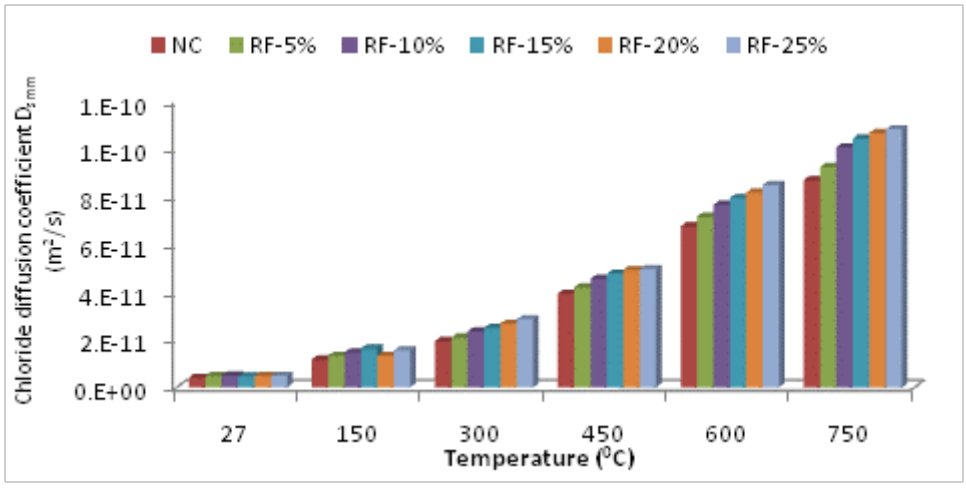

Fig. 6.78 Chloride diffusion coefficient of rubber fiber concrete (w/c ratio 0.45) after exposure to elevated temperature for 60 minutes

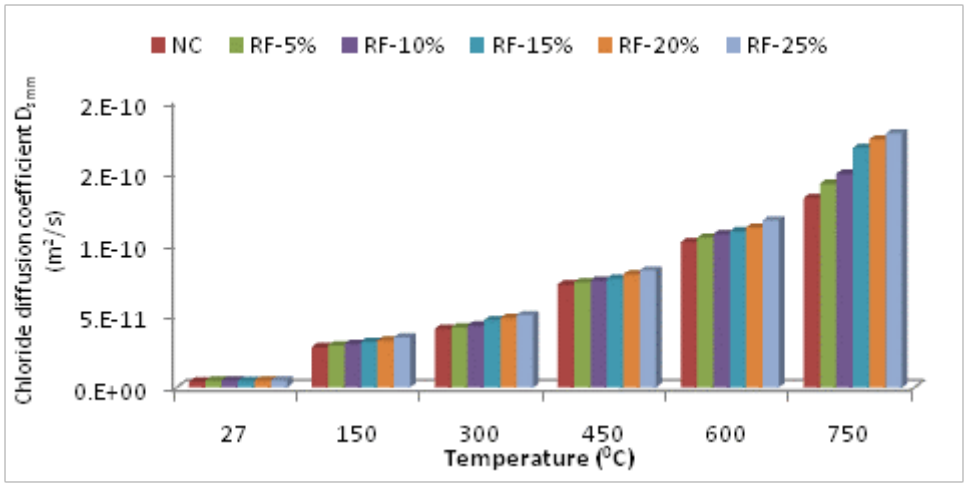

Fig. 6.79 Chloride diffusion coefficient of rubber fiber concrete (w/c ratio 0.45) after exposure to elevated temperature for 120 minutes

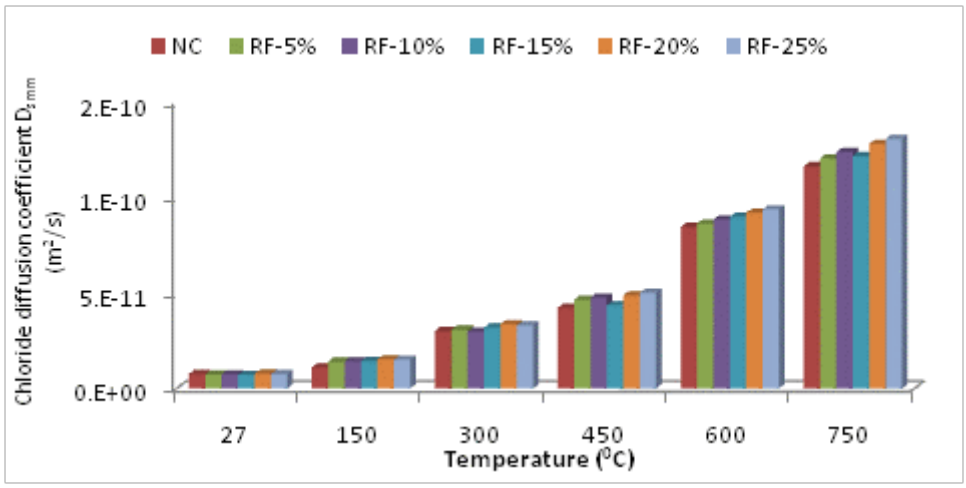

Fig. 6.80 Chloride diffusion coefficient of rubber fiber concrete (w/c ratio 0.55) after exposure to elevated temperature for 30 minutes

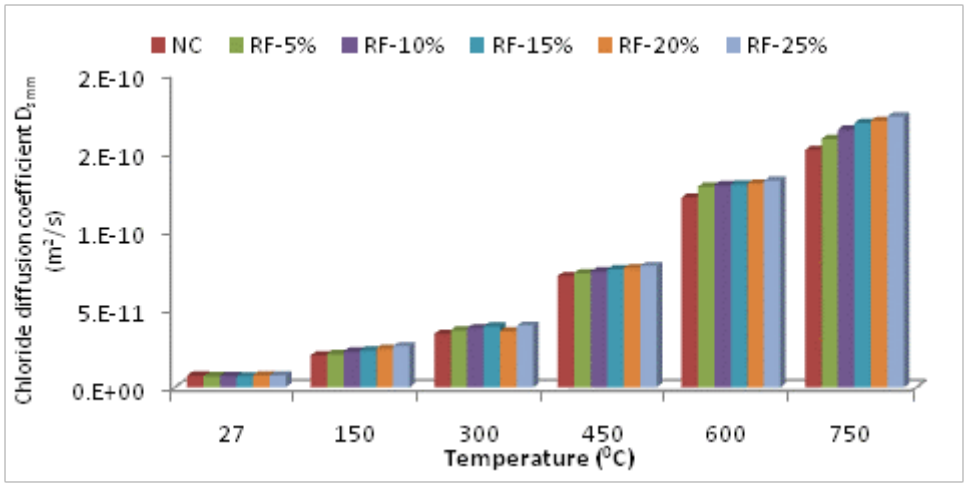

Fig. 6.81 Chloride diffusion coefficient of rubber fiber concrete (w/c ratio 0.55) after exposure to elevated temperature for 60 minutes

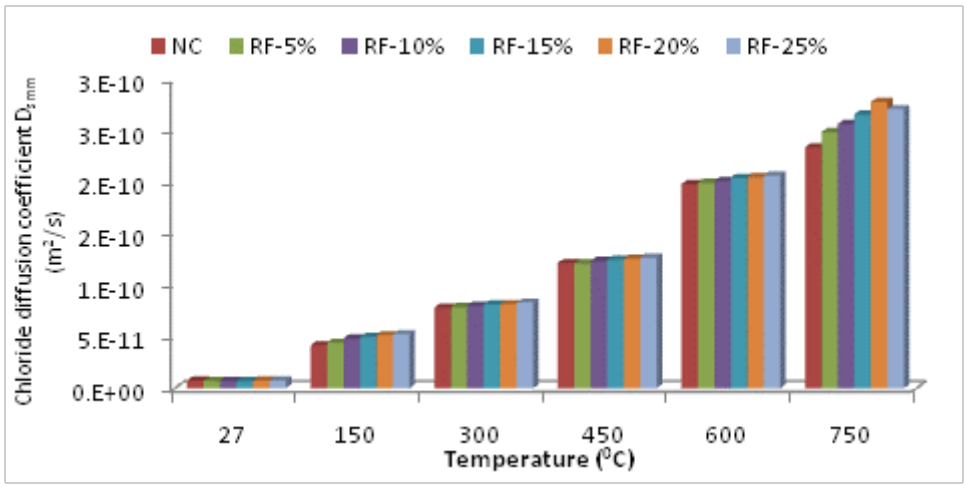

Fig. 6.82 Chloride diffusion coefficient of rubber fiber concrete (w/c ratio 0.55) after exposure to elevated temperature for 120 minutes

6.3.10 Micro structural analysis

Microscopic images of the waste rubber fiber concrete specimen are shown in Figs. 6.83-6.89. Cracks are observed in the rubber fibers in Figs. 6.83-6.84. These cracks cause reduction in the strength of the concrete. Gaps in the interface of rubber aggregate and cement matrix are observed in Fig. 6.83, and this gap reflects weak bond with cement mortar.

It is observed that gap at interface of rubber fiber and cement matrix widened with increase in temperature (Figs. 6.83-6.85). This wider gap resulted in decrease in compressive strength of concrete at elevated temperature. Crack width in the rubber fiber also increased with increase in temperature (Figs. 6.86-6.87) which is further responsible for reduction in durability of waste rubber fiber concrete. At higher temperature and longer exposure duration (750 ^{0}C and 120 minutes exposure duration), rubber fibers were completely separated from cement matrix (Fig. 6.88) which created voids in concrete. Surface cracks were also observed in concrete and Fig. 6.89 shows surface cracks in concrete at an elevated temperature of 750 ^{0}C. These gaps and crack in cement matrix and rubber fibers are responsible for reduction in mechanical strength and durability of waste rubber fiber concrete exposed to elevated temperature.

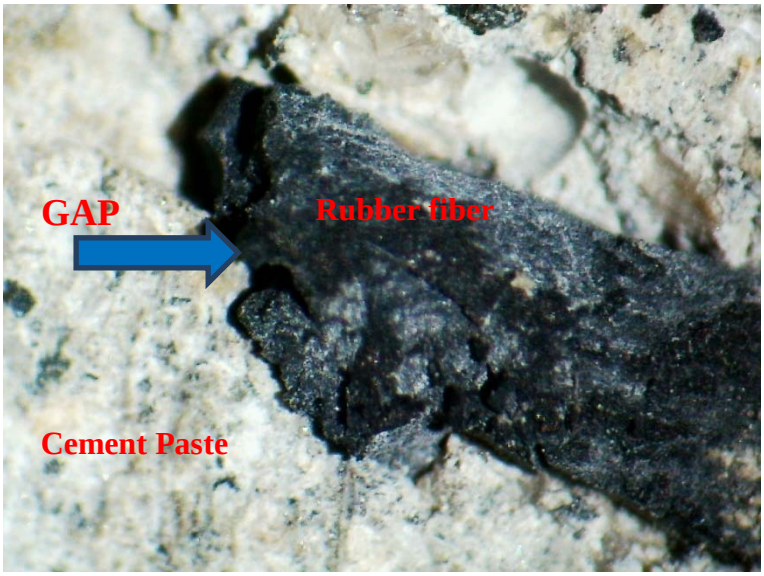

Fig. 6.83 Microstructure of concrete at 100x magnification showing gap in between cement paste and rubber fiber at normal temperature

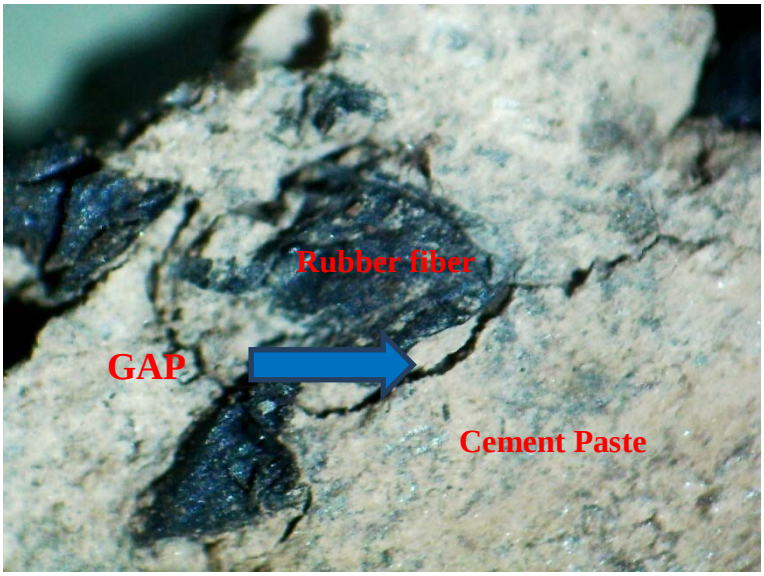

Fig. 6.84 Microstructure of concrete at 100x magnification showing wider cracks at interface of rubber fiber and cement matrix exposed to 450 ^{0}C temperature

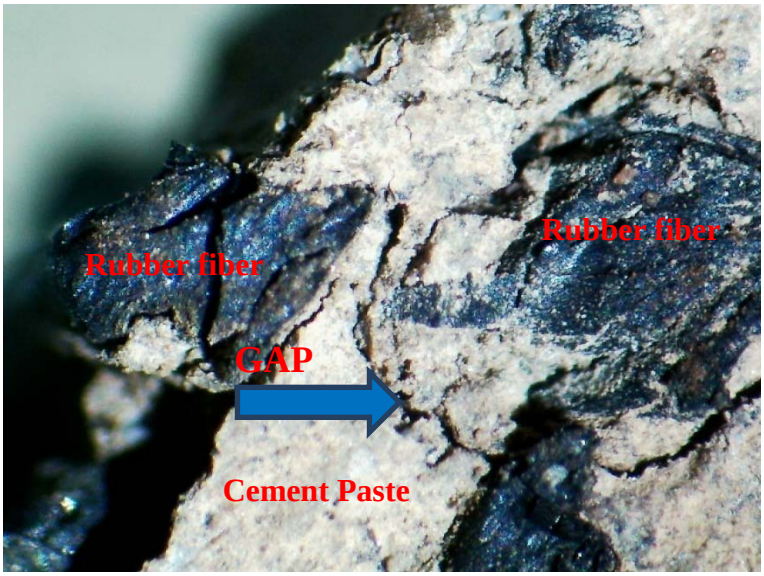

Fig. 6.85 Microstructure of concrete at 100x magnification showing wider cracks in rubber fiber and at interface of rubber fiber and cement matrix exposed to 600 ^{0}C temperature

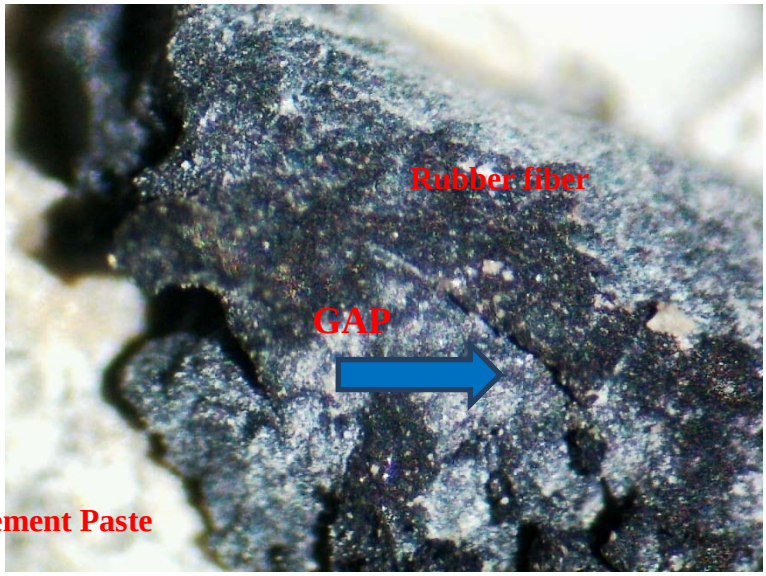

Fig. 6.86 Microstructure of concrete at 100x magnification showing cracks in rubber fiber at normal temperature

Fig. 6.87 Microstructure of concrete at 100x magnification showing wider cracks in rubber fiber exposed to 600 ^{0}C temperature

Fig. 6.88 Microstructure of concrete at 100x magnification showing gap due to rubber fiber exposed to 750 ^{0}C temperature for 120 minutes

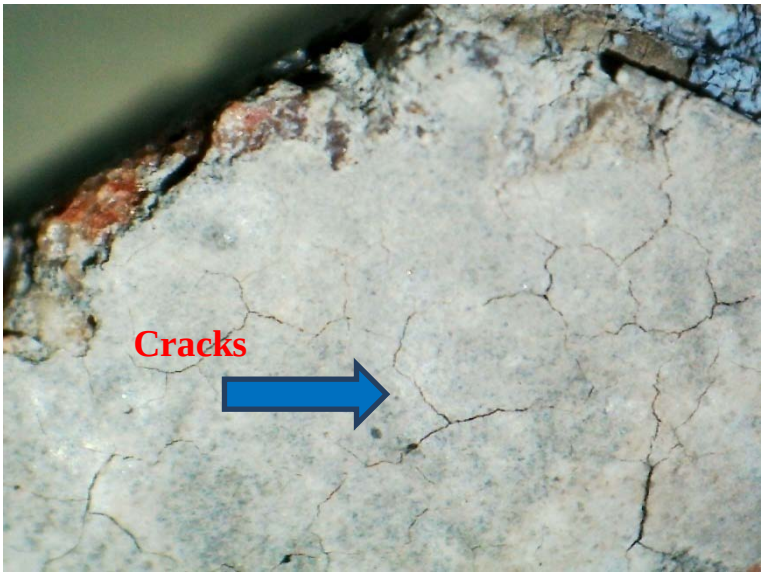

Fig. 6.89 Microstructure of concrete at 100x magnification showing surface cracks in concrete exposed to 750 ^{0}C temperature

6.4 CONCLUSIONS

The objective of this study was to evaluate the effect of elevated temperature on mass loss and change in compressive strength, ultrasonic pulse velocity, static modulus of elasticity, dynamic modulus of elasticity, water permeability and chloride-ion permeability in control mix (no replacement) and waste rubber fiber concrete. The study was undertaken for varying percentage of waste rubber fibers (0% to 25%) as fine aggregate for w/c ratios 0.35, 0.45 and 0.55. All the specimens were exposed to six levels of temperature (27 ^{0}C – 750 ^{0}C) and three

different exposure durations (30, 60 and 120 minutes). As rubber aggregate are a waste product of used rubber tyres, detailed microstructural characterization of waste rubber fiber concrete was also carried out at elevated temperature to ensure compatibility of this material with the concrete. Based on the test result and discussions following conclusions are drawn:

1. The reduction in compressive strength, on exposure to elevated temperature, is more in case of fast cooling as compared to the case of normal cooling for all the specimens of control mix as well as waste rubber fiber concrete.
2. The reduction in compressive strength on exposure to elevated temperature increases with the increase in exposure duration for control mix as well as waste rubber fiber concrete. The increase in reduction with the increase in exposure time is more in case of waste rubber fiber concrete than in case of control mix.
3. The mass loss, on exposure to elevated temperature, increases with the increase of elevated temperature and exposure duration for control mix as well as waste rubber fiber concrete. Further, the mass loss in cases of waste rubber fiber concrete is similar to the corresponding case of control mix.
4. The ultrasonic pulse velocity decreases on exposure to elevated temperature for control mix as well as waste rubber fiber concrete. The decrease is more in case of higher temperatures and longer exposure durations. The percentage decrease in ultrasonic pulse velocity in case of waste rubber fiber concrete is similar to the corresponding case of control concrete for upto 60 minute exposure.
5. The static and dynamic modulus decrease on exposure to elevated temperature for control mix as well as waste rubber fiber concrete. The decrease is more in case of higher temperatures and longer exposure durations. The percentage decrease in static and dynamic modulus for waste rubber fiber concrete is similar to the corresponding cases of control mix.
6. The water penetration depth increases on exposure to elevated temperature for control mix as well as waste rubber fiber concrete. The increase is more in case of higher temperatures and longer exposure durations. The percentage increase in penetration depth for waste rubber fiber concrete is similar to the corresponding cases of control mix.
7. The chloride-ion permeability increases on exposure to elevated temperature for control mix as well as waste rubber fiber concrete. The increase is more in case of higher temperatures and longer exposure durations. The percentage increase in

chloride-ion permeability for waste rubber fiber concrete is similar to the corresponding cases of control mix.

8. Microscopic analysis shows that gap at interface of rubber fiber and cement matrix increases with increase in temperature. Crack width in the rubber fiber also increases with increase in temperature. When exposed to high temperature for long duration, rubber fiber is completely separated from cement matrix which creates voids in concrete.

CHAPTER 7

SUMMARY AND CONCLUSIONS

In the present work, detailed experimental studies were carried out to check the suitability of waste rubber tire aggregates as fine aggregates in concrete. Two forms of waste rubber (i) rubber ash and (ii) rubber fibers were used in this study. The study was undertaken for varying percentage of waste rubber ash (0%-20%), waste rubber fiber (0%-25%) and combined form of waste rubber ash (constant 10%) & varied percentage of waste rubber fiber (0%-25%) as fine aggregates. Three different w/c ratios (0.35, 0.45 and 0.55) were selected. Silica fume was also used as replacement of cement in rubber fiber concrete with varying percentages (0-10%).

To evaluate the workability of rubberized concrete, compaction factor and slump were examined. The mechanical properties of rubberized concrete in terms of compressive strength and flexural strength were evaluated. The depth of wear due to abrasion was measured to examine the behavior of rubberized concrete against vehicular movement over concrete surface in comparison to control.

The durability properties of waste rubber concrete were evaluated by carrying out water absorption test, water permeability test as per DIN 1048, drying shrinkage test, carbonation test through ingress of 5% CO_2, chloride diffusion test, corrosion test in terms of macrocell and half cell potential and acid attack test for sulphuric acid and hydrochloric acid.

The ductility properties of waste rubber concrete were evaluated by carrying out static modulus of elasticity test, ultrasonic pulse velocity test, dynamic modulus of elasticity test, impact resistance under drop weight test, impact resistance under flexural test, impact resistance under rebound test and fatigue test.

Detailed experimental studies were carried out for the effect of elevated temperature on mass loss and change in compressive strength, density, ultrasonic pulse velocity, static modulus of elasticity, dynamic modulus of elasticity, water permeability and chloride ion permeability in control mix (no replacement) and rubberized concrete. The microstructure analysis of waste rubber fiber concrete subjected to elevated temperature was investigated. Two types of cooling, normal cooling and fast cooling were considered for the effect of elevated temperature on compressive strength of control mix as well as waste rubber fiber

concrete. All the specimens were exposed to six level of temperature (27 ^{0}C – 750 ^{0}C) and three different exposure durations (30, 60 and 120 minutes).

Following are the important conclusions of the study:

1. The specific gravity of rubber ash and rubber fiber is less than that of fine aggregate which is helpful in production of low density concrete. Particle size of rubber ash and rubber fiber conform to the requirement of Indian Standard for fine aggregate. The rubber fiber has good tensile strength which leads to increased flexural strength of concrete.
2. Partial replacement of fine aggregate by rubber ash decreases the workability of concrete whereas partial replacement of fine aggregate by rubber fiber does not affect the workability of concrete.
3. Partial replacement of fine aggregate by rubber ash and rubber fiber decreases the compressive strength of concrete. Partial replacement of fine aggregate by rubber ash decreases the flexural strength of the concrete whereas the partial replacement of fine aggregate by rubber fiber increases the flexural strength of the concrete.
4. The maximum depth of wear in rubber ash and rubber fiber concrete is less than permissible limits. The water permeability remains in the category of medium permeability defined in literature.
5. Rubber ash and rubber fiber particles increase the drying shrinkage and leads to early corrosion initiation.
6. The carbonation depth observed from 90 days accelerated carbonation test, for rubber ash and rubber fiber concrete in the most adverse condition is less than the minimum cover required for RCC member as per Indian Standard.
7. No pattern is observed for change in chloride ion resistance with the replacement level of rubber ash and rubber fiber.
8. Loss in weight and compressive strength due to attack of sulphuric acid and hydrochloric acid increases with the increase in replacement levels of rubber ash and rubber fiber.
9. The reduction in static and dynamic modulus on partial replacement of fine aggregate by rubber ash and rubber fiber indicates higher flexibility.
10. The impact resistance of concrete improves on replacement of fine aggregate by rubber ash and rubber fiber content. Fatigue strength of concrete improves on replacement of fine aggregate by rubber ash and rubber fiber content.

11. The percentage decrease in compressive strength, UPV, static and dynamic modulus for waste rubber fiber concrete at elevated temperature is similar to the respective cases of control mix.
12. Cavities and micro cracks are observed in rubber ash and rubber fiber, which reduce strength of concrete. Micro structural analysis shows weak interface between the rubber ash/rubber fiber and cement matrix. Rubber fiber is completely separated from cement matrix on exposure to elevated temperature for long duration.
13. Silica fume is found to improve the strength, durability and ductility properties of rubber fiber concrete.

To sum up, the strength and durability of rubberized concrete is less as compared to control concrete whereas the ductility is significantly better as compared to control concrete. Silica fume can be used to improve the strength and ductility properties of rubberized concrete.

Conclusions drawn from the study indicate that fine aggregate can be replaced by rubber fiber and rubber ash where ductility is of prime concern. Rubberized concrete can be used for partition wall (due to light weight), pedestrian block/residential drive ways/garage floors, highway crash barrier (due to better impact resistance) and machine foundation pads (due to better fatigue resistance).

Recommendations for future research

The present studies may be extended in future for the following:

1. Effect of silica fume on rubber ash concrete.
2. Behaviour of rubber fiber and rubber ash concrete against freeze/thaw.
3. Effect of mineral admixtures on waste rubber concrete.
4. Behaviour of rubber ash concrete at elevated temperature.
5. Energy absorption capacity of rubberized concrete using stress-strain curve.

REFERENCES

Ababneh, A. (2002). “The coupled effect of moisture diffusion chloride penetration and freezing-thawing on concrete durability.” Ph.D. dissertation, Univ. of Colorado, Boulder, Co.

ACI. (1999). “Measurement of properties of fiber reinforced concrete (544.2R-99).” American Concrete Institute, Farmington Hills, Mich.

Aiello, M.A. and Leuzzi, F. (2010). “Waste tyre rubberized concrete: Properties at fresh and hardened state.” Waste Management, 30, 1699-1704.

Akcaozoglu, K. (2013). “Microstructural examination of concrete exposed to elevated temperature by using plane polarized transmitted light method.” Construction and Building Materials, 48, 772-779.

Al-Akhras, N.M. and Smadi, M.M. (2004). “Properties of tire rubber ash mortar.” Cement and Concrete Composites, 26, 821-826.

Al-Tayeb, M.M., Bakar, B.H.A., Akil, H.M., and Ismail, H. (2013). “Performance of rubberized and hybrid rubberized concrete structures under static and impact load conditions.” Experimental Mechanics, 53(3), 377-384.

Andrade, C. (1993). “Calculation of chloride diffusion coefficients in concrete from ionic migration measurements.” Cement and Concrete Research, 23(3), 724–742.

ASTM. (2002). “Standard test method for pulse velocity through concrete.” C597–02, West Conshohocken, Pennsylvania, United States.

ASTM. (2002). “Standard test method for static modulus of elasticity and Poisson’s ratio of concrete in compression.” C469–02, West Conshohocken, Pennsylvania, United States.

ASTM. (2005). “Standard test method for determining the effects of chemical admixtures on the corrosion of embedded steel reinforcement in concrete exposed to chloride environments.” ASTM G 109-99a, West Conshohocken, Pennsylvania, United States.

ASTM. (2008). “Standard test method for density (unit weight), yield, and air content (gravimetric) of concrete.” ASTM C 138/C 138M – 08, West Conshohocken, Pennsylvania, United States.

ASTM. (2008). “Standard test method for length change of hardened hydraulic-cement mortar and concrete.” ASTM C157/C157M-08e1, West Conshohocken, Pennsylvania, United States.

ASTM. (2009). “Standard test method for corrosion potentials of uncoated reinforcing steel in concrete.” ASTM C 876-09, West Conshohocken, Pennsylvania, United States.

Atahan, A. O., and Yücel, A. Ö. (2012). “Crumb rubber in concrete: static and dynamic evaluation.” Construction and Building Materials, 36, 617-622.

Atef, B., Ashraf, F., and Andrew, K. (2006). “Statistical variations in impact resistance of polypropylene fibre-reinforced concrete.” International Journal of Impact Engineering, 32, 1907−1920.

Azevedo, F., Pacheco-Torgal, F., Jesus, C., Barroso, J.L., and Camoes, A.F. (2012). “Properties and durability of HPC with tyre rubber wastes.” Construction and Building Materials, 34, 186-191.

Azmi, N.J., Mohammed, B.S., and Al-Mattarneh, H.M.A. (2008). “Engineering properties of concrete with recycled tire rubber.” International Conference on Construction and Building Technology, ICCBT 2008, KualaLumpur, Malaysia, B(34), 373–382.

Batayneh, M., Marie, I., and Asi, I. (2008). “Promoting the use of crumb rubber concrete in developing countries.” Waste Management, 28, 2171-2176.

Bederina, M., Makhloufi, Z., Bounoua, A., Bouziani, T., and Quéneudec, M. (2013). “Effect of partial and total replacement of siliceous river sand with limestone crushed sand on the durability of mortars exposed to chemical solutions.” Construction and Building Materials 47, 146–158.

Benazzouk, A., Douzane, O., Langlet, T., Mezreb, K., Roucoult, J.M., and Queneudec, M., (2007). “Physico-mechanical properties and waste absorption of cement composites containing shredded rubber wastes.” Cement and Concrete Composites, 29(10), 732-740.

Benazzouk, A., Mezreb, K., Doyen, G., Goullieux, A., and Queneudec, M. (2003). “Effect of rubber *aggregates* on the physico-mechanical behaviour of cement–rubber composites-influence of the alveolar texture of rubber aggregates.” Cement and Concrete Composites, 25(7), 711–720.

Bentz, D.P., Jensen, O.M., Coats, A.M., and Glasser, F.P. (2000). “Influence of silica fume on diffusivity in cement-based materials: I. Experimental and computer modeling studies on cement pastes.” Cement and Concrete research, 30(6), 953-962.

Bentur, A., and Goldman, A. (1989). “Curing effect, strength and physical properties of high strength silica fume concrete.” Journal of Materials in Civil Engineering, ASCE, 1(1), 46-58.

Bjegović, D., Baričević, A., and Serdar, M. (2011). “Durability properties of concrete with recycled waste tyres.” In 12th International Conference on Durability of Building Materials and Components Porto, Faculdade de Engenharia Universidade do Porto, 1659-1667.

Bravo, M., and Brito, J.D. (2012). “Concrete made with used tyre aggregate: durability-related performance.” Journal of Cleaner Production, 25, 42-50.

British Standards Institution (BS). (2011). “Testing concrete: Method for determination of water absorption.” BS 1881-122.

Broomfield, J.P. (2007). “Corrosion of steel in concrete, understanding, investigation and repair.” 2nd edition, Tylor and Francis, London and New York.

Bureau of Indian Standards (BIS). (1959). “Methods of sampling and analysis of concrete.” IS: 1199, New Delhi, India.

Bureau of Indian Standards (BIS). (1959). “Methods of tests for strength of concrete.” IS: 516, New Delhi, India.

Bureau of Indian Standards (BIS). (1970). “Specification for coarse and fine aggregates from natural sources for concrete.” IS: 383, New Delhi, India.

Bureau of Indian Standards (BIS). (1980). “Specification for cement concrete flooring tiles (Appendix F- Method for determination of resistance to wear).” IS: 1237, New Delhi, India.

Bureau of Indian Standards (BIS). (1989). “Specification for 43 grade ordinary Portland cement.” IS: 8112, New Delhi, India.

Bureau of Indian Standards (BIS). (2000). “Specification for plain and reinforced concrete.” IS: 456, New Delhi, India.

Byfors K. (1986). “Nordic Concrete Research.” 5, 27–38.

Byström, A., Cheng, X., Wickström, U., and Veljkovic, M. (2013). “Measurement and calculation of adiabatic surface temperature in a full-scale compartment fire experiment.” Journal of Fire Sciences, 31(1), 35-50.

Chan, Y.N., Peng, G.F., and Chan, K.W. (1996). “Comparison between high strength concrete and normal strength concrete subjected to high temperature.” Materials and Structures, 29, 616–619.

Çullu, M. and Arslan, M. (2014). “The effects of chemical attacks on physical and mechanical properties of concrete produced under cold weather conditions.” Construction and Building Materials, 57, 53–60.

De Ceukelaire, L. (1992). “The effect of hydrochloride acid on mortar.” Cement and Concrete Research, 22(5), 903-914.

Demir, A., Topcu, I.B., and Kusan, H. (2011). “Modeling of some properties of the crushed tile concretes exposed to elevated temperatures.” Construction and Building Materials, 25, 1883-1889.

Demirel, B., and Kelestemur, O. (2010). “Effect of elevated temperature on the mechanical properties of concrete produced with finely ground pumice and silica fume.” Fire Safety Journal, 45, 385–391.

DIN. (1991). “Testing Concrete: Testing of hardened concrete specimens prepared in mould, Part 5.” DIN 1048, Deutsches Institut fur Normung, Germany.

Dong, J. F., Wang, Q. Y., and Guan, Z. W. (2013). “Structural behaviour of recycled aggregate concrete filled steel tube columns strengthened by CFRP.” Engineering Structures, 48, 532-542.

Fattuhi, N.I., and Clark, L.A. (1996). “Cement-based materials containing shredded scrap truck tyre rubber.” Construction and Building Materials, 10(4), 229-236.

Feldman, R.F. and ChengiYi, H. (1985). “Properties of Portland cement-silica fume paste I. Porosity and surface properties.” Cement and Concrete Research, 15(5), 765-774.

Ganesan, N., BharatiRaj, J. and Shashikala, A.P. (2013). “Flexural fatigue behavior of self compacting rubberized concrete.” Construction and Building Materials, 44, 7–14.

Ganjian, E., Khorami, M., and Maghsoudi, A. A. (2009). “Scrap-tyre-rubber replacement for aggregate and filler in concrete.” Construction and Building Materials, 23(5), 1828-1836.

Gesoglu, M., and Guneyisi, E. (2011). “Permeability properties of self-compacting rubberized concrete.” Construction and Building Materials, 25(8), 3319–3326.

Gesoglu, M., and Guneyisi, E., (2007). “Strength development and chloride penetration in rubberized concrete with and without rubberized silica fume.” Materials and Structures, 40(9), 953–964.

Gesoğlu, M., Güneyisi, E., Khoshnaw, G., and İpek, S. (2014). “Investigating properties of pervious concretes containing waste tire rubbers.” Construction and Building Materials, 63, 206-213.

Grinys, A., Sivilevičius, H., and Daukšys, M. (2012). “Tyre rubber additive effect on concrete mixture strength.” Journal of Civil Engineering and Management, 18(3), 393-401.

Guneyisi, E., Gesoglu, M., and Ozturan, T., (2004). “Properties of rubberized concretes containing silica fume.” Cement and Concrete Research, 34, 2309-2317.

Guo, Y. C., Zhang, J. H., Chen, G. M., and Xie, Z. H. (2014). “Compressive behaviour of concrete structures incorporating recycled concrete aggregates, rubber crumb and reinforced with steel fibre, subjected to elevated temperatures.” Journal of Cleaner Production, 72, 193-203.

Hausmann, D.A. (1964). “Electrochemical behavior of steel in concrete.” Journal of American Concrete Institute, 61(2), 171-188.

Hausmann, D.A. (1967). “Steel corrosion in concrete. How does it occur?” Materials Protection, 6(11), 19-23.

Hernández-Olivares, F., and Barluenga, G. (2004). “Fire performance of recycled rubber-filled high-strength concrete.” Cement and Concrete Research, 34(1), 109-117.

Hoff GC, Bilodeau A, and Malhotra VM. (2000). “Elevated temperature effects on HSC residual strength.” Concrete International, 22(4), 41–47.

Ismail, M., Ismail, M.E.G., and Muhammad. B. (2011). “Influence of elevated temperatures on physical and compressive strength properties of concrete containing palm oil fuel ash.” Construction and Building Materials, 25, 2358–64.

Khaloo, A.R., Dehestani, M., and Rahmatabadi, P., (2008). “Mechanical properties of concrete containing a high volume of tire-rubber particles.” Waste Management, 28, 2472-2482.

Khatib, Z.K., and Bayomy, F.M. (1999). “Rubberized Portland cement concrete.” Journal of Materials in Civil Engineering, ASCE, 11(3), 206–213.

Kaloush, K., Way, G., and Zhu, H. (2005). Properties of crumb rubber concrete. Transportation Research Record: Journal of the Transportation Research Board, (1914), 8-14.

Li, G., Stubblefield, M.A., Garrick, G., Eggers J., Abadie, C. and Huang B. (2004). “Development of waste tire modified concrete.” Cement and Concrete Research, 34, 2283–2289

Li, H., Zhang, M., and Ou, J. (2007). “Flexural fatigue performance of concrete containing nano-particles for pavement.” International Journal of Fatigue, 29(7), 1292−1301.

Li, L.J., Xie, W.F., Liu, F., Guo, Y.C., and Deng, J. (2011). “Fire performance of high strength concrete reinforced with recycled rubber particles.” Magazine of Concrete Research, 63(3), 187-195.

Liu, F., Zheng, W., Li, L., Feng, W., and Ning, G. (2013). “Mechanical and fatigue performance of rubber concrete.” Construction and Building Materials, 47, 711-719.

Marques, A. M., Correia, J. R., and Brito, J.D. (2013). “Post-fire residual mechanical properties of concrete made with recycled rubber aggregate.” Fire Safety Journal, 58, 49-57.

Mavroulidou, M., and Figueiredo, J., (2010). “Discarded tyre rubber as concrete aggregate: a possible outlet for used tyres.” Global Nest Journal, 12(4), 359–367.

Miyamoto, S., Minagawa, H. and Hisada, M. (2014). “Deterioration rate of hardened cement caused by high concentrated mixed acid attack.” Construction and Building Materials, 67, 47–54.

Mohammadi, Y., Carkon-Azad, R., Singh, S.P., and Kaushik, S.P. (2009). “Impact resistance of steel fibrous concrete containing fibers of mixed aspect ratio.” Construction and Building Materials, 23, 183-189.

Nadeem, A., Memon, S.A., and Lo, T.Y. (2014). “The performance of fly ash and metakaolin concrete at elevated temperature.” Construction and Building Materials, 62, 67-76.

Najim, K. B., and Hall, M. R. (2012). “Mechanical and dynamic properties of self-compacting crumb rubber modified concrete.” Construction and building materials, 27(1), 521-530.

Nataraja, M., Dhang, N., and Gupta, A. (1999). “Statistical variations in impact resistance of steel fiber-reinforced concrete subjected to drop weight test.” Cement and Concrete Research, 29(7), 989−995.

Nayef, A.M., Fahad, A.R. and Ahmed, B. (2010). “Effect of micro-silica addition on compressive strength of rubberized concrete at elevated temperatures.” Journal of Material Cycles Waste Management, 12, 41-49.

Nguyen, T.H., Toumi, A., Turatsinze, A., and Tazi, F., (2012). “Restrained shrinkage cracking in steel fibre reinforced and rubberized cement based mortar.” Materials and Structures, 45, 899-904.

Oikonomou, N., and Mavridou, S. (2009). “Improvement of chloride ion penetration resistance in cement mortars modified with rubber from worn automobile tyres.” Cement and Concrete Composites, 31, 403-407.

Olivares, F.H., and Barluenga, G. (2004). “Fire performance of recycled rubber-filled high strength concrete.” Cement and Concrete Research, 34, 109-117.

Onuaguluchi, O., and Panesar, D.K. (2014). “Hardened properties of concrete mixtures containing pre-coated crumb rubber and silica fume.” Journal of Cleaner Production, 82, 125-131.

Ozbay, E., Lachemi, M., and Sevim, U.K. (2011). “Compressive strength, abrasion resistance and energy absorption capacity of rubberized concretes with and without slag.” Materials and Structures, 44, 1297-1307.

Papadakis, V.G., Fardis, M.N., and Vayenas, C.G. (1992). “Hydration and carbonation of pozzolanic cements.” ACI Materials Journal, 89(2), 119-130.

Pasha, G.R, Khan, M.S., and Pasha, A.H. (2006). “Empirical analysis of the Weibull distribution for failure data.” Journal of Statistics, 13(1), 33-45.

Pelisser, F., Zavarise, N., Longo, T.A., and Bernarin, A.M. (2011). “Concrete made with recycled tire rubber: Effect of alkaline activation and silica fume addition.” Journal of Cleaner Production, 19, 757-763.

Peng, G.F., Bian, S.H., Guo, Z.Q., Zhao, J., Peng, X.L., and Jiang, Y.C. (2008). “Effect of thermal shock due to rapid cooling on residual mechanical properties of fiber concrete exposed to high temperature.” Construction and Building Materials, 22, 948–55.

Pofale, A.D., and Quadri S.R. (2013). “Effective utilization of crusher dust in concrete using Portland pozzolana cement.” International Journal of Scientific and Research Publication 3(8), 1-10.

Prakash V.S. (2007). “Ready mixed concrete using manufactured sand as fine aggregate.” Proceeding of the 32nd Conference on our World in concrete & structures, 28 - 29 August 2007, Singapore (http://cipremier.com/100032053).

Raghvan, D., Huynh, H., and Ferraris, C.F. (1998). “Workability, mechanical properties and chemical stability of a recycled tyre rubber-filled cementitious composites.” Journal of Material Science, 33, 1745-1752.

Rahman, M.M., Usman, M., and Al-Ghalib, A.A. (2012). “Fundamental properties of rubber modified self-compacting concrete (RMSCC).” Construction and Building Materials, 36, 630-637.

Rahmani, T., Kiani, B., Shekarchi, M., and Safari, A. (2012). “Statistical and experimental analysis on the behavior of fiber reinforced concretes subjected to drop weight test.” Construction and Building Materials, 37, 360-369.

Raif, S., and Irfan, A. (2008). “Statistical analysis of bending fatigue life data using Weibull distribution in glass-fiber reinforced polyester composites.” Materials and Design, 29(6), 1170−1181.

Ramachandran, V.S., Feldman, R.F., and Beaudoin, J.J. (1981). “Concrete science treatise on current Research.” London: Heyden and Son Ltd. Philadelphia, USA, 317.

Raupach, M. (1996). “Chloride-induced macrocell corrosion of steel in concrete--theoretical background and practical consequences.” Construction and Building Materials, 10(5), 329-338.

Reda Taha, M. M., El-Dieb, A. S., Abd El-Wahab, M. A., and Abdel-Hameed, M. E. (2008). "Mechanical, fracture, and microstructural investigations of rubber concrete." Journal of Materials in Civil Engineering, ASCE, 20(10), 640-649.

Richardson, A., Coventry, K., Dave, U., and Pineaar, J. (2011). "Freeze/thaw protection of concrete using granulated rubber crumb." The Journal of Green Building, 6(1), 83-92.

RILEM. (1988). "Measurement of hardened concrete carbonation depth." CPC-18, Materials and Structures, 21(6), 453-455.

Roy, S.K., Poh, K.B., and Northwood, D.O. (1999). "Durability of concrete – accelerated carbonation and weathering studies." Building and Environment, 34(5), 597-606.

Sangoju, B., Gettu, R., Bharatkumar, B.H. and Neelamegam, M. (2011). "Chloride-induced corrosion of steel in cracked OPC and PPC concretes: Experimental study." Journal of Materials in Civil Engineering, ASCE, 23(7), 1057-1066

Schimizze, R.R., Nelson, J.K., Amirkhanian, S.N., and Murden, J.A. (1994). "Use of waste rubber in light-duty concrete pavements." In: Proceedings of the Third Material Engineering Conference, Infrastructure: New Materials and Methods of Repair, San Diego, CA, 367–74.

Segre, N. and Joekes, I. (2000). "Use of tyre rubber particles as addition to cement paste." Cement and Concrete Research, 30, 1421-1425.

Siddique, R., Khatib, J., and Kaur, I. (2008). "Use of recycled plastic in concrete: a review." Waste management, 28(10), 1835-1852.

Skripkiūnas, G., Grinys, A., and Černius, B. (2007). "Deformation properties of concrete with rubber waste additives." Materials science [Medžiagotyra], 13(3), 219-223.

Sohrabi, M.R., and Karbalaie, M. (2011). "An experimental study on compressive strength of concrete containing crumb rubber." International Journal of Civil & Environmental Engineering, 11(3), 24-28.

Son, K.S., Hajirasouliha, I., and Pilakoutas, K. (2011). "Strength and deformability of waste tyre rubber filled reinforced concrete columns." Construction and Building Materials, 25(1), 218–226.

Song, P.S., Hwang, S., and Sheu, B.C. (2004). "Statistical evaluation for impact resistance of steel fibre-reinforced concretes." Magazine of Concrete Research, 56(8), 437–42.

Su, H., Yang, J., Ling, T. C., Ghataora, G. S., and Dirar, S. (2015). “Properties of concrete prepared with waste tyre rubber particles of uniform and varying sizes.” Journal of Cleaner Production, 91, 288-296.

Sukontasukkul, P., and Chaikaew, C. (2006). “Properties of concrete pedestrian block mixed with crumb rubber.” Construction and Building Materials, 20, 450-457.

Sukontasukkul, P., and Tiamlom, K. (2012). “Expansion under water and drying shrinkage of rubberized concrete mixed with crumb rubber with different size.” Construction and Building Materials, 29, 520-526.

Sunthonpagasit, N., and Duffey, M.R. (2004). “Scrap tires to crumb rubber: feasibility analysis for processing facilities.” Resources, Conservation and Recycling, 40(4), 281-299.

Topcu, I.B. (1995). “The properties of rubberized concrete.” Cement and Concrete Research, 25, 304-310.

Topçu, I.B., and Bilir, T. (2009). “Experimental investigation of some fresh and hardened properties of rubberized self-compacting concrete.” Materials and Design, 30, 3056–65.

Torii, K., and Kawamura, M. (1994). “Pore structure and chloride ion permeability of mortars containing silica fume.” Cement and Concrete Composites, 16, 279-286.

Toutanji, H.A. (1996). “The use of rubber tire particles in concrete to replace mineral aggregates.” Cement and Concrete Composites, 18, 135-139.

Turatsinze, A., and Garros, M. (2008). “On the modulus of elasticity and strain capacity of self-compacting concrete incorporation rubber aggregates.” Resources, Conservation and Recycling, 52, 1209-1215.

Turki, M., Zarrad, I., Bretagne, E., and Quéneudec, M. (2012). “Influence of filler addition on mechanical behavior of cementitious mortar-rubber aggregates: experimental study and Modeling.” Journal of Materials in Civil Engineering, 24(11), 1350-1358.

Uygunoglu, T., and Topcu, I.B. (2010). “The role of scrap rubber particles on the drying shrinkage and mechanical properties of self-consolidating mortars.” Construction and Building Materials, 24, 1141-1150

Vedalakshmi, R., Rajagopal, K., and Palaniswamy, N. (2008). “Long term corrosion performance of rebar embedded in blended cement concrete under macrocell corrosion condition.” Construction and Building Materials, 22 (3), 186-199.

Wang, H.Y., Chen, B.T., and Wu, Y.W. (2013). “A study of the fresh properties of controlled low-strength rubber lightweight aggregate concrete (CLSRLC).” Construction and Building Materials, 41, 526–531.

Xiang-yu, C., Yi-ning, D., and Azevedo, C. (2011). “Combined effect of steel fibers and steel rebars on impact resistance of high performance concrete.” Journal of South Central University Technology, 18, 1677-1684.

Xue, J., and Shinozuka, M. (2013). “Rubberized concrete: A green structural material with enhanced energy-dissipation capability.” Construction and Building Materials, 42, 196–204.

Yilmaz, A., and Degirmenci, N. (2009). “Possibility of using waste tire rubber and fly ash with Portland cement as construction materials.” Waste Management, 29, 1541-1546.

Yüksel, I., Siddique, R., and Özkan, Ö. (2011). “Influence of high temperature on the properties of concretes made with industrial by-products as fine aggregate replacement.” Construction and Building Materials, 25, 967–72.

Yung, W.H., Yung, L.C., and Hua, L.H. (2013). “A study of the durability properties of waste tire rubber applied to self-compacting concrete.” Construction and Building Materials, 41, 665–672.

Yüzer, N., Aköz, F., and Öztürk, L.D. (2004). “Compressive strength-color change relation in mortars at high temperature.” Cement and Concrete Research, 34, 1803–1807.

Zhang, J., Dongwei, H., and Haoyu C. (2011). “Experimental and theoretical studies on autogenous shrinkage of concrete at early ages.” Journal of Materials in Civil Engineering, ASCE, 23(3), 312-320

Zheng, L., Huo, S.H., and Yuan, Y. (2008). “Strength, elasticity, and brittleness index of rubberized concrete.” Journal of Materials in Civil Engineering, ASCE, 22(11), 692–699.

BIO-DATA

The author is currently working as an Assistant Professor in the Department of Civil Engineering, College of Technology and Engineering, Maharana Pratap University of Agriculture and Technology, Udaipur (India) since 2005. He obtained his Bachelor of Engineering from Pune University in 2001. He completed his Master's degree with Honors from Malaviya National Institute of Technology Jaipur (Rajasthan) in 2003. He has provided his services as Structural Design Engineer at the N. M. Roof Designers Pvt. Ltd., Jaipur for three years. He joined Malaviya National Institute of Technology Jaipur in July 2012 to pursue the PhD programme. His area of specialization is "Structural Engineering".

Following is the list of the publications from the work.

Gupta, T., Tripathi, B., Sharma, R.K. and Chaudhary, S. (2013). "Flexural strength, compressive strength and workability of waste rubber concrete." The 5th Asia and Pacific Young Researchers and Graduates Symposium on Current Challenges in Structural Engineering (YRGS 2013), Jaipur, India, October 15-16th 2013, 320-327.

Gupta, T., Sharma, R.K. and Chaudhary, S. (2013). "Utilization of waste rubber tire particles in concrete pavement." 4th Nirma University International Conference on Engineering, Ahmedabad, India, November 28-30th, 2013, 55.

Gupta, T., Chaudhary, S., and Sharma, R.K. (2014). "Assessment of mechanical and durability properties of concrete containing waste rubber tire as fine aggregate." *Construction and Building Materials*, 73, 562–574. (*SCIE Indexed, I.F. 2.27*)

Gupta, T., Sharma, R.K., and Chaudhary, S. (2015). "Impact resistance of concrete containing waste rubber fiber and silica fume." *International Journal of Impact Engineering*, 83, 76-87. (*SCI Indexed, I.F. 2.01*).

Gupta, T., Chaudhary, S. and Sharma, R.K. (2015). "Mechanical and durability properties of waste rubber fiber concrete with and without silica fume." Journal of Cleaner Production, 112, 702-711 (*SCIE Indexed, I.F. 3.84*).

Gupta, T., Sharma, R.K. and Chaudhary, S. (2015). "Influence of waste tyre fibers on strength, abrasion resistance and carbonation of concrete." Scientia Iranica A, 22(4), 1481-1489 (*SCIE Indexed, I.F. 1.02*).

Gupta, T., Chaudhary, S., and Sharma, R.K. and (2015). "Influence of waste rubber tyre particles in concrete pavement." The 7th Asia and Pacific Young Researchers and Graduates Symposium on Innovations in Materials and Structural Engineering Practices (YRGS 2015), Kuala Lumpur, Malaysia, August 20-21st 2013, 32-39.